DEPARTAMENT DE ZOOLOGIA

PARASITOLOGICAL STUDY OF CULTURED AND WILD SPARIDS IN THE MEDITERRANEAN.

GEMA ALAMA BERMEJO

UNIVERSITAT DE VALÈNCIA
Servei de Publicacions
2012

Aquesta Tesi Doctoral va ser presentada a València el dia 5 de desembre de 2011 davant un tribunal format per:

- Dr. Juan Antonio Balbuena Díaz-Pinés
- Dra. Ariadna Sitjá Bobadilla
- Dra. Mónica Caffara
- Dra. Pavla Bartosova
- Dr. Francisco Esteban Montero Royo

Va ser dirigida per:
Dr. Juan Antonio Raga Esteve
Dra. Astrid Sibylle Holzer

I.S.B.N.: 978-84-370-8852-5
Edita: Universitat de València
Servei de Publicacions
C/ Arts Gràfiques, 13 baix
46010 València
Spain
Telèfon:(0034)963864115

VNIVERSITAT DE VALÈNCIA

Facultat de Ciències Biològiques

Institut Cavanilles de Biodiversitat i Biologia Evolutiva

PARASITOLOGICAL STUDY OF CULTURED AND WILD SPARIDS IN THE MEDITERRANEAN

TESIS DOCTORAL

POR

GEMA ALAMA BERMEJO

DIRECTORES

ASTRID SIBYLLE HOLZER **JUAN ANTONIO RAGA ESTEVE**

Valencia, Junio 2011

D. JUAN ANTONIO RAGA ESTEVE, Catedrático de Zoología de la Facultad de Ciencias Biológicas de la Universitat de València y

Dª ASTRID SIBYLLE HOLZER, Investigadora de la Academia de Ciencias de la República Checa

CERTIFICAN que Dª Gema Alama Bermejo ha realizado bajo nuestra dirección, y con el mayor aprovechamiento, el trabajo de investigación recogido en esta memoria, y que lleva por título: "PARASITOLOGICAL STUDY OF CULTURED AND WILD SPARIDS IN THE MEDITERRANEAN", para optar al grado de Doctora en Ciencias Biológicas.

Y para que así conste, en cumplimiento de la legislación vigente, expedimos el presente certificado en Paterna a 15 de Septiembre de 2011.

Firmado: Juan Antonio Raga Esteve Firmado: Astrid Sibylle Holzer

Para Amelia y Tasia

AGRADECIMIENTOS

En primer lugar, a la primera que quiero agradecerle toda su dedicación, esfuerzo, apoyo y amistad, es a Astrid. Qué suerte fue conocerte! Bueno, en una ocasión ya te dije lo que sentía, y ya sabes que trabajar contigo ha sido de lo mejor que me ha pasado en la vida. Sólo espero ser la mitad de buena que tú!

Quiero agradecer a Toni, por dejarme empezar a colaborar en tu grupo. Gracias por ayudarme siempre con todo, por tus desvelos por ayudarme a conseguir la beca para que pudiera hacer mi tesis. Gracias por tus enseñanzas, tus consejos y ayuda!

Paco! Gracias por compartir tus conocimientos "sanguinilocos". Gracias por estar siempre dispuesto a ayudar y por tu amistad. Gracias!

I would like to thank to Aneta Kostadinova for all the blood flukes matter and the statistics help and to Ivan Fiala for all his patience with my documents.

I would like to thank my collaborators from Stirling, especially James, for all the time we spent at the confocal. Thanks Andy for all the good and strong coffee. Thanks Christina for all the brainstorming. Gracias Sara por hacerme sentir como en mi casa y a Mayra por todas las recetas mexicanas.

Mil gracias a todos los que colaboraron con las jaulas! Quiero darle las gracias a nuestro capitán Claudio, por tu dedicación y paciencia, y también por tener ese estado de ánimo tan optimista, a pesar de las tormentas! Sin ti, no habría sido posible todo el trabajo de campo. Muchas gracias también a Alfonso por dedicarnos su tiempo en vacaciones. Al Canario, por tu buen talante, por las risas subacuáticas, por ser como un pez en el agua y por tu pelo hidrofóbico. A Ana Born, por tu ayuda con todos los muestreos de sargos (las medusas apestan!), por nuestras charlas y por tu apoyo. A Natalia, gracias por tu ayuda beia! con todas las extracciones que hubo que hacer. Gracias a Valerio por las fotografías acuáticas, que han embellecido tanto este trabajo, grazie mille. Gracias, gracias!

Quiero agradecer a toda la gente de la UAB por su buen trato, en especial a Montseta, por todo tu tiempo enseñándome como iba eso del microscopio electrónico. Moltes gràcies!

Durante este camino que ya se está acabando (eh! pero empiezan otros!) he conocido a mucha gente y me quiero quedar con los mejores recuerdos y enseñanzas. Quiero agradecer a toda la gente de la unidad de Zoología Marina y de varamientos, que tantas situaciones, tanto buenas como malas, hemos pasado juntos: Abril, Ana A, Ana P., Aigües, Carmen, Celia, Chati, Diana, Eugenia, Isa A., Isa B., Javi A., Jesús T., Juan Antonio, Juanma, Marga, Merche, Monica, Neus, Ohiana, Patricia, Paula, Raúl, Vicky... Al final de todo se aprende y uno se queda con lo mejor!

A mis compañeros del máster de acuicultura, también les quiero dar las gracias. Ya han pasado un montón de años desde esos cafés y esos buenos ratos.

Quiero agradecer a mis padres, Luis y Camino por todo su apoyo y paciencia durante este largo camino.

A Kira y a Nevat, mis animalillos blancos siempre me han dado la más calurosa de las bienvenidas al llegar a casa.

Jesús, mi mexicano, tengo más cosas que agradecer a esta tesis de las que creo!

Este trabajo ha sido posible gracias a una beca predoctoral de la Consellería d'Educació, Generalitat Valenciana. Los permisos para la instalación de jaulas marinas fueron concedidos por la Consellería d' Agricultura, Pesca i Alimentació, Generalitat Valenciana. Esta tesis doctoral fue posible gracias a los proyectos MEC AGL 2005-01221 (Ministerio de Educación y Ciéncia) y GVPRE/2008/185 de la Generalitat Valenciana.

TABLE OF CONTENTS

SUMMARY

Aquaculture is a growing agricultural sector that supplies nearly half of the food fish consumed by humans worldwide. In the Mediterranean, the aquaculture market is dominated by two species, the sea bass (*Dicentrarchus labrax*, Moronidae) and the gilthead sea bream (*Sparus aurata*, Sparidae). The excess of production has led to a market saturation and an important decrease in price, which has provoked an urgent need for establishing new fish species in aquaculture in order to diversify the market. Species of the family Sparidae are important candidates for species diversification in the Mediterranean aquaculture because they are highly appreciated for commercial use due to their excellent flesh. One of the main handicaps in the commercial culture of fish is disease. Infectious diseases are produced by a variety of pathogens, i.e. bacteria, viruses or parasites. While parasites generally occur in low numbers in the natural environment, under culture conditions, they may multiply more rapidly, cause disease and mortalities and have an important impact on the production of fish. Some of the most problematic parasites in the Mediterranean aquaculture belong to the Myxozoa (Cnidaria), the Monogenea (Platyhelminthes) and to the Aporocotylidae (Trematoda).

This thesis aims to improve our knowledge of myxozoan and aporocotylid parasites in sparids which are new candidates or existing Mediterranean aquaculture species. The species studied are the sand steenbras *Lithognathus mormyrus*, the picarel *Spicara smaris*, the annular seabream *Diplodus annularis*, the common two-banded seabream *Diplodus vulgaris,* the sharpsnout seabream *Diplodus puntazzo* and the gilthead seabream *Sparus aurata*. The present study seeks to identify, describe and clarify the taxonomic position of the parasite taxa present in these hosts by using morphological and molecular based approaches, and by defining their phylogenetical position and relationship with previously described species. Furthermore, development and habitat selection in the host, as well as pathology are analysed in order to evaluate the pathogenic potential of the parasites described in the present work. Another aspect of this thesis focuses on the study of parasite life cycles, seasonality, transmission and routes of infection in the fish host, with the final aim to provide information allowing for the development of management strategies for aquaculture systems.

The study led to the following findings and conclusions:

1) A new genus and species of blood fluke, *Skoulekia meningialis* n. gen., n. sp. was described from the common two-banded seabream *D. vulgaris.* The erection of the new genus was strongly supported by morphological data as well as molecular phylogeny (SSU, ITS2 and LSU rDNA). *Skoulekia* was demonstrated to have a close relationship with the genera *Psettarium* and *Pearsonellum*. *S. meningialis* was detected in a special location, the ectomeningeal veins surrounding the optic lobes of the brain of *D. vulgaris*. This contrasts studies on the majority of aporocotylids, which usually inhabit the heart or the blood vessels of the gills. While blood fluke pathology is normally almost exclusively related to the eggs trapped within the gill vessels, it is the adults of *S. meningialis* which were found to cause mild, chronic, localised meningitis. *S. meningialis* did not seem to cause an important pathological effect on wild *D. vulgaris*. However, its special location surrounding a vital organ should be kept in mind when establishing *D. vulgaris* in aquaculture systems.

2) Macroscopic, elongate plasmodia containing myxosporean spores belonging to the genus *Unicapsula* were found in the skeletal muscle of the striped seabream, *L. mormyrus*. The only species of *Unicapsula* described from the Mediterranean to date is *Unicapsula pflugfelderi* from the picarel *Spicara smaris*. A morphological and molecular comparison (SSU rDNA) was carried out between *U. pflugfelderi* from *S. smaris* and *Unicapsula* sp. from *L. mormyrus*. Despite differences related to the size of plasmodia, spore morphology showed minor differences and SSU rDNA sequences were identical, thus determining conspecificity of the myxozoans from the two hosts. Ultrastructural data revealed the presence of two previously undescribed structures in the sporoplasm of *U. pflugfelderi* spores: a crystalline structure and a vesicular body, which may be related to osmotic changes and the production of material for polar capsule formation. Morphological comparison of all species of the genus *Unicapsula* described to date revealed that, according to shell valve distributions in the spores, two basic types can be defined, dividing the genus *Unicapsula* into two groups. As molecular data are missing, it is unclear whether this separation is artificial or is mirrored by phylogenetic clustering. Disruption of the muscle tissue (myoliquefaction) is common for species of *Unicapsula* and *Kudoa* and may render fillets liquefied and unfit for marketing. This condition does not occur in *U. pflugfelderi*-infected *S.*

smaris, however, the massive occurence of macroscopic plasmodia in the fillets of *L. mormyrus* could produce marketing problems due to rejection by the consumer.

3) Myxosporean spores belonging to the genus *Ceratomyxa* were detected in the gall bladder of the sharpsnout seabream *D. puntazzo*. A detailed morphological and molecular (SSU rDNA) characterisation of these spores and a comparison with existing descriptions of ceratomyxids resulted in the erection of a new species, *Ceratomyxa puntazzi* n. sp. *C. puntazzi* was found to cause necrosis and epithelial sloughing in the gall bladder, and to provoke mild pericholangitis in the liver tissue surrounding the bile ducts of *D. puntazzo*. Whereas no direct mortalities were observed, *C. puntazzi* may be considered an opportunistic parasite as shown in a previous study on ceratomyxid infection in steroid-treated, potentially immunosuppressed *D. puntazzo*. SSU rDNA data of three other ceratomyxids from two sparids sharing the habitat with *D. puntazzo*, i.e. *D. annularis* and *S. aurata* were also collected and indicate that the genus *Ceratomyxa* is very host-specific in sparids This agrees with data on ceratomyxids previously obtained from other fish families. The phylogenetical results revealed that all available ceratomyxid species from sparids in the Mediterranean arise from a common ancestor. The present results indicate that a high species diversity can be expected from ceratomyxids in Mediterranean sparids.

4) The combination of light microscopy, confocal laser scanning microscopy using specific stains and electron microscopy was used for a detailed study of the three-dimensional morphology, ultrastructure and cellular composition of *C. puntazzi* parasite stages in the bile. It was shown that the combined use of several microscopic methods can considerably improve the morphological characterization of myxozoan microparasites and allows for unique insights into the organisation of different cellular components. *C. puntazzi* showed two developmental pathways in the bile of *D. puntazzo*, i.e. pre-sporogonic proliferation and sporogony. In the pre-sporogonic development proliferation occurred by means of plasmotomy with frequent budding. Pre-sporogonic stages were also shown to be highly motile. For the first time, myxozoan locomotive behaviour and the distribution and potential effectors of motility were analysed providing unique information on the processes of directional locomotion and budding: F-actin rich cytoskeletal elements were found to

concentrate at one end of the parasite, which produces localised filopodia, thus facilitating parasite motility. Furthermore, the mechanism of budding was identified, for the first time, as a process dependent on F-actin concentration at opposite ends of the separating stages, thus causing their active separation. Other structures detected in the present study were lipid droplets and external blebs which might facilitate buoyancy of the parasites. In sporogonic stages, F-actin was more evenly disperse, coinciding with the end of the swimming period of the stages and the release of the mature spores.

5) Monthly natural exposures of sharpsnout seabream *D. puntazzo* to infective actinosporean stages of *C. puntazzi* throughout a full year was conducted during the present study and demonstrate the first attempt of a seasonal infection study in marine myxozoans. Natural exposure of fish in a small cage and subsequent maintenance of fish in the laboratory for 60 days at 20-23ºC resulted in *C. puntazzi* infection in the receptor fish. The parasite presented a marked temperature-related seasonality, with microscopical detection of proliferative stages and spores in the bile exclusively from April until November. Two peaks of infection prevalence were registered during this period: in April-May (80%), when seawater temperature first reached 16ºC, and in October (86%), while prevalences were lower from June to September (46-64%). These two peaks of infection prevalence could be related to actinospore production and/or viability. However, PCR detection in the bile was possible all year round, which indicates that the parasite can infect and stay in the fish in low numbers (latent infection) during the winter months. Blood stages were detected by PCR in sentinel fish and presented a very high prevalence after exposure and all year round, but the infection was sometimes cleared or lost over time, as not all fish initially infected successfully established in the bile. This may be dependent on the infective parasite dose or on the immunological condition of host in the winter months. The combination of PCR results obtained from blood, gall bladder and liver suggests the following route of infection: entry into the blood system in the gills, as suggested for other myxozoans, exit into the liver tissue, entry into the bile ducts, through which the parasite reaches the gall bladder, where it starts pre-sporogonic proliferation and sporogony with the consequent release of spores with the bile via the intestine into the environment. Artificial transmission of different developmental stages, i.e. blood stages as well as pre-sporogonic proliferative and sporogonic stages

of *C. puntazzi* via oral, intracoelomic, bath application or cohabitation was not successful. This indicates that fish-to-fish transmission as demonstrated previously for *Enteromyxum* spp. is unlikely to occur in *C. puntazzi*. The natural exposure study implicates that initial exposure of fish/transfer from the hatchery to sea cages is best done in late autumn/early winter, as the parasite would then establish in low number and potentially cause some kind of immunization, potentially resulting in higher resistance to re-infection with high numbers of parasites in the following summer. This has been demonstrated in other myxozoans and is an important implication for control measures of *D. puntazzo*.

RESUMEN

ESTUDIO PARASITOLÓGICO DE ESPÁRIDOS EN CULTIVO Y SILVESTRES DEL MEDITERRÁNEO

1.-Introducción

La acuicultura es la técnica o el sistema de cría de organismos acuáticos en agua dulce o marina. En el Mediterráneo, la acuicultura tiene una larga tradición, con primeros indicios de cultivo de peces y mariscos 2500 años a.c. Sin embargo, el desarrollo de la acuicultura Mediterránea moderna se inició hace unos 30 años, gracias a la investigación en campos como la reproducción de peces, el cultivo de larvas, el manufacturado de piensos y la ingeniería aplicada a mejorar los sistemas de producción. Actualmente, la acuicultura es considerada como el sector de producción animal con más rápido crecimiento, representando más de un tercio de la producción global de alimentos provenientes del mar. La acuicultura produce un 45,7% de los alimentos del mar de consumo humano (FAO 2010). Es estima una tendencia ascendente para cubrir la demanda ya que la acuicultura se considera como una fuente importante y asequible de proteínas.

En el Mediterráneo, el cultivo de peces está dedicado casi exclusivamente al cultivo de dos especies: la lubina (*Dicentrarchus labrax* (L.), Moronidae) y la dorada (*Sparus aurata* L., Sparidae). Sin embargo, la saturación del mercado y el exceso de producción han derivado a un nivel de competitividad muy alto y a unos márgenes reducidos de beneficios, lo que ha provocado la necesidad de diversificar especies para el cultivo (Rigos y Katharios 2010). El futuro de este sector depende de la investigación de nuevas especies cultivables para ofrecer mayor variedad de productos al consumidor, pero también que sean especies con altas tasas de crecimiento y costes de producción bajos (Barazi-Yeroulanos 2010). Las especies de la familia de los espáridos son firmes candidatas a ser nuevas especies en la acuicultura Mediterránea.

Los espáridos (Teleostei: Perciformes: Sparidae) son una familia de peces marinos con una amplia distribución, encontrándose cerca de la costa en zonas tropicales y templadas. En general son peces carnívoros pero también hay algunas especies omnívoras. Son peces muy apreciados gastronómicamente y comercialmente importantes para pesquerías, pesca deportiva y acuicultura.

El mayor reto para el cultivo de peces es las enfermedades. Las enfermedades pueden ser provocadas por diversos motivos, entre los que se encuentran los agentes infecciosos, ya sean virus, bacterias o parásitos (Woo y col. 2002). Los parásitos pueden afectar a la producción de peces de diferentes modos: afectando al aspecto del producto final, o causando morbilidad y mortandad en los stocks o incluso

pueden afectar a la salud humana. En ocasiones, existen medidas profilácticas que pueden evitar los problemas antes de que aparezcan. Se sabe que la transmisión de los parásitos se ve favorecida por las condiciones de cultivo (Hemmingsen 2008). Algunos de los grupos patógenos más problemáticos son los microparásitos del filo Mixozoa (Palenzuela 2006), los monogeneos (Thoney y Hargis 1991) y los digeneos sanguíneos de la família de los aporocotílidos (Bullard y Overstreet 2008).

Las especies de la subclase Digenea Carus 1863 son parásitos platelmintos de la clase Trematoda Rudolphi 1808 con más de 2500 especies descritas. Morfológicamente, se caracterizan por sus órganos de fijación: una ventosa oral o anterior y una ventosa ventral o posterior. Estas ventosas sin embargo se pueden perder en algunas especies. Presentan ciclos de vida complejos con varios estadios larvarios. El adulto normalmente produce huevos que se liberan al medio con las heces de su hospedador. De los huevos eclosiona un miracidio que nada y busca activamente al primer hospedador intermediario, normalmente un molusco. El miracidio desarrolla un esporocisto que produce asexualmente múltiples larvas esporocistos o redias, que darán lugar a larvas cercarias. Las cercarias salen del molusco y buscan activamente al hospedador definitivo vertebrado (ciclos de vida con dos hospedadores) o se enquistan como metacercarias en un segundo hospedador intermediario y esperan pasivamente hasta que ese hospedador es ingerido por el hospedador definitivo, donde se desarrollará el adulto (ciclos de vida con tres hospedadores). Normalmente, el hábitat de estos parásitos es el tubo digestivo, pero también se encuentran en otras cavidades corporales y tejidos. Los digeneos adultos que se encuentran en otros hábitats que no son el tubo digestivo, suelen ser los que más problemas causan en sus hospedadores. Entre ellos, los helmintos que se encuentran el sistema sanguíneo son los más problemáticos. En los peces, encontramos a helmintos de la familia Aporocotylidae. La familia Aporocotylidae Odhner 1912 (sinónimo Sanguinicolidae Poche 1926, Bullard y col. 2009) son trematodos que habitan el sistema sanguíneo de elasmobranquios, holocéfalos y teleósteos. Los aporocotílidos son difíciles de detectar y colectar en sus hospedadores definitivos y suelen pasarse por alto en los exámenes parasitológicos estándar (Smith 1997; Cribb y col. 2001). Se encuentran infectando el corazón, las arterias branquiales y arteriolas de los peces (Bullard y Overstreet 2008), pero también se han descito aporocotílidos de otras localizaciones como los vasos mesentéricos (Herbert y col. 1994), el riñón (Bullard y col. 2006) y las cinturas pectorales

(Montero y col. 2003; 2009). Morfológicamente los aporocotílidos son aplanados dorsoventralmente, con espinas tegumentarias marginales y se diferencian de otros digeneos por tener una ventosa anterior muy poco desarrollada y por carecer de ventosa ventral. La familia Aporocotylidae carece de una hipótesis filogenética clara para todo el grupo (Bullard y Overstreet 2008) y por el hecho de ser al único clado con adultos exclusivamente en peces son candidatos a ser un grupo clave para entender la evolución de los digeneos (Cribb y col. 2001). Su ciclo de vida incluye dos hospedadores, siendo los únicos digeneos que pueden no utilizar un molusco como hospedador intermediario, ya que algunas especies marinas desarrollan cercarias en poliquetos (Køie 1982; Køie y Petersen 1988). Los adultos se desarrollan en el sistema sanguíneo de los peces y liberan huevos que quedan atrapados en los capilares de las branquias, donde maduran. Los huevos obstruyen, producen lesiones epiteliales y cardiacas, y hemorragias en las branquias, lo que puede dar lugar a asfixia y finalmente a la muerte del hospedador (Ogawa y col. 1989; Crespo y col. 1992; Kirk y Lewis 1998; Padrós y col. 2001; Colquitt y col. 2001; Ogawa y col. 2007). Por ello, los aporocotílidos son conocidos por causar efectos patológicos y mortalidades en acuicultura. Los problemas patológicos raramente los producen los vermes adultos (Schell 1974; Thulin 1980; Overstreet y Thulin 1989; Padrós y col. 2001).

El filo Myxozoa Grassé 1970 son metazoos parásitos de vertebrados e invertebrados con más de 2300 especies descritas, muy conocidos por las enfermedades que producen en peces de interés comercial. Las infecciones por mixozoos en espáridos y en otras especies en cultivo han sido muy investigadas en los últimos años (Alvarez-Pellitero y Sitjà-Bobadilla 1993; Agius y Tanti 1997; Palenzuela 2006). Los mixozoos presentan esporas multicelulares formadas por células capsulogénicas que forman las cápsulas polares, su estructura más característica, células valvogénicas que forman las valvas y un esporoplasma infectivo. Las cápsulas polares son estructuras similares a los nematocistos formadas por un filamento polar enroscado que se extruye y permite la adhesión a su hospedador y la invasión por parte del esporoplasma (Lom y Dyková 2006). Antiguamente, los mixozoos fueron clasificados como protistas, pero debido a la existencia de características propias de metazoos como sus esporas multicelulares (Štolc 1899), uniones celulares y producción de colágeno (Sidall y col. 1995) y cápsulas polares similares a

nematocistos (Weill 1938), se planteó su posible origen metazoo. Este parentesco se confirmó en 1994 por el análisis de secuencias de ADN ribosomal (Smothers y col. 1994). A partir de entonces, su posición filogenética ha sido motivo de controversia, existiendo dos hipótesis: la que relaciona este grupo con los cnidarios (Siddall y col. 1995; Zrzavý y Hypša 2003; Jiménez-Guri y col. 2007; Holland y col. 2010) y la que describe afinidades con animales bilaterales (Smothers y col. 1994; Okamura y col. 2002; Monteiro y col. 2002). Los mixozoos son un grupo muy divergente y son necesarios más datos, secuencias y modelos para posicionarlos filogenéticamente (Evans y col. 2010).

La clasificación tradicional de los mixozoos se basa en la morfología de las esporas, dividiéndose en las clases Malacosporea (esporas con valvas blandas) y Myxosporea (esporas con valvas duras). Dentro de los myxosporea, existen dos órdenes: Bivalvulida (esporas con dos valvas) y Multivalvulida (esporas con tres o más valvas). El uso de filogenia molecular ha demostrado que muchos géneros son parafiléticos y polifiléticos y que existe una gran divergencia entre la taxonomía tradicional y los resultados de estudios moleculares.

La mayoría de los mixozoos pertenecen a la clase Myxosporea. El ciclo de vida de los mixosporidios incluye hospedadores alternantes. La fase myxosporea ocurre en los vertebrados, normalmente peces, donde producen mixosporas. La fase actinospora incluye a una fase sexual y tiene lugar en un invertebrado, normalmente anélidos oligoquetos en agua dulce y poliquetos en agua marina. Las actinosporas infectaran de nuevo al hospedador vertebrado. Las actinosporas en contacto con la piel o las branquias, liberan el esporoplasma. Éste migra intercelularmente por la epidermis y el epitelio branquial. Se inicia así un desarrollo pre-esporogónico proliferativo que permite la diseminación del parásito por los órganos del hospedador. Estos estados pre-esporogónicos llegan al órgano diana y empiezan la fase de esporogénesis, que desembocará en la producción de mixosporas que se formarán dentro de plasmodios o trofozoitos que pueden contener una, dos o miles de esporas. Las mixosporas se liberan al exterior a través del digestivo, el sistema excretor o tras la muerte del hospedador. Las mixosesporas serán ingeridas por el hospedador invertebrado donde el esporoplasma iniciará la merogonia. A continuación, por gametogonia, estos estados se dividen y producen un pansporocisto que producirá ocho zigotos que darán ocho actinosporas. Sólo hay cuatro ciclos de vida descritos en el medio marino (Køie y col. 2004; 2007; 2008; Rangel y col. 2009)

debido a la dificultad de encontrar al hospedador invertebrado en un ambiente tan diverso y rico en invertebrados (Køie y col. 2004). La transmisión "pez a pez" sólo ha sido observada en especies del género *Enteromyxum* Palenzuela, Redondo y Alvarez-Pellitero 2002. En estas especies la infección en peces receptores se produce no sólo por las mixosporas si no por estados proliferativos que se encuentran dentro de las célula epiteliales del intestino (Diamant 1997; Redondo et al. 2002). Esto es de especial relevancia en sistemas de cultivo, con altas densidades de peces.

Los mixozoos pueden infectar cualquier órgano o tejido: pueden ser celozoicos, cuando habitan cavidades corporales como la vesícula biliar o el tracto urinario, o histozoicos, cuando se encuentran en tejidos, intracelularmente o intercelularmente. Dependiendo de la especie, los mixozoos pueden ser muy específicos, (encontrándose en un sólo hospedador) o pueden ser muy inespecíficos (varios hospedadores) (Lom y Dyková 2006).

De todas las especies descritas, sólo una pequeña parte es notablemente patogénica. Los mixozoos pueden perjudicar el crecimiento y la reproducción de los peces o causar daño en tejidos y órganos, llegando a producir la muerte del hospedador. En estado natural, los mixozoos no suelen producir mortandades, con lo que las infecciones se vuelven crónicas. Pero en acuicultura, los mixozoos son un grave problema ya que las altas densidades, los factores de estrés secundarios y el sistema inmunitario debilitado de los peces en jaulas son una oportunidad favorable para los parásitos: Las especies *Myxobolus cerebralis* Hofer 1903, *Tetracapsuloides bryosalmonae* (Canning, Curry, Feist, Longshaw y Okamura 1999) y *Ceratomyxa shasta* (Noble 1950) son responsables de serias pérdidas económicas en cultivos de salmónidos (Hofer 1903; Bartholomew y col. 1989b; Bartholomew y col. 2004). Las especies del género *Ceratomyxa* (Thélohan 1892), que habitan en la bilis, se ha visto que causan mortalidades en peces inmunocomprometidos (Company y col. 1999; Katharios y col. 2007). Las especies de los géneros *Kudoa* Meglitsch 1974 y *Unicapsula* Davis 1924 producen quistes macroscópicos de esporas y degradación enzimática post-mortem de filetes de pescado (Moran y col. 1999). En el Mediterráneo, la enteromixosis producida por el parásito *Enteromyxum leei* (Diamant, Lom y Dyková 1994) produce importantes mortalidades en sistemas de cultivo por enteritis crónica severa (Diamant y col. 1994; Athanassopoulou y col. 1999).

2.- Objetivos

Esta tesis doctoral busca aportar conocimientos sobre parásitos aporocotílidos y mixozoos en nuevas especies de espáridos para la acuicultura mediterránea y especies de espáridos de cultivo tradicional. Las especies estudiadas son: la herrera *Lithognathus mormyrus* (L.), el caramel *Spicara smaris* (L.), el raspallón *Diplodus annularis* (L.), la mojarra *Diplodus vulgaris* (Geoffroy Saint-Hilaire 1817), el sargo picudo *Diplodus puntazzo* (Walbaum 1792) y la dorada *S. aurata*. Los objetivos de esta tesis son identificar, describir y determinar taxonómicamente a los parásitos encontrados en estos hospedadores utilizando un enfoque morfológico y molecular (SSU, ITS2 y LSU rDNA) y mediante posicionamiento filogenético y comparando con especies previamente descritas. Este es el caso de una nueva especie de helminto sanguíneo que se encontró en la mojarra con unas características y un hábitat poco común. También se observaron quistes macroscópicos en la musculatura de la herrera, conteniendo esporas de mixozoos. Se hallaron estados de un mixozoo moviéndose activamente en la bilis del sargo picudo. El desarrollo y la selección del hábitat del parásito en el hospedador, así como la patología han sido analizadas para evaluar el potencial patogéno de los parásitos descritos en este trabajo, combinando una gran variedad de técnicas microscópicas, entre ellas, el microscopio confocal láser de barrido, raramente utilizado con mixozoos. También se han tratado otros aspectos como el ciclo de vida, la estacionalidad, la transmisión y las rutas de infección de los parásitos, mediante la instalación mensual de jaulas marinas durante un año y mediante transmisiones experimentales con peces libres de infección con el objetivo de aportar información que permita desarrollar estrategias profilácticas de manejo en cultivos.

3.- Material y métodos

Muestreo de peces y obtención de parásitos

Los peces se obtuvieron de la costa mediterránea de las comunidades valenciana y murciana entre 2006 y 2010. Los peces silvestres se obtuvieron de pesca comercial de arrastre y de pesca costera. Estos peces se transportaron refrigerados hasta el laboratorio de la unidad de investigación Zoología Marina. Los peces libres de infección y de cultivo se obtuvieron de criaderos y granjas marinas. Estos peces se transportaron vivos a las instalaciones del "Servei Central de Suport a l'Investigació Experimental" de la Universidad de Valencia (SCSIE) donde se alimentaron con

piensos comerciales. Todos los peces de este estudio se sacrificaron por disección medular o por una sobredosis de anestésico.

Los peces fueron diseccionados y los órganos examinados usando microscopía óptica. Los parásitos se recolectaron y se utilizaron en fresco para la descripción morfológica por microscopía óptica, extracción de ADN, microscopía láser confocal, microscopías electrónicas de barrido y transmisión, y para histopatología.

Análisis morfológico

Microscopía óptica, videos y dibujos

Fotografías digitales de los parásitos y su localización en fresco se tomaron con una cámara digital Leica DC300 en un microscopio Leica DMR con interferencia Nomarski a diferentes aumentos. Asimismo se obtuvieron vídeos de parásitos vivos y, en algunos casos se tiñeron con la tinción vital rojo neutro al 1%. Las medidas de los parásitos se obtuvieron desde fotografías digitales con el programa de análisis de imagen UTHSCSA Image Tool 3.0 (mixozoos) o mediante dibujos (trematodos). Los dibujos se realizaron con Microsoft Office PowerPoint 2003 basándose en fotografías digitales y en imágenes de microscopía. Los frotis de esporas se tiñeron con Diff-Quick® y se montaron con un medio de montaje libre de xilol. Los digeneos se fijaron en alcohol 70º, se tiñeron con acetocarmín férrico o carmín alumínico, se deshidrataron en una cadena de alcoholes, se transparentaron con dimetil ftalato y se examinaron como preparaciones permanentes en bálsamo de Canadá. Los especímenes tipos se depositaron en colecciones del Museo de Historia Natural de Londres, Reino Unido.

Microscopía electrónica de barrido

Las esporas y trofozoitos de mixozoos depositaron sobre cubres recubiertos de 0,1% de “Poly-D-lisina”, se fijaron con 2,5 % glutaraldehído en 0,1M tampón fosfato (PBS). Después se realizó una segunda fijación con una solución al 1% de tetraóxido de osmio en PBS. Los cubres se deshidrataron en una cadena de alcoholes crecientes y se le aplicó el punto crítico. Los digeneos fueron fijados con 2,5 % glutaraldehído en PBS, se deshidrataron en una cadena de alcoholes y se les aplicó el punto crítico. Los cubres con estados de mixozoos y los digeneos fueron montados en soportes, recubiertos con oro y examinados en el microscopio de barrido FeG-SEM Hitachi S4100.

Microscopía electrónica de transmissión

Los plasmodios de la musculatura y vesículas biliares infectadas con mixozoos se fijaron con 2,5% glutaraldehído en PBS. Se realizó una segunda fijación con 1% tetraóxido de osmio en PBS y se deshidrató con una cadena creciente de alcoholes. Las muestras de etanol 100º se transfirieron a epoxipropano. Se embebieron añadiendo 60% epoxipropano - 40% epon araldita, y se dejó secar 12 horas a 4ºC. Se transfirieron a epon nuevo y se dejaron secar 48 horas a 60ºC. Se hicieron secciones semifinas que se tiñeron con 1% azul de toluidina y ultrafinos que se dispusieron en gradillas y se tiñeron con una solución al 5% de acetato de uranilo en agua destilada y la solución de Reynolds de citrato de plomo. Las gradillas se examinaron en los microscopios electrónicos de transmisión JEM 100B y Tecnai™ G2 Spirit TWIN / BioTWIN. Para un procesado más rápido se aplicó un protocolo alternativo con resina de agar de baja viscosidad.

Microscopia láser confocal de barrido

La bilis con estados proliferativos y esporogónicos de mixozoos se centrifugó, se descartó el sobrenadante y se fijó con formalina al 4% en PBS. Los parásitos se dejaron depositar sobre portas recubiertos de 0,1% de "Poly-D-lisina". Las tinciones que se utilizaron fueron: Rojo Nilo, tinción lipofílica; Faloidina, la cual se une a subunidades de actina filamentosa; y DAPI, el cual se une al ADN. Se cubrió con un porta y se selló con barniz para uñas para evitar la evaporación del medio y se observó en el microscopio Leica TCS SP2 AOBS.

Análisis estadístico de datos morfométricos de mixozoos

Para determinar diferencias morfológicas en las mixosporas, se obtuvieron medidas de las esporas y se analizaron estadísticamente. Se aplicó el test Kolmogorov-Smirnov para comprobar que la distribución era normal. Las diferencias entre las esporas de diferentes hospedadores se comprobaron con un test-T. Se llevó a cabo un análisis de componentes principales para explorar los datos. Finalmente, se aplicó un test-T para detectar diferencias entre los dos componentes obtenidos con el análisis de componentes principales. Todos los análisis se llevaron a cabo con el programa de análisis estadístico SPSS 15.

Histología

Los órganos fijados en 10% formalina fueron orientados en cassettes, deshidratados en series crecientes de alcohol y transferidos de xylol a parafina, en la que fueron embebidos. Los cortes de 6µm se tiñeron con hematoxilina-eosina, tinción de Gram y 1% azul de toluidina.

Análisis molecular

Extracción de ADN, PCR, secuenciación y alineamiento

Los parásitos se dispusieron en tampón de extracción "TNES-urea" (Asahida y col. 1996). Las muestras se digirieron con 100µg/ml de proteinasa K a 55ºC y el ADN se extrajo siguiendo un protocolo convencional de fenol-cloroformo (Holzer y col. 2004). El ADN extraído se resuspendió en agua libre de ARN/ADNasa.

La PCR, o reacción en cadena de la polimerasa, se llevó a cabo en un termociclador con un volumen final de 30µl de 0,5 U de polimerasa Thermoprime Plus DNA, 10X tampón con 1,5 mM $MgCl_2$, 0,2 mM de cada nucleótido, 0,5 µM de cada cebador y aproximadamente 100 ng de ADN. Se amplificaron tres fragmentos del gen ribosomal: la secuencia parcial de SSU rDNA, la secuencia parcial de LSU rDNA y la secuencia completa de ITS2.

El protocolo de PCR consistió en una desnaturalización inicial a 95ºC (3-5 min), seguido de 35 a 40 ciclos de amplificación: desnaturalización a 95ºC (50s), la temperatura de específica para cada pareja de cebadores utilizados (30s-1min) y la extensión a 72ºC (1-2 min) y una extensión final a 72ºC (4-7 min). Cuando fue necesario, se llevaron a cabo PCR anidadas utilizando un microlitro de la primera PCR en la segunda ronda.

Se confirmó la presencia de fragmentos amplificados con un gel 1% agarosa en tampón sodio acetato. Los productos se purificaron con el kit "GFX PCR DNA and Gel Band Purification Kit". La secuenciación se llevó a cabo en un secuenciador de 48 capilares ABI 3730 utilizando el BIG Dye Terminator v 3.1 Ready Sequencing Kit según las instrucciones del fabricante. Todas las secuencias obtenidas se enviaron a "Basic Local Alignment Search Tool" (BLAST) en GenBank™ para confirmar su origen. Todas las secuencias nuevas se depositaron en GenBank™ (números de acceso en Apéndice 1). Las secuencias fueron ensambladas con el programa "BioEdit". Las secuencias más cercanas se obtuvieron de GenBank™ y se alinearon con el programa "Clustal X" (Thompson y col. 1997). Las regiones ambiguas del

alineamiento se identificaron con el programa "GBlocks 0.91b" (Castresana 2000) y se excluyeron de los análisis filogenéticos.

Análisis filogenético

La posición filogénetica de las secuencias se estimó con un método de inferencia bayesiano usando "MrBayes v3.1.2" (Ronquist y Huelsenbeck 2003) y un método de máxima parsimonia usando "PAUP* Version 4.0b10" (Swofford 2002). El modelo general reversible en el tiempo (GTR+I+Γ; Tamura y Nei 1993) se estimó como el mejor modelo para todos los datos usando el programa jModeltest version 0.1.1 (Posada 2008). El programa "FigTree v1.3.1" (Rambaut 2009) se utilizó para visualizar los árboles.

Diseño de cebadores específicos para ensayos de PCR

Basándose en las nuevas secuencias obtenidas y su alineamiento con las de especies cercanas, se diseñaron cebadores con el programa "Primo Pro 3.4" o con "Primer Express Software" (Applied Biosystems, Life Technologies Corporation, California, USA). Los cebadores específicos CDF y CDR fueron analizados para excluir uniones autocomplementarias, reacciones cruzadas mediante una búsqueda en el BLAST y seleccionada un temperatura específica para el cebador con un gradiente de PCR. Estos cebadores se aplicaron a un ensayo específico de PCR para detectar a *C. puntazzi* n. sp. en muestras de tejidos obtenidas después de exposiciones experimentales y naturales de peces al parásito (ver más abajo).

Transmisiones experimentales del mixozoo C. puntazzi *n. sp.*

La bilis con estados pre-esporogónicos y esporogónicos de *C. puntazzi* se obtuvo de *D. puntazzo* silvestres, con un prevalencia del 26.87%. 3µl de bilis se utilizó para cuantificar el número de parásitos con un hemocitómetro. Se centrifugó la bilis a 800 RCF, se descartó el sobrenadante y el pellet de estados de *C. puntazzi* se resuspendió en 0,1M tampón fosfato a una concentración de 212 estados por microlitro. Se comprobó la viabilidad de los estados con la tinción vital rojo neutro. La mezcla se homogenizó y se refrigeró hasta su uso en el plazo de una hora.

La sangre infectada con *C. puntazzi* se obtuvo también de sargos picudos silvestres. Los peces donantes presentaron una prevalencia microscópica del parásito en la bilis de un 87.5%. Tras su llegada al laboratorio, las muestras de sangre se tomaron de la

aleta caudal, usando una jeringa heparinizada con una aguja de 0,3 mm de diámetro. Se realizaron frotis de sangre y se tiñeron con "Diff Quick" ®. Se analizaron 4µl por análisis de PCR. Las muestras de sangre de todos los peces se mezclaron, se refrigeraron y se utilizaron para infectar en el plazo de una hora.

Diseño experimental y mantenimiento de los peces receptores

Se realizó una infección con estados pre-esporogónicos y esporogónicos de la bilis: *D. puntazzo* libres de infección se usaron como peces receptores. Las infecciones experimentales se llevaron a cabo por las siguientes vías: oral, intracelómica, cohabitación y baño. Transmisión oral, los peces se intubaron con 50µl de la mezcla (10.600 parásitos) con una micropipeta. Transmisión intracelómica, se inyectó a los peces con 50µl de la mezcla (10600 parásitos) por pez. Transmisión por baño, a los peces receptores se les expuso a 3,5 ml de la mezcla (742000 parásitos) en agua de mar durante 4 días. Transmisión por cohabitación, los peces receptores se mantuvieron en tanques con sargos picudos infectados por *C. puntazzi* n. sp.

La infección con estados de la sangre se realizó vía intracelómica. Cada pez recibió 0,2 ml de la sangre heparinizada, obtenida de peces infectados.

Para pruebas orales e intracelómicas los peces se sedaron con 60 ppm de 1:10 aceite de clavo:etanol. Todos los peces se mantuvieron a 18-20ºC. El grupo control no se expuso al parásito.

Estudio parasitológico de los peces infectados artificialmente

Se muestrearon sangre (4µl), bilis (20-30µl) e hígado (aproximadamente 2 m^3) para análisis molecular utilizando el ensayo especifico de PCR (ver más arriba). Los peces fueron muestreados los días 13, 21, 28, 35, 50, 64, 78, 92 y 113 después de la infección, excepto los peces de cohabitación que se muestrearon los días 27, 49, 77 y 102, y los peces de la prueba intracelómica de sangre que fueron muestreados a los días 60 y 75 después de la infección.

Transmisiones naturales a un medio enzoótico de C. puntazzi

Exposición

Entre diciembre 2008 y noviembre 2009, se mantuvieron en el mar sargos picudos libres de infección cerca del Cabo de San Antonio, Jávea, Alicante (38º 47' 56.0'' N; 0º 11' 32.9'' E). Entre 14 y 20 peces se expusieron cada mes durante 7 días, durante

todo un año. Los parámetros del mar, la temperatura, visibilidad y condiciones del mar se anotaron. Los peces se colocaron en una jaula hecha a mano (73 x 28 x 29 cm) con una apertura de malla de 2 cm, y un soporte de plexiglass con nuversosos agujeros de 7 mm distribuidos por todos la superficie. La jaula se ató con cadenas a un lastre a 9,2 m de profundidad. Después de 7 días, se recogieron los peces; se trasladaron a las instalaciones de la Universidad de Valencia donde se mantuvieron en tanques de 80-120L a 20-23ºC. Una parte de los peces se muestrearon al día 1 tras la exposición y el resto a día 60 tras exposición. Los peces control no se expusieron y se mantuvieron en tanques de 20L en instalaciones de la Universidad de Valencia.

Estudio parasitológico de los peces infectados de forma natural

Los peces analizados 1 día después de la exposición se examinaron macroscópicamente para detectar ectopárasitos. De todos los peces se muestreó sangre (4µl), hígado (aprox. 2 m^3) y vesicular biliar que se preservaron en nitrógeno líquido y se guardaron a -20ºC para su posterior análisis molecular. Los peces muestreados el día 60 después de la infección se analizaron, como se ha detallado anteriormente y además se observaron preparaciones frescas a una magnificación de 400x de vesícula biliar, riñón e intestino, y el cerebro, ojos, branquias, corazón, bazo, digestivo y músculo se analizaron para la búsqueda de parásitos a 80x. Los frotis de sangre se tiñeron con Diff Quick®.

4.-Resultados

4.1. El helminto sanguíneo *Skoulekia meningialis* n. gen., n. sp. en *Diplodus vulgaris*

Un género y especie nuevas de helminto sanguíneo *Skoulekia meningialis* n. gen., n. sp. se halló y se describió en la mojarra o *D. vulgaris*. La comparación morfológica, los datos moleculares (SSU, ITS2 y LSU rDNA) así como los análisis filogenéticos, apoyaron firmemente la erección de un nuevo género. *Skoulekia* se caracteriza por una combinación única de caracteres morfológicos: un abultamiento a nivel dorsal del saco del cirro, presencia de una ventosa oral, un único testículo localizado sobretodo entre los ciegos, un poro genital masculino dorso-marginal, ausencia de una vesícula auxiliar seminal externa, ovario y útero laterales y un receptáculo seminal lateral en el oviducto. Tanto los datos morfológicos como moleculares

demostraron una estrecha relación de este nuevo género con los géneros *Pearsonellum* Overstreet y Køie 1989 y *Psettarium* Goto y Ozaki 1930.

S. meningialis se detectó *in situ* en fresco y mediante cortes histológicos en una localización especial: las venas ectomeningiales que están alrededor de los lóbulos ópticos del cerebro de *D. vulgaris*. Este hábitat difiere del resto de los aporocotílidos, ya que normalmente se encuentran en el corazón o en vasos sanguíneos de las branquias. Habitualmente la patología asociada a helmintos sanguíneos se da por la presencia de los huevos en los vasos de las branquias. Aunque se encontraron huevos de *S. meningialis* en cortes histológicos de branquias, no se observó ninguna patología asociada. En cambio la presencia de los adultos de *S. meningialis* en las venas de las meninges provoca una moderada y localizada meningitis crónica. Esta meningitis se caracterizó por una respuesta inflamatoria con infiltración de células mononucleares y granulocitos eosinofílicos.

A efectos prácticos, el mejor método de diagnosis para *S. meningialis* en la mojarra fue la detección de huevos en branquias por cortes histológicos (prevalencia 45%) seguido de la detección de adultos en material fresco (20%) y por último la detección de adultos en cortes histológicos de cerebro (4%). *S. meningialis* no parece provocarle un daño importante a *D. vulgaris* silvestres, a pesar de la alta incidencia (111 helmintos/215 peces) e intensidad (2,6 parásitos/pez) observadas. Sin embargo, la localización especial, próxima al cerebro, un órgano vital, debe de tenerse en cuenta si se instalan sistemas de cultivo de la mojarra.

4.2. Plasmodios macroscópicos del mixozoo *Unicapsula pflugfelderi* en la musculatura de *Lithognathus mormyrus*

Entre los mixozoos marinos histozoicos, dos géneros, *Kudoa* y *Unicapsula*, pueden provocar lesiones musculares importantes y pérdidas económicas en peces vivos y procesados. Los daños principales son producidos por la presencia de plasmodios macroscópicos de mixosporas entre la musculatura, lo que afecta al aspecto del pescado. También tras la muerte del pez o a la muerte del pez, las enzimas proteolíticas se liberan de los plasmodios y causan un proceso de degradación enzimática post-mortem de los filetes de pescado (Moran y col. 1999). Dos especies de *Unicapsula* producen este fenómeno: *Unicapsula muscularis* Davis 1924 en el fletán del Pacífico *Hippoglossus stenolepis* Schmidt 1904 y *Unicapsula seriolae* Lester 1982 en el músculo del medregal rabo amarillo *Seriola lalandi* Valenciennes

1833. Existen otras seis especies descritas en este género, todas en teleósteos de diferentes familias y con una amplia distribución. Hasta la fecha, las especies de *Unicapsula* han sido descritas en un sólo hospedador.

Se encontraron plasmodios macroscópicos y alargados con mixosporas típicas del género *Unicapsula* en el músculo esquelético de la herrera o *L. mormyrus*. La única especie de *Unicapsula* descrita en el Mediterráneo es *Unicapsula pflugfelderi* Schubert, Sprague y Reinboth 1975 en el caramel *S. smaris*. Se llevó a cabo una comparación morfológica y molecular (SSU rDNA) entre *U. pflugfelderi* de *S. smaris* y *Unicapsula* sp. de *L. mormyrus*. Los plasmodios de *S. smaris* eran 2-3 veces más grandes que los encontrados en *L. mormyrus.* Se observaron también diferencias significativas en las esporas tanto en su longitud como en la anchura de las cápsulas polares. Pero, a pesar de estas diferencias, las secuencias moleculares que se obtuvieron resultaron 100% idénticas, lo que indica que estos mixozoos de diferentes hospedadores son coespecíficos. La construcción del árbol filogenético indicó que las especies de *Unicapsula* forma un clado monofilético basal al clado que contiene a las especies de *Kudoa* y que ambos clados se agrupan en el clado general de mixozoos marinos descrito por Fiala (2006).

A nivel ultraestructural, se encontraron dos estructuras no descritas previamente: una estructura cristalina, posiblemente relacionada con cambios osmóticos cuando el esporoplasma es liberado de las valvas, y un cuerpo vesicular que puede estar relacionado con la producción de materiales necesarios para la construcción de las cápsulas polares.

La revisión del género *Unicapsula* llevada a cabo durante este estudio indica que según la distribución de las valvas de las esporas se puede dividir el género *Unicapsula* en dos grupos de especies. Unas especies presentan esporas en las que la valva impar, que cubre a la única capsula polar desarrollada, es más grande que las otras dos valvas. Otras especies presentan la valva impar más pequeña que las otras dos valvas. Hasta que no se obtengan más datos moleculares sobre especies de este género, no se podrá determinar si esta separación es artificial o si puede estar reflejando una agrupación filogenética.

No se observaron cambios histopatológicos en los filetes de *L. mormyrus* infectados con *U. pflugfelderi*, ni se observó el fenómeno de mioliquefacción, sin embargo, la presencia masiva de plasmodios macroscópicos en los filetes puede producir

problemas de comercialización ya que puede causar rechazo por parte del consumidor.

4.3. El mixozoo biliar *Ceratomyxa puntazzi* n. sp. en *Diplodus puntazzo*

Ceratomyxa es un género de mixozoos celozoicos. En general, las especies de este género no suele producir daños o problemas a sus hospedadores, aunque existen algunos casos en que se dan importantes cambios histopatológicos (Bartholomew y col. 1989a; Palenzuela y col. 1997) o que se han descrito como patógenos oportunistas en hospedadores inmunodeprimidos (Katharios y col. 2007). Durante el estudio parasitológico del sargo picudo, se hallaron esporas del género *Ceratomyxa* en la bilis. El estudio morfológico y molecular (SSU rDNA) detallado de estas esporas y su comparación con descripciones previas derivó en la descripción de una nueva especie *Ceratomyxa puntazzi* n. sp. *C. puntazzi* provoca necrosis y pérdida de las células epiteliales de la vesicular biliar, y pericolangitis en el tejido hepático cercano a los conductos biliares de *D. puntazzo*. Aunque no se observaron mortalidades, *C. puntazzi* podría ser un patógeno oportunista en hospedadores inmunodeprimidos. Especialmente considerando que el sargo picudo parece ser menos inmunoresistente que la dorada (Muñoz y col. 2007). Factores como la temperatura o la calidad del agua, deben de tenerse en cuenta en los cultivos de *D. puntazzo* ya que pueden afectar negativamente en caso de infección por *C. puntazzi*.

Durante este estudio, se consiguieron esporas de vesículas biliares de otros dos espáridos: el raspallón *D. annularis* y la dorada *S. aurata*. Se encontró un morfotipo en *D. annularis* y dos morfotipos en *S. aurata*. El morfotipo encontrado en *D. annularis* resultó ser muy similar morfológicamente a *C. puntazzi* pero molecularmente divergente, con 1,7% de diferencias en la secuencia. Esto contrasta con los datos obtenidos al comparar *C. puntazzi* y *Ceratomyxa* sp. de *D. annularis* con los morfotipos de la dorada, ya que aunque morfológicamente son muy diferentes, molecularmente presentaron valores similares o más bajos de divergencia en la secuencia (1,4-1,6%). Este hecho resalta la importancia de combinar datos morfológicos y moleculares para la correcta identificación y discriminación de especies de *Ceratomyxa*.

El análisis filogenético realizado situó a las cuatro nuevas secuencias de este estudio en un mismo clado junto con *Ceratomyxa sparusaurati* Sitjà-Bobadilla, Palenzuela y Alvarez-Pellitero 1995, la única secuencia de *Ceratomyxa* spp. previamente

publicada de un espárido. Esta agrupación sugiere que todas las especies de *Ceratomyxa* de espáridos del Mediterráneo provienen de un antecesor común. Estudios previos sugieren que la radiación en *Ceratomyxa* podría haber ocurrido entre familias de hospedadores e incluso entre géneros y especies (Gunter y col. 2009). El presente estudio parece indicar que también la localización geográfica puede afectar a la agrupación de especies pero se necesita más secuencias de ADN de *Ceratomyxa* spp. de espáridos de otras regiones del mundo para confirmar esta hipótesis.

Los nuevos datos obtenidos de cuatro especies de espáridos más las descripciones previas de especies en espáridos parecen indicar que entre los espáridos mediterráneos existe una alta riqueza de especies de *Ceratomyxa*, lo cual coincide con datos de otras familias de peces (Gunter y Adlard 2008; 2009; Heiniger y col. 2008). Es probable que cada especie de espárido presente por lo menos una especie de *Ceratomyxa*.

4.4. Morfología tridimensional, ultraestructura y composición de estados proliferativos y esporogónicos de *Ceratomyxa puntazzi*. Primera observación de las estructuras y mecanismos que subyacen a la motilidad y gemación.

La patología que producen los mixozoos suele estar relacionada con la presencia de un gran número de parásitos, producidos por la rápida proliferación de los estados vegetativos (Canning y col. 1999; Redondo y col. 2003). Sin embargo, se sabe muy poco sobre las secuencias del desarrollo que llevan a la multiplicación de los estados parásitos mixozoos. La gemación endógena o la formación de células dentro de otras células ha sido el proceso básico de proliferación aceptada para mixozoos (Lom y Dyková 2006). Pero este proceso fue rechazado por Morris (2010), que observó que las células interiorizan otras células produciendo así células secundarias y terciarias en una célula primaria. Asimismo, se ha sugerido que la formación de las células terciarias sólo ocurre al iniciarse la esporogénesis (Morris y Adams 2008). Según esta hipótesis, se podría definir una secuencia del desarrollo para los mixozoos de un mismo clado filogenético. Poco se sabe del desarrollo pre-esporogónico del género *Ceratomyxa*. La información sobre el desarrollo de las esporas de *Ceratomyxa* en la bilis es fragmentario, sin embargo Noble (1941) describió que tanto proliferación como formación de esporas tenían lugar en la bilis.

Algunos autores observaron que los estados de *Ceratomyxa* en la bilis presentaban motilidad y movimientos ameboides (Noble 1941; Meglitsch 1960; Sitjà-Bobadilla y col. 1995; Cho y col. 2004). También este movimiento ha sido descrito para los esporoplasmas cuando son liberados de las valvas de las esporas (Eszterbauer y col. 2009; Kallert y col. 2009; Grabner y El-Matbouli 2010). La especial localización de los estados que habitan la bilis, facilita el estudio de la motilidad de los estados y los mecanismos que subyacen, de lo que apenas se sabe algo hasta la fecha.

El estudio de los mixozoos se ve muy limitado debido a su pequeño tamaño. Tradicionalmente se utiliza microscopía óptica y electrónica para describirlos morfológicamente. En 2005, McGurk y col. publicaron el primer estudio tridimensional de un mixozoo. Esta técnica permite, con un procesado mínimo del material, el uso de una gran variedad de tinciones fluorescentes para la visualización de diferentes características morfológicas (McGurk y col. 2005).

En este capítulo, el uso combinado de diferentes técnicas microscópicas (microscopía óptica, microscopía láser confocal de barrido con tinciones específicas y microscopía electrónica), supuso una mejora considerable de la caracterización de un mixozoo y permitió obtener una visión única de la morfología tridimensional, de la ultraestructura y de la organización de los componentes celulares relacionados con el desarrollo y la motilidad de los estados de *C. puntazzi*.

C. puntazzi presentó dos vías de desarrollo en la bilis de *D. puntazzo*: pre-esporogénesis proliferativa y esporogénesis. Esto permite al parásito multiplicarse antes de iniciar la formación de esporas e incrementa considerablemente las oportunidades del parásito de infectar al hospedador invertebrado.

El desarrollo proliferativo pre-esporogónico se observó que ocurre mediante plasmotomia, con frecuente gemación. Los estados proliferativos presentaron una gran plasticidad morfológica, desde redondeados y elipsoides, los estados más juveniles, a estados piriformes, cuando el desarrollo avanzaba. Los estados iniciales esféricos estaban formados por una célula primaria con 1-2 núcleos. Los estados más grandes y piriformes, contenían 1-2 núcleos de la célula primaria con hasta 6 células secundarias y, más tarde, las células secundarias presentaban 1-2 células terciarias. Los estados proliferativos más grandes presentaban 12 núcleos. Los grupos de 1-3 células secundarias presentaban de 0-2 células terciarias, que se separaban de los estados más grandes por gemación.

Los estados proliferativos presentaban gran actividad locomotora, con movimientos ameboides. Los elementos citoesqueléticos ricos en actina filamentosa (actina-F) fueron relacionados con la motilidad. Se observó que la actina-F se concentró en un lado de los parásitos, formando una zona hialina definida como lamellipodium, y también en los abundantes filopodios. La zona hialina presentaba un movimiento ondulante producido por la proyección hacia adelante de los filopodios, los cuales se forman en la parte más anterior del parásito y se fusionan continuamente a la superficie celular en la parte lateral y posterior. Los filopodios se proyectan hacia la dirección del movimiento del parásito y, luego, lateralmente, desde la parte media anterior, dónde se encuentran los filopodios más largos, a las partes laterales y posterior del parásito. En la parte posterior del parásito, se encontró un larga y rígida extensión citoplasmática que puede estar favoreciendo la hidrostasis. De este modo, los parásitos se empujan a sí mismos en el medio. Estos elementos permiten la motilidad del parásito pero también explican el mecanismo de gemación como un proceso activo de separación; Los estados emergen activamente del parásito "madre" original, gracias a que el polo, rico en actina filamentosa, se encuentra orientado en otra dirección que la del parásito "madre", permitiendo así la separación de los nuevos estados, y no por un anillo contráctil de actina como el descrito en la citocinesis general (Pelham y Chang 2002). Sin embargo, no se pudo determinar con fiabilidad la composición celular de los parásitos "hijos" resultado de la proliferación, ni si los núcleos de las células primarias están incluidas en los nuevos estados junto con células secundarias o si están formados por células secundarias y terciarias, las cuales se liberarían del parásito "madre" por ruptura de su membrana celular, como el presente estudio sugiere. A pesar de la gran cantidad de material analizado, el mecanismo que produce células secundarias y terciarias en *C. puntazzi* no se pudo determinar, sin embargo, si se pudo observar células secundarias envolviendo a otras células secundarias. Esto apoya la idea de que la formación de las células terciarias se produce por que una célula envuelve a otra (Sitjà-Bobadilla y col. 1995; Morris 2010). Sin embargo, este proceso no se ha observado en las células primarias y se necesitan más estudios para determinar si un sólo mecanismo explica el proceso de formación de células endógenas a la proliferación rápida de los parásitos mixozoos.

Se observaron abundantes gotas lipídicas en los estados de *C. puntazzi* probablemente asociadas a reservas de energía para la proliferación y esporogénesis.

También se hallaron vesículas externas, que junto con los lípidos, pueden estar facilitando la flotabilidad de los parásitos en el medio.

La esporogénesis se iniciaba cuando células primarias piriformes o pseudoplasmodios contenían 4 células secundarias. Las divisiones celulares llevaban a la formación de 8 células secundarias y 4 células terciarias. Estas células se separan en dos pares de 4 células secundarias y 2 terciarias, cada par formando una espora con forma de media luna. Las células de las valvas se forman de las células secundarias y las capsulogénicas de las terciarias, cuyas células secundarias que las envuelven formaron el esporoplasma. Los estados iniciales de esporogonia eran estados piriformes muy activos, con movimiento ameboide y con un borde rico en actina filamentosa, como en los estados proliferativos. Al avanzar el desarrollo, los parásitos presentaron menos actividad locomotora y perdieron flexibilidad, ya que presentaban actina filamentosa más dispersa y por el efecto mecánico de la presencia de esporas casi maduras. Esto coincide con el fin del período activo y con la liberación de esporas maduras.

Por primera vez en los mixozoos se ha analizado el comportamiento locomotor, la distribución y la acción potencial de efectores de la motilidad y se aporta información única de los procesos de la locomoción direccional y la gemación.

4.5. Estacionalidad y rutas en el hospedador de *Ceratomyxa puntazzi*: transmisiones naturales y experimentales

La información sobre la transmisión y los ciclos de vida de mixozoos marinos es escasa ya que encontrar al hospedador invertebrado específico es extremadamente difícil debido a la gran diversidad y riqueza de invertebrados en el medio natural (Køie y col. 2004). A pesar de estos obstáculos se han descrito dos ciclos de especies del género *Ceratomyxa* incluyendo a un hospedador alternante poliqueto (Bartholomew y col. 1997; Køie y col. 2008). El hospedador alternante de *C. puntazzi* se desconoce.

Debido al pequeño tamaño de las actinosporas (<10μm), su eliminación de las fuentes de agua de los sistemas de cultivo en el caso de instalaciones en el mar es muy complicada o imposible. Sin embargo, el conocimiento de la estacionalidad y transmisión de los mixozoos puede ayudar a diseñar estrategias de manejo dirigidas a reducir la exposición a los estados infectivos.

En este capítulo, con la exposición de peces libres de infección a un medio enzoótico de *C. puntazzi* se ha buscado investigar la estacionalidad para sugerir estrategias para los cultivos de *D. puntazzo* en el Mediterráneo. Además, la exposición de peces durante un tiempo conocido puede permitir la reconstrucción de la ruta de infección y vía que sigue el parásito en el hospedador.

En muchos parásitos, el orden de desarrollo de los diferentes estados está genéticamente determinado y no puede ser alterado, por lo que no todos los estados del ciclo de vida pueden desarrollarse cuando son transferidos a otros tejidos u hospedadores. Ya se observó que el uso de mixosporas en transmisiones experimentales para intentar infectar peces receptores libres de infección fue infructuoso (McGeorge y col. 1996; Moran y col. 1999). Sin embargo, se ha observado que algunos estados pre-esporogónicos sí mantienen capacidad infectiva (Grossheider y Körting 1993; Hedrick y col. 1993; Diamant 1997; Moran y col. 1999; Redondo y col. 2002; Diamant y col. 2006), como es el caso de especies del género *Enteromyxum,* donde la transmisión pez a pez se da por estados pre-esporogónicos dentro de las células epiteliales del intestino que se desprenden y liberan al agua y son incorporados por otros peces libres de infección (Diamant 1997; Redondo y col. 2002). Asimismo, en este capítulo se determinó si estados del ciclo de *C. puntazzi* en el pez (estados en la sangre, estados proliferativos y esporogónicos) son capaces de causar infección artificial por via oral, intracelómica, baño y cohabitación. El presente capítulo busca investigar en detalle las rutas y el desarrollo de *C. puntazzi* en el sargo picudo y la estacionalidad de la infección en el Mediterráneo.

Las exposiciones mensuales de sargos picudos a actinosporas infectivas de *C. puntazzi* durante un año completo son el primer intento de un estudio de infección estacional de un mixozoo marino. Las exposiciones naturales de peces en una jaula especialmente diseñada para este estudio y el mantenimiento de estos peces en el laboratorio durante 2 meses a una temperatura de entre 20-23ºC permitió la obtención de una infección de *C. puntazzi* en los peces receptores.

C. puntazzi presentó una estacionalidad con una marcada dependencia de la temperatura, donde la detección microscópica de los estados proliferativos y esporas sólo fue posible desde abril hasta noviembre. Dos picos de prevalencia de infección se registraron: uno tuvo lugar en abril-mayo (80%), coincidiendo con una subida de 4ºC de la temperatura hasta alcanzar los 16ºC, y otro ocurrió en octubre (86%).

Contrariamente, se observaron valores más bajos de prevalencia entre junio y septiembre (46-64%). Estos dos picos de prevalencia de infección alta podrian estar relacionados con la producción de actinosporas y con su viabilidad en altas temperaturas. No obstante, la detección por PCR en la bilis fue posible durante todo el año, lo cual indica que el parásito puede infectar y estar en el pez en bajo niveles durante los meses de invierno. Los estados de la sangre fueron detectados mediante PCR en los peces receptores y presentaban una prevalencia muy alta (85.7-100%) tanto después de la exposición, como durante todo el año. Sin embargo, la infección tiende a perderse o disminuir, ya que no todos los peces inicialmente infectados, presentaron infección en la bilis. Esta situación puede ser dependiente de la dosis infectiva del parásito o de las condiciones inmunológicas del hospedador durante el invierno.

La combinación de resultados de PCR de sangre, vesícula biliar e hígado, sugiere la siguiente ruta de infección: El parásito entraría al sistema sanguíneo a través del epitelio branquial, como ya ha sido descrito para otros mixozoos (Bjork y Bartholomew 2010), saldría al tejido hepático, entrando en los conductos biliares, a través de los cuales el parásito alcanzaría la vesícula biliar, el órgano diana donde iniciaría la proliferación pre-esporogónica y la esporogénesis con la consecuente liberación de esporas con la bilis vía intestino al medio.

La transmisión artificial de los diferentes estados de desarrollo (estados sanguíneos, estados proliferativos pre-esporogónicos y estados esporogónicos) de *C. puntazzi* fueron infructuosos tanto por via oral, intracelómica, baño o cohabitación. Esto revela que la transmisión “pez a pez” de *C. puntazzi* en el cultivo de *D. puntazzo* es improbable que ocurra.

El estudio de exposición natural recomienda que la exposición inicial de los peces o el traslado de granjas de cría en tierra a jaulas marinas para el engorde se haga al final de otoño o al principio del invierno. En este período, el parásito sobrevive con una menor cantidad de estados infectivos y, potencialmente, causa inmunidad durante la reinfección en el siguiente verano, período con mayores cantidades de estados infectivos. Esto se ha demostrado en otros mixozoos y posee importantes implicaciones para las medidas de control sanitario de *D. puntazzo*.

5.- Conclusiones

Esta tesis investiga parásitos aporocotílidos y mixozoos en especies nuevas y candidatas para la acuicultura de la familia de los espáridos en el Mediterráneo. En esta sección indicamos cuales son las conclusiones más relevantes para la ciencia en general, y de un modo aplicado, para la acuicultura:

1) Se aporta una descripción detallada de un nuevo taxón de helminto sanguíneo, *Skoulekia meningialis* n. gen., n. sp. de la mojarra o *D. vulgaris*. Su erección se ha basado en datos morfológicos y filogenia molecular, demostrando una relación estrecha con dos géneros de aporocotílidos: *Psettarium* y *Pearsonellum*. La caracterización molecular de aporocotílidos debería realizarse con marcadores moleculares con diferentes tasa de evolución (en este estudio SSU, ITS2 y LSU rDNA), ya que marcadores habitualmente utilizados, como el ITS2 rDNA, no están suficientemente conservados como para permitir relacionar taxones más alejados filogenéticamente. Esto explica porque todavía no hay una hipótesis filogenética para esta familia.

2) La mayoría de los aporocotílidos habitan el corazón o los vasos de las branquias. *S. meningialis* se halló en un hábitat especial: las venas ectomeningiales que se encuentran alrededor de los lóbulos ópticos del cerebro de la mojarra. Normalmente, la patología de los helmintos sanguíneos la producen los huevos en los vasos de las branquias pero, en el caso de *S. meningialis*, los adultos producen una meningitis localizada, moderada y crónica. *S. meningialis* no parece provocar un efecto patológico importante en *D. vulgaris* silvestres. Sin embargo, se debería prestar especial atención cuando se establezcan cultivos de mojarra, debido a su peculiar localización cercana al cerebro un órgano vital.

3) Los plasmodios macroscópicos y alargados, con esporas de mixozoos del género *Unicapsula*, encontraremos en la musculatura de la herrera o *L. mormyrus*, fueron coespecificos con *Unicapsula pflugfelderi*, descrita en el caramel o *Spicara smaris*. La comparación de la morfología de las esporas de los dos hospedadores sólo reveló diferencias menores y las secuencias (SSU rDNA) eran idénticas, siendo el primer caso de poca especificidad en el género *Unicapsula*, al encontrarse la misma especie en dos hospedadores diferentes. La mioliquefacción o degradación

enzimática de los tejidos musculares es típica de especies de los géneros *Unicapsula* y *Kudoa*, convirtiendo los filetes de pescado afectados en no comercializables. No se observó degradación enzimática o mioliquefacción para *U. pflugfelderi*, sin embargo, la presencia de los plasmodios en los filetes de la herrera puede producir problemas de comercialización por rechazo del consumidor. Este hecho tiene que tenerse en cuenta ya que la herrera se considera un candidato para la acuicultura.

4) Una nueva especie del género *Ceratomyxa*, *Ceratomyxa puntazzi* n. sp., se describió de la vesícula biliar del sargo picudo, *D. puntazzo*, gracias al estudio morfológico y molecular (SSU rDNA) así como por su comparación con descripciones previas. El análisis de otras especies de este género en espáridos, que comparten el hábitat con *D. puntazzo*, mostró que la especie de *Ceratomyxa* presente en *D. annularis* era morfológicamente indistinguible de *C. puntazzi*, pero presentaba un divergencia en la region SSU rDNA de 27 bases (1,7%). Esto indica, tanto para este caso como en el caso de *U. pflugfelderi*, que sólo la combinación de datos morfológicos y moleculares permiten una clasificación taxonómica correcta que permite la erección de nuevas especies o la identificación de especies coespecíficas en los mixozoos. Esto es de especial importancia en este grupo, ya que la morfología a menudo contradice a la agrupación filogenética en este grupo de parásitos.

5) *C. puntazzi* causa necrosis y pérdida de las células epiteliales de la vesícula biliar así como una inflamación en el tejido hepático o pericolangitis alrededor de los conductos biliares de *D. puntazzo.* No se observó mortalidad relacionada con *C. puntazzi*, sin embargo, este parásito debería ser considerado como un patógeno oportunista en sargos picudos inmunodeprimidos como se demostró para *C. diplodae* en *D. puntazzo* en un estudio previo.

6) Los datos preliminares de especies de *Ceratomyxa* de espáridos que comparten el hábitat con *D. puntazzo* indican que este género es muy específico y que se esperaría una gran diversidad de especies en espáridos del Mediterráneo. Los resultados filogenéticos sugieren que todas las especies de *Ceratomyxa* de espáridos del Mediterráneo provienen de un antecesor común. Para determinar si esta agrupación se basa en características geográficas o del hospedador, se debería

realizar más análisis de secuencias de SSU rDNA de otras especies de *Ceratomyxa* de espáridos de otras regiones.

7) La combinación de diferentes técnicas microscópicas, microscopia óptica, electrónica y microscopia láser confocal de barrido con parásitos vivos y tinciones específicas fluorescentes, es una técnica novedosa en la investigación de mixozoos. Esta combinación permitió visualizaciones únicas del desarrollo y la organización celular del mixozoo *C. puntazzi*. La microscopia láser confocal de barrido no se había aplicado previamente a estados de desarrollo de mixozoos y se recomienda firmemente su uso combinado con diferentes tinciones. El éxito de este estudio pone de manifiesto la necesidad de aplicar nuevas técnicas en la investigación de los mixozoos ya que pueden ayudar a dilucidar importantes lagunas en nuestro conocimiento de este filo.

8) El estudio combinado de microscopías de los estados biliares de *C. puntazzi* reveló dos vías de desarrollo: proliferación pre-esporogénica y esporogénesis. Los estados pre-esporogénicos presentan un alto grado de motilidad, de divisiones celulares y de gemación por plasmotomia, mientras que los estados esporogónicos se caracterizaron por la formación y maduración de las esporas.

9) El comportamiento locomotor y la distribución de efectores de la motilidad fueron analizados por primera vez en los mixozoos. En este estudio se aporta información única de los procesos implicados en la locomoción direccional y la gemación en *C. puntazzi*. Los elementos citoesqueléticos ricos en actina filamentosa se encontraron concentrados a un lado del parásito, el cual produce filopodios localizados, permitiendo la motilidad del parásito. Además, el mecanismo de gemación se identificó, por primera vez, como un proceso dependiente de la actina filamentosa con actina localizada en polos opuestos de los parásitos que se están separando, causando su separación activa. El estudio del comportamiento respuesta a estímulos externos e internos así como la determinación de otros componentes celulares incluidos en la motilidad, son líneas de investigación que se han iniciado de este trabajo.

10) Los estudios ultraestructurales son de especial relevancia en el estudio de microparásitos como los mixozoos. En *C. puntazzi*, las gotas lipídicas y las vesículas externas encontradas pueden facilitar la flotación de los parásitos. Además, se describió por primera vez, un cuerpo vesicular intracelular en *C. puntazzi* y *U. pflugfelderi*, el cual por su localización y posición en los estados esporogónicos puede estar relacionada con la producción de material para la capsulogénesis.

11) Las exposiciones naturales de sargo picudo a un medio enzoótico de *C. puntazzi* durante un año es el primer caso de estudio de la estacionalidad de un mixozoo marino. El parásito presenta una marcada estacionalidad dependiente de la temperatura. Los parásitos se detectaron microscópicamente desde abril a noviembre. Sin embargo, gracias al ensayo de PCR específico para *C. puntazzi*, se detectó una infección encubierta en la bilis durante los meses de invierno. Los estados en la sangre se detectaron mediante PCR durante todo el año y con una prevalencia muy alta. Esto indica que las actinosporas están presentes en el mar y que los parásitos invaden la sangre de los peces durante todo el año. Sin embargo, la infección en sangre puede perderse o reducirse, probablemente en los casos de bajas cargas parasitarias y/o por la respuesta inmunológica del hospedador. La infección encubierta durante los meses de invierno, la invasión contínua de la sangre y la presencia de infecciones de larga duración recalca la importancia de la infecciones de mixozoos con técnicas moleculares. El análisis de muestras de agua de mar a diferentes profundidades durante un año es un trabajo en curso, que permitirá reflejar la dinámica del parásito en el pez y determinar los patrones de producción de actinosporas por el hospedador poliqueto alternante. El estudio de las exposiciones naturales implica que la exposición o traslado inicial de peces, desde criaderos a jaulas marinas, sería más adecuado al final del otoño/ principio del invierno, con lo que el parásito estaría en cargas bajas y el pez podría producir algún tipo de inmunización. Esto daría lugar a una resistencia mayor a la reinfección con una carga más alta de parásitos en el verano siguiente. Esto se ha demostrado para otros mixozoos y tiene implicaciones importantes para las medidas sanitarias para *D. puntazzo*.

12) Las combinaciones de PCR de los diferentes órganos de los peces expuestos a *C. puntazzi* permitieron sugerir una posible ruta de infección de *C.*

puntazzi en su hospedador: el punto de entrada son las branquias, desde donde el parásito invade el sistema sanguíneo, sale al tejido hepático y entra en los conductos biliares, desde donde el parásito alcanza la vesícula biliar, donde inicia su proliferación y esporogénesis, con la consecuente liberación de esporas con la bilis por el intestino al medio.

13) La transmisión artificial de estados de la sangre y pre-esporogónicos y esporogónicos de la bilis de *C. puntazzi* no fue posible por ninguna de las cuatro vías: oral, intracelómica, baño.y cohabitación con peces infectados. La transmisión "pez a pez" de *C. puntazzi* en sargo picudo en cultivo es improbable que ocurra y es necesario un hospedador alternante, al contrario que con *Enteromyxum* spp.

6. Reflexión

La diversificación de la acuicultura Mediterránea es una importante estrategia para combatir la saturación del mercado y la bajada de los precios. Así, la continuidad del sector depende de la investigación básica de nuevas especies de peces y sus patógenos, y de la innovación en el área de la intervención profiláctica. La investigación de los parásitos de especies nuevas y candidatas para el cultivo debería priorizarse, ya que todavía quedan por descubrir nuevas especies y su patología asociada. Con respecto a la investigación relacionada con la intervención práctica en enfermedades, en la acuicultura de nuevas especies, las tendencias futuras de investigación deberían centrarse en completar ciclos de vida de los parásitos para conocer si es el hospedador alternante se encuentra en el biofouling de las jaulas. Es más, la especificidad del parásito debe ser determinada para obtener datos sobre la posibilidad de infecciones cruzadas entre cultivos existentes y nuevos cultivos. Las infecciones parásitas mixtas y sus dinámicas deberían ser estudiadas ya que pueden ocurrir con bastante probabilidad y tienen mucho más impacto que las infecciones simples. En general, es de gran importancia que se combine investigación experimental y básica, así como técnicas tradicionales y nuevas, cuyo uso está restringido, actualmente, a parásitos humanos o de importancia veterinaria, donde la investigación está más avanzada. Estas técnicas pueden aportar visiones únicas en áreas inexploradas de la investigación de parásitos de peces. El desarrollo de nuevos enfoques es de considerable importancia en un mundo que depende cada vez más del pescado como una fuente valiosa de proteína para consumo humano.

CHAPTER 1. Introduction

1.1. Mediterranean aquaculture

"Aquaculture is the farming of aquatic organisms in inland and coastal areas, involving intervention in the rearing process to enhance production and the individual or corporate ownership of the stock being cultivated." (FAO, Glossary of Aquaculture, 2008, http://www.fao.org/fi/glossary/aquaculture/pdf/glossary.pdf). Mediterranean aquaculture has a long history with evidence of fish and shellfish culture as old as 2500 BC. However, the beginning of the modern marine Mediterranean aquaculture started about 25 years ago, when aquaculture developed thanks to significant research in the fields of reproduction, larval culture, feed manufacturing and engineering technology.

Nowadays, aquaculture is the fastest growing livestock agricultural production sector, representing more than one third of global seafood production. Aquaculture already produces 45.7 % of seafood for human consumption and the FAO (State of World Fisheries and Aquaculture 2010, http://www.fao.org/docrep/013/i1820e/i1820e.pdf) estimates that by 2030 an additional 37 million tonnes of seafood will need to be produced to keep up with the demand. The aquaculture industry is considered of strategic importance as an inexpensive source of protein.

In the Mediterranean, finfish farming has been dominated by the culture of sea bass (*Dicentrarchus labrax* (L.), Moronidae) and gilthead sea bream (*Sparus aurata* L., Sparidae) (Figure 1.1). However, market saturation and excess of production resulting in high competition and reduced profits have provoked the need of species diversification (Rigos & Katharios 2010). The future of the aquaculture market depends heavily on research and development of new species for culture towards a wider range of products to the customer through new species whose growth rates and costs of production allow efficient processing and new product presentation (Barazi-Yeroulanos 2010). Thereby, species of the family Sparidae are firm candidates for new species in the Mediterranean aquaculture.

1.2. The Sparidae "fishes with golden heads"

The Sparidae (Teleostei: Perciformes) are a family of marine fishes with 35 genera and 130 species of sea breams or porgies. Etymologically, "sparoides" refers to a "fish with golden head" (Greek). Sea breams have a wide distribution, being present in tropical and temperate littoral or inshore waters, sometimes also brackish waters.

In general, sea breams are carnivores and bottom dwelling; most of the species possess molar-like teeth, however there are many omnivorous species such as the sharpsnout seabream *Diplodus puntazzo* (Walbaum 1792) and herviborous species as the salema *Sarpa salpa* (L.). Hermaphoditism is widespread in the family, and either protandry or protogyny occur (Whitehead et al. 1986). Recently, fishes of the genus *Spicara*, traditionally belonging to the family Centracanthidae, have been also ascribed to the family Sparidae (Orrell et al. 2002).

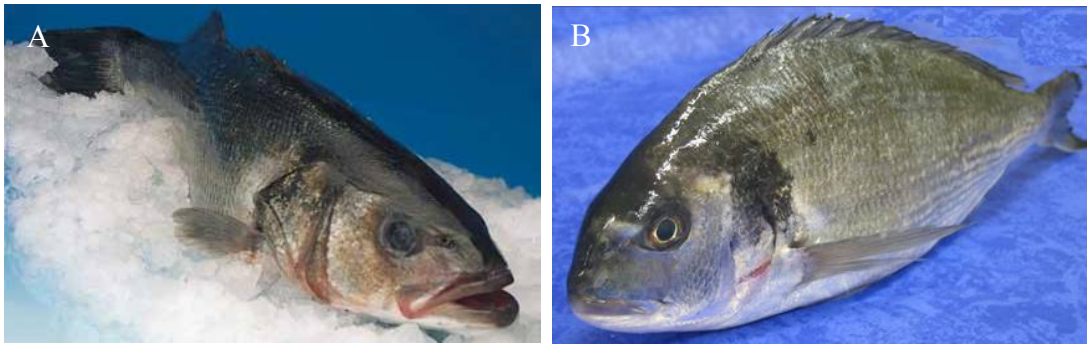

Figure 1.1 A) The sea bass *Dicentrarchus labrax* (L.) (Moronidae) and B) the gilthead sea bream *Sparus aurata* L. (Sparidae) are the two fish species predominantly cultured in the Mediterranean (Images from http://www.peixosdepalamos.com).

Most sea breams are well known as excellent food fish and as fish of commercial importance for fisheries, aquaculture and game fishing. In the Mediterranean, the best known sparid species is the gilthead sea bream *S. aurata*, an extensively farmed fish. Some other sparid species are presently cultured close to commercial scale in the Mediterranean, *e.g.* the sharpsnout sea bream *D. puntazzo*, common dentex *Dentex dentex* (L.) and common pandora *Pagellus erythrinus* (L.). Other species are in the pilot stage for aquaculture production as the sand steenbras *Lithognathus mormyrus* (L.), the white seabream *Diplodus sargus* (L.) or the common two banded seabream *Diplodus vulgaris* (Geoffroy Saint-Hilaire 1817) (Barazi-Yeroulanos 2010).

1.3. Parasites in aquaculture

One of the main challenges in the production of fish is health management. Disease may be the result of poor nutrition, genetic, adverse environmental conditions, physical injury or pathogens, either virus, bacteria or parasites (Woo et al. 2002). Parasites can affect the production of farmed fish in diverse ways: from spoiling the

appearance of the final product to causing disease and mortality of the stock or even posing a threat to humans health. As in all diseases affecting human or livestock, prophylactic strategies aiming at preventing diseases in cultures are preferable to addressing the problem once present. With regard to parasites, it is known that high density of fish in intensive cultures, eutrophication, bio-fouling on the nets and culture sites with specific environmental conditions favour their transmission (Hemmingsen 2008).

Some of the most problematic and pathogenic metazoan parasites in the Mediterranean aquaculture are microparasites of the phylum Myxozoa (Palenzuela 2006), monogenean flatworms (Thoney & Hargis 1991) and trematode blood flukes of the family Aporocotylidae (Bullard & Overstreet 2008). In the present thesis, only aporocotilids and myxozoans will be considered.

1.4. The Digenea (Trematoda)

1.4.1. General aspects

(Summarized and modified from Gibson 2002a,b; Cribb 2005)

The subclass Digenea Carus 1863 are platyhelminth parasites belonging together with subclass Aspidogastea Faust & Tang 1963 to the class Trematoda Rudolphi 1808 (Phylum Platyhelminthes). Aspidogastreans are a small group of parasites of molluscs, fishes and chelonians. The Digenea are a much larger group, with about 18000 nominal species (Cribb et al. 2001a). Digenea have complex life cycles with several larval stages and hosts belonging to the molluscs and the vertebrates. Adult digeneans are primarily parasites of the gut, but in fish they also occur in wide variety of body-cavities, organs and tissues.

The main distinctive morphological feature of the Digenea is the attachment organ. The adults have an oral (anterior) and ventral (posterior) sucker, however suckers can be lost in some species. Usually, the mouth is located within the oral sucker and the ventral sucker is usually used only for attachment. Digeneans have a syncytial tegument often armed with spines. The gut usually comprises a prepharynx, pharynx, oesophagus and a pair of blind caeca. The excretory system comprises flame cells and ducts that lead to the excretory vesicle that opens to an excretory pore at the posterior end of the body. The reproductive system usually fills most of the body. Digeneans are hermaphodites and rarely dioecius. The male system has typically two

testes. The sperm passes via ducts to the cirrus-sac, a muscular structure that has an internal seminal vesicle and an eversible ejaculatory duct that, when everted, forms the cirrus. However, many digeneans lack a cirrus-sac. The male system eventually

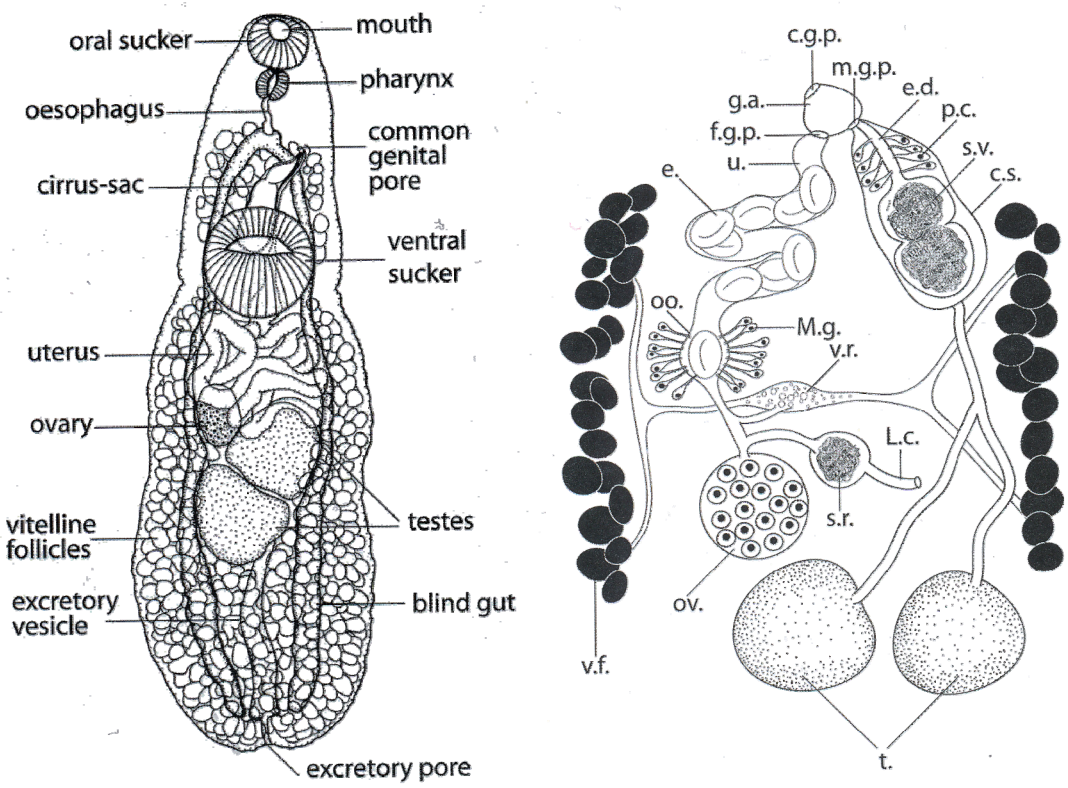

Figure 1.2 A) Typical morphology of a digenean adult. B) Male and female reproductive systems. c.g.p. common genital pore; c.s. cirrus sac; e. egg; e.d. ejaculatory duct; f.g.p. female genital pore; L.c. Laurer's canal; M.g. Mehlis'gland; m.g.p. male genital pore; oo. ootype; ov. ovary; s.r. seminal receptacle; s.v. seminal vesicle; t. testes; u. uterus, v.f. vitelline follicles; v.r. vitelline reservoir (after Cribb 2005).

opens to a male genital pore. Usually the male and female pores open next to each other in a genital atrium which itself opens to the exterior through a common genital pore. In the female system, the ovary normally is a single mass but it is occasionally follicular. The oocytes are produced in the ovary and eggs are assembled at the ootype where the oocyte becomes fertilised by incoming sperm. A sperm storage apparatus or seminal receptacle and a seminal disposal apparatus or Laurer's canal is usually also present. If not, sperm may be stored in masses in the uterus. The ootype is surrounded by gland cells forming the Mehlis' gland that stimulate the release of

eggshell precursors from the vitelline cells. The eggs pass to the exterior via the uterus. A ciliated larva or miracidium develops within the egg. The vitellarium is variable, exhibiting all forms from follicular to a single compact mass, often scattered throughout much of the body (Figure 1.2).

1.4.2. Life cycle

(Summarized and modified from Gibson 2002b)

A general digenean life cycle (Figure 1.3) involves at least two hosts with both free-living and parasitic stages, incorporating both asexual and sexual reproduction. Almost all digeneans have a mollusc first intermediate host (except for some aporocotylids that infect polychaetes) and a vertebrate definitive host.

Adults produce eggs that pass to the environment. Eggs hatch to release a motile, short-lived, non-feeding, ciliated larva, called miracidium. The miracidium swims and penetrates a molluscan first intermediate host, usually a gastropod, but also infects bivalves, scaphopods or polychaete annelids. The miracidium in the first intermediate host develops into a mother sporocyst, which is a simple sac without feeding structures or gonads. The mother sporocyst produces either multiple daughter sporocysts or rediae. A redia has a mouth, pharynx and a short saccular gut. Sporocysts and rediae reproduce asexually, producing cercariae. The cercariae emerge actively from the mollusc. Their morphology is highly variable and related to their infection behaviour. After the cercariae emerge, they can penetrate the definitive host (in a two-host life cycle) or encyst as a metacercaria in a second intermediate host and wait passively until they are eaten by the definitive host (three-host life cycle). If the life cycle is a three-host life cycle, a second intermediate host, a crustacean or fish, is involved. This is the most common life cycle in the Digenea.

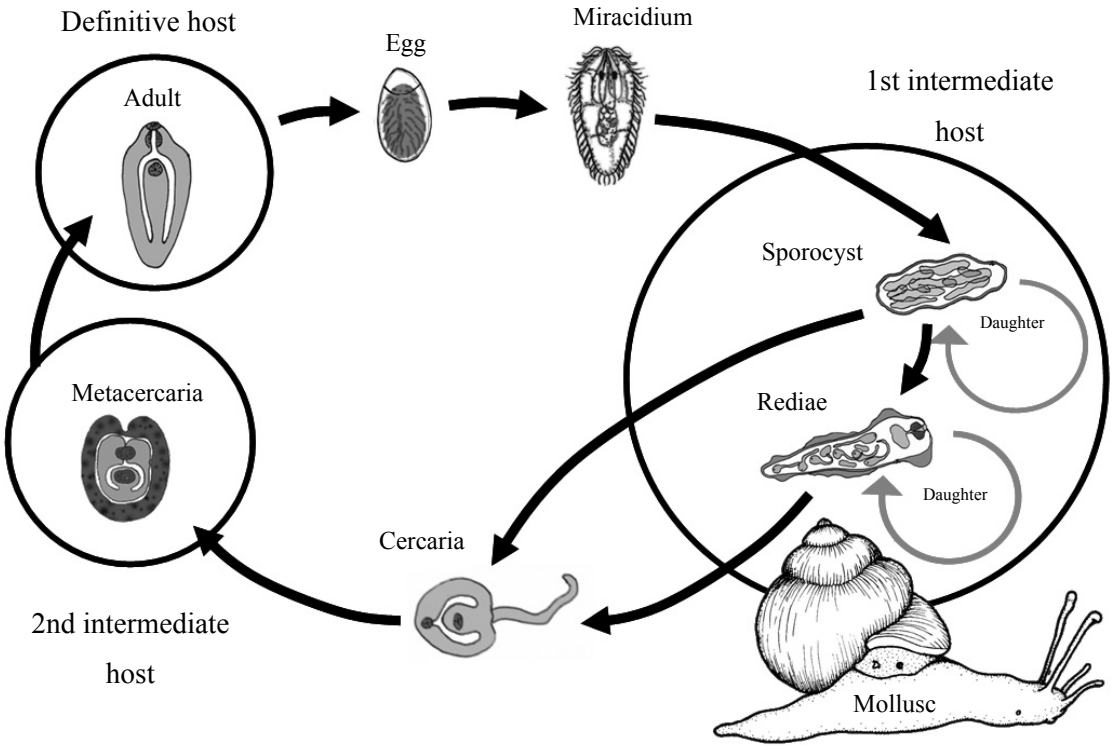

Figure 1.3 A general digenean life cycle. The eggs are released from the adults to the environment. From the egg hatches the miracidium, a ciliated larva that actively searches for the first intermediate host, usually a mollusc. In the first intermediate host the miracidium develops into sporocyst and rediae. Sporocysts and rediae are reproducing asexually, producing cercariae. The cercariae emerge actively from the mollusc. The cercariae infect the second intermediate host and form a metacercaria. The second intermediate host is eaten by the definitive host and the cycle is completed.

1.4.3. Effects on hosts

(Summarized and modified from Cribb 2005)

In the first intermediate host, digeneans live within the haemocoel and typically occur in the digestive gland or gonad of the molluscs. As the asexual reproduction takes place in the first intermediate host, many spococysts or rediae are developing cercariae. These stages may occupy more than half of the digestive gland volume and replace the gonad entirely, producing parasitic castration. In the second intermediate host, digeneans occur as encysted or unencysted metacercariae. However, most metacercarial infections appear to be relatively benign. In the definitive host, most digeneans are parasites of the digestive tract. There are few reports of pathogenesis and mortalities with such infections. Adult digeneans that cause significant problems

are those that occur in non-digestive sites. Among these, the blood flukes are the most important ones. Blood flukes occur in the blood vessels of marine birds (Family Schistosomatidae Poche 1907), marine turtles (Family Spirorchiidae Rao 1933) and fishes (Family Aporocotylidae Odhner 1912). Adult blood flukes can interfere with the normal blood flow and erode the blood vessel walls. The eggs are most problematic as there is no direct exit route into the environment so they must pass through host tissue, where they can cause major inflammatory responses. Eggs may become trapped in tissues with no exit. Miracidia of schistosomatids and spirorchiid exit their eggs and penetrate the gut wall, but aporocotylid miracidia penetrate the gill epithelim of their hosts, after eggs accumulation in the capillaries of the gills. Thereby, aporocotylids have been associated with mass mortality of fish in aquaculture.

1.4.4. Family Aporocotylidae or fish blood flukes

1.4.4.1. General aspects

The family Aporocotylidae Odhner 1912 (syn. Sanguinicolidae Poche 1926; see Bullard et al. 2009) is composed of trematodes inhabiting the blood system of elasmobranch, holocephalan and teleost fishes. Aporocotylids are difficult to detect and collect in their definitive hosts (Cribb et al. 2001b) and they are often missed in parasitological surveys of fish, especially if the circulatory system is not routinely examined (Smith 1997). Aporocotylids usually infect the heart, and the branchial arteries and arterioles of fishes (Bullard & Overstreet 2008). However, the habitat in the blood system is not as restricted as generally assumed, as some aporocotylids have been described from other intravascular locations like the mesentery vessels (Herbert et al. 1994), kidney (Bullard et al. 2006) or the pectoral girdles (Montero et al. 2003; 2009).

Adult aporocotylids (Figure 1.4) are thin-bodied, dorsoventrally flattened or tube-like and elongate or oval in shape. Some are concave and capable of using the ventral surface of the body as a suction cup for adhesion to the walls of arteries and veins. The majority of species have lateral tegumental spines, with different arrangement, and which facilitate attachment and locomotion. Aporocotylids are further differentiated from other digeneans by having a diminute or poorly developed anterior sucker and by lacking the ventral sucker. Smith (2002) listed the

morphological features used to distinguish genera, however, the family Aporocotylidae lacks a phylogenetical hypothesis as a whole (Bullard & Overstreet 2008). Molecular studies have shown that the Schistosomatoidea (including the Aporocotylidae) + Diplostomoidea may be the most basal clade within the Digenea (Cribb et al. 2001b). Aporocotylidae is the only family in this clade whose members parasitize fishes as sexual adults and as such is a strong candidate to be considered one of the more pivotal digenean taxa for the understanding of digenean evolution in general (Cribb et al. 2001b).

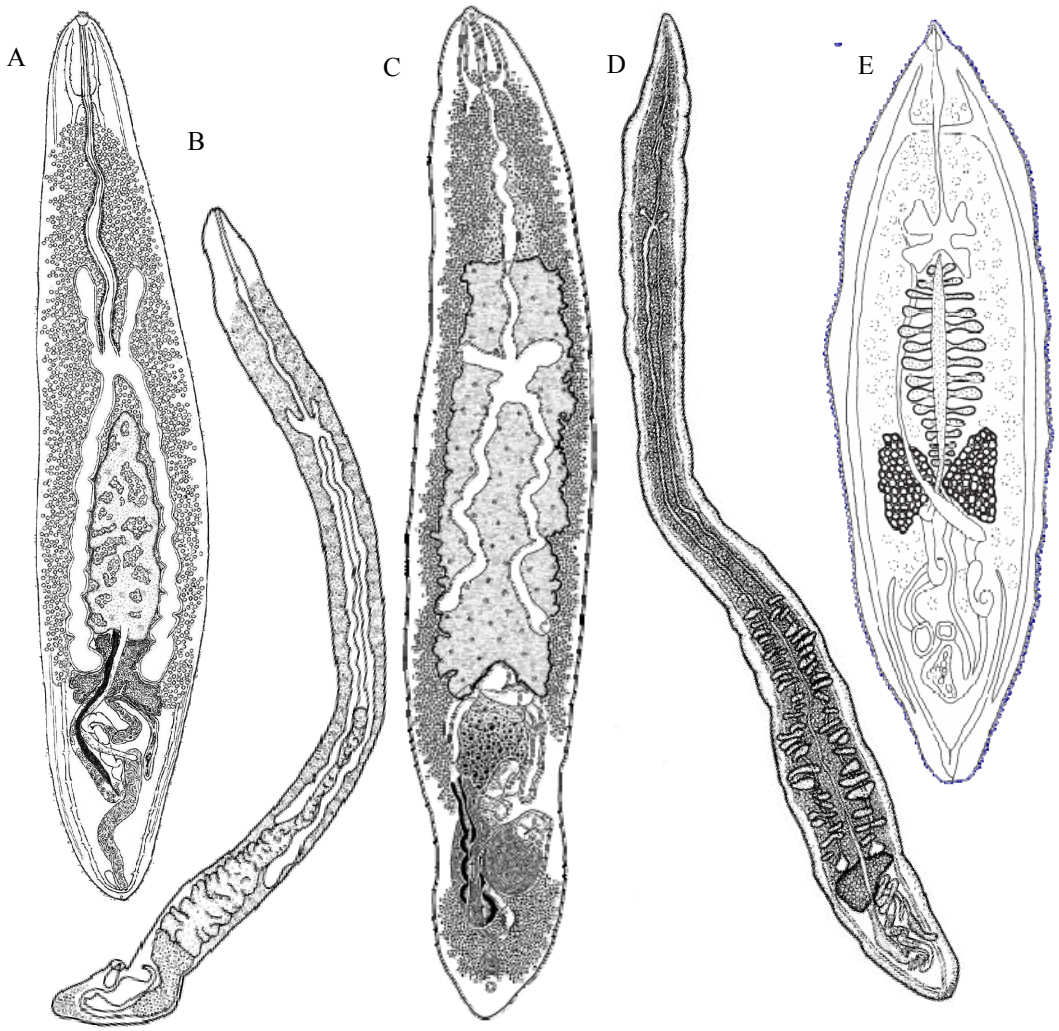

Figure 1.4 Aporocotylid blood flukes. A) *Cardicola aurata* Holzer, Montero, Repullés, Nolan, Sitjà-Bobadilla, Alvarez-Pellitero, Zarza & Raga 2008 (after Holzer et al. 2008). B) *Psettarium sebastodorum* Holmes 1971 (after Holmes 1971). C) *Pearsonellum corventum* Overstreet & Køie 1989 (Nolan & Cribb 2004b). D) *Paradeontacylix ibericus* Repullés-Albelda, Montero, Holzer, Ogawa, Hutson & Raga 2008 (after Repullés-Albelda et al. 2008). E) *Sanguinicola inermis* Plehn 1905 (after Kirk & Lewis 1993).

1.4.4.2. Life cycle

Aporocotylids lack a second intermediate host and thus a metacercarial stage. In their definitive host, they mature in the blood or occasionally in the body cavity. Most of the eggs become trapped in the gill capillaries where the egg develops a miracidium. Aporocotylids are the only digeneans that may use a non-mollusc as first intermediate host, as marine species develop cercariae inside polychaetes (Køie 1982; Køie & Petersen 1988). The cercariae penetrate the fish host through its gill, skin, eyes, fins or alimentary tract and develop into a juvenile stage called schistosomule before reaching a specific site in the circulatory system. However, the life cycles of most blood flukes are cryptic.

1.4.4.3. Pathogenicity

The host response to aporocotylids depends on the host species, site of infection, intensity of infection, season and environmental conditions. There is little information on the effect of blood flukes on wild host populations. However, blood flukes are well known for causing pathological effects and even mortalities in aquaculture (Ogawa et al. 1989; Crespo et al. 1992; Crespo et al. 1994; Kirk & Lewis 1998; Colquitt et al. 2001; Padrós et al. 2001; Ogawa et al. 2007; Ogawa et al. 2010). Acute and chronic stages of disease can be lethal. Aporocotylid eggs in the gills (Figure 1.5) may cause blood vessel obstructions, epithelial and cardiac lesions and haemorrhages. Miracidial hatching from the eggs and breaking through the gill epithelia of the secondary lamellae often leads to problems with oxygen transport in the gills and finally the death of the host (Ogawa et al. 1989; Crespo et al. 1992; Kirk & Lewis 1998; Padrós et al. 2001; Colquitt et al. 2001; Ogawa et al. 2007). In some cases, a massive number of cercariae was shown to kill fish in a few hours and produced severe oedema and epidermal haemorrhaging (Kirk & Lewis 1992). Only a few reports directly relate pathological problems to the living adult aporocotylid (Schell 1974; Overstreet & Thulin 1989; Padrós et al. 2001) and in some cases the pathology is induced by dead, disintegrated or already encapsulated adult worms (Thulin 1980).

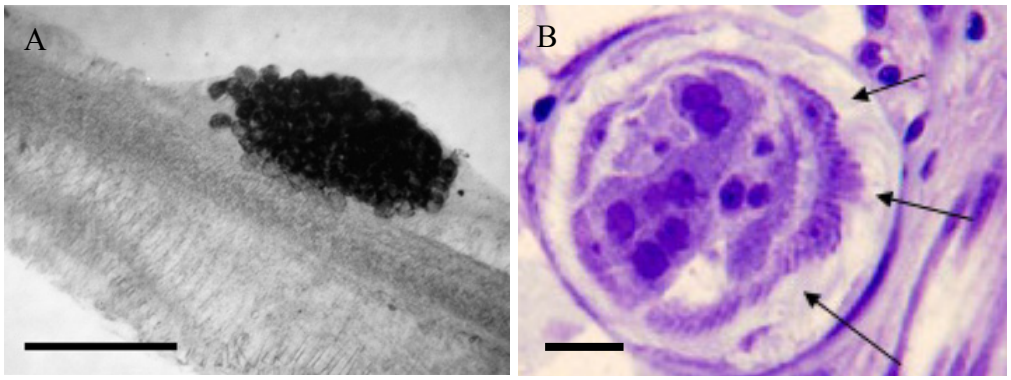

Figure 1.5 A) Large egg aggregation of *Paradeontacylix ibericus* in the primary gill lamella of *Seriola dumerili* (Risso 1810), (after Repulles-Albelda et al. 2008). B) Semithin section of a mature egg of *Cardicola aurata* stained with methylene blue containing fully developed miracidia with ciliated cells (arrows) in gills of *Sparus aurata* (after Holzer et al. 2008). Scale bar: A= 1mm; B= 10 µm.

1.5. The Myxozoa

1.5.1. General aspects

The phylum Myxozoa Grassé 1970 is a group of metazoan parasites of vertebrates and invertebrates, mainly known for the diseases they provoke in commercial fish. Despite the description of more than 2300 representatives in the phylum, only a fraction of them is pathogenic. Myxozoan infections in sparids and other mariculture species in the Mediterranean have been investigated widely in the last 15 years, and a large number of species have been reported (Alvarez-Pellitero & Sitjà-Bobadilla 1993b; Agius & Tanti 1997; Palenzuela 2006).

Myxozoans are characterized by typical multicellular spores consisting of one to several capsulogenic cells that form the polar capsules, two to seven valvogenic cells that form the shell valves and the amoeboid infective sporoplasm which consists of one to many sporoplasmic cells (Figure 1.6). The polar capsules are the most prominent structures of this parasite group. These nematocyst-like structures consist of a coiled polar filament, and the extrusion of the polar filament allows for the attachment to the host and the subsequent invasion of the sporoplasm, the infective germ (Lom & Dyková 2006).

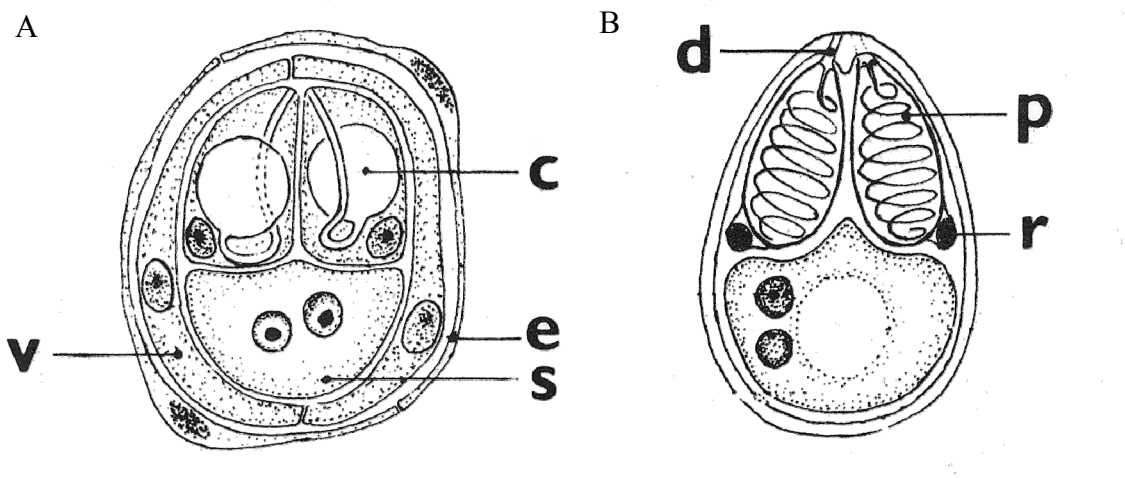

Figure 1.6 A) Sporogonic stage and B) mature myxospore of the genus *Myxobolus* Bütschli 1882. v, valvogenic cell; c, capsulogenic cell with capsular primordium; e, enveloping cell (pericyte); s, sporoplasmic cell; d, canal for polar filament discharge; p, polar filament; r, residual nuclei of capsulogenic cell (after Lom & Dyková 1992).

1.5.2. Taxonomy and phylogenetic relationships

Historically, the myxozoans were classified as protists but some metazoan characteristics like the multicellular character of the myxozoan spores (Štolc 1899), the type of cell junctions and the possibility to produce collagen (Sidall et al. 1995), the similarity between myxozoan polar capsules and cnidarian nematocysts (Weill 1938) pointed to a possible metazoan origin. The first analysis of myxozoan ribosomal DNA sequences in the early 1990ies confirmed the Myxozoa as phylum member of the metazoans (Smothers et al. 1994). However, the phylogenetic position of the myxozoans within the Metazoa is still controversial, and two main hypotheses exist, relating them to 1. The Cnidaria or 2. The Bilateria. The structural similarity between the polar capsules of myxozoans and the nematocysts of cnidarians suggested that these groups were possibly related (Weill 1938). The relationship between myxozoans and cnidarians was supported by molecular analyses of ribosomal DNA sequences including the narcomedusan species *Polypodium hydriforme* (Ussov 1885), which has been proposed as the sister group of myxozoans (Siddall et al. 1995; Zrzavý and Hypša 2003). Recently, a minicollagen gene, which encodes cnidarian nematocyst proteins was characterized in *Tetracapsuloides bryosalmonae* (Canning, Curry, Feist, Longshaw & Okamura 1999) and supports a link between the cnidarians and the myxozoans (Holland et al. 2010). Multi-gene

analyses and the detection of four radially symmetric muscle blocks in the vermiform myxozoan *Buddenbrockia plumattelae* Schröder 1910 also placed the Myxozoa within Cnidaria (Jiménez-Guri et al. 2007). However, bilateral symmetry of the worm-like myxozoan *B. plumattelae* (Okamura et al. 2002) and other molecular studies (Smothers et al. 1994; Monteiro et al. 2002) demonstrated bilaterian affinities of the myxozoans. Recently, new DNA sequence data set analyses indicated a well-supported early diverging bilaterian position for the phylum Myxozoa (Evans et al. 2010). However, the authors also suggest that the myxozoans are a highly divergent taxon, and that further data exploration and selection of a better evolutionary model are necessary to phylogenetically place highly divergent taxa.

Table 1.1 Classification of the myxozoa (Canning & Okamura 2004)

Phylum Myxozoa Grassé 1970
Class Myxosporea Bütschli 1881
Order Bivalvulida Schulman 1959
Suborder Sphaeromyxina Lom & Noble 1984
Suborder Variisporina Lom & Noble 1984
Suborder Platysporina Kudo 1919
Order Multivalvulida Schulman 1959
Class Malacosporea Canning, Curry, Feist, Longshaw & Okamura 2000
Order Malacovalvulida Canning, Curry, Feist, Longshaw & Okamura 2000
Family Saccosporidae Canning, Okamura & Curry 1996
Genus *Buddenbrockia* Schröder 1910
Genus *Tetracapsuloides* Canning, Tops, Curry, Wood & Okamura 2002

Traditionally, the classification of the Myxozoa (Table 1.1) is based on spore morphology, i.e. shape of spore, number of shell valves and number, shape and orientation of polar capsules. Two classes have been described, the Malacosporea Canning, Curry, Feist, Longshaw & Okamura 2000, which form soft-walled spores and the Myxosporea Bütschli 1881, which mostly form harder spores valves. Depending on the number of valves of the spores, two orders were determined in the class Myxosporea: Bivalvulida Shulman 1959, developing spores with two valves and Multivalvulida Shulman 1959, developing spores with three or more valves. With regard to habitat in the host, two classes of myxozoans can be distinguished:

coelozoic species which live in body cavities such as the gall bladder, bile ducts or the urinary tract, i.e. renal tubules, urethers or urinary bladder; and histozoic species, which live in various tissues, mostly intercellularly, but sometimes also intracellularly, at least during some period of the life cycle. Myxozoans are furthermore characterized by a variable degree of host specificity. Some species are strictly host specific, while others parasitize several related or non-related fish species (Lom & Dyková 2006).

The introduction of molecular tools, i.e. phylogenetic analysis based on small subunit (SSU) rDNA sequences was found to contradict traditional taxonomy, revealing many paraphyletic and polyphyletic genera within the Myxozoa (Fiala 2006). Phylogenetic analyses showed that clustering of species is strongly influenced by host tissue localisation (Holzer et al. 2004; Fiala 2006), the invertebrate host type (bryozoan, polychaete and oligochaete) (Holzer et al. 2007), habitat (Holzer et al. 2007) and the cellular development in the host (Morris & Adams 2008). The phylogenetic trees based on SSU rDNA sequences have now largely been confirmed by large subunit (LSU) rDNA sequences and a non-ribosomal gene (elongation factor 2 (EF2)) (Bartošová et al. 2009, Fiala & Bartošová 2010). The inconsistency between traditional taxonomy based on spore morphology and the results of phylogenetic studies is based on the strong plasticity of myxospore morphology during the evolution of the myxozoans (Fiala & Bartošová 2010), and thus a revision of the current taxonomy is urgently needed.

1.5.3. Hosts and life cycle of the Myxozoa

1.5.3.1. Malacosporean hosts and life cycles

Only two genera, *Tetracapsuloides* Canning, Tops, Curry, Wood & Okamura 2002 and *Buddenbrockia* Schröder 1910 and three species have been described in the class Malacosporea. These freshwater parasites have a life cycle involving a bryozoan and a fish host (Morris & Adams 2006; Grabner & El-Matbouli 2010a). The parasite infects the body cavity of bryozoans and develops sac-like or vermiform trophozoites (Figure 1.7A) inside which malacospores mature. Malacospores have eight unhardened shell valves, four polar capsules and two sporoplasms with secondary cells and sporoplasmosomes (Canning & Okamura 2004). In the fish host, the spores are called fishmalacospores and possess four valve cells, two polar capsules and one

sporoplasm with sporoplasmosomes but no secondary cells (Hedrick et al. 2004). The species *T. bryosalmonae* is the agent of proliferative kidney disease (PKD) of cultured and wild salmonid fishes that produces an inflammatory response in the kidney and can cause high levels of mortalities. In 2005, the use of confocal laser scanning microscopy (CLSM) in *T. bryosalmonae* documented the cellular components of malacosporean spores for the first time in 3D (McGurk et al. 2005) (Figure 1.7B-C).

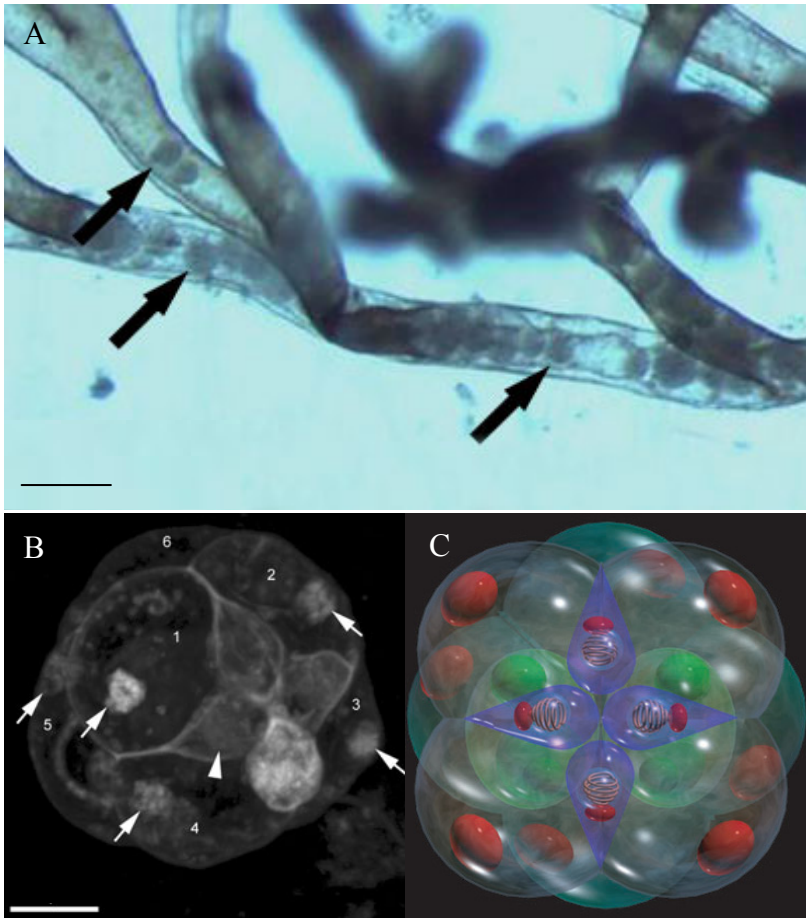

Figure 1.7 A) Sac-like stages of *Tetracapsuloides bryosalmonae* (Canning, Curry, Feist, Longshaw & Okamura 1999) (arrows) inside a bryozoan host (Image by Sylvie Tops); B) Confocal laser scanning microscopy (CLSM) 3D reconstruction of a spore of *Tetracapsuloides bryosalmonae* (from McGurk et al. 2005): arrowhead pointing to one out of four central polar capsules. Six of the eight valve cells (1–6) can be seen including nuclei (arrows); C) Schematic 3D model of *Tetracapsuloides bryosalmonae* spore showing all layers in situ (from McGurk et al. 2005). Scale bar: A= 200 µm; B= 5 µm.

1.5.3.2. Myxosporean hosts and life cycle

The majority of myxozoans described to date are included in the class Myxosporea. The life cycle of myxosporeans also includes the alternation of two hosts. The myxosporean phase occurs in the vertebrates resulting in the production of myxospores (Figure 1.8). Typically the vertebrate host is a fish, but may also be amphibians, reptiles, birds and mammals (Jirkú et al. 2006; Prunescu et al. 2007; Bartholomew et al. 2008). The actinosporean phase takes places in the invertebrate resulting in the production of actinospores (Figure 1.9). The hosts of the actinosporean phase are annelids, in freshwater generally oligochaetes, in the marine environment polychaetes, and rarely sipunculids (Ikeda 1912).

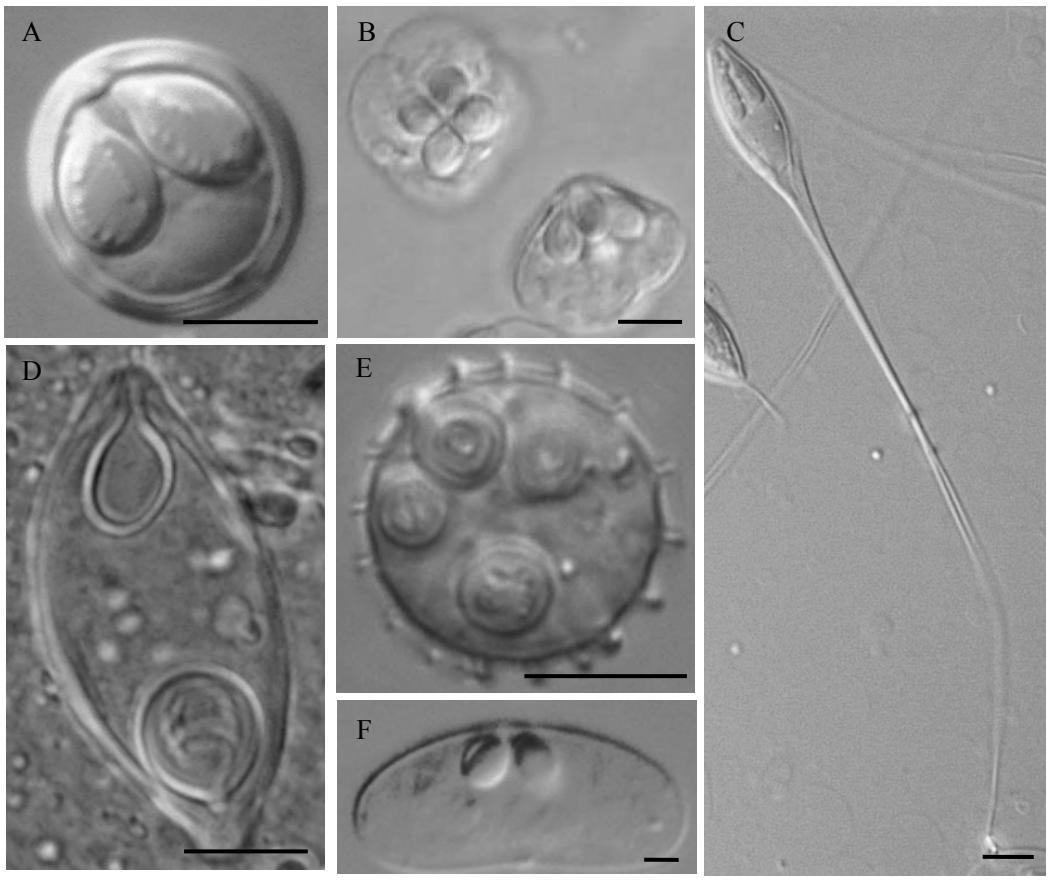

Figure 1.8 Myxospores of A) *Myxobolus neurotropus* Hogge, Campbell & Johnson 2008 (after Hogge et al. 2008); B) *Kudoa iwatai* (Egusa & Shiomitsu 1983) (after Diamant et al. 2005); C) *Henneguya pellis* (Minchew 1977) (after Griffin et al. 2009); D) *Myxidium anatidum* Bartholomew, Atkinson, Hallett, Lowenstine, Garner, Gardiner, Rideout, Keel & Brown 2008 (after Bartholomew et al. 2008); E) *Chloromyxum auratum* Hallett, Atkinson, Holt, Banner & Bartholomew 2006 (after Hallett et al. 2006); F) *Ceratomyxa honckenii* Reed, Basson, Van As & Dyková 2007 (after Reed et al. 2007). Scale bar: 5 µm.

The first life cycle of a myxozoan that was elucidated was that of *Myxobolus cerebralis* Hofer 1903 (Wolf & Markiw 1984) the agent of "whirling disease" in salmonids. While more than 30 life cycles have been elucidated in the freshwater environment (Figure 1.10A; Lom & Dyková 2006) only four marine life cycles have been described to date (Figure 1.10B; Køie et al. 2004; 2007; 2008; Rangel et al. 2009). Knowledge of myxozoan life cycles from the marine environment is poor because it is difficult to determine invertebrate hosts in an environment with an extremely rich invertebrate biodiversity (Køie et al. 2004) and a large water body. Fish-to-fish transmission of myxozoans has been observed only in the enteric genus *Enteromyxum* Palenzuela, Redondo & Alvarez-Pellitero 2002, however, proliferative stages which are protected within epithelial cells of the intestine are responsible for infection in the receptor fish and not mature spores (Figure 1.10C; Diamant 1997; Redondo et al. 2002). This indicates that even *Enteromyxum* spp. have an invertebrate host although its importance for high density aquaculture systems, where fish-to-fish infection is likely to occur, is questionable.

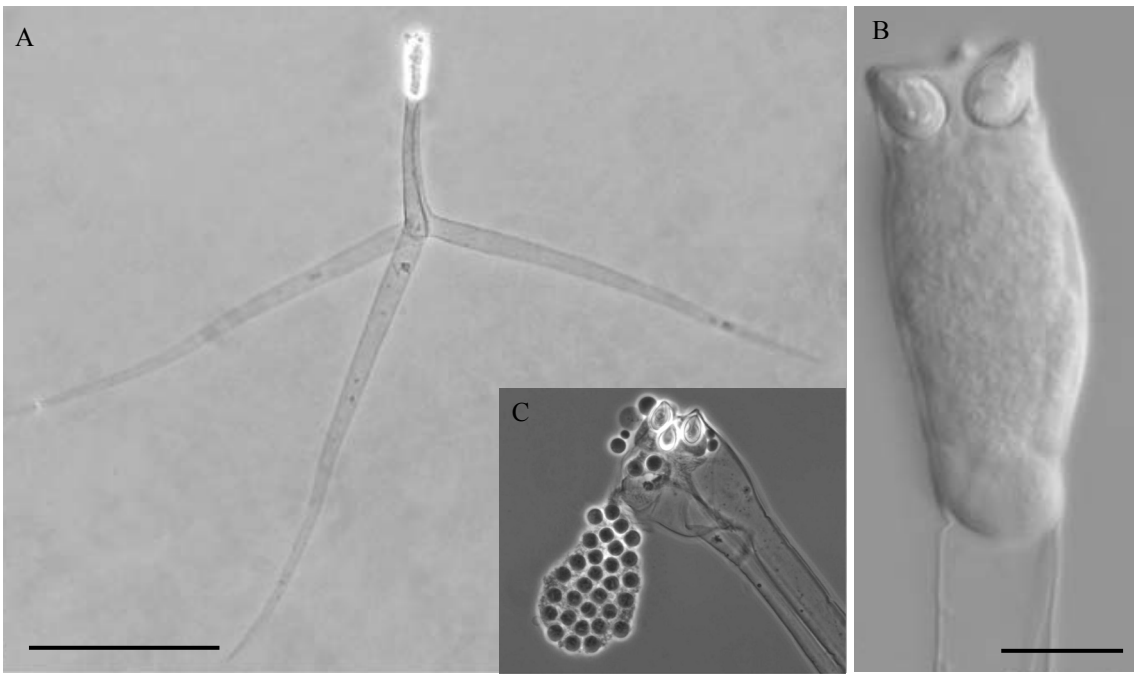

Figure 1.9 Actinospores of A-B *Myxobilatus gasterostei* (Parisi 1912) and C *Myxobolus cerebralis* Hofer 1903. A) Actinospore with large floating appendages and B) detail of apical part of actinospore, where polar capsules and sporoplasm are located (after Atkinson & Bartholomew 2009). C) Sporoplasm release from an actinospore (after Kallert et al. 2010). Scale bar: A= 100 µm; B= 10 µm.

On contact with the skin or the gills of the vertebrate host, the actinospores extrud their polar filaments and release the sporoplasm. The sporoplasm migrates intercellulary through the epidermis and the gill epithelium. Then, presporogonic development results in parasite proliferation and allows spreading of the parasite throughout the host organs. When presporogonic stages arrive at the host organ, the sporogonic phase begins and the stages transform into plasmodia or trophozoites. Plasmodia can be monosporic, disporic or polysporic. The sporogonic cells inside the plasmodia differentiate into capsulogenic, valvogenic and sporoplasmogenic cells of the spores. Myxospores are produced and they are released into the water via the gut, the excretory system or after death of the fish host.

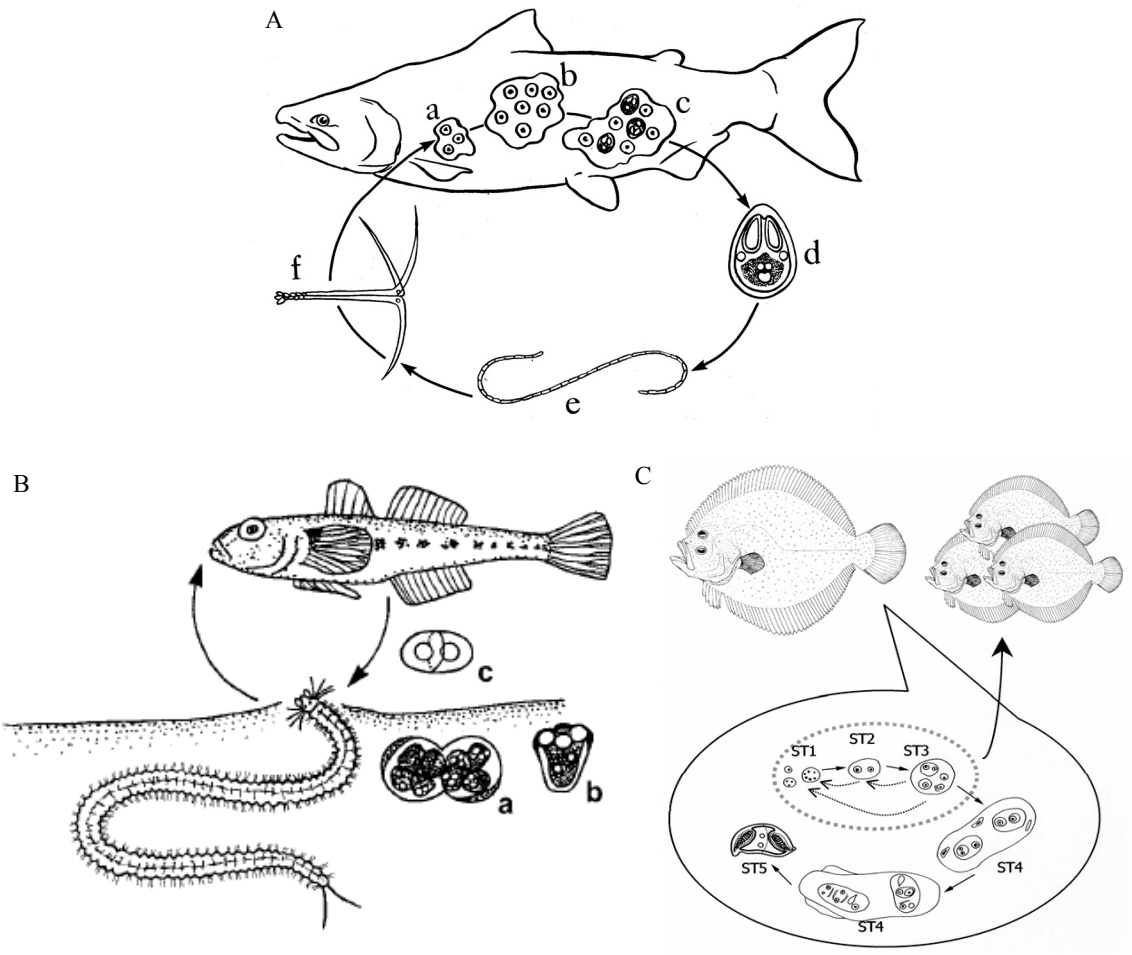

Figure 1.10 Schematic diagram of the life cycles of Myxozoa. A) Freshwater life cycle of *Myxobolus* sp. a-c: development and spore formation; d: myxospores are released from the fish; e: annelid becomes infected after ingestion of myxospores from fish; f: actinospore released from the annelid infects the fish host to complete the life cycle (after Kent & Poppe 1998). B) Marine life cycle of *Ellipsomyxa gobii* Køie 2003. Species of the

Figure1.10 continued: genus *Nereis* act as invertebrate host and the common goby as vertebrate host. a: pansporocyst with eight actinospores; b: actinospore; c: myxospore (after Køie et al. 2004). C) Fish to fish transmission of *Enteromyxum scophthalmi* Palenzuela, Redondo & Alvarez-Pellitero 2002 in turbot. ST2 to ST3 are the proliferative stages which can be transmitted and infect to other fish (when released with detached epithelial strips) through the faeces (after Redondo et al. 2004).

The myxospores are ingested by the invertebrate host where the sporoplasm of the myxospore initiates proliferation. During the subsequent gametogony (sexual reproduction), these stages divide and form a pansporocyst, which produces eight zygotes that differentiate into eight actinospores. In contrast to myxospores, actinospores have a typical triradiate symmetry with three polar capsules, three valves and a multinuclear sporoplasm (Figure 1.9A-C; Kent et al. 2001; Lom & Dyková 2006). Recently, some nucleosides produced by the fish host have been related with chemostimulation causing polar filament discharge and sporoplasm emission from the actinospores (Kallert et al. 2010). These nucleosides seem to allow fish host recognition.

1.5.4. Pathogenicity of the Myxozoa

Myxozoans can infect any host organ or tissue. Among the large number of myxozoan species described, only a small fraction is pathogenic. Myxozoans may impair the growth and reproduction of fish, cause damage in tissues and organs or even produce the death of the host. The extent of the damage depends on the myxozoan species, its life cycle stage, the intensity of infection, the host immune response and temperature conditions.

In wild fish populations, myxozoans do not usually kill their host. Consequently, myxozoan parasitism tends to be chronic. However, in aquaculture, myxozoans are a challenge for the industry as the high-density of host populations represents an opportunity for the parasites. Secondary stressors and/or reduced immunocompetence due to the culture conditions have a significant effect.

One of the best known pathogenic myxozoans is *M. cerebralis,* the causative agent of salmonid whirling disease. Disease is caused by the destruction of cartilage and associated tissue, leading to the death of the fish or life-long skeletal deformities (Hofer 1903) (Figure 1.11A). *Ceratomyxa shasta* (Noble 1950) produces extensive

haemorrhages and necrosis in the intestine of its hosts and cause substantial losses in wild and cultured salmonids (Bartholomew et al. 1989a; Bartholomew et al. 2004). The malacosporean *T. bryosalmonae* provokes PKD, responsible for serious economic loss in salmonid culture throughout Europe and North America (Feist et al. 2002) (Figure 1.11B). Multivalvulid myxosporeans of the genera *Kudoa* Meglitsch 1947 and *Unicapsula* Davis 1924 make fish fillets unmarketable due to the presence of macroscopic cysts within the musculature or by post-mortem myoliquefaction of the flesh (Moran et al. 1999a) (Figure 1.11C). Several myxosporeans species affect to the reproductive tract of the fish, as *Sphaerospora testicularis* Sitjà-Bobadilla & Alvarez-Pellitero 1990 which occurs in the seminiferous tubules of broodstocks of sea bass (Figure 1.11D) (Sitjà-Bobadilla & Alvarez-Pellitero 1993b).

In Mediterranean sparids, enteromyxosis caused by *Enteromyxum leei* (Diamant, Lom & Dyková 1994) produces serious mortality in culture systems. The parasite invades the intestinal tract causing severe chronic enteritis that frequently causes emaciation and death, reaching 80% losses in some stocks (Diamant et al. 1994; Athanassopoulou et al. 1999) (Figure 1.11E). Bile inhabiting species of genus *Ceratomyxa* (Thélohan 1892) have been related to mortalities of immunocompromised sparid fish (Company et al. 1999; Katharios et al. 2007). Also, the species *Polysporoplasma sparis* Sitjà-Bobadilla & Alvarez-Pellitero 1995 was reported to produce a glomerular disease in the kidney of gilthead sea bream (Palenzuela et al. 1999).

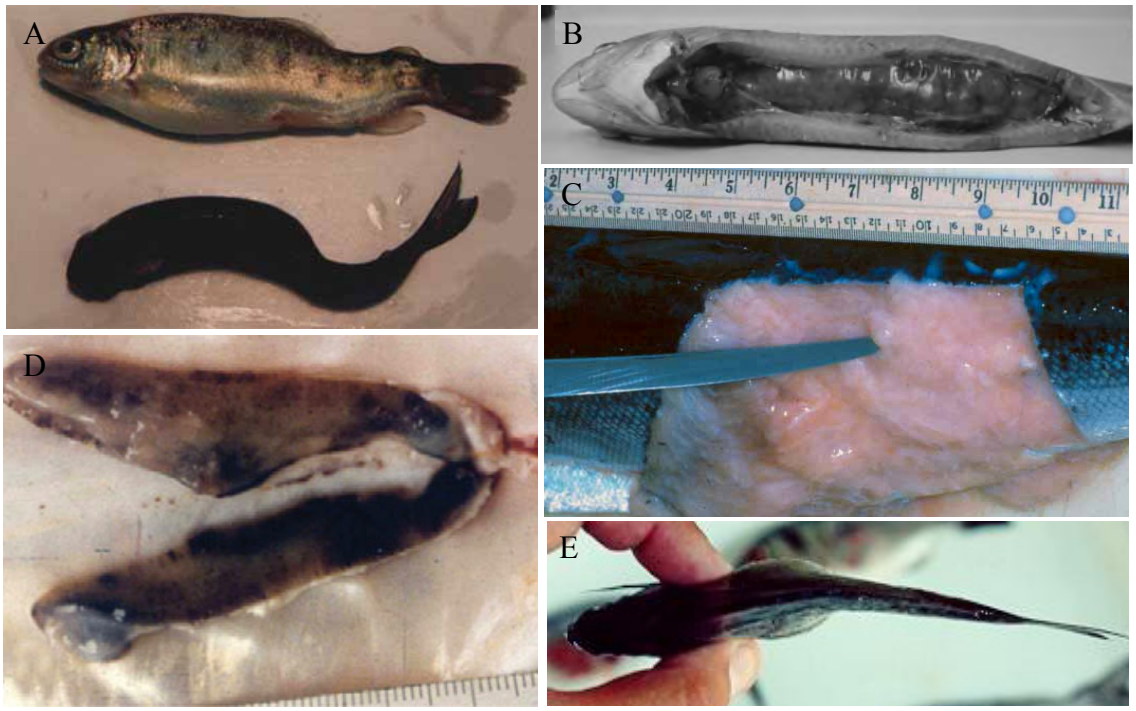

Figure 1.11 A) Whirling disease in rainbow trout *Oncorhynchus mykiss* Walbaum 1792, caused by *Myxobolus cerebralis*. Note scoliosis of vertebral column of fish and pigment abnormality (bottom). B) Proliferative kidney disease in rainbow trout fingerling provoked by *Tetracapsuloides bryosalmonae,* note extensive renal hypertrophy (after Feist & Longshaw 2006). C) Fresh Atlantic salmon held on ice for five days showing severe post-mortem myoliquefaction by *Kudoa thyrsites* (Gilchrist, 1924) infection (after Moran et al. 1999a). D) Massive necrosis in sea bass *Dicentrarchus labrax* testis produced by *Sphaerospora testicularis* (after Sitjà-Bobadilla 2009). E) Emaciated *Sparus aurata* with distended abdominal walls due to chronic enteromyxosis caused by *Enteromyxum leei* (Image by Dr. Varvarigos).

CHAPTER 2. Aims and objectives

Aims

Species diversification has become a major aim in Mediterranean aquaculture. Parasites naturally inhabiting aquaculture candidate fish species may represent a health challenge under culture conditions. Thus, investigations into the biology and life cycle of parasites infecting new candidate species is needed to assist the viability of new and existing species for aquaculture (Rigos & Katharios 2010; Feist & Longshaw 2006). This study aims to provide novel data on myxozoans and aporocotylid trematodes in new species for Mediterranean aquaculture belonging to the family Sparidae. The chosen candidates are 1) Sand steenbras *Lithognathus mormyrus*; 2) Picarel *Spicara smaris* (L.); 3) Annular seabream *Diplodus annularis* (L.); 4) Common two-banded seabream *Diplodus vulgaris*; 5) Sharpsnout seabream *Diplodus puntazzo* and 6) Gilthead seabream *Sparus aurata* (Figure 2.1).

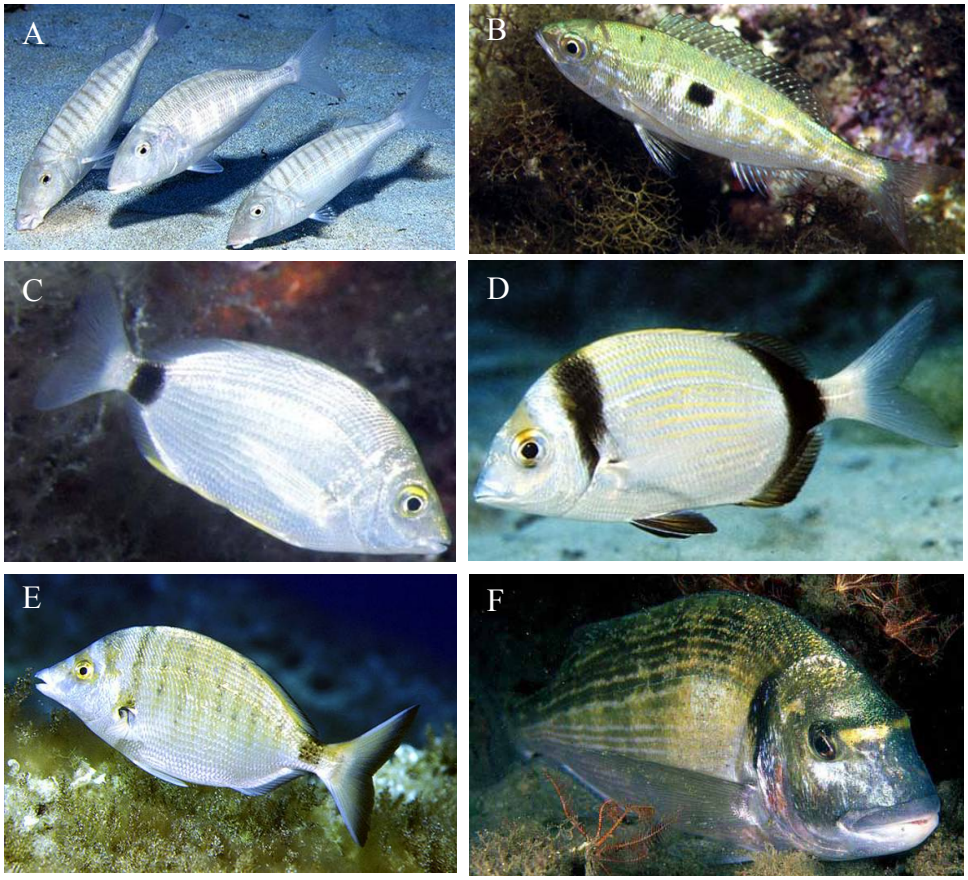

Figure 2.1 Sparid host species analysed. A) Sand steenbras *Lithognathus mormyrus*. B) Picarel *Spicara smaris*. C) Annular seabream *Diplodus annularis*. D) Common two-banded seabream *Diplodus vulgaris*. E) Sharpsnout seabream *Diplodus puntazzo*. F) Gilthead seabream *Sparus aurata*. Images from www.FishBase.org.

The present work pursues to identify and morphologically describe the parasites species of these hosts, and determine their systematic position and relationship with previously described species. In order to better understand the biology and pathogenic potential of the newly identified parasites, their development, life cycle, habitat selection within the fish and their pathology will be studied. Finally, the aim is to understand the transmission, seasonality and pathway of infection of the detected myxozoan parasites. It is expected that this information will allow the development of control policies for the aquaculture of the investigated sparid species, thus contributing to the development and diversification of Mediterranean fish farming in EU member states.

Objectives

The specific objectives are to:

1- Describe a new blood fluke species found in the blood vessels of the meninges of the common two banded seabream *D. vulgaris*. Identify and characterise this blood fluke morphologically, compare it with similar species, analyse it molecularly (SSU, LSU and ITS regions of rDNA), and finally estimate its phylogenetic position within the Aporocotylidae. Determine its exact location and pathological potential in the brain of infected fish.

2- Describe and molecularly characterise (SSU rDNA) a myxozoan parasite belonging to the genus *Unicapsula* found to form large cysts in the muscle of the sand steenbras *L. mormyrus*, and compare it with previously described records. Carry out a histopathological study to clarify whether the *Unicapsula* sp. can cause problems in the marketing of *L. mormyrus* fillets as species belonging to the genus *Unicapsula* and the closely related genus *Kudoa* have been reported to cause post-mortem myoliquefaction, thus digesting the muscle tissue of the host and rendering it unmarketable.

3- Identify and morphologically describe a myxozoan belonging to the genus *Ceratomyxa,* found in the bile of the sharpsnout seabream *D. puntazzo*. Provide basic information on the host-parasite relationship by studying the pathology observed in

relation to the occurrence of the parasite in different organs. Molecularly characterise (SSU rDNA) this *Ceratomyxa* species from *D. puntazzo* and those of other sparids (*D. annularis* and *S. aurata*), occurring in the same habitat, thus providing information on host specificity of *Ceratomyxa* spp. in sparids.

4- Combine a variety of microscopical techniques to study proliferative and spore-forming stages of *Ceratomyxa puntazzi* from *D. puntazzo,* describing their three-dimensional morphology and composition by confocal microscopy, and their ultrastructure by scanning and transmission electron microscopy (SEM and TEM). Describe for the first time the specific locomotive behaviour of these stages and the structural components used therefore. Ascertain the developmental sequence of stages resulting in successful proliferation and spore formation in the bile.

5- Attempt experimental infections with *Ceratomyxa puntazzi* in naïve *D. puntazzo*. Determine whether artificial infections with different stages from donor fish are possible to cause infection in receptor fish (blood stages, developmental bile stages and spore-forming stages), investigating different pathways (bath treatment, intragastric injection and intracoelomic injection). Investigate natural infections by the exposure of naïve fish in experimental cages to a *Ceratomyxa*-enzootic habitat in the Mediterranean on a monthly basis, to understand the seasonal dynamics of the parasite. Elucidate the route of infection of *Ceratomyxa puntazzi* in *D. puntazzo*.

CHAPTER 3. General materials and methods

3.1. Host sampling and parasite collection

Sparid fishes were obtained from the regions of Valencia and Murcia (Mediterranean coast) between 2006 and 2010 (see Table 3.1). Wild fish were purchased from fishing harbours and had been obtained by commercial trawling and shore fishing. Cultured fish were obtained from fish farms (Mar Menor, Murcia). These fish were put on ice and transported to the laboratory of the Marine Zoology Unit.

Live, naïve *D. puntazzo* were obtained from a Greek fish hatchery (38º 17' 50.44''N; 21º 47' 41.04'' E). Live, wild *D. puntazzo* were obtained by shore fishing at San Pedro del Pinatar (Murcia). These fish were transported live to the aquaculture facilities at the University of Valencia (SCSIE) where they were maintained until their use for infection studies. Fish were feed with a commercial dry pellet diet. All fish were sacrificed by an overdose of anaesthetic (clove oil) and by neural pitting.

Table 3.1 Fish species, their number, origin, condition and date of capture of the sparids analysed in the present study. Live fish (*) were maintained at the laboratory for different infection trials.

Fish species	N	Origin	Condition	Date of capture
Diplodus vulgaris	215	Valencia (Spain)	Wild	Nov-Dec 2007 and 2008
Lithognathus mormyrus	24	Valencia (Spain)	Wild	Nov 2006/Oct 2007
Spicara smaris	24	Valencia (Spain)	Wild	Nov 2006/Oct 2007
Diplodus puntazzo	242	San Pedro del Pinatar (Spain)	Wild*	Dec 2007; April 2008; May 2009; May 2010
	299	Rio Achaia, Patras (Greece)	Hatchery* (naïve)	Oct 2006
Diplodus annularis	47	Valencia (Spain)	Wild	April 2008; March and Sep 2010
Sparus aurata	21	San Pedro del Pinatar (Spain)	Sea cages	May 2008; March and Sep 2010

Fish were dissected and organs were examined using a dissection and binocular microscope at 6.8X-1000X magnification. Samples used for morphological description by light microscopy, DNA extraction, confocal microscopy, scanning and transmission electron microscopy and for histopathological pursues were taken from fresh fish. The remainder of the fish, which was used to obtain prevalence data based on microscopical presence, was frozen at -20ºC and thawed on the day of examination. In the freeze-thawed fish the organs were screened and trematode worms were fixed in 70% ethanol after recovery.

Specific host data, sampling sites, organs analysed and parasites obtained are detailed for each study (see Chapters 4-8).

3.2. Morphological analysis

3.2.1. Light microscopy (LM), videos and drawings

Myxozoans

Digital photographs of spores and plasmodia were taken with a Leica DC300 camera mounted on a Nomarski interference microscope Leica DMR at 1000X (Leica Microsystems AG, Wetzlar, Germany). All measurements were taken on digital images using the computer program UTHSCSA ImageTool Version 3.0 for Windows (The University of Texas Health Science Center at San Antonio, Texas, USA). Morphological measurements of spores were taken following the recommendations of Lom & Arthur 1989. Measurements are given in µm as means ± standard deviation with range in parenthesis. Drawings were made with Microsoft Office PowerPoint 2003 (Microsoft Corporation, USA) based on digital photographs, laser confocal and electron microscopy images.

Fresh smears of myxozoan spores on microscopic slides were air dried, stained with Diff-Quick® (Medion Diagnostics International) and mounted in a xylene-free mounting medium (Panreac Química S.A.U., Spain). Syntype specimens were deposited in the Invertebrate Collection of the Natural History Museum, London, UK, and the specific codes are provided in the chapters containing the description of each species (see sections 5.3.5, & 6.3.1).

Live stages of myxozoans were recorded with a Leica DFC295 (Leica Microsystems Ltd.) on a Nomarski interference microscope Leica DMR at 1000X magnification. In

some cases, the live parasites were stained with 1% neutral red. Videos were edited with the software ArcSoft ShowBiz® DVD 2 (ArcSoft Inc., USA).

Trematodes

Fresh worms and their location in the host were photographed with a Leica DC300 camera mounted on a Leica MZ APO and a Leica DMR microscope (Leica Microsystems AG, Wetzlar, Germany). Worms were fixed in 70% alcohol, stained with iron acetocarmine (Georgiev et al. 1986) or alum carmine (Grenacher 1879), differentiated in 1% HCl in 70% ethanol, dehydrated in an ethanol series (70% to 100%), transferred to 98% dimethyl phthalate for clearing and examined as permanent mounts in Canada balsam.

Measurements were taken from illustrations, which were made using a drawing tube attached to a light microscope, Nikon Optiphot-2 (Nikon Corporation) at 100-1000x magnification. Measurements are given in μm as a mean, with range in parentheses. Width measurements refer to maximum width of the body.

Type and voucher specimens were deposited in the British Museum (Natural History) Collection at the Natural History Museum, London (BMNH) and the specific codes are provided together with the description (see section 4.3.2).

3.2.2. Scanning electron microscopy (SEM)

Myxozoans

Ethanol-washed and dried coverslips were coated with 0.1% poly-D-lysine. Myxozoan spores and trophozoites were left to settle onto the coated surface for 30 min in a saline solution and were then fixed for 30 min on the coverslips using 2.5% glutardaldehyde in 0.1 M phosphate buffer (pH 7.4). After rinsing in PBS (2x15min) the spores and trophozoites on the coverslip were post-fixed with 1% osmium tetraoxide in 0.1 M phosphate buffer for 30 min. Then the coverslips were washed for 15 min in distilled water, dehydrated in an ascending alcohol series from 30% to 100% ethanol (5 min each) and critical-point dried. Thereafter, the coverslips were mounted on stubs, gold sputtered and examined with an FeG-SEM Hitachi S4100 electron microscope (Hitachi High Technologies Co LTD, Tokyo, Japan).

Trematodes

Specimens were fixed in 2.5% glutaraldehyde in 0.1 M phosphate buffer (pH 7.4). The worms were dehydrated in ascending alcohol series from 70% to 100% ethanol

(10 min each) and critical-point dried. Thereafter, the specimens were mounted on stubs, sputter coated with gold and examined as described above.

3.2.3. Transmission electron microscopy (TEM) of myxozoans

Isolated plasmodia from the fillets and infected gall bladders were fixed with 2.5% glutardaldehyde in 0.1 M PBS (pH 7.4). The gall bladders were fixed by injecting the fixative slowly into the bladders, using a syringe with a fine needle (0.3mm diameter) in order to fix myxozoan stages and the epithelium of the gall bladder immediately and not await the slow penetration of the fixative through the gall bladder wall. Samples were then placed in an eppendorf with fixative and left to fix for several days. After several washes with PBS, samples were post-fixed with 1% osmium tetraoxide in 0.1 M PBS and dehydrated in an ascending alcohol series from 30% to 100% ethanol. Samples were transferred from 100% ethanol into epoxypropane. Embedding was performed by adding 60% epoxypropane/40% epon araldite and leaving the mixture to desiccate for 12 hours at 4ºC. Samples were then transferred into moulds with fresh epon and dried for 48 hours at 60ºC in an oven. Ultrathin sections mounted on grids were stained with 5% uranyl acetate in distilled water for 15 minutes and Reynold's lead citrate solution for 5 minutes.

An alternative protocol for rapid processing using Agar low viscosity (ALV) resin (Agar Scientific, Essex, UK) was followed for some of the infected gall bladders. After fixation with glutaraldehyde and osmium tetraoxide as described above, the samples were washed with distilled water and transferred to 2% Uranyl Acetate in 30% Acetone in the dark for 1 hour. The tissue was then dehydrated in an ascending acetone series from 30% to 100% acetone. Gall bladders were transferred from 100% acetone into ALV resin. The mixture was then transferred into moulds and left to polymerise for 16 hours at 65ºC.

Semithin sections were cut, stained with 1% toluidine blue (TB) for 1 min and mounted. Ultrathin sections were cut and mounted on grids. Grids were examined in a JEM 100B transmission electron microscope (JEOL Ltd, Peabody, MA, USA) and a Tecnai™ G2 Spirit TWIN / BioTWIN (FEI Company, Oregon, USA).

3.2.4. Statistical analyses of morphometric data of myxozoans

To determine morphological differences between myxospores, the measurements were analysed statistically. The Kolmogorov-Smirnov test was used for checking the

normal distribution and the significance of the data. Differences between spores from different hosts were tested using a t-test. Principal component analysis (PCA) was carried out for further data exploration. Finally, a t-test was applied to detect differences between the two components obtained with PCA. All statistical analyses were carried out using the computer program SPSS 15 (SPSS Inc.).

3.2.5. Histology

For histological examination, organs were fixed in 10% neutral buffered formalin. The samples were then placed in cassettes, dehydrated in alcohol series, transferred through xylene into paraffin, in which they were embedded. Six µm sections of the tissues were stained with haematoxylin and eosin (H&E), Gram stain and 1% toluidine blue.

3.3. Molecular analysis

3.3.1. DNA Extraction, PCR, sequencing and alignment

Whole worms (trematodes), large plasmodia, infected bile, gall bladder, blood and liver (myxozoans) were placed in 300 - 400µl TNES urea (10 mM Tris-HCl (pH 8), 125 mM NaCl, 10 mM ethylenediaminetetraacetic acid, 0.5% sodium dodecyl sulphate, 4 M urea) (Asahida et al. 1996), and sometimes stored over several days before DNA extraction. For extraction, the samples were digested with 100 µg/ml proteinase K overnight at 55ºC. DNA was extracted using a conventional phenol-chloroform protocol (Holzer et al. 2004). The extracted DNA was resuspended in 20-200 µl of RNAse/DNAse free water and left to dissolve overnight in the fridge.

Polymerase chain reactions were performed with a programmable thermal cycler (Techne, TC-512, GMI, Minnesota, USA) in a final volume of 30 µL containing 0.5 U of Thermoprime Plus DNA polymerase and 3 µL of the related 10X buffer with 1.5 mM $MgCl_2$ (ABgene, Epsom, UK), 0.2 mM of each dNTP, 0.5 µM of each primer and approx. 100 ng of DNA. Three fragments were amplified from the genomic ribosomal DNA (rDNA) gene tandems: partial SSU rDNA, partial LSU rDNA and the whole internal transcribed spacer 2 (ITS2).

The PCR protocol consisted of initial denaturation at 95ºC (3-5 min) followed by 35-40 cycles of amplification (denaturation at 95ºC (50s), specific annealing temperature (30s) for each primer pair used (see Table 3.2) and extension at 72ºC (1-

2 min)) and a final extension at 72ºC (4-7 min). When necessary, nested PCRs were conducted using 1 microliter of the 1st PCR in the second round.

After checking for the presence of PCR amplicons in a 1% agarose gel in sodium borate buffer, PCR products were purified for sequencing using the GFX PCR DNA and Gel Band Purification Kit (GE Healthcare UK Limited, Little Chalfont, Buckinghamshire, UK). Cycle sequencing was conducted in a 48 capillary ABI 3730 sequencer (Applied Biosystems) using the BIG Dye Terminator v 3.1 Ready Sequencing Kit (Applied Biosystems) according to the manufacturer's instructions. PCR primers and additional primers were used for sequencing in order to obtain widely overlapping parts of the sequences for assembly (see Table 3.2). Whenever possible, two replicate samples of each species/spore type were sequenced. All obtained sequences obtained were submitted to the Basic Local Alignment Search Tool (BLAST) on GenBank™ to confirm their correct origin. All new sequences were submitted to GenBank™ (http://www.ncbi.nlm.nih.gov/genbank/GenbankSearch.html) and accession numbers were obtained which are stated in Appendix 1. Sequences were assembled using the program BioEdit (Hall 1999). Based on a BLAST search for each new DNA sequence, closely related taxa as well as representatives of other previously defined phylogenetic clades were obtained from GenBank™ and were used for sequence alignment. All sequences obtained were aligned using the computer program Clustal X (Thompson et al. 1997), assigning a specific gap opening penalty and a gap extension penalty specified in each chapter (Sections 4.2.4, 5.2.3 & 6.2.3). Ambiguous regions of the alignment were identified with the help of the program GBlocks 0.91b (Castresana 2000) and were excluded from phylogenetic analyses.

Table 3.2 Name, target region, sequence, species used for (see Chapter 4, 5, 6 & 8) annealing temperature and origin of the primers used for amplification (PCR), nested PCR (nPCR) and sequencing (Seq, *). F=forward primer, R=reverse primer.

Primer	Target	Sequence	Species used for	Use	Annealing temp.	Author
ERIB1 (F)	SSU rDNA	5'-ACCTGGTTGATCCTGCCAG-3'	*Unicapsula pflugfelderi* & *Ceratomyxa* spp.	PCR; Seq	48ºC	Barta et al. 1997
ERIB10 (R)	SSU rDNA	5'-CTTCCGCAGGTTCACCTACGG-3'		PCR; Seq		Barta et al. 1997
18e (F)	SSU rDNA	5'-CTGGTTGATCCTGCCAGT-3'	*Unicapsula pflugfelderi* & *Ceratomyxa* spp.	PCR; Seq	56ºC	Hillis & Dixon 1991
18R	SSU rDNA	5'-CTACGGAAACCTTGTTACG-3'		PCR; Seq		Whipps et al. 2003
Lin 3 (F)	SSU rDNA	5'-GCGGTAATTCCAGCTCCA-3'	*Skoulekia meningialis* & *Ceratomyxa* spp.	Seq	*	Lin et al. 1999
Lin 10 (R)	SSU rDNA	5'-CACTCCACGAACTAAGAA-3'	*Ceratomyxa* spp.	Seq	*	Lin et al. 1999
Worm A (F)	SSU rDNA	5'-GCGAATGGCTCATTAAATCAG-3'	*Skoulekia meningialis*	PCR; Seq	56ºC	Littlewood & Olson 2001
Worm B (R)	SSU rDNA	5'-CTTGTTACGACTTTTACTTCC-3'		PCR; Seq		Littlewood & Olson 2001
MyxospecF	SSU rDNA	5'-TTCTGCCCTATCAACTWGTTG-3'	*Unicapsula pflugfelderi*	nPCR; Seq	52ºC	Fiala 2006
MyxospecR	SSU rDNA	5'-GGTTTCNCDGRGGGMCCAAC-3'		nPCR; Seq		Fiala 2006
U178 (F)	LSU rDNA	5'-GCACCCGCTAAYT-TAAG- 3'	*Skoulekia meningialis*	PCR; Seq	55ºC	Lockyer et al. 2003
L1642 (R)	LSU rDNA	5'-CCAGCGCCATC-CATTTTCA-3'		PCR; Seq		Lockyer et al., 2003
LSU1200 (R)	LSU rDNA	5'-GCATAGTTCACCATCTTTCGG-3'	*Skoulekia meningialis*	Seq	*	Lockyer et al. 2003
Kt28S1F	LSU rDNA	5'-CAAGACTACCTGCTGAAC-3'	*Unicapsula pflugfelderi*	PCR; Seq	56ºC	Whipps et al. 2004
28S1R	LSU rDNA	5'-GTGTTTCAAGACGGGTCG-3'		PCR; Seq		Whipps et al. 2004
GA1 (F)	ITS2 rDNA	5'-AGAACATCGACA-TCTTGAAC-3'	*Skoulekia meningialis*	PCR; Seq	53ºC	Anderson & Barker 1998
ITS2.2 (R)	ITS2 rDNA	5'-CCTGGTTAG-TTTCTTTTCCTCCGC-3'		PCR; Seq		Cribb et al. 1998
CDF	SSU rDNA	5'-TCCAAACAATGCGGCCCACTC-3'	*Ceratomyxa puntazzi*	PCR; Seq	58ºC	**Present study**
CDR	SSU rDNA	5'-TAAGCAGCGACCGCTCCAAC-3'		PCR; Seq		**Present study**

3.3.2. Phylogenetic analyses

The phylogenetic position of the investigated taxa was estimated by a likelihood-based Bayesian tree sampling procedure (BI) using MrBayes v3.1.2 (Ronquist & Huelsenbeck 2003) and a maximum parsimony (MP) approach using PAUP* Version 4.0b10 (Swofford 2002). The general time-reversible model (GTR+I+Γ; Tamura & Nei 1993) was estimated as the best substitution model for all data sets using jModeltest version 0.1.1 (Posada 2008). Thus, parameters corresponding to this model (nst=6 basefreq=empirical, rates = invgamma) were applied in the BI analysis. Posterior probability distributions were generated using the Markov Chain Monte Carlo (MCMC) method. The MCMC was run for 1,000,000 generations sampling every 100^{th} tree and burn-in was set for each run (specified in each relevant chapter), when the process had reached a stationary state. MP used a heuristic search with tree bisection-reconnection (TBR) branch swapping, random addition of taxa (n=10) and the ACCTRAN option. Transition/transversion ratio was 1:2 and gaps were treated as missing data. Clade support was assessed by bootstrapping (1000 replicates). All trees were unrooted. The computer program FigTree v1.3.1 (Rambaut 2009) was used to visualize trees.

CHAPTER 4. The blood fluke *Skoulekia meningialis* n. gen., n. sp. surrounding the brain of *Diplodus vulgaris* (Geoffroy Saint-Hilaire 1817)

4.1. Background

Currently, the family Aporocotylidae consists of 28 genera (May 2011) (Smith 2002; Nolan & Cribb 2004a; Nolan & Cribb 2004b; Nolan & Cribb 2005; Nolan & Cribb 2006a; Nolan & Cribb 2006b; Bullard et al. 2008; Bullard & Jensen 2008; Bullard 2010). Only two genera of aporocotylids have been reported in the Mediterranean: *Cardicola* Short 1953 from the gilthead sea bream *S. aurata* (Holzer et al. 2008) and *Paradeontacylix* MacIntosh 1934 from the greater amberjack *Seriola dumerili* (Risso 1810) (Repullés-Albelda et al. 2008). In both cases, the parasites have been related to pathological effects and even mortalities (Crespo et al. 1992, 1994; Padrós et al. 2001).

During the parasitological study of the Mediterranean aquaculture candidate species common two-banded seabream *D. vulgaris*, a previously undescribed blood fluke was found in the blood vessels of the meninx of the host, a rather unusual location. This species showed similarities to the genera *Pearsonellum* Overstreet & Køie 1989 and *Psettarium* Goto & Ozaki 1930 but did not match their descriptive diagnoses exactly. The combination of a detailed morphological study and phylogenetic studies based on various regions of the rDNA gene resulted in the erection of a new aporocotylid genus, *Skoulekia* n. gen. Furthermore, a histopathological study was conducted in order to determine whether the special location of the aporocotylid worm or its eggs cause any adverse effects in the host and could thus be considered a problem for cultures of *D. vulgaris* in the Mediterranean.

4.2. Materials and methods

4.2.1. Sample collection

D. vulgaris (n=215; 10.0-27.7 cm total length; 15-336 g) were purchased at Valencia's fishing harbour (Spanish Mediterranean coast; see Table 3.1). Forty specimens were examined within 6-24 h after capture. The skull of each fish was opened dorsally and the brain was gently removed as a whole. Gills and heart were also removed. The organs were examined in 0.85% saline using a dissection microscope at 6.8x-80x magnification. Additionally, fresh smears of the gills were examined under optical microscope at 400X. The worms were used for either DNA extraction (n=4) or for morphological description by LM (n=23) and SEM (n=3)

(Chapter 3, Section 3.2.1 & 3.2.2). All type specimens were obtained from fresh fish. Additionally, the heads (from mouth to operculum, including skull, eyes, gills and heart) of 25 fresh fish captured in the same location from November/December 2008 were removed and whole heads were fixed in 10% neutral buffered formalin for histopathological analysis. The remainder of the fish was frozen at -20ºC and thawed on the day of examination. In the freeze-thawed fish only the brain was screened for the presence of parasites and the worms were fixed in 70% ethanol after recovery. Infection parameters were estimated following Bush et al. 1997.

4.2.2. Morphological analysis

For morphological analysis based on LM, ethanol fixed worms were stained with iron acetocarmine (n=20) or alum carmine (n=1). Specimens were processed as described in Chapter 3, Section 3.2.1. Due to the difficulties related to recognizing the dimensions of the testis, some worms were processed following particular procedures: one worm stained with acetocarmine was cut sagitally with the help of a razor blade in slices of about 500µm in order to examine the transversal extension of the testis. Each slice was sequentially oriented and mounted in Canada balsam. Another worm was dehydrated, cleared and mounted in Canada Balsam without staining in order to study the lateral distribution and extension of the testis. Drawings and measurements of stained specimens were made as described in Chapter 3, Section 3.2.1.

4.2.3. Histopathology

The cephalic regions of *D. vulgaris* were processed as described in Chapter 3, Section 3.2.5. After fixation, an extra step was done. The cephalic regions were decalcified in 8% formic acid for 72 hours, replacing the formic acid every 24 hours. The skull containing the brain was then cut frontally in two "halves" using a scalpel blade. Worms were firstly found in 6 µm sections performed every 300 µm of tissue, stained with 1% toluidine blue (30 min). On parasite detection, more 6 µm serial sections were produced, stained with haematoxylin and eosin (H&E) and analysed for pathological changes. Two gill archs from each decalcified head were also processed histologically.

4.2.4. Molecular data and phylogeny

DNA extraction, PCR, sequencing and alignment of the obtained sequences were done as described in Chapter 3, Section 3.3.1. Three fragments were amplified from the genomic ribosomal DNA (rDNA) gene tandems: partial SSU rDNA, partial LSU rDNA and whole internal transcriber spacer 2 (ITS2).

All sequences obtained were submitted to the BLAST to identify the closest relatives published to date. Selected taxa for sequence alignment are included in Table 4.1. Phylogenetic analysis was applied as described in Chapter 3, Section 3.3.2. In Clustal X, a gap opening penalty of 15.0 and a gap extension penalty of 6.0 were applied. In the BI analysis, the MCMC burn-in was set at 55,000 generations. In the LSU rDNA phylogenetic analysis of aporocotylid taxa, *Plethorchis acanthus* Martin 1975 was used as outgroup. Due to the large ITS2 sequence divergence between more distantly related aporocotylid genera, the phylogenetic analysis of ITS2 data included only the present species and the most closely related genera *Pearsonellum* and *Psettarium.* The sequence of *Paradeontacylix sinensis* Liu 1997 was also included as this species was ascribed to the genus *Psettarium* (Ogawa et al. 2007).

Table 4.1 Aporocotylid LSU and ITS2 rDNA sequences used in the phylogenetic analyses.

Species/Type	Length (bp)	GenBank™ acc. no.
LSU rDNA sequences		
Plethorchis acanthus	1218	AY222178
Paradeontacylix kampachi	1613	AM489595
Paradeontacylix ibericus	1613	AM489593
Paradeontacylix godfreyi	1613	AM489597
Paradeontacylix grandispinus	1613	AM489596
Paradeontacylix balearicus	1613	AM489594
Cardicola forsteri isolate CF6	629	EF653388
Cardicola forsteri isolate CF1	698	EF653387
Cardicola forsteri isolate CF27	717	EF653389
Cardicola sp. AH-2007a	1619	AM910616
Paradeontacylix sinensis	1618	EU368853
Sanguinicolid sp. Moorea-DTJL-2002	1618	AY157174
ITS2 rDNA sequences		
Psettarium sp. KH-2007-1	523	EF544057
Psettarium sp. Aburatsubo 3.2	526	EF544056
Pearsonellum pygmaeus	533	AY465874
Pearsonellum corventum	569	AY465873

4.3. Results

4.3.1. Location, prevalence and abundance

The adult worms were detected within the blood vessels surrounding the optic lobes of the brain (Figure 4.1) but were absent from the blood vessels of the heart or gills. A total of 111 adult aporocotylids were detected, with an infection prevalence of 20% (43 of 215 fishes), a mean abundance of 0.52 flukes per fish and a mean intensity of 2.6 flukes per infected fish. A maximum of 11 aporocotylids were found in one fish. Blood fluke eggs were not found in the fresh material. Eggs were detected in the histological sections of the gills with a prevalence of 44% (11 of 25 fishes). Adults were detected in brain histological sections with a prevalence of 4% (1 of 25 fishes).

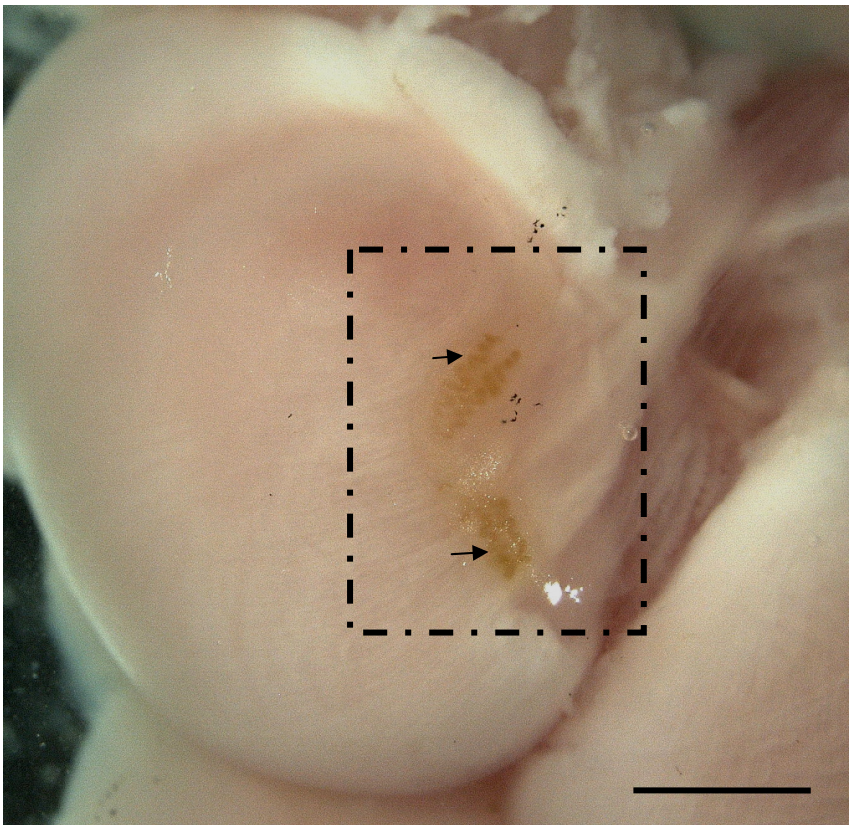

Figure 4.1 Two adult worms of *Skoulekia meningialis* n. gen., n. sp. (selected area) inside an ectomeningeal blood vessel on the surface of the optic lobes of the brain of *Diplodus vulgaris*. Intestinal caeca (arrows) of the aporocotylids are easily distinguished due to their darker color. Scale Bar: 1 mm.

The worms presented specific and unique morphological and molecular features when compared with other species. The taxonomy proposed here is based on the comparison of these features with those of known aporocotylid taxa, resulting in the erection of a new genus.

4.3.2. Morphological description

Aporocotylidae Odhner, 1912

Skoulekia n. gen.

Diagnosis

Body of adult flattened, spatulate, laterally curved, with a dorsosinistral swelling at cirrus sac level. Ventrolateral transverse rows of spines. Ventrolateral tegumental pits present. Oral sucker present. Pharynx absent. Mouth subterminal, medioventral. Oesophagus sinuous along midline. Intestine H-shaped; anterior caeca short, approximately equal in length; posterior caeca long, unequal in length. Testis single

medial, mostly between posterior caeca. Auxiliary external seminal vesicle absent. Cirrus sac post-gonadal, sinistral. Male genital pore dorsomarginal. Ovary post-caecal, post-testicular, dextral. Oviducal seminal receptacle present. Laurer's canal absent. Vitelloduct medial, extending posteriorly dorsal to the ovary. Oötype medial, predominantly post-gonadal. Uterus lateral and posterior to ovary. Female genital pore dorsosinistral, anterior to male pore. Parasites of vascular system of marine teleosts.

Taxonomic summary

Type species: *Skoulekia meningialis* n. gen., n. sp.

Etymology*:* Generic name from "Skouleki" (Greek: worm).

Remarks

Skoulekia differs from other aporocotylid genera by a unique combination of traits, mainly the body dorsally swelled at cirrus sac level, the presence of an oral sucker, the single, mostly intercaecal testis, the dorsal-marginal male genital pore, the absence of an auxiliary external seminal vesicle, the lateral ovary, the lateral uterus and the possession of an oviducal seminal receptacle. This genus has morphological similarities with two other genera: *Pearsonellum* and *Psettarium*. The three genera are compared in detail in section 4.6.

Skoulekia meningialis n. sp.

Morphological description

Based on 22 whole mounted specimens (21 stained and 1 unstained), sagittal sections of 1 stained worm, digital images of 3 living specimens, 3 SEM prepared specimens and eggs in the histological sections of the gills. See Figure 4.2, Figure 4.3 & Figure 4.4. For measurements methodology see section 3.2.1.

With features of the genus. Body flat, curved, 2226 (1642-2800) long, 483 (274-758) wide, 3-6 times longer than wide. Sinistral dorsolateral protuberance at male genital pore level; body dorsally swelled at cirrus sac level (Figure 4.3A,C). Tegument ventrally papillate and dorsally smooth. Ventrolateral rows of spines (Figure 4.2C & Figure 4.3D) present from anterior to posterior end, spines 8.7 (7-10) long and 1.3 (1-1.8) wide (n=14), 10 spines per row, 343-346 rows per side (n=2); rows each

measuring 9.3 (7.23-11.61). Ventral tegumental papillae 1.1 (0.8-1.4) in diameter (Figure 4.3F,G). Ventrolateral tegumental pits 2.3 (1.86-2.75) diameter (n=3), 13.4 (11.67-15.20) distance between them, rather regularly distributed (Figure 4.3F,H). In some stained specimens dorsoventral muscular fibers were visible at the area of posterior caeca. Nerve cords 17.2 (12-24) wide, 39.8 (18-60) from lateral body margin; indistinct posteriorly; nerve commissure medial, 126 (71-164) from anterior end, 76.7 (60-108) wide, 24.6 (16.5-36) long. Vague oral sucker, 31.9 (25.8-36.6) in length, 39.3 (26-50.5) in width. Mouth ventromedial, 10.3 (4.3-12.9) in diameter, 7.5 (4.2-16.8) from anterior end (Figure 4.3B). Oesophagus straight at first half of length, then sinuous, 492 (228-596) long or 8-27% of body length, 30.7 (15-54) of maximum width. Oesophageal glands approx. in mid-oesophageal area, occupying 199 (114-258) in length (26-89% of oesophageal length) and 113 (72-174) in width. Anterior intestinal caeca short, almost equal, 66 (21-126) long or 1-5% of body length, 39.9 (30-54) wide; posterior caeca of unequal length, sinuous; dextral posterior caecum 865 (589-1221) long, 31-47% of body length, 15 times longer than dextral anterior caecum, 49.2 (24-87) wide; sinistral posterior caecum 905 (505-1284) long, 27-47% of body length, 16 times longer than sinistral anterior caecum, 51.1 (30-90) wide; intersection of anterior and posterior caeca 508.4 (384-696) or 15-32% of body length from anterior end. Post-caecal area 679.2 (438-894) long or 26-40% of body length. Testis single, diffuse, mostly positioned in posterior intercaecal field, extending laterally beyond some portions of caeca; 476 (288-726) long, 17-27% of body length, 269 (144-444) wide, 49-78% of body width (n=12); 1.8 times longer than wide; anterior margin of testis posterior to intersection of caeca. Post-testicular area 962.6 (672-1216) or 34-54% of body length. Vasa eferentia not observed. Vas deferens slightly sinuous 762 long, 12.6 (9-18) wide (n=1), extending posteriorly along dorsal surface of ovary, turning sinistrally to enter into cirrus sac; often not observed. Cirrus sac spherical to oval, 82 (46-122) long and 71 (34-118) wide; 1.2 times longer than wide; cirrus sac wall 7.6 (4.5-13.5) thick; post-cirrus sac area 264 (214-319) long or 10-14% of body length; cirrus not observed; male pore 7.4 (6- 11), post-male pore area 328 (265-403) to posterior body end or 13-17% of body length; dorsolateral protuberance surrounding male pore observed externally in SEM specimens (Figure 4.3C,E). Seminal vesicle ovoid, 53 (33-82) long, 43 (27-60) wide.

Ovary dextral, post-caecal, 376 (200-516) long, 8-21% of body length, and 269 (158-420) wide, 36-81% of body width at its level; 1.4 times longer than wide; post ovarian area 342 (267-417) long or 13-19% of body length. Oviduct originating at posterior midline of ovary, 212.5 (147-264) long, 13.7 (9-18) wide, 137.1 (111-204) or 5-10% of body length to posterior end; going dorsosinistral and expanding to form the oviducal seminal receptacle, then narrowing, and entering oötype. Oviducal seminal receptacle 168 (109-252) long and 25 (13-55) wide; 43-89% of oviduct length. Vitellarium follicular extending anteriorly from nerve commissure to dextral posterior end of ovary and to anterior end of uterus, and laterally to body margins. Vitelloduct passing posteriorly along midline and along dorsal surface of ovary; 560 (378-804) long, 14 (6-18) wide; overlapping the vas deferens; continuing sinistrally and ventral to the oviduct and the oviducal seminal receptacle; vitelloduct widens close to its posterior end 166 (88-248) long and 41 (25-53) wide, joining distal portion of oviduct and forming a short common duct before entering oötype posteriorly. Oötype spherical, lateral to oviduct and vitelloduct, 43.6 (33-54) long and 35.9 (24-54) wide; distance between oötype and posterior body end 162 (126-213) or 6-9% of body length. Mehlis'gland surrounding oötype. Uterus convoluted; on exit of the oötype going forward, occasionally describing a single backwards loop beyond oötype, extending parallel to the sinistral margin of ovary until anterior end of ovary, occasionally extending anterior to ovary, then looping backwards sinistral to first section of uterus, before ending in female pore, 25.3 (15-36) wide near oötype, 35.5 (24-57) maximum width. Metraterm indistinct. Female pore, 11.8 (8-20.8) in diameter, opening close to midline and anterior to male pore and cirrus sac; post-female pore area 338 (252-405) to posterior body end or 13-17% of body length. Uterine eggs irregular to spherical and thin-shelled in proximal part of the uterus, regular ellipsoidal, elongate and thicker well defined shell in distal part of uterus (Figure 4.4A); 38 (30-71) long and 15 (11-21) wide (n=56) in distal part of uterus; 30-59% uterus width; shell thickness 2 (1.4-3.6); some uterine eggs contained a large amount of black pigment (Figure 4.4B). Eggs free in gills, consistently elongate 71 (60-80) (n=11) long and 29 (20-40) diameter (n=27) (Figure 4.4C); opercula not observed. Excretory vesicle and collecting ducts not observed. Excretory pore subterminal, dorsomedial, 12.7 (9-18) in diameter.

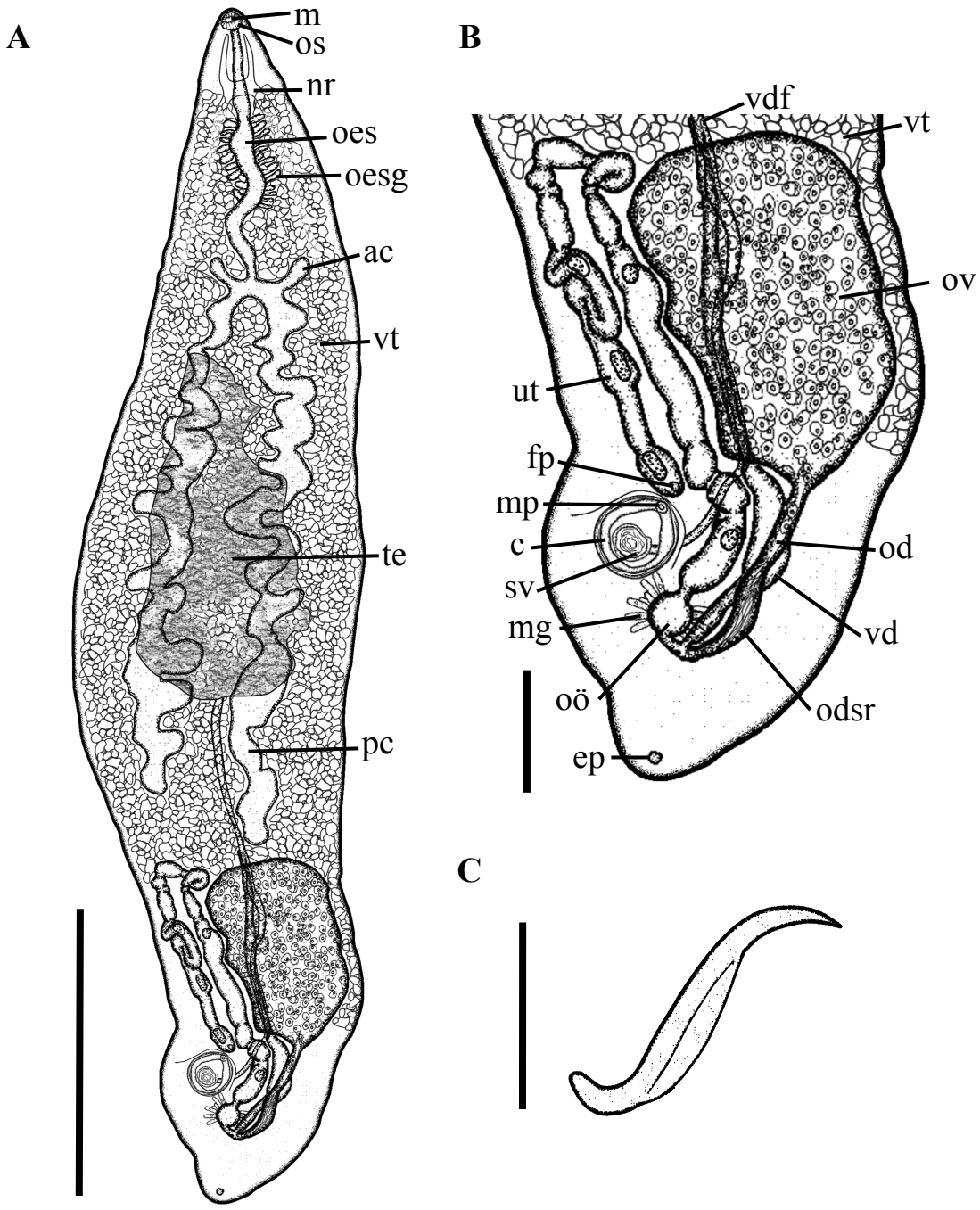

Figure 4.2 Drawing of *Skoulekia meningialis* n. gen., n. sp. isolated from the ectomeningeal veins of *Diplodus vulgaris* off Valencia, Spain. A) Adult, whole worm, dorsal view. B) Detail of posterior body part with reproductive organs, dorsal view. C) Tegumental spine. Abbreviations: m, mouth; os, oral sucker; nr, nerve ring; oes, oesophagus; oesg, oesophageal gland; ac, anterior intestinal caeca; vt, vitellarium; te, testis; pc, posterior intestinal caeca; vdf, vas deferens; ov, ovary; od, oviduct; vd, vitelloduct; odsr, oviducal seminal receptacle; ep, excretory pore; oö, oötype; mg, mehlis' gland; sv, seminal vesicle; c, cirrus sac; mp, male pore; fp, female pore; ut, uterus. Scale Bar: A= 500 µm; B= 250 µm; C= 5 µm.

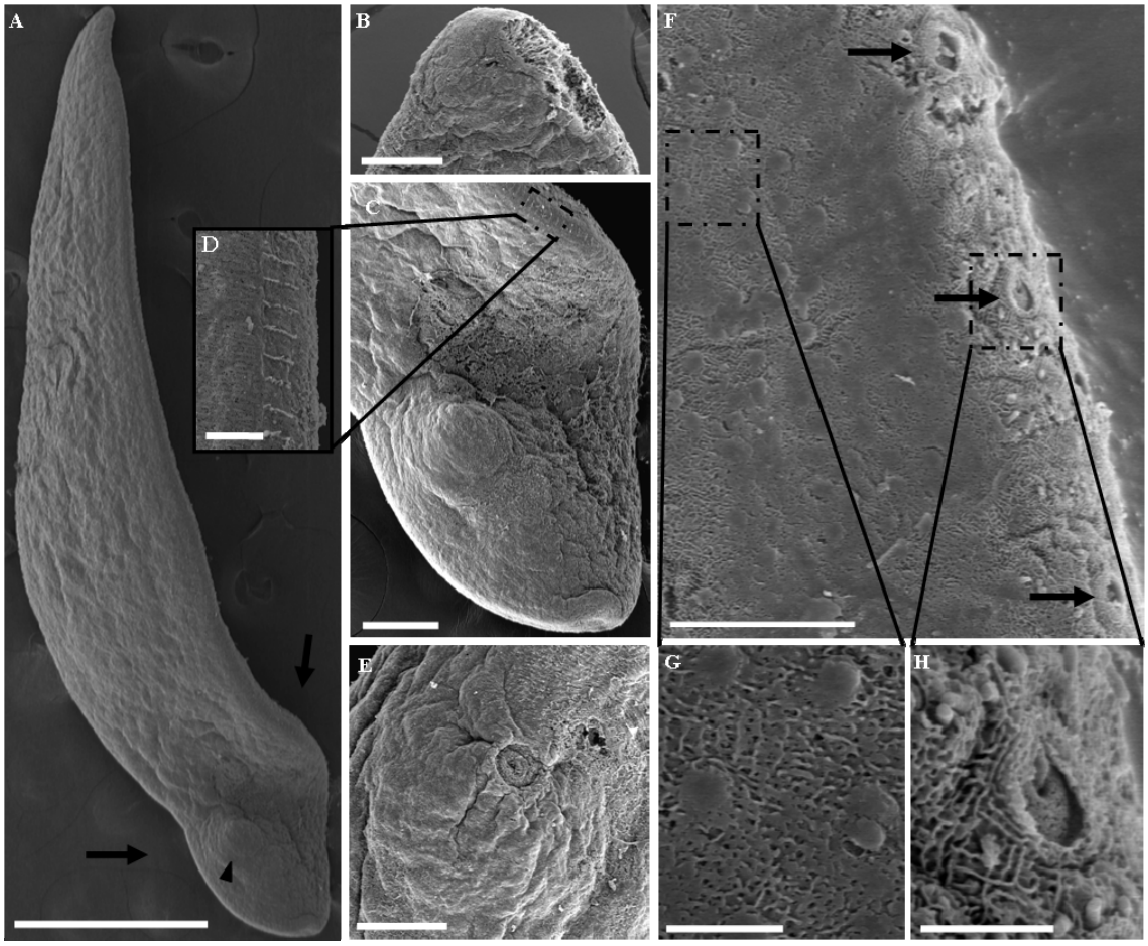

Figure 4.3 *Skoulekia meningialis* n. gen., n. sp. SEM. A) Whole adult worm showing typical body dorsally swelled at cirrus sac level (arrows) and sinistral dorsolateral protuberance at male genital pore level (arrow head). B) Subterminal mouth and oral sucker. C) Sinistral dorsolateral protuberance at male genital pore level in the posterior region of the body. D) Detail of the ventrolateral rows of spines. E) Sinistral dorsolateral protuberance where male pore is located. F) Ventral papillate tegument (selected area) and ventrolateral tegumental pits (arrows). G) Detail of several tegumental papilla. H) Detail of a ventrolateral tegumental pit. Scale Bar: A= 500 µm; B= 30 µm; C= 100 µm; D= 10 µm; E= 50 µm; F= 10 µm; G-H= 250 nm.

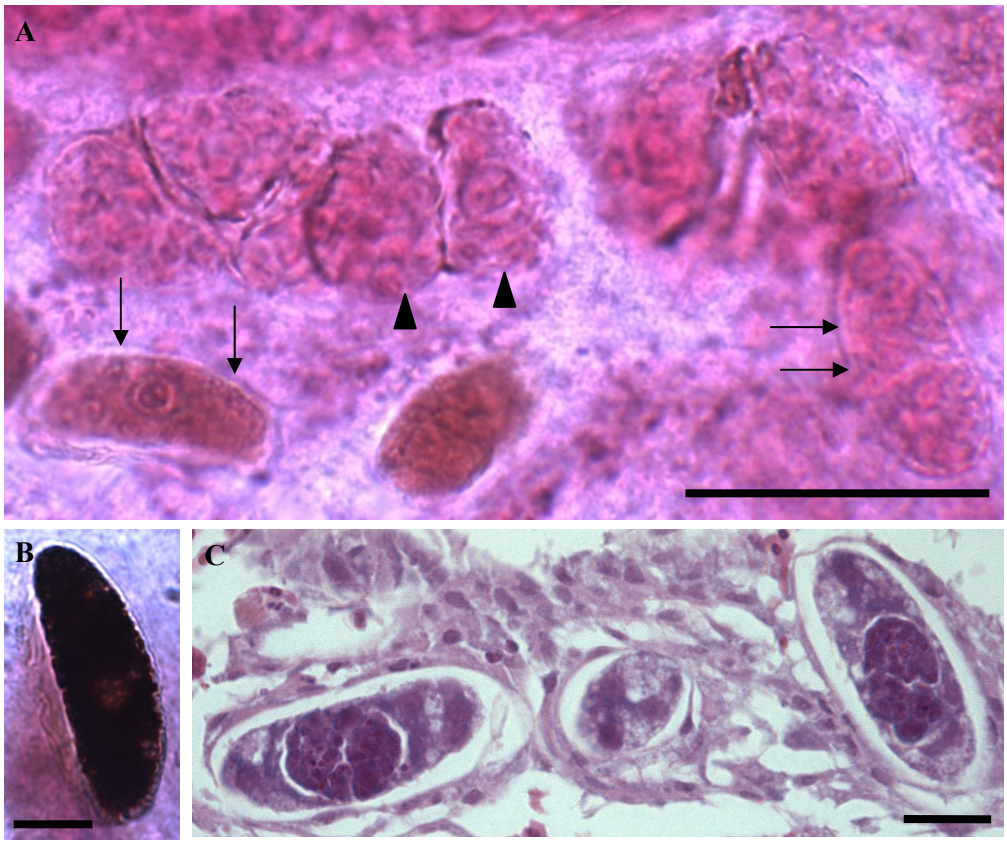

Figure 4.4 Eggs of *Skoulekia meningialis* n. gen., n. sp. A-B. Uterine eggs in stained specimens. A) Varying morphology from irregular spheroid, flexible and thin shelled eggs (arrow heads) to regular ellipsoid, elongate and well defined eggs with shell (arrows). B) Egg containing black pigment. C) Eggs in histological cross-sections of the gills. Note constant elongate shape. Scale Bar: A= 100 µm; B-C= 25 µm.

Taxonomic summary

Type host: *Diplodus vulgaris* (Geoffroy Saint-Hilaire 1817), common two-banded seabream (Perciformes: Sparidae). Length 13.2-24.4 cm; weight 31.75-226 g.

Site in host: meningeal veins.

Type-locality: Gulf of Valencia, Valencia, Spain.

Type specimens: Holotype (2010.9.8.1) and paratype (2010.9.8.2; 2010.9.8.3, 2010.9.8.4; 2010.9.8.5) specimens of *S. meningialis* (microscopic slides of iron acetocarmine stained specimens mounted in Canada Balsam) were deposited in the Collection of the Parasitic Worms Division of the Natural History Museum, London, UK.

Infection parameters: prevalence, 20%; mean abundance, 0.52; mean intensity, 2.6 flukes per fish.

Sequence data: *Skoulekia meningialis* n. gen., n. sp. SSU, internal transcriber space 2 and LSU rDNA sequence, ex. *Diplodus vulgaris*. See Appendix 1.
Etymology: Specific name refers to the site in the host, meningeal veins.

Remarks

The ventral tegumental papillae and the ventrolateral tegumental pits were only visible by SEM but not by LM. These structures have not been described in the species of the closest genera (*Pearsonellum* spp. and *Psetarium* spp.), but not all descriptions included SEM observations. Caeca contained brownish-yellowish material visible in living and mounted specimens. The testis was clearly distinguished in only a few specimens of *S. meningialis*. Testis limits are diffuse and the tissue is extremely difficult to recognise in stained worms. The sections of the acetocarmine stained worm and the DMP cleared worm were most informative for indicating the exact extension and position of the testis. The testis may be undistinguishable due to its involution or degeneration, which was seen to occur when the sperm had been spent in the marine aporocotylids *Aporocotyle simplex* (Odhner 1900) (Thulin 1980) and *Cruoricola lates* Herbert, Shaharom-Harrison & Overstreet 1994 (Herbert et al. 1994). However, the sperm was distinct in most of the specimens of *S. meningialis*. Testes of aporocotylids are not always well-defined but often represent a tissue which is scattered throughout the parenchyma without a defined margin. This idea is supported by the observations that some aporocotylid testes are reticulated and perforated by islands of vitellarium (Manter 1947; Holzer et al. 2008).

The vitelloduct was only visible when passing dorsally to the ovary, until its entry into the oötype. The vitelloduct length given was based on this visible section. The arrangement of the uterus in *S. meningialis* was found to be somewhat variable: i) the first section of the uterus extending forward or backward to the oötype; ii) the following anteriormost section extending to the anterior margin of the ovary or anteriorly to the ovary. The variable arrangement of the uterus is probably related to its position at the moment of fixation, since movements of the uterus were observed in living specimens.

4.4. Specific location and histopathology

Parasites were detected *in situ* (Figure 4.1) in fresh fish and in histological sections (Figure 4.5) within the blood vessels surrounding the brain. In the histological analysis, *S. meningialis* was found inside a thin-walled blood vessel on the surface of the brain (Figure 4.5A,C). This vessel was embedded in the meninges, more specifically in the ectomeninx, and was identified as an ectomeningeal vein. Cross-sections of *S. meningialis* were identified by the presence of sigmoid spines in the tegument, a body consisting of a matrix of parenchymatic cells within which different parts of the female and male genitalia and elongated eggs were recognizable (Figure 4.5B).

A localised, mild but chronic inflammatory response was detected in the ectomeninx (Figure 4.5D-H), which was characterised by infiltration of the blood vessel wall and adjacent ectomeningeal tissue by mononuclear cells, lymphocytes and macrophages (Figure 4.5D). Eosinophilic granulocytes were also present in a smaller proportion (Figure 4.5E). This inflammation of the meninges was accompanied by clotted erythrocytes Figure 4.5B,D). However, the inflammatory response was localised and complete occlusion of the blood vessel was not observed.

Free eggs were observed in the afferent vessels of the primary gill filaments, mainly concentrated at the apex of the filaments. The eggs were embryonated and had an elongate shape (Figure 4.5C). Eggs were not operculated and cilia were not observed in the embryos or larvae within the egg. No direct pathological changes could be detected in gills containing eggs.

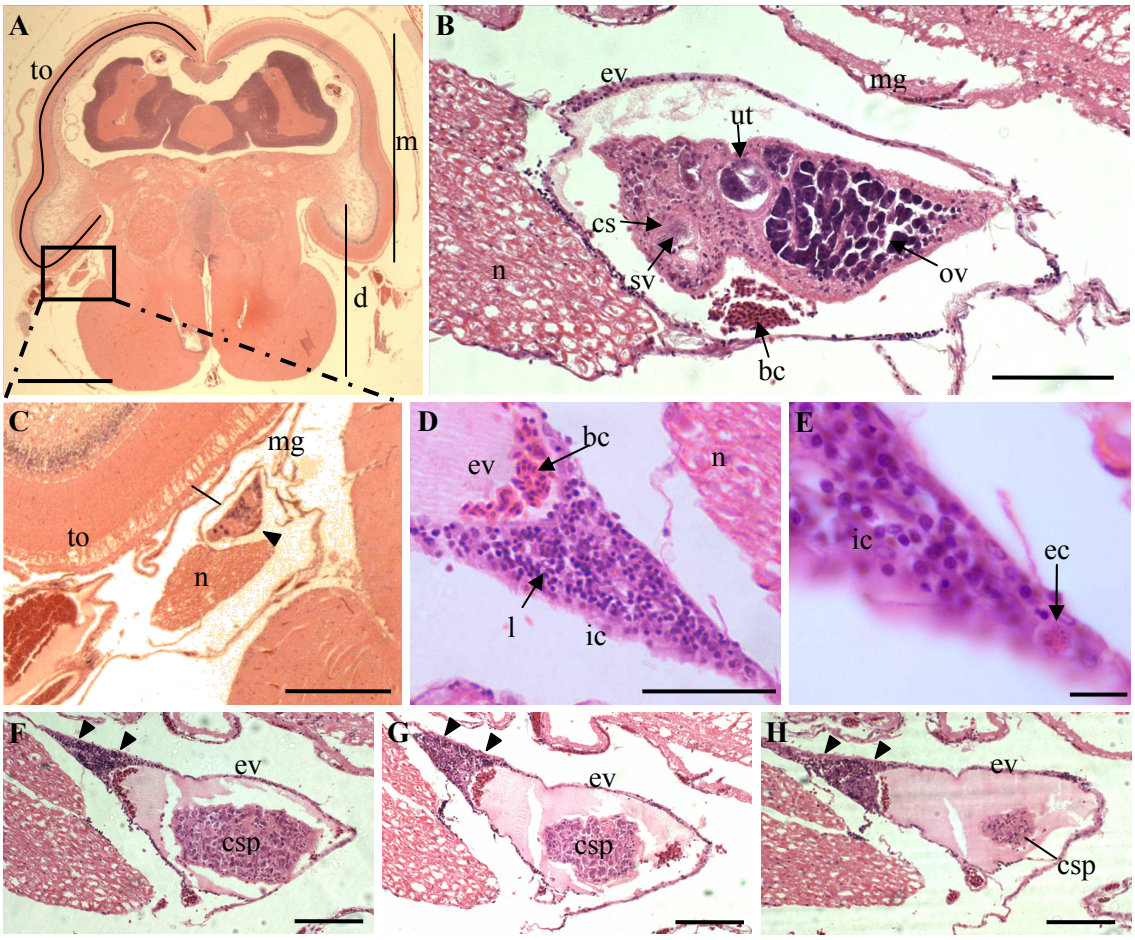

Figure 4.5 *Skoulekia meningialis* n. gen., n. sp. in histological cross-sections of the brain capsule of *Diplodus vulgaris*. A) Location of meningial vein infected by *S. meningialis* (box). B) Magnification of *S. meningialis* inside the vein, with details of parasite visible. C) Detail of Figure 4.5A showing location of *S. meningialis* (arrow head). D-E. Magnification of host tissue response: D) Accumulation of inflammatory cells (mainly lymphocytes). E) Presence of eosinophilic granulocytes. F-H) Sequential sections (every 24µm) showing the extension of the inflammatory response (arrow head). Abbreviations: m, mesencephalon; d, diencephalon; to, tectum opticum; ev, ectomeningeal veins; mg, meninges; n, nerve; sv, seminal vesicle; cs, cirrus sac; ut, uterus; ov, ovary; bc, blood clot; csp, cross-section of parasite; ic, inflammatory cells; l, lymphocytes; ec, eosinophilic cell. Scale Bar: A= 2 mm; B= 100 µm; C= 500 µm; D= 50 µm; E= 10 µm; F-H= 100 µm.

4.5. Molecular characterization and phylogeny

Partial SSU rDNA (1668 bp), partial LSU rDNA (1506 bp) and complete ITS2 rDNA (580 bp) sequences were obtained from *S. meningialis*.

Submission to the BLAST server showed that the SSU rDNA closest sequence matches were *P. sinensis* (GenBank Accession Number EU081899; Query coverage 100%; Maximun identity 98%) and Sanguinicolid sp. Moorea-DTJL-2002 (GenBank Accession Number AY157184; Query coverage 100%; Maximun identity 97%). The LSU rDNA closest sequence matches were also Sanguinicolid sp. Moorea-DTJL-2002 (GenBank Accession Number AY157174; Query coverage 99%; Maximun identity 90%) and *P. sinensis* (GenBank Accession Number EU368853; Query coverage 99%; Maximun identity 90%). The ITS2 rDNA closest sequence matches were obtained by species of the genus *Psettarium*, with query coverage varying between 70% and 80% and sequence identities between 86% and 98%.

SSU rDNA phylogenetic analysis was not carried on as not enough sequences of this region are available in the database to compare properly the new obtained sequence of *S. meningialis*.

The alignment of the partial LSU rDNA sequence of *S. meningialis* with sequences from other aporocotylid taxa showed intergeneric sequence similarities of between 74.6% and 92.1% over an alignment of 3821bp. The highest sequence similarity was obtained with the sequences of Sanguinicolid sp. Moorea-DTJL-2002 (92.1%) and of *P. sinensis* (91.8%).

In order to place *S. meningialis* amongst other, closely related members of the aporocotylids, a phylogenetic study using LSU and ITS2 rDNA was carried out. For the LSU rDNA analysis using BI and MP, 580 informative characters were used (as suggested by GBlocks). The result (Figure 4.6A) shows that *S. meningialis* forms a well-supported sister clade to [Sanguinicolid sp. Moorea-DTJL-2002 and *P. sinensis*]. The next closest clade to *S. meningialis* and [Sanguinicolid sp. Moorea-DTJL-2002 and *P. sinensis*] is occupied by members of the genera *Cardicola* and *Paradeontacylix*.

The alignment of the ITS2 rDNA region showed high sequence divergences between aporocotylid taxa of different genera. Thus, for reliable alignment of *S. meningialis* with other aporocotylids only closely related species, belonging to the genera *Psettarium* and *Pearsonellum* were used. The alignment of all the ITS2 rDNA

sequences available of the genus *Psettarium* proved that the three sequences of *Psettarium* sp. KH-2007 (EF544057, EF544058 and EF544059) are identical. Furthermore, the sequences of *P. sinensis*, *Psettarium* sp. from Kagawa, Oita, China and Aburatsubo (EU082007, EF544037, EF544038, EF544039, EF544040, EF544041, EF544042, EF544043, EF544044, EF544045, EF544046, EF544047, EF544048, EF544049, EF544050, EF544051, EF544052, EF544053, EF544054, EF544055 and EF544056) are conspecific. Thus, only two ITS2 rDNA sequences of *Psettarium* representing the two species were used for phylogenetic analyses: *Psettarium* sp. KH-2007-1 and *Psettarium* sp. Aburatsubo 3.2.

The alignment of the ITS2 rDNA sequences of *S. meningialis* with sequences from *Psettarium* and *Pearsonellum* (641 bp) showed intergeneric sequence similarities of 81.2%-81.4% between *S. meningialis* and the genus *Psettarium,* 72.5%-73.0% between *S. meningialis* and the genus *Pearsonellum*, and 72.8%-73.1 % between *Psettarium* and *Pearsonellum*. Intrageneric similarities between the two sequences of *Psettarium* spp. was 98.7% and between two species of *Pearsonellum* was 95.9%. In the BI and MP phylogenetic analyses of the ITS2 rDNA sequences, 316 informative characters were used (GBlocks results). The cladogram of ITS2 rDNA sequence analysis (Figure 4.6B) shows three well supported clades: [*S. meningialis*], [*Pearsonellum* spp.] and [*Psettarium* spp], supporting the erection of the new genus *Skoulekia*.

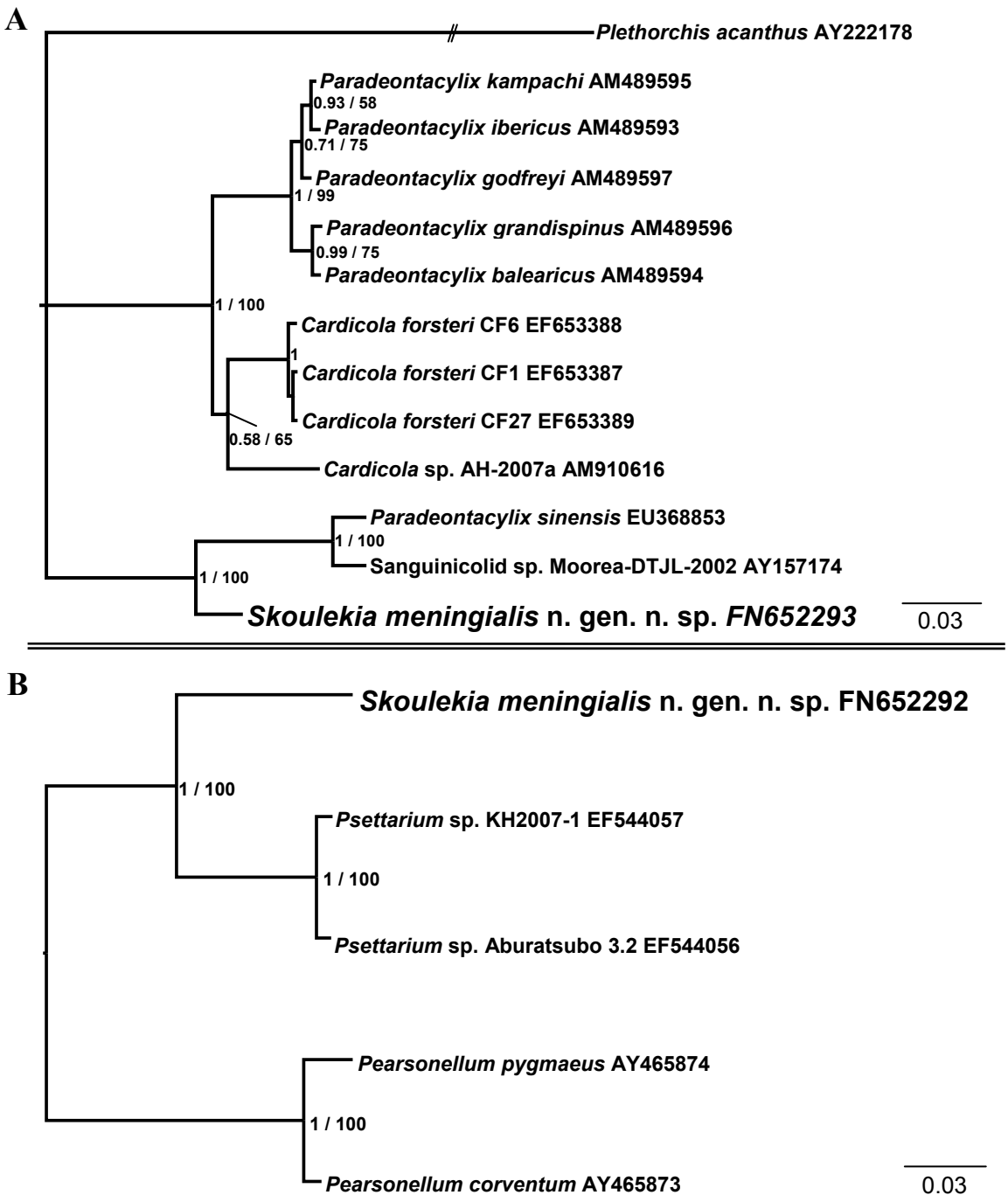

Figure 4.6 Phylogenetic trees based on A) LSU rDNA sequences and on B) ITS2 rDNA sequences of selected aporocotylids, showing the position of *Skoulekia meningialis* n. gen., n. sp. inferred by Bayesian inference (BI) and maximum parsimony (MP). BI analysis selected tree showed. Numbers at nodes represent clade posterior probabilites (BI) and bootstrap values (MP). *Plethorchis acanthus* was used as outgroup for LSU rDNA tree. *Paradeontacylix sinensis* was ascribed to the genus *Psettarium* (Ogawa et al. 2007). Note *Cardicola forsteri* isolates formed a polytomy in the LSU rDNA tree produced by MP. No outgroup was employed for the ITS2 rDNA analysis (tree is midpoint rooted).

4.6. Morphological comparison of the genera *Pearsonellum*, *Psettarium* and *Skoulekia*

Due to the molecular and morphological proximity of the genera *Pearsonellum, Psettarium* and *Skoulekia*, a detailed morphological comparison of the three genera was conducted. All morphological details of the three genera are summarized in Table 4.2 (Goto & Ozaki 1930; Overstreet & Køie 1989; Smith 2002; Bullard & Overstreet 2006).

→*Similarities between Pearsonellum, Psettarium and Skoulekia*

Skoulekia is morphologically similar to *Pearsonellum* and *Psettarium* as they share the following common features: tegumental spines not larger at body end, anterior caeca shorter than posterior ones, testis single, female pore opens anteriorly to male pore, ovary post-caecal. *Skoulekia* shares with *Pearsonellum* the following features: body spatulate, presence of oral sucker, cirrus sac short ellipsoidal, male pore dorsal, presence of an oviducal seminal receptacle - referred to as ovarian seminal receptacle for *Pearsonellum corventum* Overstreet & Køie 1989 - and vitellarium follicular. *Skoulekia* shares with *Psettarium* the following features: body asymmetrical, sinistral body protuberance at male genital pore level, intestinal caeca H-shaped, absence of the auxiliary external seminal vesicle and indistinct metraterm.

→*Differences between Pearsonellum, Psettarium and Skoulekia*

Skoulekia differs from *Pearsonellum* in the following features: *Skoulekia* presents a body dorsally swelled at cirrus sac level whereas *Pearsonellum* has a straight body. The testis of *Skoulekia* lies mostly intercaecal while it extends anteriorly and posteriorly to caeca in *Pearsonellum*. *Skoulekia* lacks an auxiliary external seminal vesicle which *Pearsonellum* posses. *Skoulekia*'s ovary is lateral while *Pearsonellum*'s ovary is medial. The metraterm is indistinct in *Skoulekia* whereas it is conspicuously muscular in *Pearsonellum*. The vitelloduct position is medial in *Skoulekia* but dextral in *Pearsonellum*. *Skoulekia* differs from *Psettarium* in the following features: *Skoulekia* presents an oral sucker whereas in *Psettarium* it is absent. In *Skoulekia* the testes are mostly intercaecal while in *Psettarium* the testes also extend posteriorly to caeca. *Skoulekia* posses an ellipsoideal, short cirrus sac whereas *Psettarium* posses an ellipsoideal but elongate cirrus sac. The position of the male pore is dorsal in *Skoulekia* but marginal in *Psettarium*. The shape of the ovary is round in *Skoulekia* but lobed in *Psettarium*. *Skoulekia* has an oviducal seminal

receptacle which is absent in *Psettarium*. The vitellarium is follicular in *Skoulekia* while it forms tubular acini in *Psettarium*. The vitelloduct position is medial in *Skoulekia* but dextral in *Psettarium*.

Table 4.2 Comparison of morphological characters between the genera *Skoulekia* n. gen., *Pearsonellum* and *Psettarium* (based on original descriptions of the three genera: Goto & Ozaki 1930; Overstreet & Køie 1989; Smith 2002; Bullard & Overstreet 2006 and on the present study).

	***Skoulekia* n. gen. sp.**	***Pearsonellum* spp.**	***Psettarium* spp.**
Body shape	Flattened, spatulate, body laterally curved, sinistral dorsolateral protuberance at cirrus sac level	Flattened, spatulate, body straight	Flattened, elongate, hindbody curved, sinistral lateral protuberance at male pore level
Oral sucker	Present	Present	Absent
Intestinal caeca	H-shaped, anterior caeca shorter than posterior ones	X- or H-shaped, anterior caeca shorter than posterior ones	H-shaped, anterior caeca shorter than posterior ones
Tegumental spines	Not larger at body end	Not larger at body end	Not larger at body end
Male reproductive organs			
Number of testes	1	1	1
Position of testes	Mostly intercaecal	Mostly intercaecal, extending anteriorly and posteriorly to caeca	Intercaecal, extending posteriorly to caeca
Auxiliary external seminal vesicle	Absent	Present	Absent
Cirrus sac	Cirrus sac ellipsoidal short	Cirrus sac ellipsoidal short	Cirrus sac ellipsoidal elongate
Position of male pore	Sinistral, dorsal, postovarian	Sinistral, dorsal, postovarian	Sinistral, marginal, postovarian
Female reproductive organs			
Ovary shape	Ellipsoidal or irregular, entire	Ellipsoidal or irregular, lobed or entire	Irregular, lobed
Ovary position	Lateral	Medial	Medial or lateral
Oviducal (Ovarian) seminal receptacle	Present	Present	Absent
Uterus position	Lateral and posterior to ovary, sometimes anterior to ovary and/or posterior to oötype	Lateral, anterior and posterior to ovary	Posterior to ovary, sometimes with loops lateral to ovary
Metraterm	Indistinct	Conspicuously muscular	Indistinct
Vittelarium	Follicular, extending from dorsal nerve commissure level, to posterior margin of ovary and/or to anterior margin of uterus	Follicular, extending from dorsal nerve commissure level, to termination of posterior caeca or to cirrus sac	Tubular acini, extending from near the anterior end, mid-level of oesophagus or intestinal bifurcation to anterior margin of ovary
Viteloduct	Medial	Dextral	Dextral
Position of female pore	Dorsal, anterior to male pore	Dorsal, anterior to male pore	Dorsal, anterior to male pore
Eggs	Ellipsoidal elongate	Ovoid	Ovoid

4.7. Discussion

The present study describes *Skoulekia meningialis* as a new aporocotylid genus and species discovered in the Mediterranean. After *Cardicola*, this is the second genus described from the host family Sparidae. *Cardicola cardiocola* (Manter 1947) and *Cardicola aurata* Holzer, Montero, Repullés, Nolan, Sitjà-Bobadilla, Alvarez-Pellitero, Zarza & Raga 2008 have previously been described from the sparids *Calamus bajonado* (Bloch & Schneider 1801) in Florida and *S. aurata* in the Mediterranean, respectively. Apart from the present study and during parasitological studies in our laboratory, other aporocotylid species have been detected in other sparid species (authors unpublished data; Isbert W. & Montero F. E. personal communication, Autonomous University of Barcelona). This suggests that Mediterranean sparids are usual hosts for aporocotylids and that a number of aporocotylid species are yet to be discovered. Sparid blood flukes in the Mediterranean may have been overlooked to date due to the fact that this trematode group is difficult to detect and collect (Cribb et al. 2001b; Smith 1997).

The morphological and molecular results provided evidence for *Skoulekia* being closely related with the genera *Pearsonellum* and *Psettarium*. Relatedness of the three genera was not found to be based on the host family, as the members of *Pearsonellum* parasitize the Serranidae, the members of *Psettarium* the Tetraodontidae, Sebastidae and Rachycentridae, and *Skoulekia* the Sparidae.

The analysis of both, LSU and ITS2 rDNA sequences showed that the genus *Skoulekia* occupies a clade which is separated from other genera, supported by high nodal support, thus suggesting that the erection of a new genus is justified, based on both, morphological and molecular characteristics.

In the LSU rDNA sequence analysis, the clade formed by *P. sinensis* and Sanguinicolid sp. Moorea-DTJL-2002 is a sister clade of *Skoulekia*. *P. sinensis* was reascribed to the genus *Psettarium* and is molecularly identical with *Psettarium* sp. described in Ogawa et al. (2007). Sanguinicolid sp. Moorea-DTJL-2002 has not been described morphologically but is likely to be a member of the genus *Psettarium*. Unfortunately, LSU rDNA sequences of the genus *Pearsonellum* are not available which is problematic as ITS2 sequences differ considerably (27%-27.5% sequence divergence), especially in the 3' part of the sequence, corresponding with helix IV of the ITS2 secondary structure (Schultz et al. 2005), and rendering this ITS2 region

without possibility for intergeneric comparison. The phylogenetic analysis of the remainder of the ITS2 rDNA sequences showed a clear separation of the genera with *Skoulekia* being positioned between *Psettarium* and *Pearsonellum*. Thereby *Psettarium* is molecularly more closely related to *Skoulekia*. Despite the fact that *Pearsonellum* has more morphological features in common with *Skoulekia* than with *Psettarium*, the latter two genera share particular traits which are unusual for aporocotylids, as the asymmetry and the sinistral body protuberance at male genital pore level. However, because ITS2 rDNA sequences can only be used for differentiation between members of the same or very closely related genera, it has to be stressed that sequences for more conservative regions of the ribosomal gene (SSU and LSU rDNA) are necessary for the phylogenetic analysis of the Aporocotylidae in order to postulate a phylogenetical hypothesis for this group, which is still lacking (Bullard & Overstreet 2008).

S. meningialis was found to use the meningeal veins as a specific habitat in *D. vulgaris*. Although the vast majority of aporocotylids infect intravascular sites in the gills and the heart (Smith 1997), this is not the first record of aporocotylids in the cephalic region: *A. simplex* has been found in the major arteries of the head of fish belonging to the family Pleuronectidae (Thulin 1980), *Sanguinicola rutili* Simón-Martín, Rojo-Vázquez & Simón-Vicente 1987 was described in the cerebral vessels of *Rutilus arcasi* (Steindachner 1866) (Simón-Martín et al. 1988), and *Sanguinicola idahoensis* Schell 1974 was found in the blood vessels and connective tissue of the head, the choroid coat, the iris stroma, the vitreous humor of the eye and the brain surface of *Oncorhynchus mykiss* (Walbaum 1792) (Schell 1974). The latter author (Schell 1974) also suggested that the flukes found on the brain surface could be located in the *Pia mater*, which is possibly the same location as in the case of *S. meningialis*. Fish meninges are composed of four layers (from outside to inside): the ectomeninx and the endomeninx, which is sub-divided into an outer, intermediate and inner layer. The ectomeninx contains mucuous tissue, collagen fibers and blood vessels (Caruncho et al. 1993), which were identified as the specific habitat of *S. meningialis*. However, it is possible that *S. meningialis* also inhabits other cephalic veins. Thulin (1980) described *A. simplex* from arteries of the brain of *Hippoglossoides platessoides* (Fabricius 1780). This location is inopportune as this suggests that eggs released by the adult worms would get trapped in the brain. In contrast, *S. meningialis* can release its eggs into the ectomeningeal veins which drain

into the dorsal sagittal vein, which splits into the right and left posterior cerebral veins, and which finally become the anterior cardinal veins (Aurboonyawat et al. 2007). Thus the blood transporting the eggs reaches the duct of Cuvier and then the heart, from where the eggs can enter the gills, the common exit site for the aporocotylid miracidia from their fish hosts (Bullard & Overstreet 2008). The hypothetical route of the eggs of *S. meningialis* to the exit site (illustrated in Figure 4.7) is considerably longer than that of aporocotylids which are located in the gills or the heart, and eggs may become trapped on the way. It remains unclear what advantages the unusual location in the meningeal veins offer to compensate for the obstacles related to egg release.

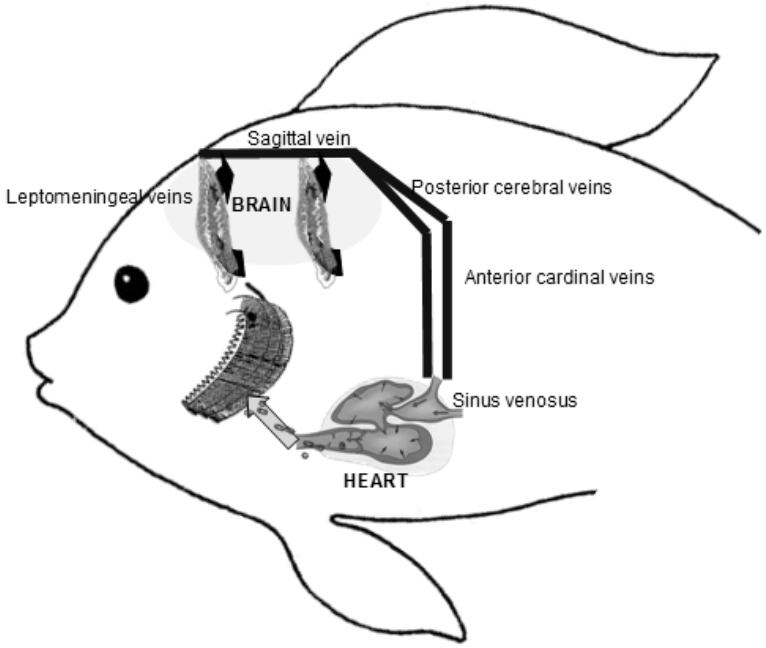

Figure 4.7 Diagram of the potential exit route of the eggs of *Skoulekia meningialis* n. gen., n. sp.

On the other hand, aporocotylids may change their habitat prior to egg release and following seasonal dynamics: species of the genus *Paradeontacylix* migrate to the branchial vessels to deposit eggs during a specific season (Ogawa et al. 1993). *Sanguinicola inermis* Plehn 1905 distribution in *Cyprinus carpio* L. changed with season occurring in the gill vessels in summer months but in the heart in winter time (Iqbal & Sommerville 1984). Thus, the ectomeningeal veins could be a temporal place for *S. meningialis* and the adult might migrate closer to the gills for egg release. However, the large number of specimens of *S. meningialis* found in the

ectomeningeal vessels and not in other locations, the advanced degree of sexual maturation in almost all specimens, as well as the presence of mature eggs in the uterus and in the gills seem to indicate that this habitat is chosen independently from the egg release period.

Blood fluke pathology is produced predominantly by the parasite eggs which accumulate in parts of the circulatory system, mainly the gills (Paperna & Dzikowski 2006). Pathology related to the adult flukes has very rarely been reported in aporocotylids. Disintegrated or degenerated adult flukes in the gill arteries were found to produce necrosis (Thulin 1980) and an increased abundance of melanomacrophages centers was observed in the heart (Overstreet & Thulin 1989). Partial occlusion of blood vessels by dead adults has also been described (Kirk & Lewis 1998). But in other cases the presence of dead worms did not cause a host response at all (Herbert et al. 1995). The present study showed that live adults of *S. meningialis* cause mild histopathological changes, which were restricted to the area surrounding the site the blood fluke resided at. The mild chronic inflammatory meningitis observed involved lymphocytes, macrophages and eosinophilic granulocytes, and the formation of blood clots in the vessel, which could partially obstruct the affected blood vessel. Thus, *S. meningialis* is one of the few reports of pathology caused by living adult aporocotylids in fish.

From a practical point of view, the best method for diagnosis of the presence of *S. meningialis* in *D. vulgaris* has been the detection of eggs in histological sections of the gills. This method presented a higher prevalence (P=45%) than that of adults in fresh material (P=20%) or that of adults in histological sections of the brain (P=4%) for the same fish individuals.

Aporocotylid egg accumulations have been seen to cause important mortalities (Ogawa et al. 2007; Bullard & Overstreet 2008) or to have sublethal effects including reduced food conversion ratios and increased susceptibility to diseases in cultured fish (Herbert et al. 1995). Despite the high prevalence of *S. meningialis* eggs in the gills of the host, no important pathological changes have been detected. The mild chronic parasitic meningitis caused by *S. meningialis* is unlikely to have an important effect on wild *D. vulgaris* populations. However, *S. meningialis* affects the brain, a vital organ, and its effects in culture conditions could be more harmful. Thus the presence of the parasite should be kept in mind in future attempts of *D. vulgaris*

culture in the Mediterranean Sea, especially because of the high incidence and intensity of infection with *S. meningialis* observed in wild fish.

CHAPTER 5. Large cysts of the myxozoan *Unicapsula pflugfelderi* Schubert, Sprague & Reinboth 1975 in the fillets of *Lithognathus mormyrus* (L.)

5.1. Background

Amongst the marine histozoic species, two closely related genera, *Kudoa* and *Unicapsula* (Myxozoa: Myxosporea: Multivalvulidae) can cause important muscle lesions and economical losses in both, live and processed fish. These parasites can make fish unmarketable due to the presence of macroscopic cysts of myxospores within the musculature. Furthermore, it has been reported from several species, that after death of the fish, proteolytic enzymes are released from the plasmodia in the muscle, causing an autolytic process called post-mortem myoliquefaction (Moran et al. 1999a). Two species of *Unicapsula* have been shown to cause myoliquefactive autolysis, i.e. *Unicapsula muscularis* Davis 1924 in Pacific halibut, *Hippoglossus stenolepis* Schmidt 1904, and *Unicapsula seriolae* Lester 1982 in the muscle of *Seriola lalandi* Valenciennes 1833.

Apart from *U. muscularis* and *U. seriolae,* six other species have been described in the genus. Most *Unicapsula* spp. infect the skeletal muscle (Lom & Dyková 2006), only two species were found in the gills and the urinary bladder (Diebakate et al. 1999; Aseeva & Krasin 2001). The teleost hosts belong to several families and have a wide distribution. To date, each species of *Unicapsula* has been reported from only one teleost host.

The sparid sand steenbras *Lithognathus mormyrus* is an important species for aquaculture diversification (Barazi-Yeroulanos 2010) due to its high commercial value and its importance to coastal fisheries. In Turkey and Greece, the biology and culture of this species is being investigated (Firat et al. 2005; Kallianiotis et al. 2005). The parasitological study of *L. mormyrus* in the course of the present work showed that macroscopic cysts filled with spores matching the descriptive diagnosis of the genus *Unicapsula* were present in the muscle of this fish species. The only *Unicapsula* species previously described from the Mediterranean is *Unicapsula pflugfelderi* Schubert, Sprague & Reinboth 1975, occurring in the muscle of the picarel, *Spicara smaris* (Centracanthidae), which is morphologically similar to the one found in *L. mormyrus*. The present chapter aims to elucidate the similarities between *U. pflugfelderi* and the species detected in *L. mormyrus* and to determine whether pathological changes or myoliquefaction occurs in infected *L. mormyrus*.

5.2. Materials and methods

5.2.1. Sampling site and methodology

L. mormyrus (n=24; 22.5-32.5 cm total length; 126.1-499.34 g; 12 females / 12 males) and *S. smaris* (n=24; 13.5-23.5 cm total length; 25.7-161.81 g; 12 females / 12 males) were bought at Valencia's fishing harbour (Spanish Mediterranean coast, see Table 3.1).

Twelve specimens of each species were examined within 24 hours after capture. The skeletal muscle of these fish was separated, squashed between 3 mm thick glass plates, and scrutinized for the presence of myxozoan plasmodia at x80 magnification. Plasmodia were then isolated and examined at x1000 magnification before samples were taken for DNA extraction and morphological description by LM, including histology, SEM and TEM. The remaining fish (used for analysis of prevalence) were frozen at -20ºC and thawed on the day of examination.

5.2.2. Morphological examination

Individual plasmodia were examined and measured at x125 magnification. Measurements of length and width of 101 plasmodia (56 from 4 *L. mormyrus* and 45 from 5 *S. smaris*) were taken. Thirty spores from each host species, derived from 3 plasmodia each of 5 host fish were measured using the parameters defined in Figure 5.1. In order to measure the length of the polar filament, spores were exposed to a 0.2 M KOH solution. Fifty one polar filaments were measured: 25 polar filaments of 2 *L. mormyrus* and 26 polar filaments of 2 *S. smaris* derived from 2 plasmodia of each fish. The rudimentary polar capsules were measured manually on SEM photographs (4 spores of *L. mormyrus* and 3 spores of *S. smaris*).

In order to determine if any morphological differences exist between the spores obtained from the two fish hosts, spore measurements (Figure 5.1) were analysed statistically (see Chapter 3, Section 3.2.4).

SEM and TEM samples were processed as described in Chapter 3, Section 3.2.2 & 3.2.3. For TEM, additionally, several sections were mounted on gold grids and stained by Thiéry reaction for carbohydrates (Thiéry 1967) and by the osmium-thiocarbohydrazide-osmium (OTO) technique for lipids (Seligman et al. 1966).

For histological examination, infected muscle was processed as described in Chapter 3, Section 3.2.5 and the sections were stained with haematoxylin and eosin (H&E) and according to Gram.

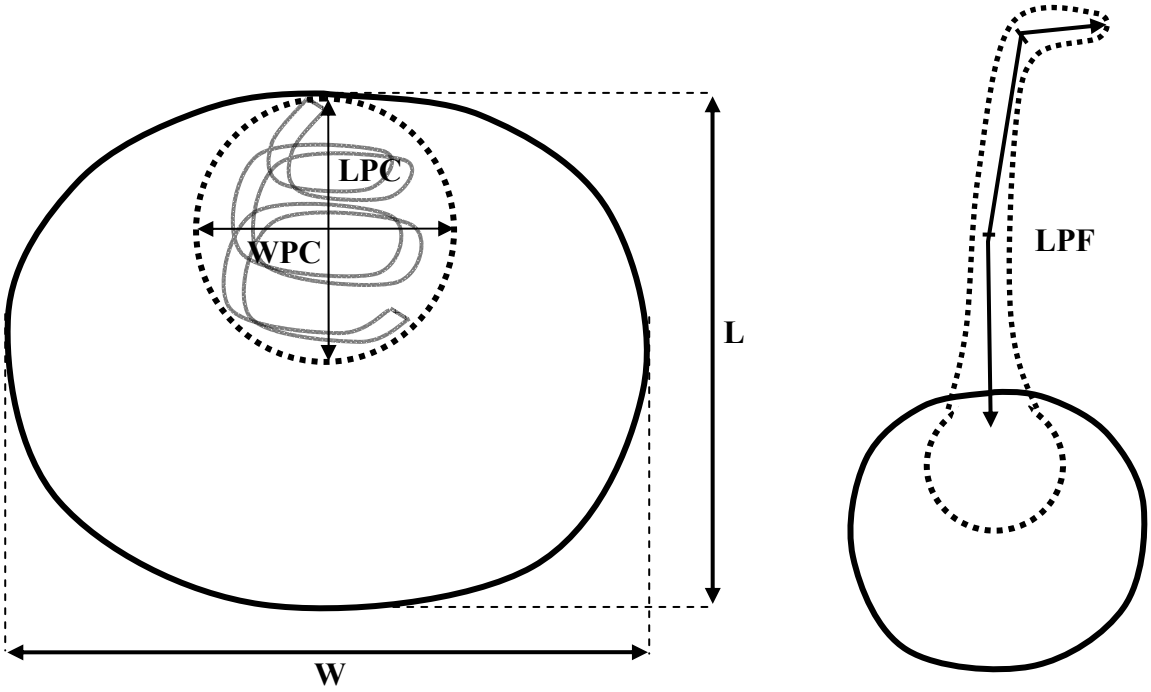

Figure 5.1 Diagram of the measurements taken on the spores of *Unicapsula* sp. L, length of the spore body; W, width of the spore body; LPC, length of the polar capsule; WPC, width of the polar capsule; LPF, length of polar filament.

5.2.3. Molecular data and phylogeny

DNA extraction, PCR, sequencing and alignment of the obtained sequences were done as described in Chapter 3, Section 3.3.1. Two fragments were amplified from the genomic rDNA gene tandems: partial SSU rDNA and partial LSU rDNA.

The SSU rDNA sequences obtained from both fish species were submitted to the BLAST to identify the closest relatives published to date. In order to determine the phylogenetic position of the *Unicapsula* isolates, they were aligned with other myxozoan sequences summarized in Table 5.1. In Clustal X, a gap opening penalty of 8.0 and a gap extension penalty of 5.0 were applied. The phylogenetic position of the *Unicapsula* isolates was estimated by a maximum likelihood (ML) and maximum parsimony (MP) approach using PAUP* Version 4.0b10 (Swofford2001). The general time-reversible model (GTR+I+C; Tamura & Nei 1993) was estimated as the best substitution model for the data set using Modeltest version 3.7 (Posada &

Crandall 1998). Thus, parameters corresponding to this model (nst = 6 basefreq = empirical, rates = invgamma) were applied in the ML analysis. MP was conducted as described in Chapter 3, Section 3.3.2. *Tetracapsuloides bryosalmonae* was used as outgroup in the phylogenetical analyses.

Table 5.1 Myxozoan species and their SSU rDNA sequences used in the phylogenetic analyses.

Species/Type	**Length (bp)**	**GenBank™ acc. No.**
Tetracapsuloides bryosalmonae	1802	U70623
Unicapsula sp.	1683	AY302725
Kudoa iwatai	1602	AY514038
Kudoa rosenbuschi	1740	AY623795
Kudoa miniauriculata	1563	AF034639
Kudoagrammatorcyni	1680	AY302739
Kudoa scomberomori	1680	AY302737
Kudoa thyrsites	1564	AF031413
Kudoa megacapsula	1564	AB188529
Kudoa thalassomi	1565	AY302738
Kudoa yasunagai	1679	AY302741
Kudoa neurophila	1552	AY172511
Sphaerospora dicentrarchi	844	AY278564
Sphaerospora sp	772	DQ377695
Kudoa amamiensis	1739	AY152748
Kudoa shiomitsui	1719	AY302724
Kudoa hypoepicardialis	1721	AY302722
Myxidium bergense	1752	DQ377702
Auerbachia pulchra	1745	DQ377703
Zschokkella mugilis	1632	AF411336
Ellipsomyxa gobii	1697	AY505126
Myxidium incurvatum	1735	DQ377708
Sinuolinea phyllopteryxa	1740	DQ645952
Ceratomyxa shasta	1643	AF001579
Ceratomyxa sparusaurati	1741	AF411471
Palliatus indecorus	1734	DQ377712

5.3. Results

As a consensus of the morphological, ultrastructural and molecular data from this study, the *Unicapsula* spp. found in *S. smaris* and *L. mormyrus* were identified as conspecific and identical with *U. pflugfelderi* (Schubert et al. 1975). Our observations, thus, resulted in the redescription of the species including novel information:

5.3.1. Redescription of *Unicapsula pflugfelderi* (Schubert, Sprague & Reinboth 1975)

5.3.1.1. Morphological data

LM: Elongate and macroscopic plasmodia (Table 5.2) intracellularly in the skeletal muscle (Figure 5.2A-B), with individual muscular fibres infected by individual plasmodia (Figure 5.2C). Polysporic plasmodia consisting of an smooth ectoplasm layer and an endoplasm which contains the spores (Figure 5.2D). Spores sub-spherical (Table 5.2). One refractile, spherical polar capsule visible by light microscopy (Figure 5.2E). Sutural lines indicate the presence of three valves, one larger than the other two, the latter being bilaterally symmetrical. Sporoplasm sometimes visible in the basal part of the spores. In some fresh smears, few aberrant spores with ellipsoidal, “rugby ball”-like shape were observed (Figure 5.2F).

SEM: Subspherical spores without surface ornamentation (Figure 5.3A-C). Three shell valves: one occupying approximately half of the spore, the other two smaller and bilaterally symmetrical (Table 5.2). Shell valves delimited by distinct sutural lines that form a pronounced ridge on spore surface and join forming a Y shape on the apical pole and a T shape on the basal pole (Figure 5.3B-C). Largest polar capsule appeared as an elevation at the surface of the largest valve cell (Figure 5.3B). Two further elevations visible in the smaller valve cells were identified as rudimentary polar capsules by TEM. Ellipsoidal or “rugby ball-shaped” spores were more frequently observed at SEM than at LM (Figure 5.3D). In these spores the large valve cell was collapsed.

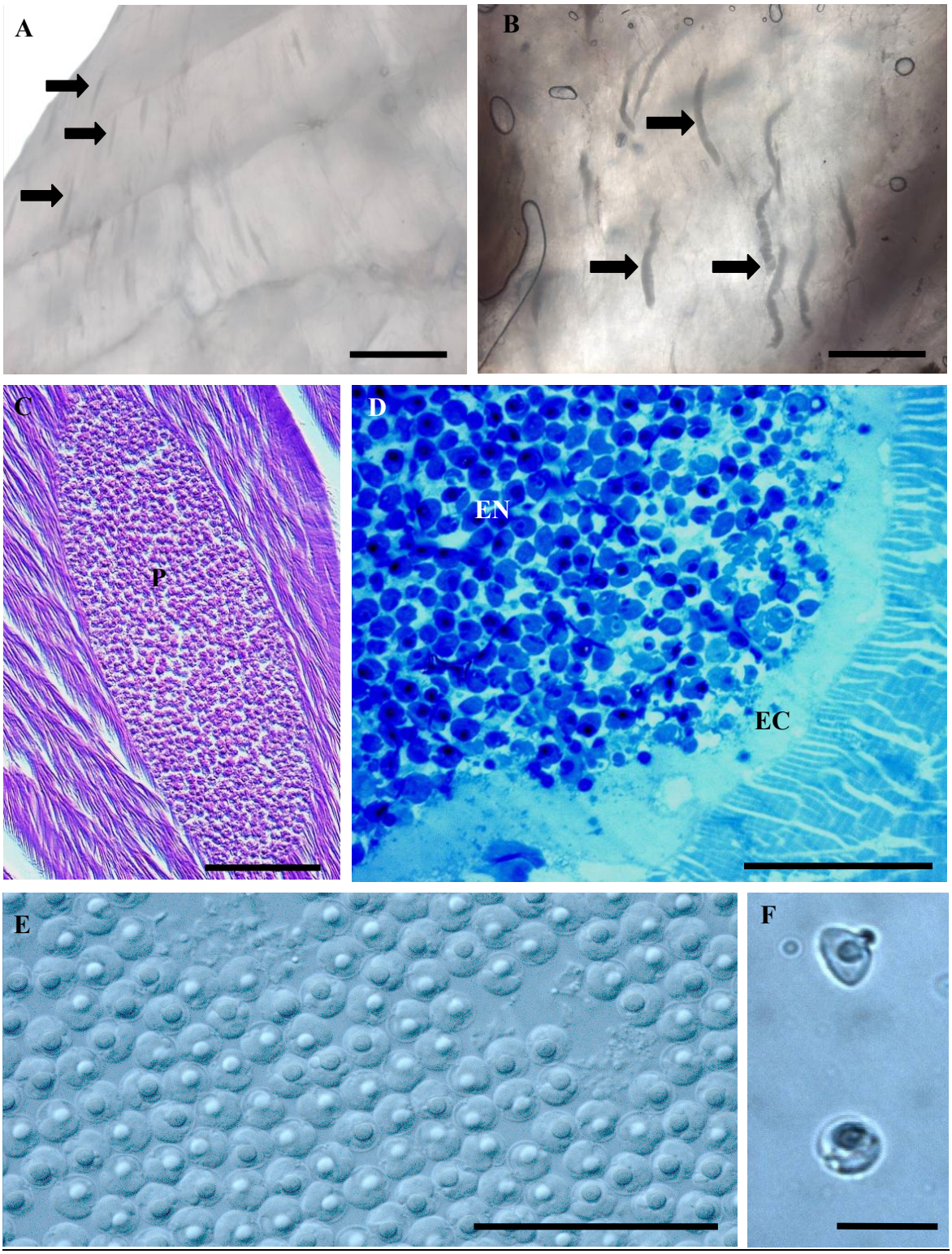

Figure 5.2 *Unicapsula pflugfelderi*: Plasmodia in the muscle of A) *Lithognathus mormyrus* and B) *Spicara smaris*; note plasmodial size difference between the two hosts. C) Section through muscle of *L. mormyrus* showing intracellular position of plasmodium (P), stained according to Gram. D) Semithin section of infected muscle of *S. smaris*, showing ectoplasm (EC) and endoplasm (EN) of the plasmodium. E) Fresh smear of spores from *S. smaris*. F) Fresh preparation of spores from *S. smaris* with normal(bottom)

Figure 5.2 continued: and aberrant ("rugby ball", top) form of spores. Scale bar: A-B= 2mm; C= 50 µm; D-E= 30 µm; F= 10 µm.

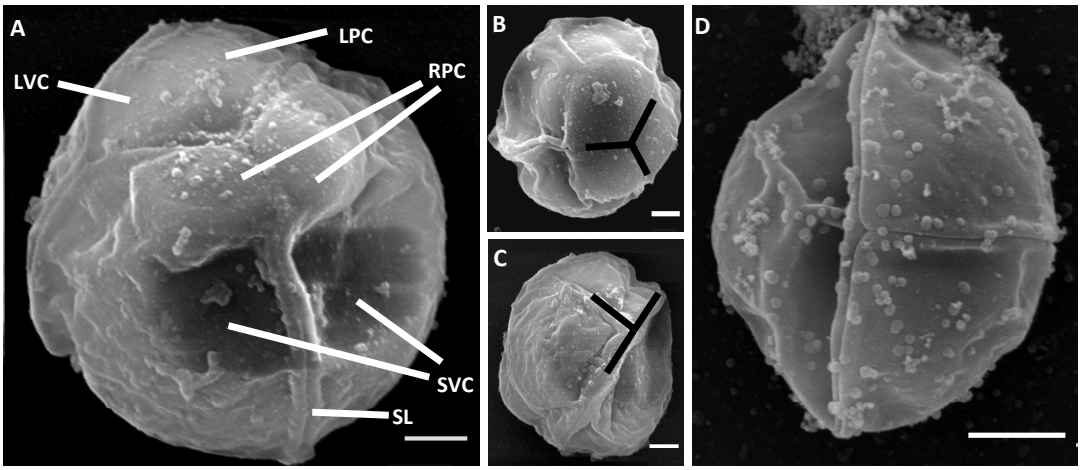

Figure 5.3 Scanning electron microscopy (SEM) images. A) SEM of spores of *Unicapsula pflugfelderi* from *Lithognathus mormyrus* indicating ultrastructural features. B) lateral-apical and C) lateral-basal view of spores indicating patterns of connection between shell valves. D) Spore of *U. pflugfelderi* from *Spicara smaris* with aberrant shape (rugby ball) due to collapse of large valve cell. Abbreviations: LVC, large valve cell; SVC, small valve cell; LPC, large polar capsule; RPC, rudimentary polar capsule; SL, sutural lines. Scale bar: A-C= 500 nm; D= 1 µm.

TEM: Large (1-2 µm) lipid vesicles (OTO-positive) inside granular endoplasm of plasmodia. Ectoplasmic layer ranging 1.61-3.92 µm in thickness.

Spores composed of three capsulogenic cells, three enveloping valve cells and two uninucleate sporoplasms, one enveloping the other one (Figure 5.4A-B). Valve cells appeared as an amorphous dense matrix delimited by an external membrane of two layers. At the suture line, valve cells formed deep invaginations projecting into the spore (Figure 5.4A, D). Both, the enveloping and the enveloped sporoplasm cell contained rosette-shaped, carbohydrate-rich (Thiéry-positive) granules (Figure 5.4D-E), abundant endoplasmic reticulum and numerous elongate mitochondria (Figure 5.4D). The outer sporoplasm cell showed a crystalline structure of 0.35 x 0.19 µm with dots of 0.06 x0.01 µm diameter (Figure 5.4A, G). The inner sporoplasm cell was densely packed with ribosomes (Figure 5.4B).

Three capsulogenic cells: the largest harboring a fully developed polar capsule and the other two harboring rudimentary polar capsules (Figure 5.4A). Polar capsules consisted of two layers: an inner lucent layer and an outer dense layer. Inside the fully developed polar capsule, two turns of the polar filament within a granular matrix were observed. Surface of polar filament irregularly twisted with longitudinal folds which disappear towards the end of the filament. Opening for polar filament discharge was located in the largest shell valve near the suture line with the smaller two valves (Figure 5.4C). Rudimentary polar capsules showed small polar filaments (Figure 5.4A). Electron-dense bodies, located between each polar capsule and its corresponding shell valve, were observed within capsulogenic cells (Figure 5.4B-C, E). These bodies were smaller when polar capsule was fully developed than when it was rudimentary. Accumulations of carbohydrate-rich granules (Thiéry-positive) were observed in the capsulogenic cells (Figure 5.4E-F). Moreover, a "vesicular body" harbouring small "vesicles" ranging from 0.04 to 0.06 µm in diameter and surrounded by carbohydrate-rich granules was located in the capsulogenic cell containing the largest polar capsule (Figure 5.4F, H).

Figure 5.5 summarizes the 3-dimensional features of the cells constituing the spores of *U. pflugfelderi*.

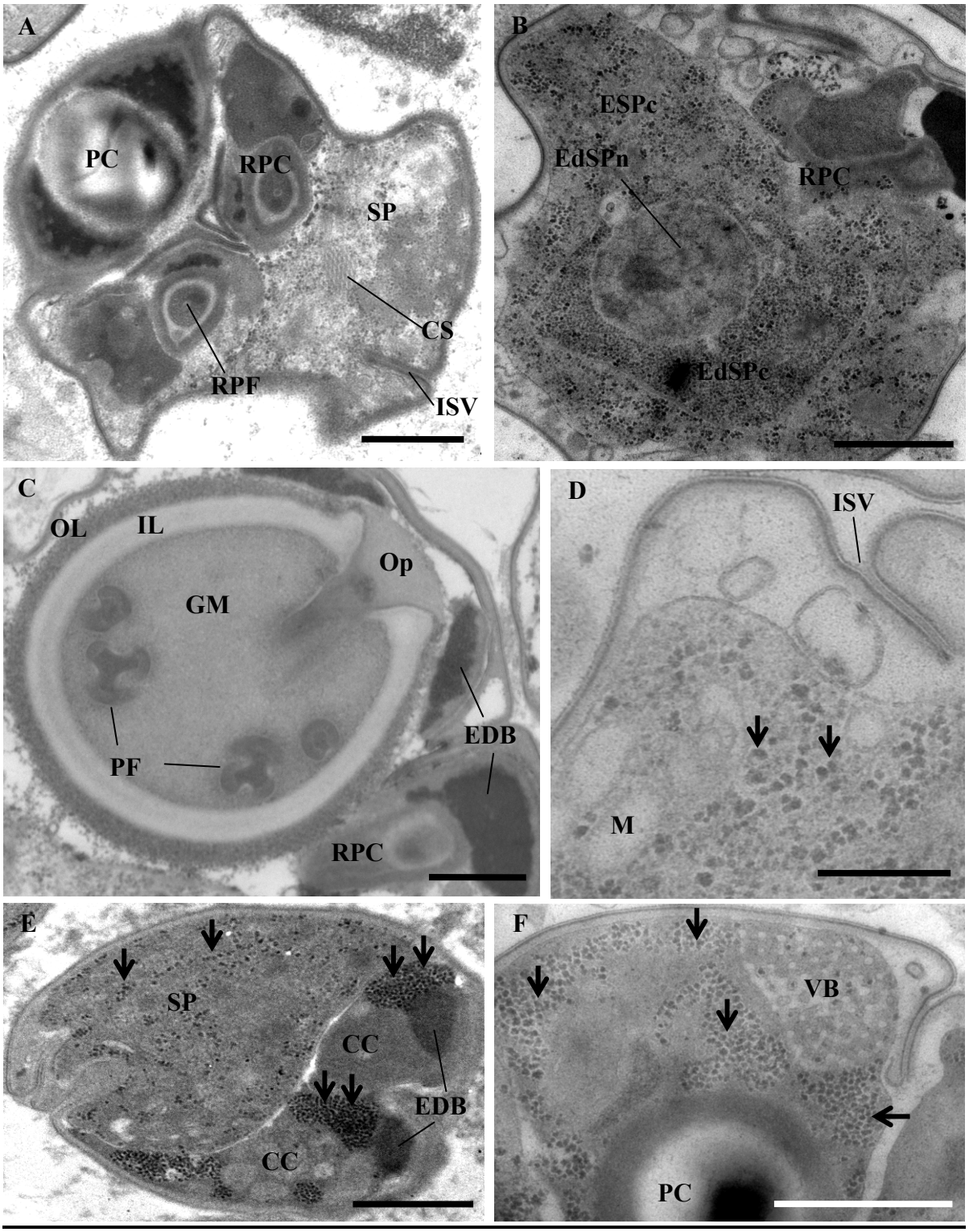

Figure 5.4 Legend on following page.

Figure 5.4 continued.

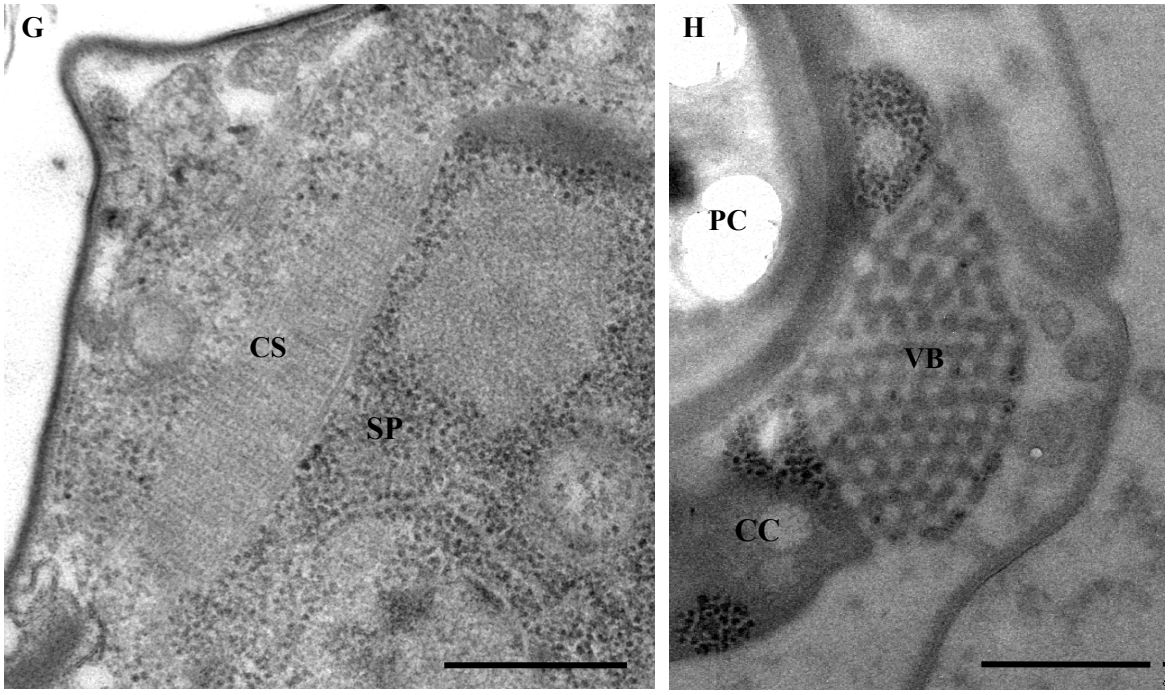

Figure 5.4 TEM images of spores of *Unicapsula pflugfelderi*. A) Section through a spore with sporoplasm (SP) and crystalline structure (CS); three capsulogenic cells, one containing large polar capsule (PC), the other two containing rudimentary polar capsules (RPC) with a rudimentary polar filament (RPF). Notice the deep invagination of the shell valve (ISV). B) Section through a spore showing the enveloping (ESPc) and the enveloped (EdSPc) sporoplasm cells with the enveloped sporoplasm cell nucleus (EdSPn) and one capsulogenic cell with its rudimentary polar capsule (RPC) and its electron-dense body (EDB). C) Detail of Figure 5.4 continued: polar capsule: outer electron-dense layer (OL), inner electron-light layer (IL), opening for the extrusion of the polar filament (OP), granular matrix (GM) containing polar filament (PF); four sections through the polar filament are visible. D) Detail of a valve junctions with deep invagination of the shell valves (ISV), sporoplasm with mitochondria (M) and carbohydrate-rich particles (arrows). E) Thiéry-positive reaction of carbohydrates, showing the distribution of carbohydrate-rich particles (probably glycogen, arrows) in the capsulogenic cells (CC) and in the sporoplasm (SP). F) Detail of a capsulogenic cell with vesicular body (VB) and abundant carbohydrate-rich granules (probably glycogen, arrows) close to a developed polar capsule (PC). G) Detail of a large crystalline structure (CS) in the sporoplasm (SP). H) Detail of a vesicular body (VB) of a capsulogenic cell (Thiéry reaction). Scale bar: A-B= 1 µm; C-D= 0,5 µm; E-F= 1 µm; G-H= 0,5 µm.

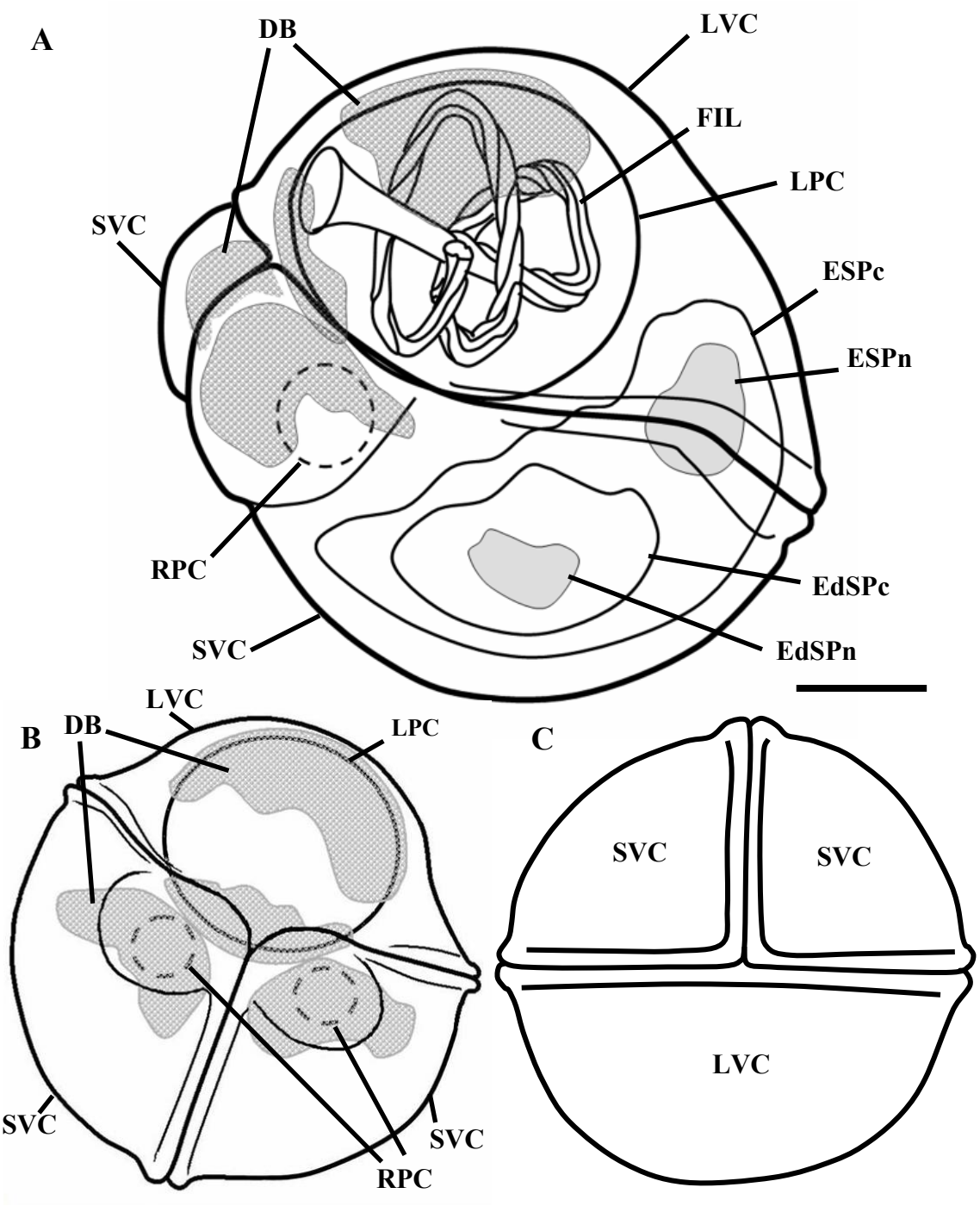

Figure 5.5 Schematic drawing of the spores of *Unicapsula pflugfelderi*. A) Lateral view, B) apical view and C) basal view. LVC, Large valve cell; SVC, small valve cell; LPC, large polar capsule; RPC, rudimentary polar capsule; DB, electron-dense body; FIL, polar filament; ESPc, enveloping sporoplasm cell; EdSPC, enveloped sporoplasm cell; ESPn, enveloping sporoplasm nucleus; EdSPn, enveloped sporoplasm nucleus. Scale bar: 1 μm.

5.3.2. Statistical results of morphometry

The summary (mean, standard deviation and range) of the measurements taken on 30 spores of *U. pflugfelderi* from each, *L. mormyrus* and *S. smaris,* in fresh smears are shown in Table 5.2. The Kolmogorov-Smirnov test indicated a normal distribution of the data. Statistically significant differences between the spores of *U. pflugfelderi* from the two hosts were observed only with regard to total spore length ($p = 0.004$) and polar capsule width ($p = 0.002$). Width of the spore ($p = 0.906$), polar capsule length ($p = 0.069$) and polar filament length ($p = 0.008$) were not significantly different between *L. mormyrus* and *S. smaris*.

In the PCA, principal component I explained 44.67% and component II explained 23.34% of the total morphometric variability. Representation of components I and II in a dispersion diagram shows that the morphometrical data from the spores of the two hosts did not form clearly separated groups, although data seemed to separate to some degree along the x-axis (Figure 5.6). The t-test of the principal components (component I: $p = 0.002$; component II: $p = 0.302$) indicated that differences were observed for component I, which is related to the size of the spores, but not for component II, which is related to the shape of the spores.

With regard to the plasmodia, the t-test showed significant differences between the length ($p = 0.000$) and the width ($p = 0.000$) of the plasmodia from the two hosts. *U. pflugfelderi* plasmodia in *S. smaris* were 2-3 times larger than those in *L. mormyrus* (Table 5.2).

Table 5.2 Average and standard deviation and range of measurements from plasmodia and spores of *Unicapsula pflugfelderi* from *Lithognathus mormyrus* and from *Spicara smaris*, compared with those of the previous description by Schubert et al. (1975). Spore measurements are in micrometers. Plasmodia measurements are in millimetres.

Present study			**Schubert et al. 1975**
SPORES			**SPORES**
	***L. mormyrus* (5 hosts; n=30) Mean (range)**	***S. smaris* (5 hosts; n=30) Mean (range)**	***S. smaris* Diameter**
Total length	5.37 ± 0.31 (4.63-6.07)	5.16 ± 0.24 (4.66-5.73)	4-5
Total width	6.02 ± 0.29 (5.19-6.74)	6.02 ± 0.31 (5.33-6.56)	
Large PC length	2.59 ± 0.18 (2.2-2.93)	2.5 ± 0.18 (2.15-2.86)	2
Large PC width	2.49 ± 0.19 (1.89-2.74)	2.33 ± 0.18 (1.88-2.7)	
POLAR FILAMENT			
	***L. mormyrus* (2 hosts; n=25) Mean (range)**	***S. smaris* (2 hosts; n=26) Mean (range)**	
Large PF length	8.17 ± 0.81 (6.39-9.47)	7.54 ± 0.8 (6.14-8.98)	
RUDIMENTARY POLAR CAPSULES			
	***L. mormyrus* (n=4) Mean (range)**	***S. smaris* (n=3) Mean (range)**	
Small PC length	0.85 ± 0.09 (0.77 –0.97)	0.89 ± 0.07 (0.83 – 0.98)	
Small PC width	1.1 ± 0.03 (1.05 – 1.14)	1.03 ± 0.04 (0.98 – 1.07)	
PLASMODIA			
	***L. mormyrus* (4 hosts; n=56) Mean (range)**	***S. smaris* (5 hosts; n=45) Mean (range)**	
Length	0.81±0.28 (0.33-1.56)	2.47 ± 1.09 (0.69-5.3)	
Width	0.1 ± 0.04 (0.02-0.21)	0.22 ± 0.07 (0.09-0.41)	

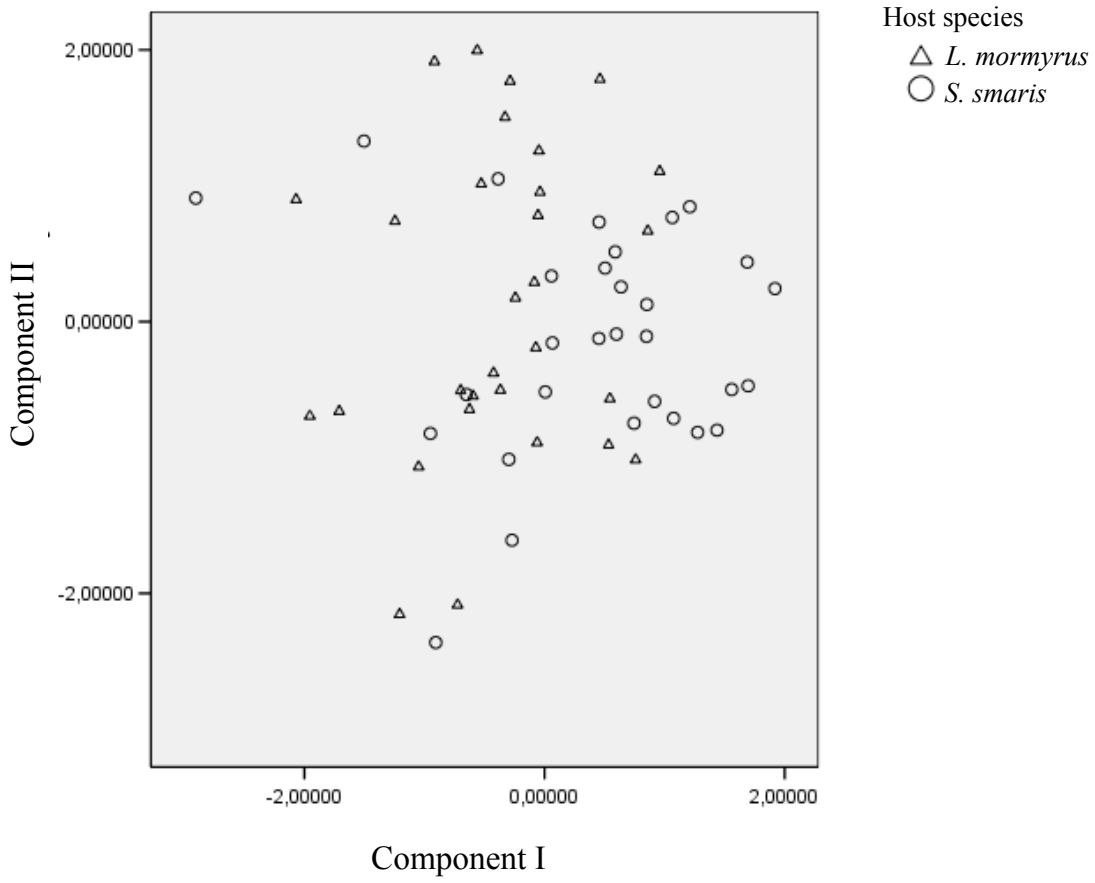

Figure 5.6 Dispersion diagram between component I (size-related, X-axis) and II (shape-related, Y-axis) after PCA obtained with the measurements of the spores of *Unicapsula pflugfelderi*. Δ, *Lithognathus mormyrus*; ○, *Spicara smaris*.

5.3.3. Histopathology

No histopathological changes (Figure 5.2C), i.e. inflammatory response involving increased numbers of white blood cells, granulomatosis, melanization, necrosis or other tissue alterations were observed in the infected muscle fibres. No myoliquefaction in fresh or conserved (>24 hrs at 4ºC) fillets was observed, neither in *L. mormyrus* nor in *S. smaris*.

5.3.4. Molecular characterization and phylogeny

DNA sequencing of *Unicapsula* from both teleost hosts produced approx. 700 bp partial sequences of SSU and LSU rDNA that were 100% identical. Submission to the BLAST server showed that the closest sequence matches was obtained from the only *Unicapsula* sequence available on GenBank, i.e. *Unicapsula* sp. (Whipps et al. 2004, GenBank accession number AY302725) from *Argyrosomus japonicus*

(Temminck & Schlegel 1843). Alignment of the sequences with the other representative of the genus resulted in sequence identity of 96.9% for SSU rDNA and 79.4 % for LSU rDNA.

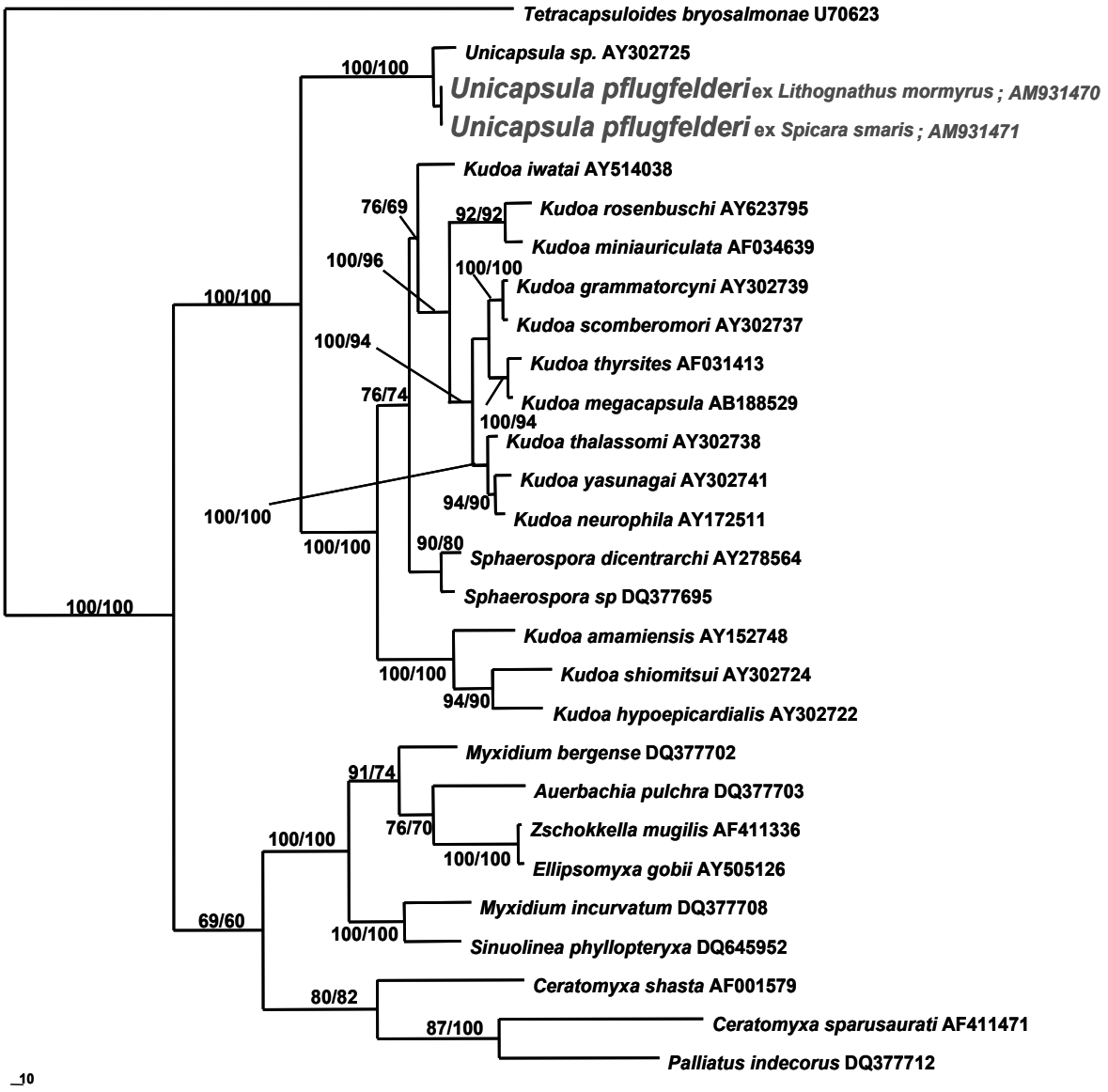

Figure 5.7 Phylogenetic tree resulting from the maximum parsimony analysis of SSU rDNA data of selected myxozoan species, showing the position of the *Unicapsula pflugferlderi* isolates sequenced in the current study. *Tetracapsuloides bryosalmonae* is used as outgroup. Numbers at the branches represent bootstrap values for the maximum parsimony and the maximum likelihood analysis (MP/ML, 1000 replicates each).

The phylogenetic tree constructed using ML and MP (Figure 5.7) revealed that the two species of *Unicapsula* form a monophyletic clade, basal to the clade containing

Kudoa spp. Both clades are embedded in the "generally marine clade of myxozoans" as defined by Fiala (2006).

5.3.5. Taxonomic summary

Type host: picarel *Spicara smaris* (L.) (Centracanthidae), number of hosts studied, sex and morphometrical data hosts not provided by Schubert et al. (1975); current study: weight 25.7 - 153.3 g; length 13.5 - 23 cm; 7 females / 8 males.

Type locality: Banyuls-sur-Mer, France.

Other localities: off Valencia, Spain.

Other hosts: sand steenbras *Lithognathus mormyrus* (L.) (Sparidae); weight 174.24 - 291.0 g; length 23.8 - 28.3 cm; 6 females / 5 males.

Locality: Valencia, Spain.

Site of infection: skeletal muscle, plasmodia intracellularly in muscle fibres.

Prevalence: current study: 62.5% in *S. smaris*; 45.8% in *L. mormyrus.*

Material deposited: Neotype (2008.3442) and voucher (2008.3443) specimens from host *Spicara smaris*; Neotype (2008.3444) and voucher (2008.3445) specimens from host *Lithognathus mormyrus* (microscopic slides of spores in glycerol-gelatine) were deposited in the Invertebrate Collection of the Natural History Museum, London, UK.

Sequence data: *Unicapsula pflugfelderi* partial SSU and LSU rDNA sequence, ex. *L. mormyrus* and *Unicapsula pflugfelderi* partial SSU and LSU rDNA sequence, ex. *S. smaris*. See Appendix 1.

Remarks

In contrast to Schubert el al. 1975, which suspected the valve cell covering the developed polar capsule to be smaller than the other two, the current study proves that the unpaired valve cell is considerably larger and covers approximately half of the spore (Table 5.2).

According to Schubert et al. 1975, fixed spores measure 4-5 µm in diameter whereas unfixed spores measure 4.63-6.07 µm in length and 5.19-6.74 µm in width. This coincides with the percentage of shrinkage by fixation observed in other myxozoans (e.g. in *Chloromyxum schurovi* Shul'man & Ieshko 2003 (Holzer et al. 2006a)).

With regard to the polar filament, Lester (1982) found that the polar filament of *U. pflugfelderi* was coiled in one and a quarter turns. In the current study, the polar

filament appeared coiled in two complete turns, visible as four cross-sections in TEM. However, these differences might be due to the angle at which the spore is cut or to the intra-specific variability in the spore morphology also described in other species (Egusa 1986; Whipps et al. 2003).

In the present study, *U. pflugfelderi* was found in multiple hosts, being the first report of low host specificity within the genus. Furthermore, the present report expands the geographical distribution of *U. pflugfelderi* from Banyuls-sur-Mer, gulf of Lyon (France, Schubert et al. 1975) to the southern Mediterranean, gulf of Valencia.

5.3.6. Morphological analysis of the spores of *Unicapsula* spp. described to date

A comparative study of the members of the genus *Unicapsula* (Table 5.3; Figure 5.8) showed that *U. pflugfelderi* is not the only species that presents the unpaired valve cell covering not only half of the spore but also the polar capsule: *U. galeata* Naidjenova & Zaika 1970, *U. schulmani* Aseeva & Krasin 2001 and *U. pacifica* Aseeva & Krasin 2001 show the same valve cell organisation. Although being described with only two valve cells, the type species *U. muscularis* also shows the largest valve cell covering the polar capsule. The remainder of the species: *U. pyramidata* Naidjenova & Zaika 1970, *U. seriolae* Lester 1982 and *U. marquesi* Diebakate, Fall, Faye & Toguebaye 1999 show large paired valve cells whereas the unpaired one is reduced. In conclusion, the valve cell organisation divides the genus in two groups: one with the unpaired valve cell larger and the other one with the unpaired valve cell smaller than the two paired ones.

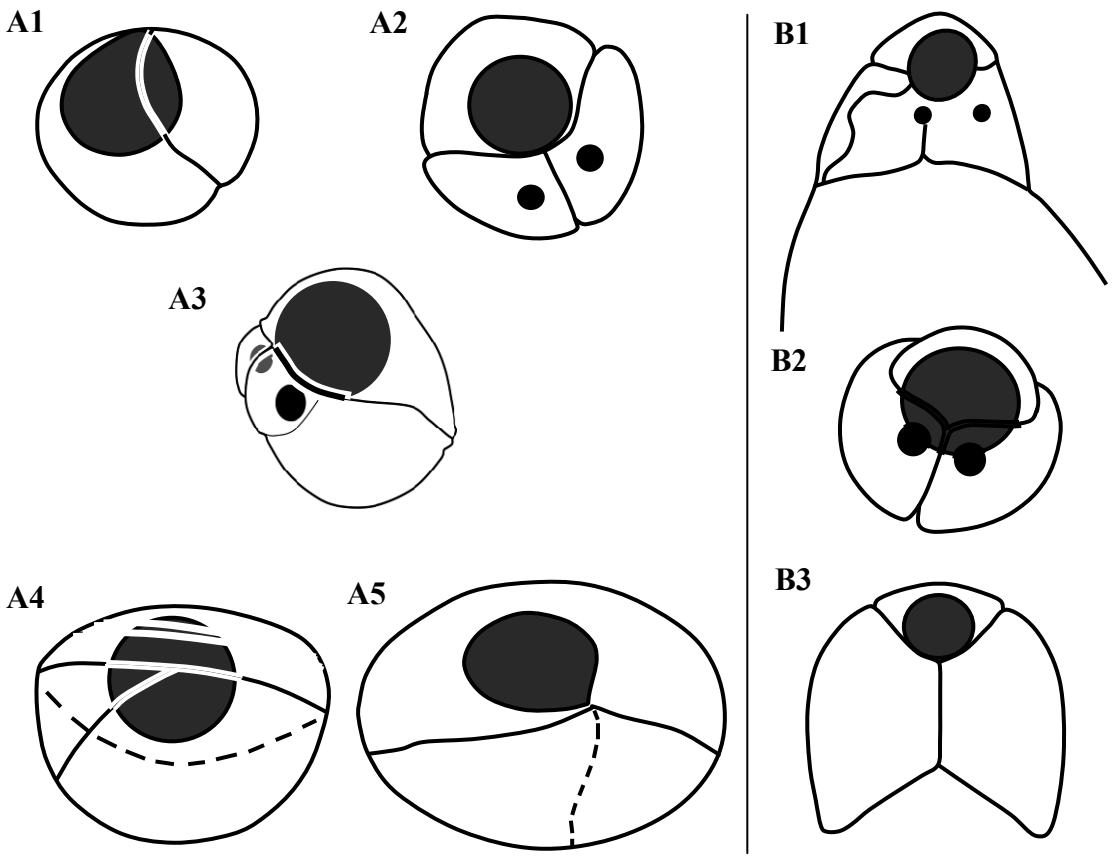

Figure 5.8 Schematic drawings of A1) *Unicapsula muscularis* (after Davis 1924), A2) *Unicapsula galeata* (after Naidjenova & Zaika 1970), A3) *Unicapsula pflugfelderi*, A4) *Unicapsula pacifica* (after Aseeva & Krasin 2001) and A5) *Unicapsula schulmani* (after Aseeva & Krasin 2001). A1-5) Note that the unpaired valve cell is larger than the other two. Schematic drawings of B1*) Unicapsula pyramidata* (after Naidjenova & Zaika 1970), B2) *Unicapsula seriolae* (after Lester 1982) and B3) *Unicapsula marquesi* (after Diebakate et al. 1999). B1-3) Note that the unpaired valve cell is smaller than the other two. Scale bar: 10 µm.

Table 5.3 Summary of descriptions of species of *Unicapsula*, indicating fish host and their family, geographic location, site of infection, prevalence (%), total length or length x width of plasmodia, diameter or length x width of spores, diameter or length x width of large polar capsule (PC), turns and length of its polar filament (PF) and shell valves patterns: 1) the unpaired valve cell is larger and 2) the unpaired valve cell is smaller than the two paired ones. The presence or absence of myoliquefaction (MYL) in the flesh of fish is also noted (* indicates data from present study). [a] Fishes of the genus *Spicara* , traditionally belonging to the family Centrachanthidae have been ascribed to the family Sparidae (Orrell et al. 2002).

Species	Host & Family host	Geographic location	Site of infection	Prevalence (%)	Plasmodia (mm)	Spores (µm)	Large PC (µm)	Turns PF	Length PF	Shell valve pattern	MYL
Unicapsula muscularis Davis 1924	*Hippoglossus stenolepis* (Pleuronectidae)	Pacific Ocean	Muscle	-	2-6	6	3	5	-	1	Yes
Unicapsula galeata Naidenova & Zaika 1970	*Pseudopeneus pleurotaenia* (Mullidae)	Indian Ocean	Muscle	-	-	5 x 5-6	3	-	7	1	-
Unicapsula pyramidata Naidenova & Zaika 1970	*Nemipterus japonicus* (Nemipteridae)	Indian Ocean	Muscle	-	1-3	4.6-5 x 6.8-7	1.7-2	-	7	2	-
Unicapsula pflugfelderi Schubert, Sprague & Reinboth 1975	*Spicara smaris* (Centracanthidae)[a]	Banyuls-Sur-Mer, France, Mediterranean	Muscle	-	-	4-5	2	1.25	-	1*	No
		Valencia, Spain, Mediterranean*		62.5%*	2.47 x 0.22*	5.16 x 6.02*	2.5 x 2.33*	2 *	7.5*		
	Lithognathus mormyrus (Sparidae)	Valencia, Spain Mediterranean *		45.8%*	0.81 x 0.1*	5.37 x 6.02*	2.59 x 2.49*	2*	8.2*		
Unicapsula seriolae Lester 1982	*Seriola lalandi* (Carangidae)	Brisbane, Australia Pacific Ocean	Muscle	61.54 %	7 x 0.2	5.6	2.9	2.5	18	2	Yes
Unicapsula marquesi Diebakate, Faye & Toguebaye 1999	*Polydactylus quadrifilis* (Polynemidae)	Dakar, Senegal Atlantic Ocean	Gills	5.6%	1-3	6.13 x 7.18	3	2-3	-	2	-
Unicapsula pacifica Aseeva & Krasin 2001	*Coryphaenoides pectoralis* (Macrouridae)	Okhotsk Sea, Pacific Ocean	Muscle	4.5%	- (only 1 spore per plasmodium)	7.31-8.64	3.9-4	-	-	1	-
Unicapsula schulmani Aseeva & Krasin 2001	*Coryphaenoides pectoralis* (Macrouridae)	Okhotsk Sea, Pacific Ocean	Urinary bladder	4.6%	-	7.78 -10.28	2.75-3.82	4	-	1	-

5.4. Discussion

Of the eight species described in the genus *Unicapsula*, only one, i.e. *U. pflugfelderi* has been described from the Mediterranean. *U. pflugfelderi* was firstly found in *S. smaris* from Banyuls-Sur-Mer (France) by Schubert et al. (1975). The discovery of a similar *Unicapsula* species in the sparid *L. mormyrus* initiated the present comparative study. The morphological and molecular results showed that the two *Unicapsula* sp. were conspecific and represent *U. pflugfelderi,* resulting in a new teleost host record and a re-description of the species. Whereas data on the host range of other *Unicapsula* spp. are not currently available, *U. pflugfelderi* seems to be little host-specific. Low host specificity has also been observed in several members of the multivalvulid sister genus of *Unicapsula*, i.e. *Kudoa*, e.g. for *K. thyrsites* which is known from 37 hosts from 18 different fish families (Whipps & Kent 2006). *U. pflugfelderi* infects two hosts belonging to different families, however these fish species might be more closely related than previously believed as *S. smaris* has been suggested to be included in the Sparidae (Day 2002). Thus, the present findings may support the idea of parasitic range enlargement among closely related hosts, based on common niche (Riedl 1986; Whitehead et al. 1986) and on evolutionary relatedness (Day 2002).

Statistical analyses of the morphometrical data of *U. pflugfelderi* from *L. mormyrus* and *S. smaris* showed highly significant differences with regard to the plasmodia size but only for a few spore measurements. The length and width of plasmodia in *S. smaris* were 2-3 times larger than in *L. mormyrus*. With regard to the spore measurements, only spore length and polar capsule width seem to be significantly different between the fish hosts. Host-related variability in spore size has been demonstrated (Diamant 1998; Aseeva 2002; George-Nascimento et al. 2004). The morphological variability related to the plasmodia of *U. pflugfelderi* is also host-related and could be explained by differences in the immunological potential to combat *U. pflugfelderi* infection. Despite morphological differences, molecular analysis based on SSU and LSU rDNA sequences showed that *U. pflugfelderi* from *L. mormyrus* and from *S. smaris* are 100% identical.

An aberrant, “rugby-like” spore was sometimes observed by LM and SEM. Collapse and subsequent deformation of the largest valve cell, possibly due to disinflation of the spore caused by osmotic imbalance, might be the cause for this aberrant form. It

is suggested that sutures form a hard, skeleton-like structure. However, the soft shell valves are likely to change shape when exposed to different osmolarities (saline) or to the light of the microscope. Due to the larger size of one valve cell, this cell provides less resistance to deformation than the other two, which present a much smaller surface area between the supportive sutures than the large valve.

Ultrastructural results are in accordance with those found by Schubert et al. (1975) but provide several additional details. Abundant ribosomes were described by Schubert et al. (1975) in the cytoplasm of the sporoplasm cells. In the current study, the majority of ribosomes were packed in the inner sporoplasm cell, whereas a large quantity of rosette-shaped carbohydrate-rich particles, probably representing glycogen, were observed in both, the inner and the outer sporoplasm cells. These carbohydrate-rich particles could represent an energy storage that allows the spore to remain in the water column over a long period of time before finding an alternate invertebrate host. Alternatively, this storage might be useful for the mobility of the sporoplasm when exiting the spore and burrowing into the host´s epithelium.

At the suture line, the shell valves were found to form a deep invagination into the spore body. This condition has also been reported in *U. seriolae* (Lester 1982), *U. marquesi* (Diebakate et al. 1999) and, earlier on, in *U. pflugfelderi* (Schubert et al. 1975) but has not been reported from other genera and might thus represent a genus-specific structure. However, a similar genus-specific suture structure has been ascribed to the genus *Kudoa* (Diamant et al. 2005), which shows overlapping flanges of the cell valves, whereas in all other myxosporeans (bivalvulids), simple, non-overlapping valve joints are present.

The electron-dense body associated with each polar capsule might represent material for the construction of the polar capsule as the structure of the electron-dense body is homogenous and similar to that of the outer electron-dense layer of the polar capsule and because the capsulogenic cell with the developed polar capsule show a much smaller electron-dense body than in those presenting rudimentary polar capsules. In some myxozoans this electron-dense mass next to the polar capsules has been referred to glycogen (Sitjà-Bobadilla & Alvarez-Pellitero 1992). However, we observed extensive accumulations of small carbohydrate-rich (Thiéry positive) granules next to the polar capsules and alongside the homogenous electron-dense material. These accumulations could provide energy for the polar capsule

development, whereas the homogenous material in the electron-dense body represents its construction material.

In the previously undescribed "vesicular body" detected close to the developed polar capsule, in some cases, it was possible to observe electron-dense dots inside the "vesicles". This is similar to the external tubule described in other myxozoa, however, sections of external tubule were generally few (<10) and were only observed in developing spores (Cho et al. 2004; Diamant et al. 2005). In the present case, the mature spores with a well-developed polar capsule show a large area of regularly organised and numerous (approx. 70) cross-sections of considerably smaller units than the sections of external tubules. It is suggested that the regularly organised structure of "vesicles" observed in *U. pflugfelderi* could have secretory function.

With respect to the crystalline structure found in the sporoplasm, a similar feature was described in *Henneguya adiposa* Current 1979. However, there are some significant differences: the so-called "paracrystalline" structure of *H. adiposa* was found inside the mitochondria of the plasmodium, and its size was larger (0.5 x 0.49 µm in contrast to 0.35 x 0.19 µm) than that of *U. pflugfelderi*. Current (1979) indicated that this structure could be a proteinaceous body for translational products or an extensive incorporation and storage of extra-mitochondrial proteins. The crystalline structure found in the sporoplasm of the spores of *U. pflugfelderi* consists neither of carbohydrates nor of lipids (negative for Thiéry and OTO reaction) and, due to its specific structure and based on the localisation, it is suggested to be an accumulation of minerals. This structure could allow the sporoplasm to cope with osmotic and pH changes when leaving the spore valves and entering into host tissues.

The results of the phylogenetic analyses indicate that the evolution of the multivalvulids is based on a bivalvulid origin. Based on the bivalvulid morphology, two lines evolved: the *Unicapsula* clade with three shell valves and the *Kudoa* clade with four or more shell valves (*Kudoa* clade). In the latter clade, more valves were added in some species, creating penta- and hexacapsulid forms (Whipps et al. 2004). Thereby, *Kudoa* consistently increases the number of valve cells together with the number of polar capsules. The biological significance of this increase could be explained by a higher probability for attachment to the host when infection takes place. The increase of the number of valve cells cannot be explained in the same manner in *Unicapsula* as only one polar capsule is developed and functional in the

spore. However, an increased number of suture lines might improve the stability of the spore.

Finally, no histopathological changes in the muscle and no myoliquefaction were observed in fish infected with *U. pflugfelderi*. However, high numbers of plasmodia in the fillets were found to create a negative aesthetic aspect that could considerably lower the market value due to rejection by the consumer, like in *Kudoa* spp. (Moran et al. 1999a). Thus, *U. pflugfelderi* may somehow impact on the potential of *L. mormyrus* as a candidate species for Mediterranean aquaculture.

The revision of the *Unicapsula* spp. described to date (Table 5.3) showed that various species are poorly characterised with regard to morphology, host tissue localisation and molecular data. In their genus diagnosis, Lom & Dyková (2006) state that there are eight *Unicapsula* species, with all of them occurring in tissues. However, the original description of *U. schulmani* (Aseeva & Krasin 2001) describes it as a parasite of the urinary bladder but the exact location (coelozoic / histozoic) and the plasmodia were not described. The remainder of the *Unicapsula* spp. are truly histozoic, inhabiting the muscle or the gill filaments (*U. marquesi*). Revision of the *Unicapsula* spore morphology showed that the organisation of the valve cells in this genus divides it into two groups, one where the developed valve cell is larger and the other one where it is smaller than the two rudimentary ones. Although this classification may be artificial, it is important to know that one of these morphotypes contradicts the current diagnosis of the genus. It is also suggested that the ultrastructural detail referring to the invagination of the shell valves of the spore at their suture is a genus-specific feature to be included in the diagnosis. As a result, the following amended diagnosis is suggested:

Amended diagnosis of the genus *Unicapsula* (Davis 1924)

Spores subspherical, with three polar capsules, 1 fully developed and 2 rudimentary ones. Three unequally sized valve cells: one larger or smaller than the other two which are paired, symmetrical, and equal in size and shape. The first covers the developed polar capsule whereas the latter cover the capsular rudiment. At suture line, valve cells adjoin parallel and penetrate deep into the spore body, forming characteristic invaginations. Spore contains two uninucleate sporoplasms, one enveloping the other. In marine and brackish fishes. Large polysporic plasmodia

usually in the muscle, exceptionally found in gills and urinary bladder. Type species *U. muscularis* Davis 1924.

CHAPTER 6. The bile myxozoan *Ceratomyxa puntazzi* n. sp. in *Diplodus puntazzo* (Walbaum 1792): description, host-parasite relationship and first data on host specificity of ceratomyxids in sparids

6.1. Background

Ceratomyxa (Thélohan 1892) is a genus of predominantly coelozoic myxozoan parasites. Over 270 species have been described (Eiras 2006; Mladineo & Bočina 2006; Ali et al. 2006; Reed et al. 2007; Abdel-Ghaffar et al. 2008; Heiniger et al. 2008, Gunter & Adlard 2008, 2009, 2010; Gunter et al. 2009; Gunter et al. 2010a), most of them infecting the gall bladders of marine teleosts.

In general, *Ceratomyxa* species seem to cause little or no damage to their hosts, possibly due to their coelozoic development, however, some species have been shown to cause important pathological changes in their hosts. The best known pathogen is *C. shasta*, which occurs in salmonids in North America (Bartholomew et al. 1989b). *C. shasta* produces extensive haemorrhages and necrosis in the intestine of its hosts and cause substantial losses in wild and cultured salmonids (Bartholomew et al. 1989a; Bartholomew et al. 2004). However, *C. shasta* is not a typical representative of the genus as it differentiates itself from all other *Ceratomyxa* spp. by various characters, most importantly, its histozoic nature. It also clusters separately from the otherwise monophyletic genus *Ceratomyxa* when analysed phylogenetically (Fiala 2006, Fiala & Bartošová 2010).

In the Mediterranean, bile-inhabiting species of *Ceratomyxa* have been shown to cause pathogenic changes in a number of sparids. *Ceratomyxa sparusaurati* Sitjà-Bobadilla, Palenzuela & Alvarez-Pellitero 1995 is a highly prevalent parasite of gilthead seabream *S. aurata* in Mediterranean culture systems and produces notable histopathological damage including swelling, vacuolization and sloughing of the epithelial cells of the gall bladder, associated with mortalities (Palenzuela et al. 1997). *Ceratomyxa diplodae* (Lubat, Radujkovic, Marques & Bouix 1989) has been related to mortalities as an opportunistic pathogen in potentially immunosuppressed, steroid treated sharpsnout seabream *D. puntazzo* (Katharios et al. 2007). During the parasitological study of the newly established aquaculture species *D. puntazzo*, ceratomyxid spores were found in the bile. The relation of this species with previously described species and with those obtained from sparids sharing the same habitat was determined and the related pathology in *D. puntazzo* was studied.

6.2. Materials and methods

6.2.1. Source of fish

Between 2007 and 2010, *D. puntazzo*, *D. annularis* and *S. aurata* from different sites along the Spanish Mediterranean coast were studied for infection with ceratomyxids. Specimens of *D. puntazzo* (n=94, 6-37 cm total length; 3.75-733.9 g), annular seabream *D. annularis* (n=47, 12.5-20 cm total length; 39.22-158 g) and gilthead seabream *S. aurata* (n=21, 11.5-28 cm total length; 18.43-385.4 g) were obtained by local shore fishing in the Mediterranean off Jávea (Alicante) and off San Pedro del Pinatar (Murcia), from Valencia's fishing harbour and from a fish farm, off San Pedro del Pinatar (Murcia) (Spanish Mediterranean coast; see Table 3.1).

6.2.2. Morphological analysis of bile myxozoans

The gall bladder of each fish was isolated, held with forceps directly above the opening of an autoclavated 1.5 ml eppendorf and ruptured. From the collected bile, 4 µl were placed on a microscopic slide, covered with a cover-slip and examined using light microscopy at 400x magnification. Spores detected in the bile of six *D. puntazzo*, of three *S. aurata* and of two *D. annularis* were measured (parameters see Figure 6.1) and described. The posterior spore angle of ceratomyxid spores was measured as described in Heninger et al. 2008. The remainder of each sample was used for DNA extraction and SSU rDNA sequencing.

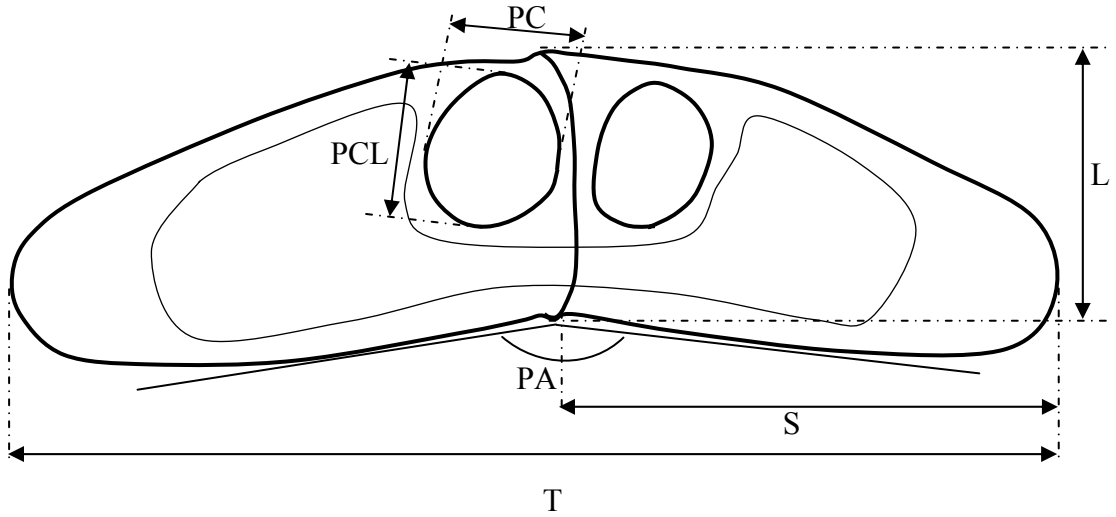

Figure 6.1 Schematic diagram of a ceratomyxid spore measurements. L, length; PA, posterior angle; PCL, polar capsule length; PCW, polar capsule width; S, sutural position; T, thickness.

To determine differences between the morphologically similar spores obtained from *D. puntazzo* and from *D. annularis*, spore measurements were analysed statistically, as described in Chapter 3, Section 3.2.4.

For TEM, the protocol described in Chapter 3, Section 3.2.3 was followed. For histological analysis, gall bladder, liver, intestine, kidney and spleen of five infected *D. puntazzo* were processed as described in Chapter 3, Section 3.2.5. The sections were stained with haematoxylin and eosin (H&E) and 1% toluidine blue.

6.2.3. Molecular data and phylogeny

DNA extraction, PCR, sequencing and alignment of the obtained sequences was conducted according to the methodology described in Chapter 3, Section 3.3.1. Partial SSU rDNA sequences of four ceratomyxid spore morphotypes were amplified from genomic rDNA tandems. In all cases, sequences were obtained from two fish, except for *Ceratomyxa* sp. 2 ex *Sparus aurata*, which sequence was obtained from a single fish.

The obtained SSU rDNA sequences were submitted to the BLAST to identify the closest relatives published to date. The myxozoan sequences used for alignment and phylogenetic analyses are included in Table 6.1. Phylogenetic analyses were conducted as described in Chapter 3, Section 3.3.2. In Clustal X, a gap opening penalty of 8.0 and a gap extension penalty of 5.0 were applied. In the BI analysis, the MCMC burn-in was set to 80,000 generations. *E. leei*, *Kudoa septempunctata* Matsukane, Sato, Tanaka, Kamata & Sugita-Konishi 2010 and *Kudoa shiomitsui* Egusa & Shiomitsu 1983 were used as outgroup.

Table 6.1 Myxozoan SSU rDNA sequences used in the phylogenetic analyses.

Species/Type	Length (bp)	GenBank™ acc. no.
Enteromyxum leei	1588	AB243447
Kudoa shiomitsui	1719	AY302724
Kudoa septempunctata	1701	AB553293
Ceratomyxa sp. SRR	1732	DQ333431
Ceratomyxa sp. RM	1705	DQ333429
Ceratomyxa kenti	1418	EU440363
Ceratomyxa bryanti	1421	EU440357
Ceratomyxa capricornensis	1410	EU440364
Ceratomyxa choerodonae	1432	EU045333
Ceratomyxa heinigerae	1354	FJ204249
Ceratomyxa milleri	1426	FJ204251
Ceratomyxa nowakae	1479	FJ204252
Ceratomyxa seriolae	1862	AB530265
Ceratomyxa sp. SAR	1723	DQ333430
Ceratomyxa ernsti	1420	FJ204247
Ceratomyxa talboti	1403	EU440368
Ceratomyxa cribbi	1409	EU440367
Ceratomyxa dennisi	1388	EU440358
Ceratomyxa diamanti	1447	FJ204246
Ceratomyxa moseri	1403	EU440360
Ceratomyxa jonesi	1413	FJ204250
Ceratomyxa labracis	1763	AF411472
Ceratomyxa auerbachi	1778	EU616732
Ceratomyxa sp. 2 IF-2006	1741	DQ377699
Palliatus indecorus	1734	DQ377712

6.3. Results

Spores typical for the genus *Ceratomyxa* (Thélohan 1892) were found in the bile of the gall bladders of all fish species analysed. Trophozoites were only observed in *D. puntazzo*. Infection was detected in 58.5% (55/94) of *D. puntazzo*, 4.3% (2/47) of *D. annularis*, 9.5% (2/21) of *S. aurata* (*Ceratomyxa* sp. 1) and 4.7% (1/21) of *S. aurata*

(*Ceratomyxa* sp. 2). A new species of *Ceratomyxa*, *Ceratomyxa puntazzi* n. sp. is described from *D. puntazzo* and a differential diagnosis is provided.

6.3.1. Description of *Ceratomyxa puntazzi* n. sp.

Phylum Myxozoa

Class Myxosporea

Order Bivalvulida

Family Ceratomyxidae Doflein 1899

Genus *Ceratomyxa* (Thélohan 1892)

Ceratomyxa puntazzi n. sp.

Description (based on light microscopy and TEM; see Figure 6.2A,E, Figure 6.3, Figure 6.4, Figure 6.5A,B & Table 6.2): Spores (n=30, live spores in bile) typical of the genus *Ceratomyxa*. Mature myxospores slightly crescent shaped, 9.2 ± 0.7 µm (8.03-10.72) in length and 29 ± 2.9 µm (23.83-34.5) in thickness. Posterior angle slightly concave to straight (146.4-179.2º). Two valves, roughly equal, smoothly ovoid in lateral view. Straight sutural line visible between valves, connected with desmosome-like junctions. Polar capsules (n=60) (sub)spherical, 4.1 ± 0.4 µm (2.95-4.77) in length, equalling 43.9 % of spore length, and 4 ± 0.4 µm (2.9-4.6) in width, possessing an outer electron-dense layer and an inner electron-lucent layer. Two capsulogenic nuclei located close to the polar capsules. Twisted polar filament allocated in five turns. Single, binucleated sporoplasm occupying most of the spore body. Sometimes, atypical 3-valved spores, possessing three polar capsules, were observed.

Trophozoites (n=21, live trophozoites) floating in the bile, in different stages of maturation, disporous, elliptical to sub-spherical 30.1 ± 1.3 µm (25.2-37.4) in length and 21.8 ± 2.7 µm (17-25.4) in width. One primary cell with abundant vacuoles present in the cytoplasm. One to two secondary cells observed. One to two tertiary cells observed. Trophozoites frequently with cytoplasmic extensions in the shape of filopodia.

Figure 6.2 Photomicrographs of ceratomyxid spores in sutural view. A) *Ceratomyxa puntazzi* n. sp. ex *Diplodus puntazzo*. B) *Ceratomyxa* sp. ex *Diplodus annularis*. C) *Ceratomyxa* sp. 1 ex *Sparus aurata*. D) *Ceratomyxa* sp. 2 ex *Sparus aurata*. E) Two disporous plasmodia and an atypical 3-valved spore of *Ceratomyxa puntazzi* n.sp. from *Diplodus puntazzo*. Scale bar: 10µm.

Taxonomic summary

Host: *Diplodus puntazzo* (Walbaum, 1792), sharpsnout seabream (Perciformes: Sparidae) (n=6; 6-28.5 cm total length; 3.75-448.6 g).

Type locality: Mediterranean off San Pedro del Pinatar (Mar Menor, Murcia), Spain.

Other locality: Mediterranean off Jávea (Alicante), Spain.

Site: Within gall bladder.

Prevalence: 58.5% (55/94)

Etymology: The species name refers to the specific name of its host, *D. puntazzo*.

Material deposited: Syntype (2011.53; 2011.54) specimens (two air-dried slides stained with Diff-Quick®) and DNA sample (2011.55; 2011.56) (two bile samples in 100% ethanol) were deposited in the Invertebrate Collection of the Natural History Museum (NHMUK), London, UK.

Sequence data: *Ceratomyxa puntazzi* n.sp. SSU rDNA sequence (from two fish, identical sequences from both PCR products). See Appendix 1.

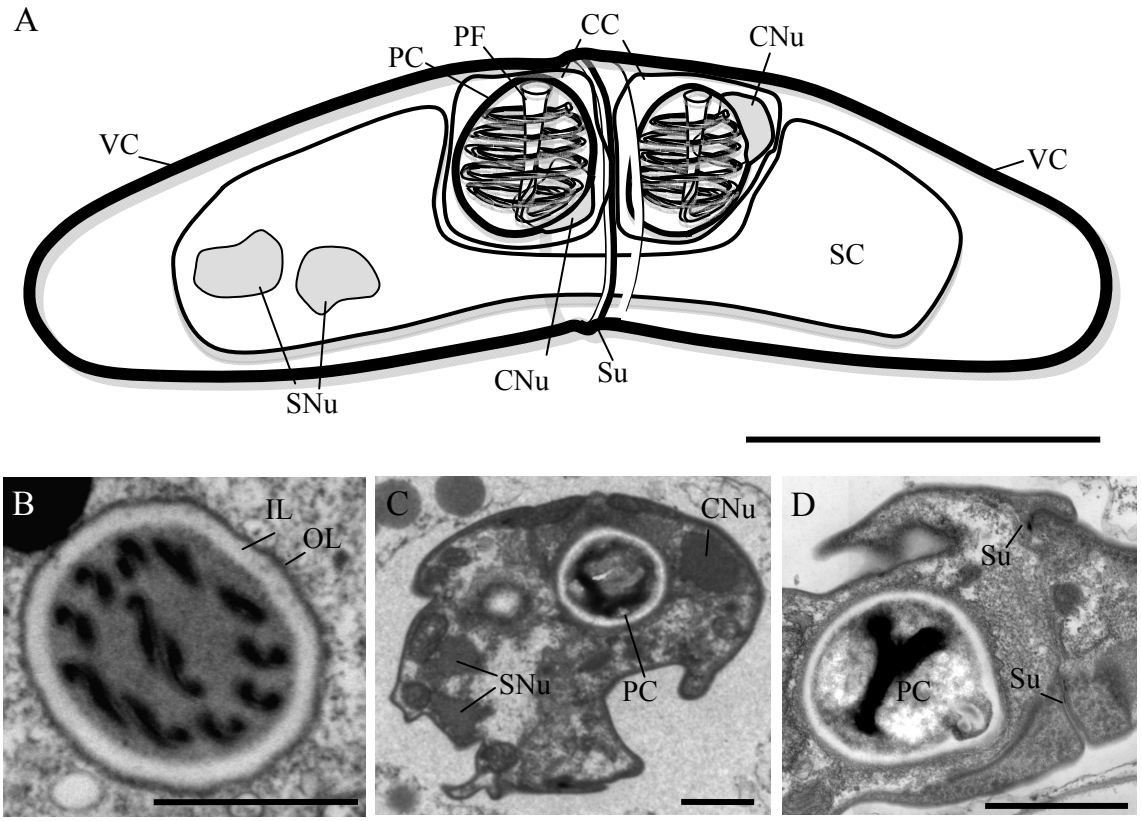

Figure 6.3 *Ceratomyxa puntazzi* n. sp. ex *Diplodus puntazzo*. A) Schematic drawing of a spore in sutural view. VC, valve cell; SC, sporoplasm cell; CC, capsulogenic cell; SNu, sporoplasm nucleus; CNu, capsulogenic nucleus; PC, polar capsule; PF, polar filament; Su, suture between valves. B-D) Transmission electron microscopy (TEM) images. B) Detail of a polar capsule, with twisted polar filament in five coils. Notice an outer electron-dense layer (OL) and an inner electron-lucent layer (IL) of polar capsule wall. C) Mature spore with a capsulogenic cell, its nucleus (CNu) and a polar capsule (PC). Binucleate sporoplasm with two sporoplasmic nuclei (SNu) can be observed. D) Detail of a mature spore with a polar capsule (PC) and suture between valves showing desmosome-like junction. Scale bar: A= 10 µm; B-D=1 µm.

Remarks

Ceratomyxid spores found in the gall bladders of *D. puntazzo* were identified as *C. diplodae* by Katharios et al. in 2007. *C. diplodae* was originally described from *D. annularis* (Lubat et al. 1989) and also from *D. labrax* (Sitjà-Bobadilla & Alvarez-Pellitero 1993c). However, spores of *C. puntazzi* n. sp. are considerably larger than the

spores of *C. diplodae* described previously from all three hosts (Table 6.2). No molecular data of *C. diplodae* is available from any of the previously reported hosts.

Submission to the BLAST server showed that the closest sequence matches of *C. puntazzi* n. sp. SSU rDNA were *Ceratomyxa sparusaurati* (from *Sparus aurata*, GenBank Accession Number AF41147; Query coverage 96%; Maximum identity 97%) and *Ceratomyxa* sp. SRR (from *Siganus rivulatus*, GenBank Accession Number DQ333431; Query coverage 95%; Maximum identity 91%).

The alignment of the partial SSU rDNA sequence of *C. puntazzi* n. sp. with sequences from other *Ceratomyxa* spp. showed intrageneric sequence similarities from 68.2% to 98.2% over an alignment of 2012 bp. The highest sequence similarity was obtained with the sequences of *Ceratomyxa* sp. ex *D. annularis* (98.2%) and of *Ceratomyxa* sp. 2 ex *S. aurata* (98.2%) (both obtained in present study; see section 6.3.3).

Table 6.2 Summary of data of Mediterranean species of *Ceratomyxa* in fish of the family Sparidae. Measurements are given in µm as means ± standard deviation with range in parenthesis. Sutural position as described in Heiniger et al. 2008. PCL: polar capsule length; PCW: polar capsule width; PA: posterior angle; *:diameter.

Host	***Pagellus bogaraveo***	***Sarpa salpa, Boops boops***	***Sarpa salpa***	***Diplodus annularis***		***Dicentrarchus labrax***	***Diplodus puntazzo***		***Sparus aurata***		
Species	*Ceratomyxa arcuata* (Thélohan 1892)	*Ceratomyxa pallida* Thélohan 1894	*Ceratomyxa herouardi* Georgévitch 1916	*Ceratomyxa diplodus* (Lubat, Radujkovic, Marques & Boux,1989)	***Ceratomyxa* sp. ex *Diplodus annularis***	*Ceratomyxa diplodus*	*Ceratomyxa diplodus*	***Ceratomyxa puntazzi* n. sp.**	*Ceratomyxa spanusaurati* Sitjà-Bobadilla, Palenzuela & Álvarez-Pellitero 1995	***Ceratomyxa* sp. 1 ex *Sparus aurata***	***Ceratomyxa* sp. 2 ex *Sparus aurata***
Study	Kalavati & Mackenzie 1999	Thélohan 1894	Georgévitch 1916	Lubat et al. 1989	Present study (n=27)	Sitjà-Bobadilla & Álvarez-Pellitero 1993b (n=38)	Katharios et al, 2007 (n=30)	Present study (n=30)	Sitjà-Bobadilla et al. 1995 (n=30)	Present study (n=10)	Present study (n=20)
Thickness	36.2 ± 2.7 (32.5-40.0)	25-30	--	20 (18-22)	28.8 ± 3.7 (21.5-32.7)	20.9 ± 2.759 (17-27)	24.0 ± 0.8	29 ± 2.9 (23.83-34.5)	15.76 ± 1.01 (14-17.5)	17.2 ± 3.4 (13.1-22.5)	20 ± 2.1 (16.7-24.7)
Length	6.8 ± 0.9 (6.0-9.0)	5	--	6 (5-7)	9.8 ± 0.8 (7.1-13)	6.2 ± 0.425 (5-7.5)	6.6 + 0.5	9.2 ± 0.7 (8.03-10.72)	5.65 ± 0.74 (4.5-7.5)	5 ± 0.5 (3.9-5.6)	9.9 ± 0.6 (8.7-11.4)
Sutural position	--	--	--	--	14.7 ± 0.3 (10-18.2)	--	--	14.3 ± 1.9 (10.5-19.1)	--	8.6 ± 1.8 (5.7-11.8)	10 ± 1.3 (8.2-12.9)
PCL	3.7 ± 0.7 (2.5-5.0)	--	--	2.25	4.1 ± 0.6 (3.2-5.2)	3.0 ± 0.303 (2.5-3.8)	2.7 ± 0.2*	4.1 ± 0.4 (2.95-4.77)	2.79 + 0.27* (2.2-3.4)	2.2 ± 0.4 (1.6-2.7)	3.8 ± 0.3 (3.2-4.5)
PCW	3.0 ± 0.2 (2.5-4.0)	--	--	2	4.1 ± 1.1 (3.1-5.1)	2.8 ± 0.363 (2-3.8)		4 ± 0.4 (2.9-4.6)		2.1 ± 0.3 (1.5-2.5)	3.8 ± 0.4 (3.2-4.5)
PA	--	--	--	--	164.8° ± 2 (147- 176.2)	--	--	166.2° ± 7.4 (146.4-179.2)	--	175.2° ± 4.1 (166.9-179.9)	169.2° ± 6.5 (155.4-178.8)
Host Location	Mediterranean off France, Italy, Monaco, & Northeast Atlantic	Mediterranean off France. Croatia & Monaco	Mediterranean off Monaco	Mediterranean off Montenegro	Mediterranean off Spain	Mediterranean off Spain	Not indicated, presumably Mediterranean off Greece	Mediterranean off Spain	Mediterranean off Spain & South Atlantic	Mediterranean off Spain	Mediterranean off Spain
Prevalence	--	--	--	15.38%	4.26%	--	51% ; 2%	58.51%	2.15%; 48.7%; 28.6%	9,53%	4,76%
Preparation of spores	Fresh	--	--	--	Fresh	Fresh	--	Fresh	Fresh	Fresh	Fresh

6.3.2. Histopathology of *C. puntazzi* in *D. puntazzo*

Infected fish showed no external signs of disease, neither was mortality recorded from the stocks used in the present study. In some cases, enlargement of infected gall bladders was noted, although heavy parasite load was not necessarily related to an enlargement of the bladder. Thickening of the subepithelial connective tissue of the gall bladder was frequently observed. Trophozoites in different degrees of maturation as well as mature spores released into the bile were observed in the lumen of the gall bladders (Figure 6.4). In some cases, localised loss of epithelial cells and their microvilli was observed close to parasites and surrounded by areas of intact epithelium (Figure 6.4). In TEM, a number of necrotic cells with darker appearance, abundant vacuoles, loss of mitochondrial structure and loss of connection to the basal lamina (Figure 6.5A,C) were observed close to or in areas showing epithelial sloughing (Figure 6.5A-C). Despite the close vicinity of the trophozoites and the epithelium they were never detected intracellularly, nor clearly attached to the epithelium. However, connection between some parasites and detached cells or cell debris was sometimes observed (Figure 6.5A). The epithelial cells of the gall bladder often exhibited bulging apices showing fine granular cytoplasm segregation (Figure 6.5D).

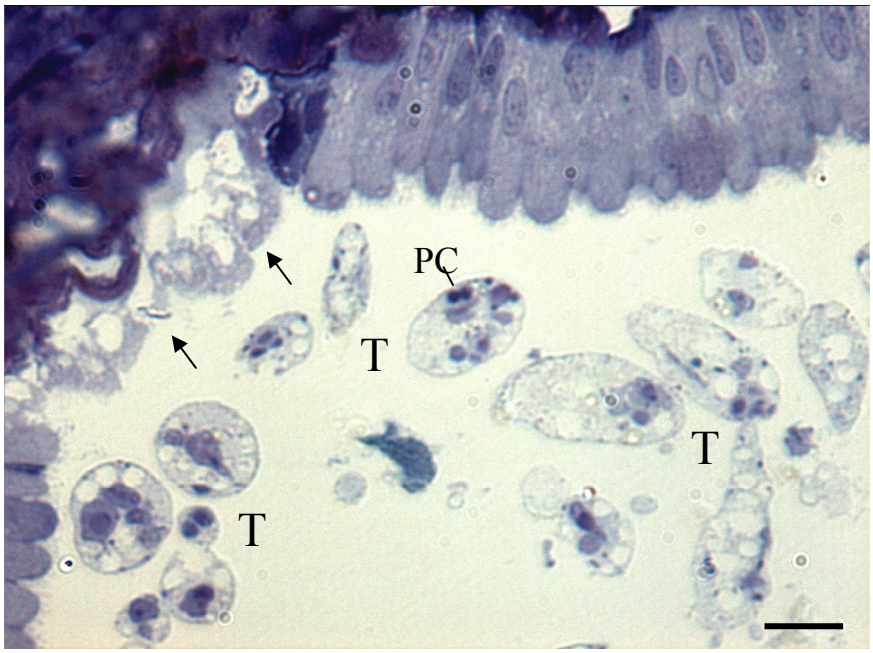

Figure 6.4 Semithin section of *Ceratomyxa puntazzi* n. sp. infected gall bladder of *Diplodus puntazzo*. Affected gall bladder area with a large group of trophozoites (T), one of them more mature harbouring two polar capsules (PC). Notice the loss of epithelial cells (arrows). Scale bar: 10 µm.

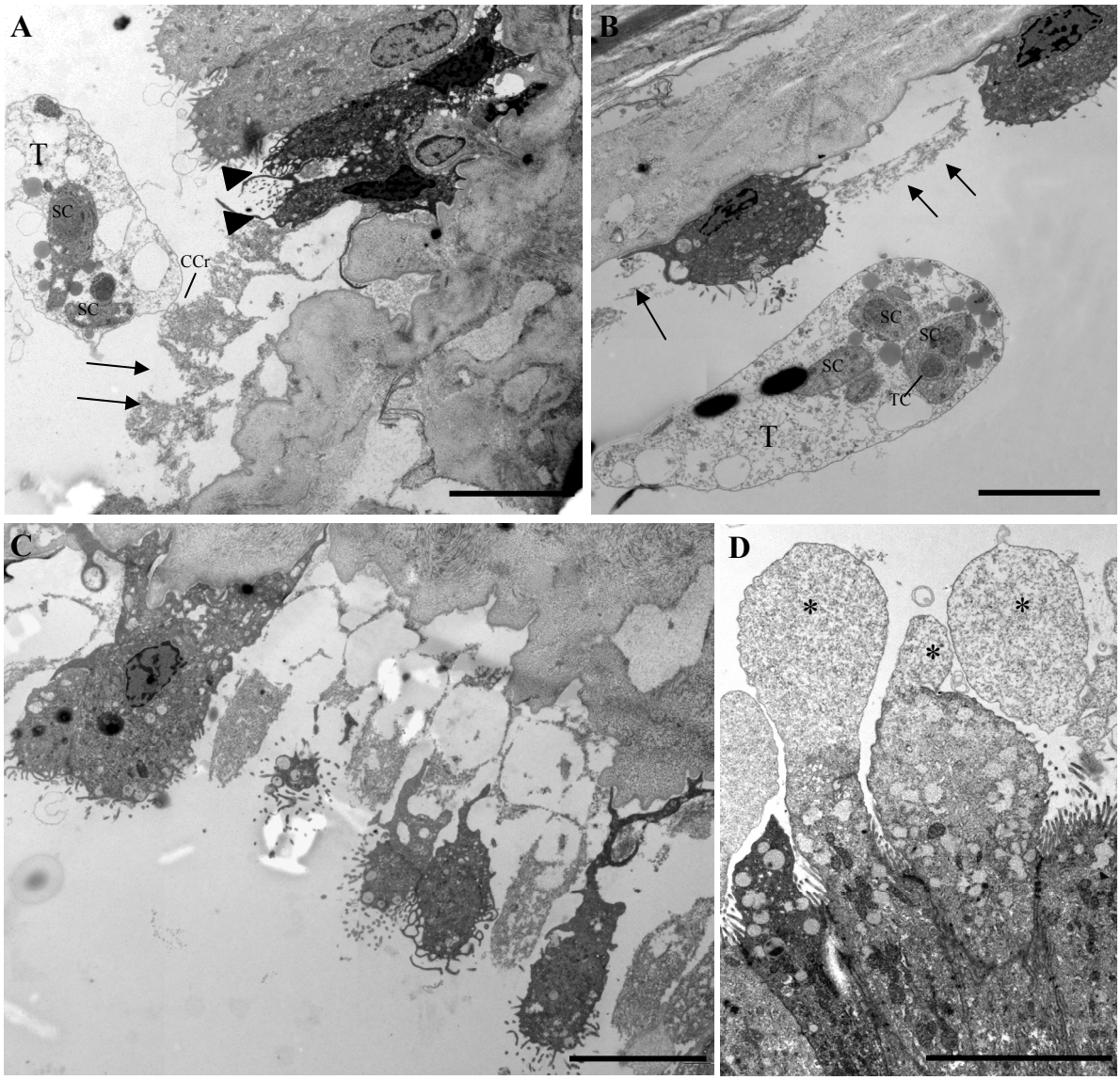

Figure 6.5 Transmission electron microscopy (TEM) images of the epithelium of *Ceratomyxa puntazzi* n. sp. infected gall bladders of *Diplodus puntazzo*. A) A trophozoite (T) with several secondary cells (SC) close to an affected epithelial area apparently connected to detached epithelial cell residues (CCr). Notice the loss of epithelial cells (arrows) and the presence of two darker, necrotic cells, showing vacuolisation, loss of mitochondrial structure and detachment (arrow head). B) Trophozoite (T) with several secondary cells (SC) and a tertiary cell (TC) close to an affected area with loss of epithelial cells (arrows). C) Sloughing of epithelium with extensive loss of epithelial cells. Notice necrotic appearance (as in Figure 6.5A) of the epithelial cells, which are still attached. D) Detail of epithelial cells with bulging apices (*) showing fine granular cytoplasm segregation inside. Scale bar: 5 µm.

In the liver (Figure 6.6A), an inflammatory response or pericholangitis was detected in infected fish, which was characterised by infiltration of eosinophilic granulocytes and lymphocytes into the tissue adjacent to the bile ducts (Figure 6.6B). An increased number of basophilic granulocytes was detected in the liver close to the blood vessels (Figure 6.6C). No histopathological changes were observed in the other organs, i.e. gills, spleen, intestine and kidney.

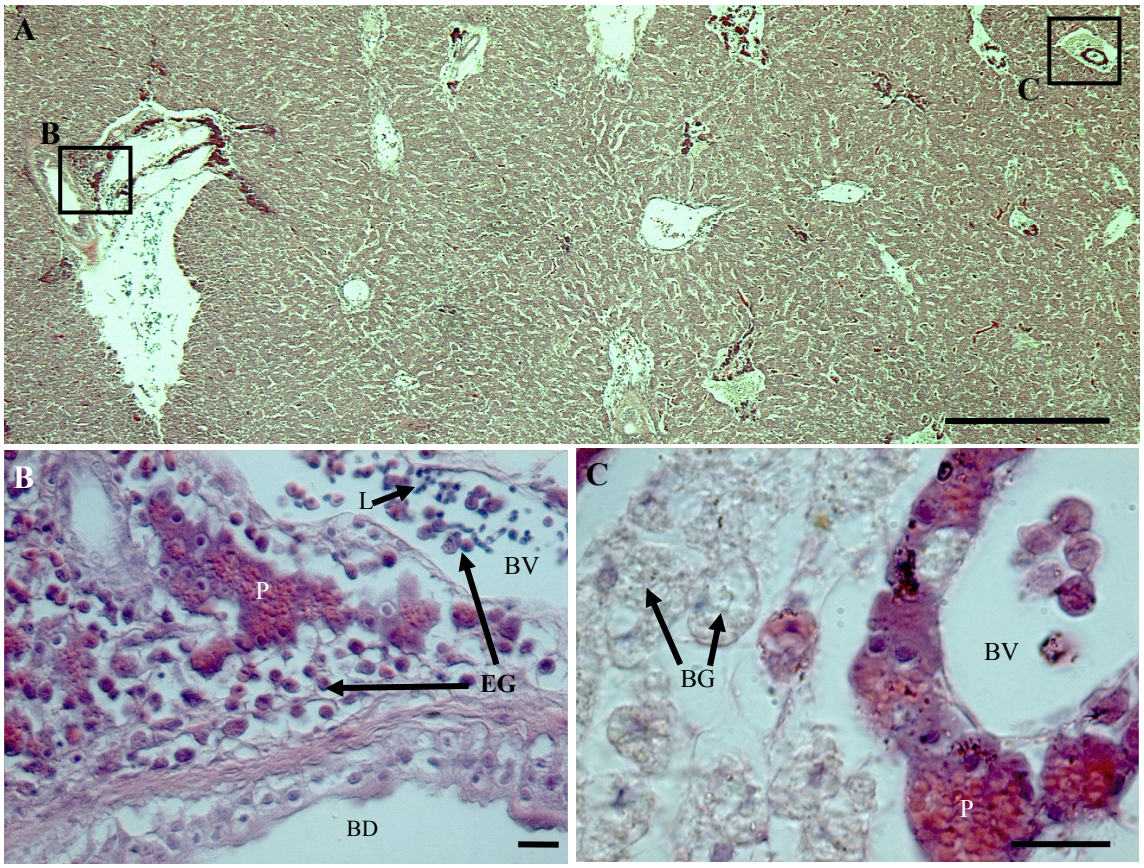

Figure 6.6 Histological cross-sections of *Ceratomyxa puntazzi* n. sp. infected liver of *Diplodus puntazzo*. A) Location of infiltration of leukocytes, detailed in Figure 6.6B & Figure 6.6C. B) Tissue adjacent to a bile duct (BD) and a blood vessel (BV) showing infiltration of eosinophilic granulocytes (EG) and lymphocytes (L), indicating pericholangitis. C) Presence of basophilic granulocytes (BG) close to a blood vessel (BV). P, pancreas. Scale bar: A= 500 µm; B-C= 20µm.

6.3.3. Ceratomyxids of some sparids sharing the habitat with *D. puntazzo*

Ceratomyxid spores of a single morphotype were detected in *D. annularis* (Figure 6.2B), and spores of two different morphotypes in *S. aurata* (Figure 6.2C-D). Due to the lack of detailed information, these spores are not described as new species. However,

morphometrics, prevalence and origin of the material are provided in Table 6.2. SSU rDNA sequences from the three *Ceratomyxa* spores types (see Appendix 1) were obtained and used for morphological comparison and phylogenetical analysis. In all cases, sequences obtained from two fish resulted in identical sequences from PCR product.

6.3.4. Morphological differences between *C. puntazzi* and *Ceratomyxa* sp. ex *D. annularis*

Due to their strong morphometrical similarity (see Table 6.2), measurements of 30 spores of *C. puntazzi* and 27 spores of *Ceratomyxa* sp. from *D. annularis* were analysed statistically. Thereby, statistically significant differences between the spores of *C. puntazzi* and *Ceratomyxa* sp. ex *D. annularis* were observed only with regard to total spore length ($p=0.017$). Thickness of the spore ($p=0.843$), posterior angle of the spores ($p=0.518$), sutural position of the spore ($p=0.337$), polar capsule length ($p=0.192$) and polar capsule width ($p=0.996$) were not significantly different between *C. puntazzi* and *Ceratomyxa* sp. ex *D. annularis*. In the PCA, principal component I (size-related, *X*-axis) explained 34% and component II (shape-related, *Y*-axis) explained 54.62% of the total morphometric variability. Representation of components I and II in a dispersion diagram shows that the two species did not form clearly separated groups (Figure 6.7). The t-test of the principal components (component I: $p=1.000$; component II: $p=1.000$) indicated no differences between the spores from the two hosts.

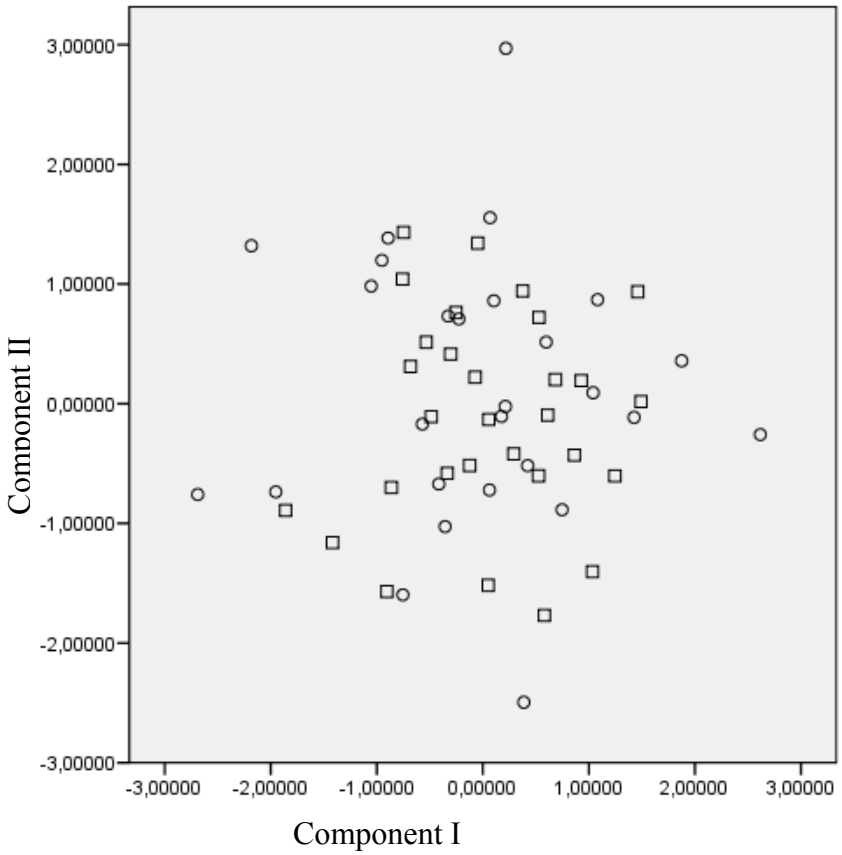

Figure 6.7 Dispersion diagram of component I (size-related, *X*-axis) and II (shape-related, *Y*-axis) after PCA obtained with the measurements (detailed in Table 6.2) of the spores of (○) *Ceratomyxa* sp. ex *Diplodus annularis* and (□) *Ceratomyxa puntazzi* n. sp. ex *Diplodus puntazzo* demonstrates that separation of the two species on the basis of morphological data is not possible.

6.3.5. Molecular and phylogenetical results

Submission to the BLAST server on GenBank showed that all new sequences were most closely related to 1) *C. sparusaurati* (GenBank Accession No. AF41147) from Mediterranean *S. aurata* (Palenzuela et al. 2002), to 2) *Ceratomyxa barnesi* Gunter, Whipps & Adlard 2009 (GenBank Accession No. FJ204245) from a siganid from the Great Barrier Reef, Australia (Gunter et al. 2009) and to 3) two *Ceratomyxa* spp. (GenBank Accession No. DQ 333431 and DQ333429) from the Red Sea (Diamant & Lipshitz unpublished). Interspecific genetic variation in the SSU rDNA sequence between the new sequences from ceratomyxids from sparids and *C. sparusaurati* was as high as 1.4-3.7% with 22 to 59 bp differing between the sequences (Table 6.3). Interspecific genetic variation of all ceratomyxids from sparids in the Mediterranean

with ceratomyxids from siganids was 9.6-13.9%, showing a higher similarity with *C. barnesi* from Australia (9.6-10.7%) than with *Ceratomyxa* sp. SRR and RM from Red Sea (11.3-13.9%).

Table 6.1 Pairwise divergences in the SSU rDNA sequences of *Ceratomyxa* spp. from sparids expressed in percentage (1.7-3.7%, upper right part) and in nucleotide differences (22-59 bp, lower left part).

	1	**2**	**3**	**4**	**5**
1. *Ceratomyxa puntazzi* n.sp.	--	1.7	3.6	1.6	3.1
2. *Ceratomyxa* sp. ex *Diplodus annularis*	27	--	3.6	1.4	2.5
3. *Ceratomyxa* sp. 1 ex *Sparus aurata*	58	57	--	3.7	2.2
4. *Ceratomyxa* sp. 2 ex *Sparus aurata*	25	22	59	--	2.2
5. *Ceratomyxa sparusaurati*	49	40	35	34	--

In order to determine the phylogenetic position of the four new sequences obtained in this study and the relation with the most closely related taxa, 31 SSU rDNA sequences of myxozoans, 27 of which belong to the genus *Ceratomyxa* (including all close BLAST matches) were included in the phylogenetic analysis. BI and MP analyses were based on 1020 informative characters (as suggested by GBlocks) and produced a tree (BI tree showed; Figure 6.8) which placed the new sequences in a single well-supported clade [*Ceratomyxa* sp. ex *D. annularis*, *Ceratomyxa* sp. 1 ex *S. aurata*, *Ceratomyxa* sp. 2 ex *S. aurata*, *C. sparusaurati* and *C. puntazzi* n. sp.] in close relationship with the siganid ceratomyxids. Other well-supported clades were [*Ceratomyxa kenti* Gunter & Adlard 2008 and *Ceratomyxa bryanti* Gunter & Adlard 2008], [*Ceratomyxa choerodonae* Heiniger, Gunter & Adlard 2008, *Ceratomyxa heinigerae* Gunter, Whipps & Adlard 2009 and *Ceratomyxa milleri* Gunter, Whipps & Adlard 2009] and [*C.* sp. 2 IF-2006 and *Palliatus indecorus* Shulman, Kovaleva & Dubina 1979] in accordance with a recent phylogentic study of the genus *Ceratomyxa* (Gunter et al. 2009).

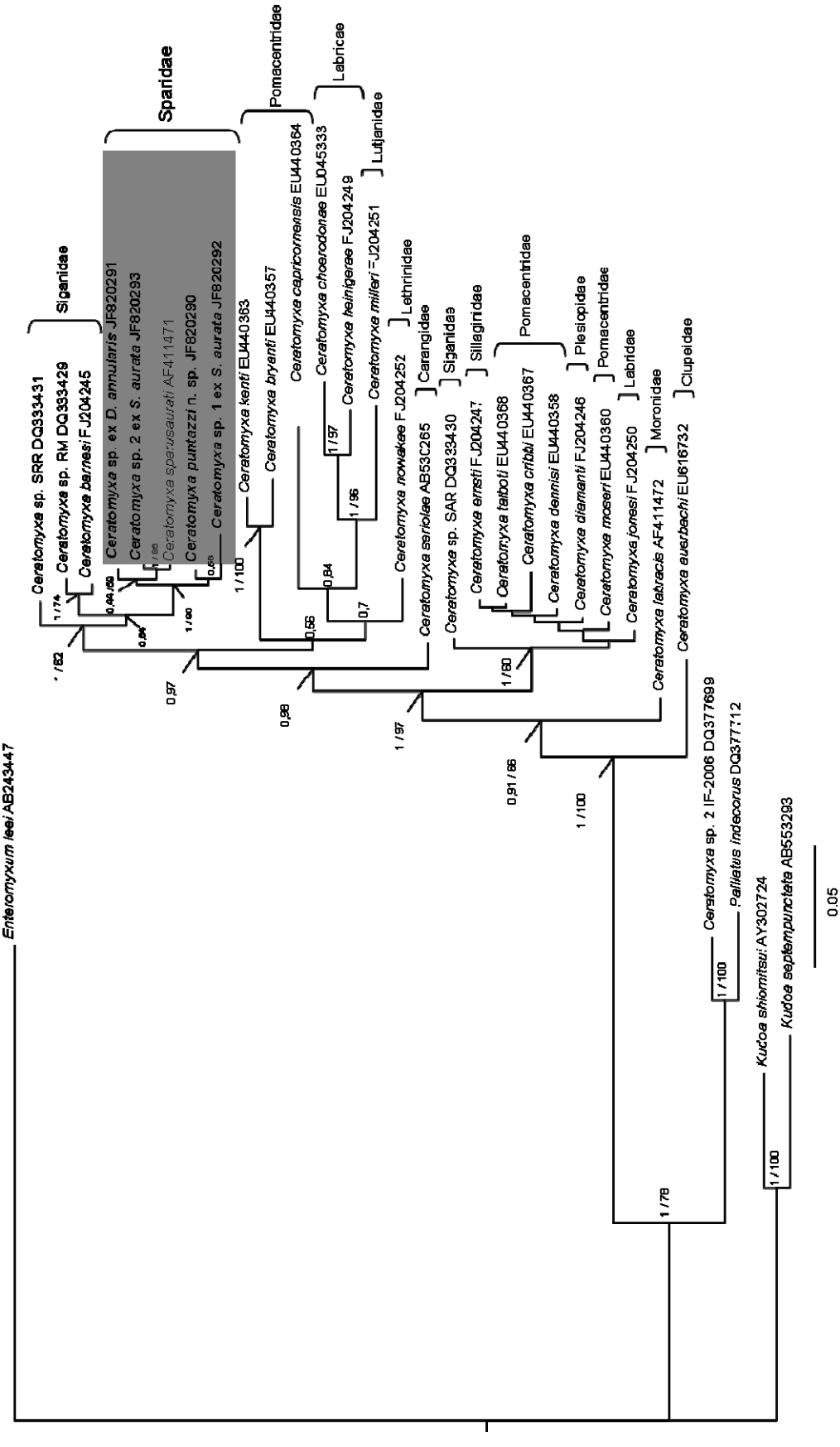

Figure 6.8 Phylogenetic tree based on SSU rDNA sequences of selected myxozoan species, showing the position of the *Ceratomyxa* spp. sequenced in the present study, inferred by Bayesian inference (BI) and maximum parsimony (MP). BI analysis selected tree showed. Family host indicated. Grey box indicates species from sparid fishes, which form a well-supported clade. *Enteromyxum leei*, *Kudoa septempunctata* and *Kudoa shiomitsui* were used as outgroups. Numbers at nodes represent clade posterior probabilites (BI) and bootstrap values (MP).

6.4. Discussion

Ceratomyxa is considered as a "super-rich" genus of myxozoans: in the Great Barrier Reef (Australia), where most hitherto described *Ceratomyxa* species originate, between 0.91 - 1.0 species of *Ceratomyxa* occur per fish species and several thousands of species are likely to exist (Gunter et al. 2010b). While previous phylogenetic studies focussed on ceratomyxids in the fish families Serranidae, Labridae and Pomacentridae, sequence information is only available for a single species from the family Sparidae, i.e. *C. sparusaurati* (Palenzuela et al. 2002). The present study provides morphological and molecular data of *C. puntazzi* in *D. puntazzo* and of three further *Ceratomyxa* species from other sparids in the same habitat. In addition to the present data, eight species of *Ceratomyxa* have been described in the family Sparidae: *Ceratomyxa arcuata* (Thélohan 1892) in *P. bogaraveo*, *Ceratomyxa pallida* Thélohan 1894 in *Sarpa salpa* L. and *Boops boops* L., *Ceratomyxa herouardi* Georgévitch 1916 in *S. salpa*, *Ceratomyxa mylionis* syn. *Leptotheca mylionis* (Ishizaki 1960) in *Acanthopagrus schlegelii* (Bleeker 1854), *C. diplodae* in *D. annularis*, *D. puntazzo* and *Dicentrarchus labrax* (L.), *C. sparusaurati* in *S. aurata, Ceratomyxa acanthopagri* syn. *Leptotheca acanthopagri* (Zhao & Song 2003) from *A. schlegelii* and *Ceratomyxa* sp. from *D. dentex* (Kudo 1919; Ishizaki 1960; Lubat et al. 1989; Sitjà-Bobadilla & Alvarez-Pellitero 1993c; Sitjà-Bobadilla et al. 1995; Company et al. 1999; Zhao & Song 2003; Merella et al. 2005; Katharios et al. 2007). The fact that all these species, except *C. mylionis* and *C. acanthopagri*, have been described from the Mediterranean, suggests that species richness of *Ceratomyxa* in Mediterranean sparids is similarly high as previously reported from serranids, labrids and pomacentrids (Gunter & Adlard 2008; 2009; Heiniger et al. 2008).

According to the present findings, it is furthermore likely that more than one species of *Ceratomyxa* may be present in a single sparid host. We detected two *Ceratomyxa* spp. in *S. aurata* which were both morphologically as well as molecularly different from *C. sparusaurati*, found in the same host, indicating that at least three different species are present in *S. aurata*. Similarly, *C. puntazzi* was described as a new species in this study as morphological data differed considerably from *C. diplodae*, which was originally described from *D. annularis* (Lubat et al. 1989) but found to occur in *D. puntazzo* from Greece (Katharios et al. 2007). Unfortunately, only morphological data are available for *C. diplodae*, and our attempts to obtain molecular data of this species were

unsuccessful, as the only ceratomyxid detected in *D. annularis* seems to be yet another species, morphologically different from both, *C. puntazzi* and *C. diplodae*. Morphologically, *C. puntazzi* and *Ceratomyxa* sp. ex *D. annularis* were extremely similar and could not be separated by statistical analysis or principal component analysis of morphometric data, although significant differences were found with regard to spore length. However, the SSU rDNA sequences of these morphologically similar species possessed an interespecific genetic variation of 1.7%, representing 27 bp of divergence (Table 6.3). Our results agree with the reported interspecific genetic distances between species of the genus *Ceratomyxa* which have been recorded as low as 1.29% corresponding to only 17 bp (Gunter & Adlard 2009). Moreover, *C. puntazzi* and *Ceratomyxa* sp. ex *D. annularis* are reported from different sparid host, which agrees with the idea that *Ceratomyxa* spp. are generally constrained to a single host species (Gunter et al. 2009).

The fact that two species have 1.7% sequence divergence but almost identical morphology, contrasts with the results obtained from other species analysed in the present study. The interspecific sequence divergence between *C. puntazzi* and *Ceratomyxa* sp. 2 ex *S. aurata* is 1.6%, representing 25 bp, and that of *Ceratomyxa* sp. ex *D. annularis* with *Ceratomyxa* sp. 2 ex *S. aurata* is 1.4%, representing 22 bp (Table 6.3). However, the morphometric differences between these species are considerable with regard to spore size and proportions. Thus, the combination of morphometric features and molecular data are essential for the discrimination and correct diagnosis of new and previously described species of *Ceratomyxa*.

Our phylogenetic analysis placed the new sequences from this study together with *C. sparusaurati*, the only other *Ceratomyxa* SSU rDNA sequence from sparids available to date, thus forming a well-supported clade of ceratomyxid species from sparid hosts in the Mediterranean and indicating that they might have a common ancestor. Previous studies suggested that radiation of *Ceratomyxa* spp. has occurred also within other host families (Serranidae and Pomacentridae), and even within host genera and species (Gunter et al. 2009). However, the present results also support a clustering according to geographic location as all species contained within the well supported clade were obtained from the Mediterranean and the closest taxa outwith the clade were obtained from fishes in the Red Sea (Diamant and Lipshitz unpublished), which is geographically close and connected to the Mediterranean via the Suez Canal. To understand if radiation of ceratomyxids is influenced more strongly by host family or by geographical barriers,

further SSU rDNA sequences from sparids outwith the Mediterranean region would be desirable.

Compared with the strongly pathogenic effect of the unusual (histozoic) ceratomyxid *C. shasta*, pathological effects related to coelozoic *Ceratomyxa* species from the gall bladder have been described as moderate. However, *Ceratomyxa* spp. have been determined as important opportunistic parasites, especially in the sharpsnout sea bream. *C. diplodae* showed increased intensity of infection causing a 2-3 times enlargement of the gall bladder in fish heavily infected with the polyopisthocotylean *Atrispinum salpae* (Parona & Perugia 1890) (Merella et al. 2005). In another case, steroid injected *D. puntazzo* which were potentially immunosuppressed, showed heavy infestation with *C. diplodae*, resulting in a high incidence of mortality (Katharios et al. 2007).

The typical types of lesions caused by ceratomyxids in gall bladders were described for *Ceratomyxa* spp. in *S. aurata* and *D. labrax* and include swelling, vacuolization, deformation, sloughing and even necrosis of the epithelial cells of the gall bladder wall and thickening and inflammation of the subepithelial connective tissue (Alvarez-Pellitero & Sitjà-Bobadilla 1993b; Palenzuela et al. 1997), similar as in the present case of *C. puntazzi*. Attachment of the trophozoites to the epithelial cells of the gall bladder, as *Ceratomyxa* spp. in *D. labrax* and *Ceratomyxa dehoopi* Reed, Basson, Van As & Dyková 2007 in *Clinus superciliosus* (L.), has been identified as the cause of this damage to the epithelium (Alvarez-Pellitero & Sitjà-Bobadilla 1993a; Reed et al. 2007). However, in the case of *C. puntazzi* the connection between parasite and epithelium was rather loose, although the parasite obviously caused epithelial changes.

Epithelial cells of *D. puntazzo* often presented bulging apices showing fine granular cytoplasm segregation. Similar structures have been observed in gall bladder of tench, described as droplets of degenerated cytoplasm (Viehberger 1982). Bulging epithelial apices in the sparid *Boops boops* (L.) have been related to normal secretory function of film mucus (Oldham-Ott & Gilloteaux 1997). However, although the bulging apices may represent a normal condition in gall bladder epithelia in various fish species, parasitic stages of *C. sparusaurati* were found in close contact with or even embracing finger-like protrusions in the gall bladder epithelium of *S. aurata* and noticeable signs of damage were observed in these cells (Palenzuela et al. 1997). In the case of *C. puntazzi*, no direct relationship between bulging epithelial apices and the parasite was observed, but a potential effect of hypersecretion of mucus by the host due to the presence of the parasite could exist.

The pericholangitis in the liver of *D. puntazzo* infected with *C. puntazzi* included the infiltration of different leukocytes from the blood vessels in the areas surrounding the bile ducts. Under normal conditions, the small number of *C. puntazzi* detected in the bile ducts is not likely to affect the normal bile drainage of the liver as observed in the case of *C. dehoopi* which completely obstructs and distends the bile ducts (Reed et al. 2007). However, the potential of a parasite to proliferate and considerably expand the infection depends to a great part on the condition of the host immune system. In the case of the pathogenic intestinal myxozoan *E. leei*, the immune response to this parasite is weaker in *D. puntazzo* than in *S. aurata*, which might explain the much higher severity of infection in *D. puntazzo* (Muñoz et al. 2007). According to our observations, the same dose of infective stages of the ciliate protozoan *Cryptocaryon irritans* Brown 1951 causes high mortalities in *D. puntazzo* but not in *S. aurata* (unpublished data). This suggests that the immune system of sharpsnout seabream is less capable of coping with different immunological challenges than that of *S. aurata*. It might thus also be more susceptible to uncontrolled proliferation of *C. puntazzi* in case of opportunistic situations, similar as described for *C. diplodae* in the same host species (Merella et al. 2005, Katharios et al. 2007). This should be kept in mind when establishing new *D. puntazzo* culture sites, as temperature stress, decreased water quality and other factors may have a negative effect on an existent *C. puntazzi* infection.

CHAPTER 7. Three-dimensional morphology, ultrastructure and composition of *Ceratomyxa puntazzi* proliferative and sporogonic stages from the bile – A first insight into the structures and mechanisms underlying motility and budding of plasmodia

7.1. Background

Pathology in myxozoans is usually associated with the presence of large numbers of parasites, produced by rapid proliferation of vegetative stages (Canning et al. 1999; Redondo et al. 2003a). However, little is known about the developmental sequences resulting in the multiplication of myxozoan parasite stages.

The Myxozoa have been reported to show a unique process of proliferation with new cells forming within other cells by a process referred to as endogenous budding (Lom & Dykóva 2006). For many years, endogenous budding had been regarded as the basic method of parasite proliferation in myxozoans. Recently, this process was proposed to be dogma (Morris 2010), as it was observed that cells internalize other cells, resulting in the production of so called secondary and tertiary cells, which lie within the primary cell. Morris & Adams (2008) furthermore suggested that the formation of tertiary cells in all myxozoans only occurs at the onset of sporogony, and that, based on this hypothesis, a common sequence of development can be defined for all myxozoans from the same phylogenetic clade.

Little is known of the pre-sporogonic development of the members of the phylogenetic clade which harbours *Ceratomyxa* spp. (Thélohan 1892) (marine clade of Fiala 2006, and marine clade III of Morris & Adams 2008). Only recently, Björk & Bartholomew (2010) demonstrated that pre-sporogonic stages of *C. shasta* develop in the endothelium of the blood vessels of the gills, and that they release small, binuclear stages which migrate to the intestine, where proliferation and sporogony takes place. While *C. shasta* is considered an extraordinary member of the genus with regard to tissue location, as *Ceratomyxa* spp. usually inhabit the bile of marine teleosts, and possibly also with regard to phylogenetic position (Fiala 2006; Fiala & Bartošová 2010), information on the developmental sequence of ceratomyxids that develop spores within the bile is fragmentary. One of the most complete studies is that of *Ceratomyxa blennius* (Noble 1941), but the author only provides information on the nuclear divisions during development, without being able to study the cytokinetics, which is possibly related with the limited methods available at the time. However, Noble (1941) already recognised that both, proliferation (schizogony) and spore-formation (sporogony) take place in the bile.

Noble (1941) and several other authors (*e.g.* Meglitsch 1960; Sitjà-Bobadilla et al. 1995; Cho et al. 2004) observed that *Ceratomyxa* spp. stages in the bile show motility

and amoebic movement. Amoebic movement has also been reported from sporoplasms after release from the spore valves, *e.g.* in *T. bryosalmonae* (Grabner & El-Matbouli 2010b) and *M. cerebralis* (Eszterbauer et al. 2009; Kallert et al. 2009). While motility of the sporoplasms allows the parasite to burrow into the epithelia of the fish, thus promoting entry into or, thereafter, active displacement within the host's tissues, motility in myxozoans inhabiting body cavities filled with fluids probably serves buoyancy rather than displacement. Amoeboid movement of cells is generally accepted to be based on an actin cytoskeleton (Mitchison 1995) which allows membrane protrusion. Protrusion is based on the extension of pseudopodia that could be of three kinds: filopodia, lamellipodia or blebs (Small & Rottner 2010). Filopodia and lamellipodia are produced by polymerization of actin but blebs are membrane bulgings and are actomyosin-dependent (Charras & Paluch 2008). Furthermore, actin filaments are the key in the process of cell divisions by the formation of a contractile ring during cytokinesis in eukaryotes (Pelham & Chang 2002). As myxozoans occurring in the bile are often present in large numbers and can be easily extracted without host tissue contamination, they provide a special opportunity to study the structures facilitating parasite motility and the mechanisms underlying parasite movement, topics about which hardly anything is known to date.

For the study of myxozoans, the main limiting factor is their small size. Traditionally, light microscopy and electron microscopy have been used to morphologically describe different stages in myxozoans. In 2005, McGurk et al. published the first three-dimensional view of myxozoans by studying spores of *T. bryosalmonae* using confocal laser scanning microscopy. This technique allows for the visualization of different cell components in whole parasites, with minimal processing of the material and a wide range of fluorescent dyes available for the visualization of different morphological features (McGurk et al. 2005).

A large number of different developmental stages of *C. puntazzi* were detected in the bile of *D. puntazzo* (see Chapter 6, Section 6.3.1), and these stages showed active motility. A variety of microscopy techniques were combined, *i.e.* light microscopy, videos, scanning and transmission electron microscopy and confocal laser microscopy, to study *C. puntazzi*'s three-dimensional morphology, ultrastructure and composition, as well as its locomotive behaviour and the structural components promoting parasite motility. Furthermore, live, fixed and differentially stained parasite stages from the bile of *D. puntazzo* were studied to ascertain the developmental sequence of parasite stages

resulting in successful proliferation and spore formation. This sequence was then compared with existing descriptions of other *Ceratomyxa* spp.

7.2. Materials and methods

7.2.1. Fish and parasite collection

D. puntazzo (n=81; 6-29 cm total length; 3.75-448.6 g) were obtained from San Pedro del Pinatar, Mar Menor, Murcia (Spanish Mediterranean coast, see Table 3.1). Fish were transported live to the aquaria facilities at the University of Valencia. Bile was collected as described in Chapter 6, Section 6.2.2. Parasites were observed *in vivo*, as well as after fixation and differential staining, using a variety of microscopic techniques to obtain the most comprehensive information on the morphology and development of *C. puntazzi* in the gall bladder of *D. puntazzo*.

7.2.2. Morphological examination

LM digital images, measurements and videos of live parasites were taken as described in Chapter 3, Section 3.2.1. SEM and TEM were conducted as describe in Chapter 3, Section 3.2.2 & 3.2.3. TEM was conducted using the alternative protocol for rapid processing with Agar low viscosity (ALV) resin.

7.2.2.1. Confocal laser scanning microscopy (CLSM)

For CLSM, bile containing proliferative and sporogonic myxozoan stages was centrifuged for 3 min at 1800 x g to pellet the myxozoans. The supernatant was then removed and replaced by 4% formalin in 0.1M PBS. After overnight fixation, the parasite stages were left to settle onto 0.1% poly-D-lysine coated slides for 30 min. The parasites were then stained with the following differential dyes: 1. Nile Red (7-diethylamino-3, 4-benzophenoxazine-2-one), which is lipophilic and stains intracellular lipid droplets red, 2. Phalloidin (Alexa Fluor® 488 phalloidin, Invitrogen), which binds specifically at the interface between the subunits of F(ilamentous)-actin, which forms the cytoskeleton and functions as an important mediator of cell mobility, and 3. DAPI (4,6-diamidino-2-phenylindole,dilactate; Molecular probes), which binds to DNA. Nile Red stock solution (0.5 mg/ml in acetone) was diluted by mixing 1.7 ml of the stock solution with 50 ml of a 75:25 glycerol:water mixture. Nile red staining was conducted for 30 min in the dark, thereafter with the samples were washed with 0.1M PBS. Phalloidin was applied at 2.5 µL/100 µL in 0.1M PBS and DAPI at 300nM in

dechlorinated tap water. Parasites were stained for 30 min, and no post-staining rinses were conducted before viewing. Cover slips were placed over all the samples and sealed with nail varnish to prevent evaporation of the medium. All CLSM samples were examined using a Leica TCS SP2 AOBS confocal laser scanning microscope (Leica Microsystems AG, Wetzlar, Germany).

7.3. Results

A variety of different stages of *C. puntazzi* were found to develop in the bile of *D. puntazzo*. None of these stages were found to be attached or occur inter- or intracellularly in the epithelium of the gall bladder. Most importantly, the bile was determined as the site of two different developmental cycles of *C. puntazzi*: 1. pre-sporogonic proliferative development and 2. sporogony. Both developmental cycles were found to occur in parallel but fish were observed to have either predominantly stages lacking mature spores or stages with predominantly mature spores.

The combination of different microscopic techniques allowed for the observation of the behaviour, structure, morphology, cellular anatomy and composition of the different stages, as well as for the estimation of their developmental sequence and succession.

7.3.1. Pre-sporogonic stages

Gross morphology, differential staining and behaviour

Proliferating stages presented high morphological plasticity and locomotive activity, showing amoeboid movement. The earliest and smallest stages were round or ellipsoidal (Figure 7.1A and Figure 7.8A), measured 3.7-6.5 μm in diameter, and showed dispersed refractive bodies in their cytoplasm as well as the presence of 1-3 filopodia of 0.9-3.1 μm length. As development progressed, the parasites acquired a larger size (9.7-35.2 μm length, 5.89-20.52 μm width; 3-11 filopodia of 1.7-7.5 μm length) and a characteristic pyriform shape, which seemed to be closely associated with the direction of movement (Figure 7.1B-D and Figure 7.8B). The round side was found to represent the anterior end of parasites in motion, and it was characterized by a hyaline area (ectoplasm) of 2.3-3.5 μm width and a concentration of filopodia which were moving actively (Figure 7.1B,I). Sometimes, the filopodia appeared to be ramified. Using CLSM, a high concentration of filamentous actin (F-actin, cytoskeleton) was detected at the round, active, anterior end of the parasites (fluorescent green phalloidin staining in Figure 7.1H-K), corresponding to the hyaline ectoplasm area, which can thus

be defined as a lamellipodium, and the filopodia. The posterior end of the parasites was typically pointed forming a single, large cytoplasmatic extension (8.1-13.9 μm length, 1.1-2 μm and 0.3-1.3 μm width at base and at the tip, respectively) which had a much more rigid appearance than the delicate filopodia at the anterior end of the parasites, and which lacked accumulations of F-actin (Figure 7.1C-D,I). The hyaline area or lamellipodium showed an undulating motion, provoked by the projection of the filopodia, which were formed at the anterior end of the parasite and merged again with the cell surface in the lateral, posterior area. The filopodia were projected in the direction of parasite movement and then laterally, from the median anterior end, which usually had the largest filopodia, to the lateral and most posterior part of the body. Thereby the parasites pulled themselves forward in the medium (Figure 7.2). In the endoplasm of the live parasites, cytoplasmic streaming was observed.

In the pyriform stages, vacuoles measuring 2.8-4.3 μm (neutral red-positive) (Figure 7.1D) and refractive bodies measuring 0.9-1.8 μm (Figure 7.1B,D) were observed, and the latter seemed to be concentrated at the rounded end, posterior to the hyaline area (Figure 7.1B-D). Parasite stages without spores inside them showed intense exogenous budding by plasmotomy (Figure 7.1E-G, J-K). The buds seemed to emerge actively from the "mother" parasite with the F-actin-rich ectoplasmic border of the still attached buds usually found to have a different orientation than that of the "mother" parasite (Figure 7.1J-K), thus causing separation from it. Parasites prepared for SEM showed a slightly different morphology than fresh material, possibly due to fixation. Filopodia and the posterior, pointed cytoplasm extension were often difficult to distinguish (Figure 7.1F). However, the buds were clearly visible, and some of them showed a well defined demarcation line, a cytoplasmic constriction, at the point where they would eventually separate from the "mother" parasite (Figure 7.1E-F). In addition, using SEM, some small blebs (0.22-0.64 μm in diameter) were detected on the surface of the proliferating parasites (Figure 7.1E-G). Nile red-positive lipid droplets (1-2 μm in diameter) were very common in the larger pyriform parasites but not in the smallest ellipsoid stages.

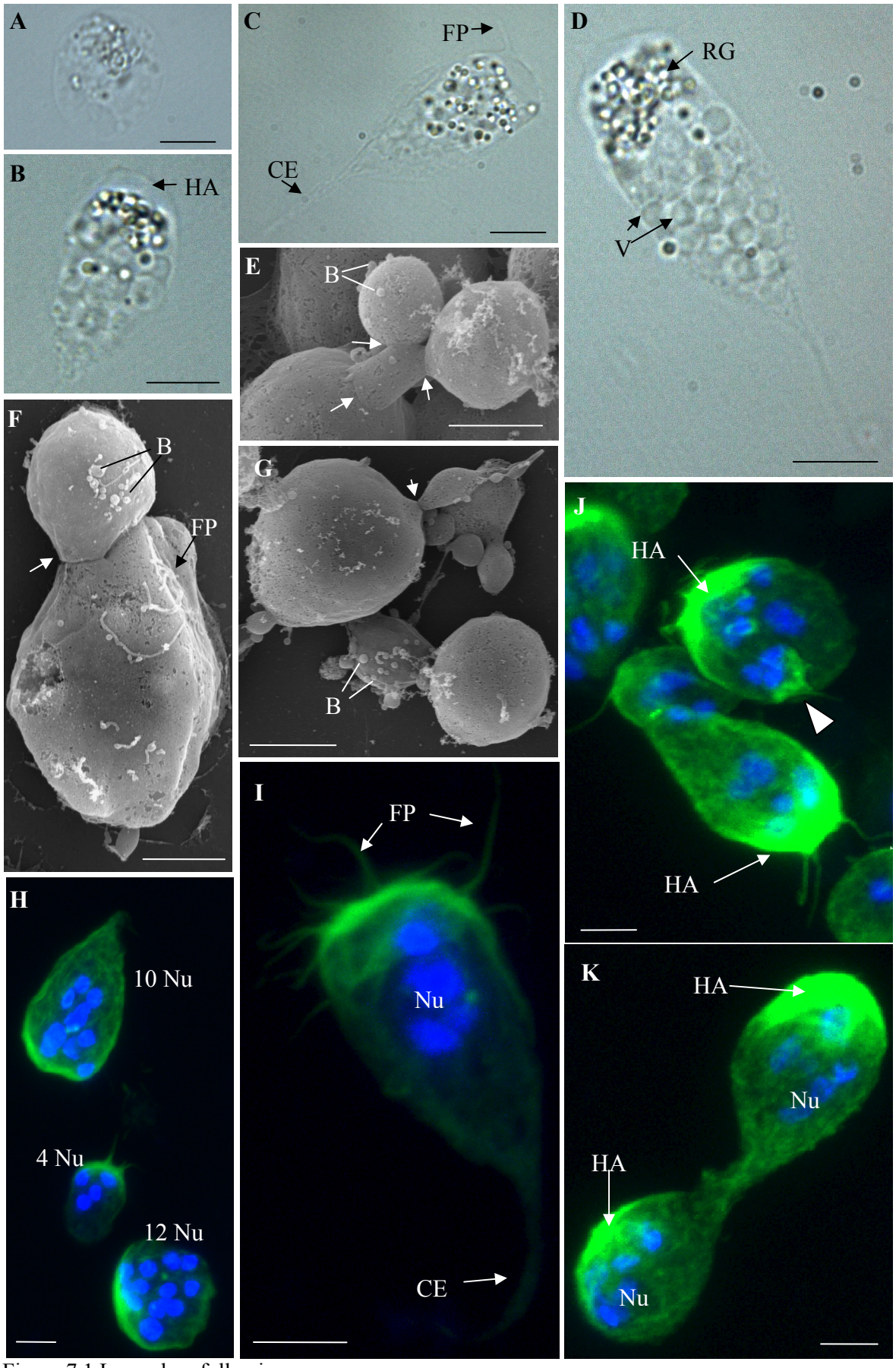

Figure 7.1 Legend on following page.

Figure 7.1 Pre-sporogonic proliferative development of *Ceratomyxa puntazzi* from the bile of *Diplodus puntazzo*. A-D: LM, E-G: SEM, H-K: CLSM (DAPI and Phalloidin stained). A) Small ellipsoidal stage. B) Pyriform stage with a wide hyaline area and refractive granules at rounded, anterior end of parasite. C) Pyriform stage showing large filopodia and abundant refractive bodies at rounded end and a large, rigid cytoplasm extension at posterior end. D) Pyriform stage with abundant vacuoles present in almost the whole body. Refractive bodies were concentrated at anterior end. E-G) Exogenous budding with several stages dividing by plasmotomy. Arrows indicate cytoplasm constrictions. Some filopodia and blebs can be seen on the surface in F and G. H) Three stages, a small ellipsoidal stage with 4 nuclei and two larger stages with 10 and 12 nuclei. I) Pyriform stage with abundant filopodia at round side, where F-actin (green stain) accumulated, and rigid cytoplasmic extension at the posterior end. Four nuclei are visible. J) Several stages with a clear pattern of accumulation of F-actin in the hyaline area at the anterior end of the parasites where the filopodia are located. Upper parasite: exogenous budding of a round stage with three nuclei (head arrow) and an F-actin rich surface at opposite end from the "mother" parasite it is emerging from. K) Two stages showing exogenous budding with still attached buds moving in opposite directions. Abbreviations: HA, hyaline area; CE, cytoplasmic extension; FP, filopodia; RG, refractive granules; V, vacuole; B, bleb; Nu, Nuclei. Scale bar: A= 3 µm; B-D= 10 µm; E-K= 4 µm.

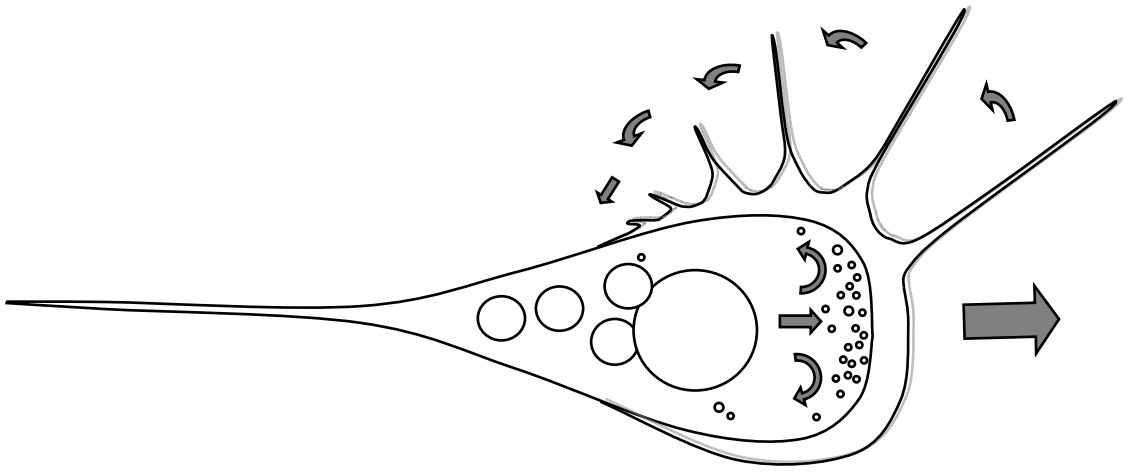

Figure 7.2 Schematic drawing of the locomotive action of an active pyriform stage. Projection of filopodia from the anterior, median part laterally to most posterior part of the hyaline area, allowing active parasite movement.

Cellular ultrastructure and developmental sequence

The earliest, spherical stages observed in the lumen of the gall bladder represented a primary (P) cell containing one or two nuclei (Figure 7.3A), which occupied most of the cell lumen. Larger, pyriform stages with 1-2 nuclei in the P cell contained up to 6

secondary (S) cells (Figure 7.3B-C), and later, secondary cells were found to harbour 1-2 tertiary (T) cells (Figure 7.3C,E-F). The largest proliferative stages were found to contain 12 nuclei (CLSM observation; Figure 7.1H). Commonly, units of 1-3 S cells, harbouring 0-2 T cells each (Figure 7.3F) were found to be separated from larger stages and to bud off (Figure 7.1E-F,J). Often, proliferation inside the different compartments would continue while the buds were still attached.

P cells had the largest nuclei and generally showed dispersed heterochromatin. The cytoplasm of the P cell was generally less electron-dense than that of S or T cells as it was less densely packed with ribosomes. The smallest stages, *i.e.* the ones harbouring 0-2 S cells, often contained very large mitochondria (0.9-1.2 μm length) with various pronounced cristae (Figure 7.4A). The number of mitochondria increased as the P cells grew (Figure 7.3E) but their size was considerably smaller (0.2-0.8 μm length) in larger parasites. Lipid droplets (Figure 7.4B) in the P cell were absent or few and small in the youngest proliferative stages (Figure 7.3A-C) but numerous and larger in multicellular stages (Figure 7.3E). Lipid droplets were rarely observed in the cytoplasm of S or T cells. The P cell of proliferative stages of all sizes had a large number of non electron-dense vacuoles (Figure 7.4C). These had a single membrane and were of variable size, measuring 0.9-2.3 μm in diameter (Figure 7.4A), sometimes filled with granular material (Figure 7.4D).

The cytoplasm of S cells contained mitochondria, abundant ribosomes and rough endoplasmic reticulum (Figure 7.3F). Mitochondria of S cells were normally smaller (0.2-0.4 μm in length) than mitochondria of early P cells. Between some S cells, prominent cell junctions were observed (Figure 7.3D,G). In some cases, partial engulfment was detected between attached S cells (Figure 7.3G). Prominent eccentric nucleoli were sometimes present in the nuclei of S cells (Figure 7.3C-D). A liberated cell doublet was observed, with a highly electron dense cytoplasm, probably representing an S cell harbouring a T cell in its cytoplasm, and with remnants of the P cell membrane attached (Figure 7.3H).

Generally, the T cell cytoplasm was even more densely packed with ribosomes than that of S cells, and some small mitochondria were also present (Figure 7.3F).

The cytoplasmic extensions corresponding to the rhizoid filopodia at the anterior end and the rigid posterior cytoplasm extension were also observed in TEM sections (Figure 7.4D). Small blebs were identified on the surface of the P cell by SEM (Figure 7.4E,F-

H) and were also detected in TEM sections. Their content was either transparent (Figure 7.4E) or presented the same structure as the cytoplasm of the P cells (Figure 7.4F-H).

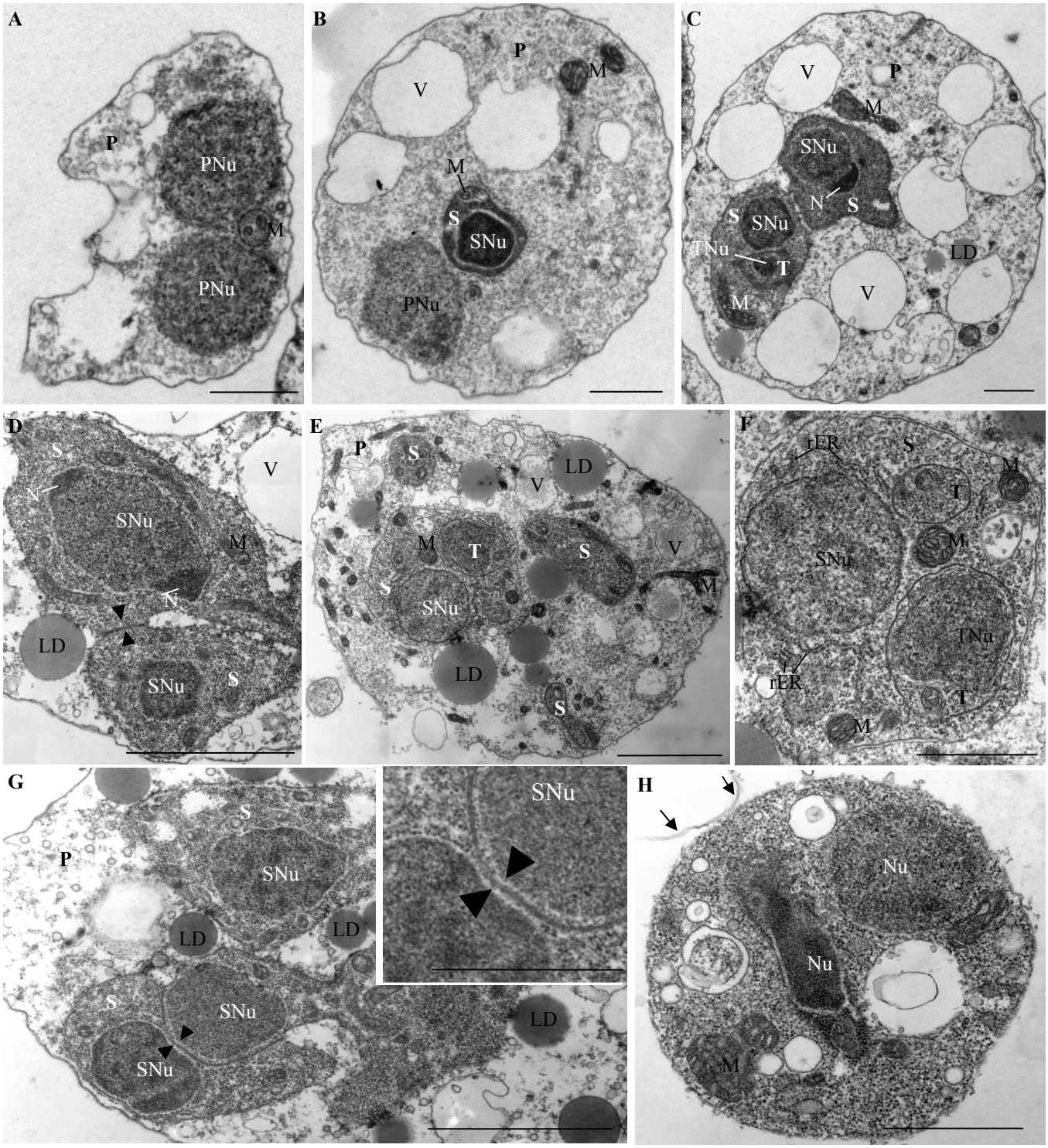

Figure 7.3 Legend on following page

Figure 7.3 Pre-sporogonic proliferative development of *Ceratomyxa puntazzi* from the bile of *Diplodus puntazzo* (TEM). A) Early stage consisting of a P cell with two P cell nuclei. Notice the presence of vacuoles, mitochondria and absence of lipid droplets. B) Stage consisting of a P cell and a S cell with their respective nuclei. In the P cell, vacuoles are well defined and large mitochondria. In the S cell, small mitochondria are visible. C) Stage consisting in a P cell with two S cells, one of them with a forming tertiary cell (S-T doublet). Large mitochondria are present in the P cell and in the S cells. One of the S cell nuclei has an eccentric nucleoli. Notice the presence of small lipid droplets in the P cell. D) Detail of a stage showing two S cells and their nuclei, one of them with two eccentric nucleoli. Notice junction of the S cells (arrow head). Electron-dense lipid droplets where observed in the cytoplasm of the P cell and abundant mitochondria in the S cells. E) Large stage with several S cells and S-T doublet. Abundant electron-dense lipid droplets and mitochondria in the P cell. F) Detail of S-T doublet shown in Figure 7.3E, composed of an S cell and two T cells. Notice abundant rough endoplasmic reticulum in S cell cytoplasm. G) A stage with three S cells in a P cell. Notice cell junction of two S cells (arrow head, see detail insert), where partial engulfment was detected. H) Liberated cell doublet with a high electron dense cytoplasm, probably a S cell with a T cell in its cytoplasm. Note remnants of P cell membrane (arrows). Abbreviations: P, primary cell; PNu, primary cell nucleus; M, mitochondria; S, secondary cell; SNu, secondary cell nucleus; V, vacuole; LD, lipid droplet; N, Nucleoli; T, tertiary cell; TNu, tertiary nucleus; rER, rough endoplasmic reticulum; Nu, nucleus. Scale bar: A-C= 1 µm; D-E= 2 µm; F= 1 µm; G= 2 µm; H= 1 µm.

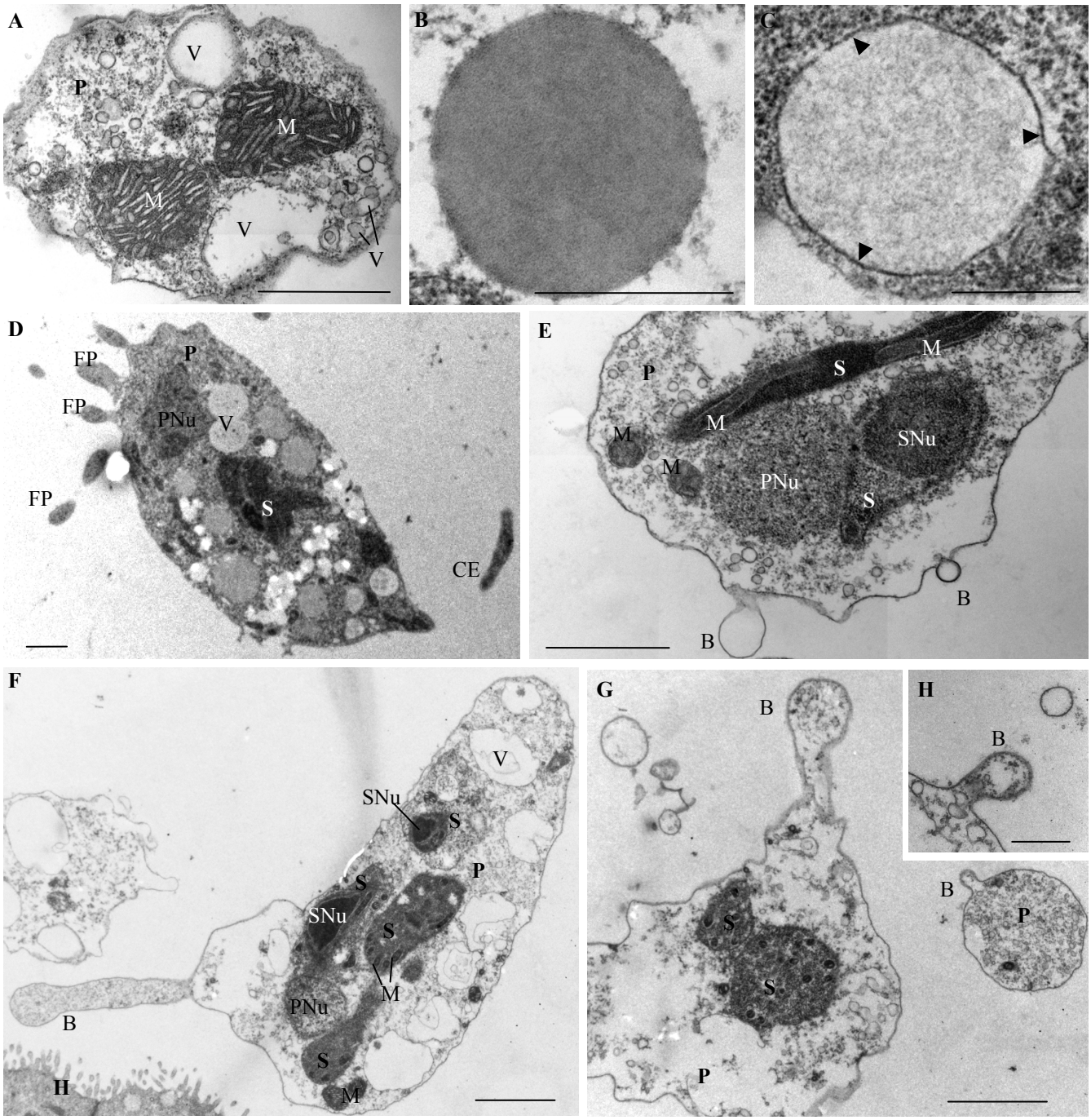

Figure 7.4 Pre-sporogonic proliferative development of *Ceratomyxa puntazzi* from the bile of *Diplodus puntazzo* (TEM). A) Two large mitochondria in the P cell with numerous well-developed cristae. B) Detail of electron-dense lipid droplet in a P cell. Notice the lack of a delimiting membrane. C) Detail of non electron-dense vacuole with a single membrane (arrow head) filled with granular material. D) Pyriform stage with filopodia at rounded side and a large cytoplasmic extension at posterior end. Notice vacuoles with granular material. E) Stage with blebs on the surface. Notice electron-dense cytoplasm of an S cell densely packed with ribosomes. F) Large stage close to the epithelium of the gall bladder, with a large bleb filled with the same material as the cytoplasm of the P cell. G) Stages with blebs.

Figure 7.4 continued: Notice the presence of material inside, similar to the P cytoplasm content. H) Detail of a bleb. Abbreviations: P, primary cell; PNu, primary cell nucleus; M, mitochondria; S, secondary cell; SNu, secondary cell nucleus; V, vacuole; FP, filopodia; CE, cytoplasmic extension; B, bleb; H, host epithelium. Scale bar: A= 1 μm; B-C= 0.5 μm; D-E= 1 μm; F-G= 2 μm; H= 1 μm.

7.3.2. Sporogonic stages

Gross morphology, differential staining and behaviour

Sporogonic stages of *C. puntazzi* were represented by pseudoplasmodia developing two crescent-shaped spores (Figure 7.5A-B and Figure 7.8C). Early sporogonic stages were pyriform showing a high degree of activity and amoeboid-like movement as well as an F-actin-rich anterior edge, as seen in proliferative stages. Later, the parasite stages showed less locomotive activity and were more rigid, due to the mechanical effect of the almost mature spores. As sporogenesis proceeded, F-actin was more dispersed and no longer concentrated at one extremity (Figure 7.5D and Figure 7.8D). Filopodia were present throughout the initial stages of sporogony (Figure 7.5F-G) but had disappeared by the time spores neared maturity (Figure 7.5H and Figure 7.8D). The pyriform shape was found to change to an oval one and lipid droplets were less abundant and had a more random distribution (Figure 7.5H and Figure 7.8D) in mature pseudoplasmodia. Mature spores were free in the bile (Figure 7.8E).

Cellular ultrastructure and developmental sequence

Sporogony was initiated from a pyriform P cell (the pseudoplasmodium) containing 4 S cells. Further division led to the formation of 8 S cells and 4 T cells. These would separate in two pairs of 4 S cells and 2 T cells, each forming a spore. Valve cells were formed from S cells, whereas capsulogenic cells were formed from T cells whose enveloping S cells were found to form the sporoplasm (Figure 7.6A-B). In the beginning, the sporoplasmogenic cells would take up most of the space inside the developing spore. More mature capsulogenic cells were found to be attached to the valve cells (Figure 7.6A).

The pseudoplasmodia (P cells) were electron-lucent and, in the early stages of sporogony, the P cells contained a large number of mitochondria, lipid droplets and vacuoles (Figure 7.6A-B), but as spore formation proceeded, the P cell cytoplasm appeared less defined and less electron-dense, still containing lipid droplets but having

less vacuoles (Figure 7.7A-B). At the end of sporogenesis, the P cell cytoplasm had degenerated and contained hardly any organelles apart from abundant lipid droplets (Figure 7.7B).

During sporogony, the valvogenic cells soon occupied an external position enveloping all other sporogonic cells (Figure 7.6A & Figure 7.7A). In one case, during early sporogony, the cytoplasm of a valvogenic cell showed a constriction connecting an area containing the nucleus of one valvogenic cell with the remainder of the valvogenic cell and all other spore-forming cells (Figure 7.6B). During spore maturation, the cytoplasm of the valvogenic cells became progressively thinner. The two valvogenic cells joined to form the suture (Figure 7.6F & Figure 7.7A), in which the two cells overlapped and formed a desmosome-like junction (Figure 7.7C-E). Mature valve cells formed only a thin line surrounding the other sporogonic cells and the valve cell nuclei had disintegrated (Figure 7.5E).

Capsulogenic cells developed a capsular primordium with an external tube in the cytoplasm (Figure 7.6A,D). As capsulogenesis advanced, the capsular primordium and the external tube grew. Later on, the polar filament was found to condense (Figure 7.7A,D) and coil up inside the polar capsule, forming five coils. The mature polar filament was typically twisted and lay in a granular matrix (Figure 7.7D). Polar capsules had an outer electron-dense layer and an inner electron-lucent layer (Figure 7.7D). At the end of capsulogenesis, the polar capsules acquired a pointed tip where the plug for polar filament discharge was located (Figure 7.7C-D). Next to the plug, the junctions between the capsulogenic cells and the valve cells were surrounded by fibrous material (Figure 7.7D). Capsulogenesis was not synchronised between the four capsulogenic cells of a pseudoplasmodium (Figure 7.7 A).

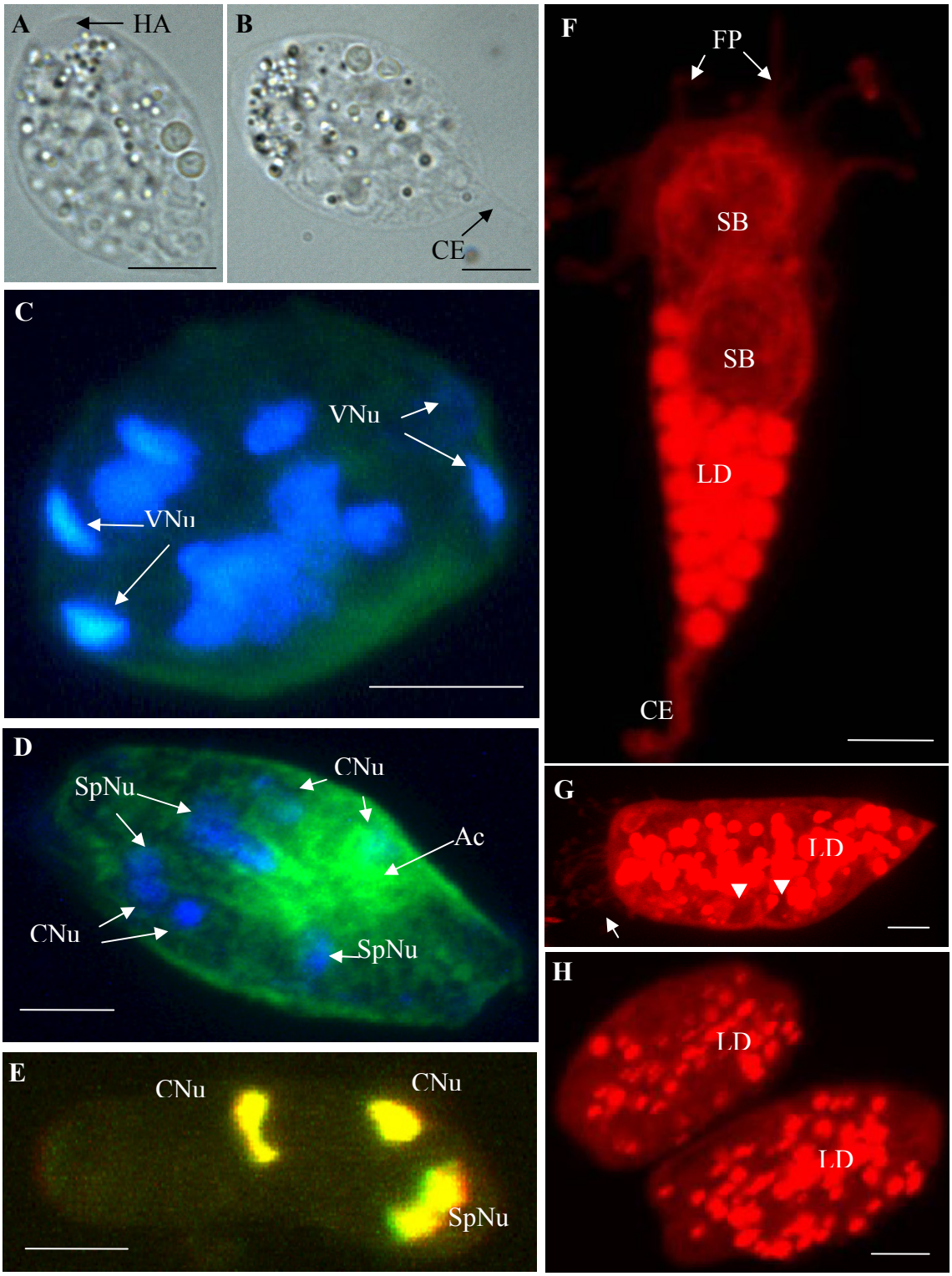

Figure 7.5 Sporogenesis of *Ceratomyxa puntazzi* from the bile of *Diplodus puntazzo*. A-B: LM, C-H: CLSM. C-E: DAPI and phalloidin stains, F-H: Nile Red stain. A-B) Pseudoplasmodia with two almost mature spores. Hyaline area visible at rounded side of parasites and one cytoplasmic extension at posterior end. C) Late pseudoplasmodium with two spores, where all nuclei, including the valvogenic ones are visible. D) Mature stage with two spores, where F- actin accumulation can be noted. Valvogenic nuclei have desintegrated.

Figure 7.5 continued: E) Mature spore liberated into the bile with two capsulogenic nuclei and two sporoplasm nuclei. Valve nuclei are absent. F) Pyriform stage with two early sporoblasts, abundant lipid droplets, filopodia and one larger cytoplasmic extension. G) Almost mature stage showing abundant filopodia at rounded side (arrow) and abundant lipid droplets. Two polar capsules can be estimated (arrow head). H) Two mature stages harbouring two spores each, presenting smaller and randomly distributed lipid droplets than in early pseudoplasmodia. Abbreviations: HA, hyaline area; CE, cytoplasmic extension; VNu, valvogenic nuclei; Ac, F-actin; SpNu, sporoplasmogenic nuclei; CNu, capsulogenic nuclei; FP, filopodia; SB, sporoblast; LD, lipid droplets. Scale bar: A-B= 10 µm; C-H= 4 µm.

The two sporoplasmogenic cells (Figure 7.6A) formed a single binucleate sporoplasm in mature spores (Figure 7.6C). The nuclei of the sporoplasmogenic cells contained heterochromatin, only in mature stages one eccentric nucleoli was detected in each nucleus (Figure 7.6C). In contrast to the P cell, the cytoplasm of sporoplasmogenic cells showed abundant rough endoplasmic reticulum (Figure 7.7A). In the cytoplasm and between the membranes of the two capsulogenic cells, an organized vesicular body was observed (Figure 7.6D,F). The "vesicles" ranged from 32 to 60 nm in diameter: in some cases small electron-dense dots were present inside the "vesicles" (Figure 7.6E,G). Sporoplasmosomes and membrane bound structures appeared in the cytoplasm of the sproplasm close to the end of sporogenesis (Figure 7.7C,E).

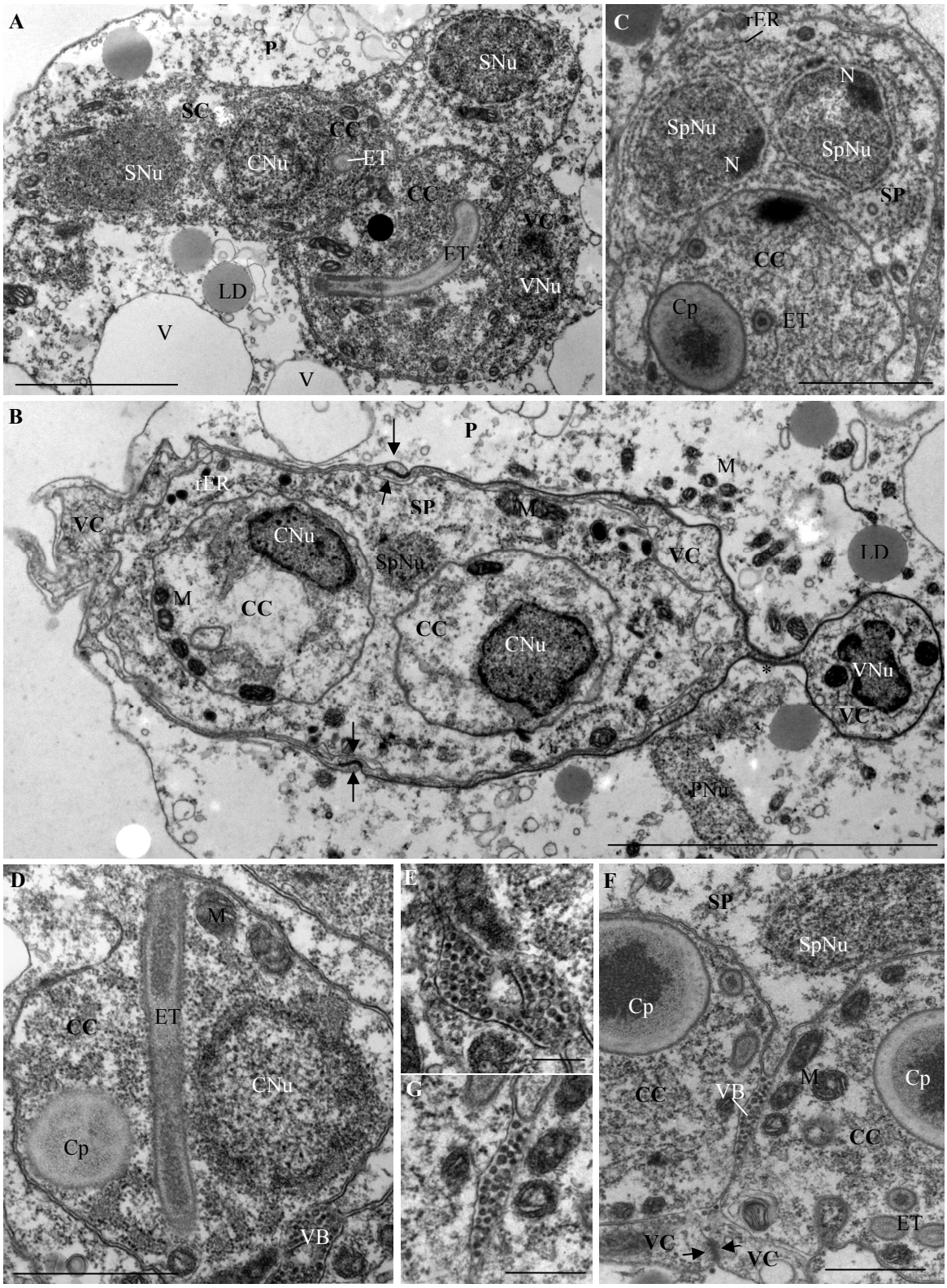

Figure 7.6 Legend on the following page.

Figure 7.6 Sporogenesis of *Ceratomyxa puntazzi* from the bile of *Diplodus puntazzo* (TEM). A) Initial sporoblast with two capsulogenic cells developing the external tube. Both capsulogenic cells are enveloped by a sporoplasmogenic cell harbouring two sporoplasmic nuclei. Laterally, a valvogenic cell and its nucleus. Lipid droplets and vacuoles are abundant in the cytoplasm of the P cell. B) Sporoblast with two capsulogenic cells, a sporoplasmogenic cell with two nuclei and two valvogenic cells. The nucleus of the valvogenic cell is connected by a cytoplasmic bridge (*). Notice formation of suture (arrows). C) Detail of a sporoblast, showing the binucleate sporoplasm, with two eccentric nucleoli. Abundant rough endoplasmic reticulum is present in the cytoplasm of the sporoplasmogenic cell. D) Capsulogenic cell with a prominent external tube and a capsular primordium. Note vesicular body associated to the membrane of the capsulogenic cell. E) Detail of the vesicular body of Figure 7.6D. F) Detail of a sporoblast with vesicular body between the membranes of the two capsulogenic cells and the sporoplasmogenic cell. Suture forming between the two valvogenic cells (arrows). G) Detail of vesicular body shown in Figure 7.6F. Abbreviations: P, primary cell; PNu, primary nucleus; CC, capsulogenic cell; CNu, capsulogenic nucleus; SP, sporoplasmogenic cell; SpNu, sporoplasmogenic nuclei; VC, valvogenic cell; VNu, valvogenic nucleus; ET, external tube; rER, rough endoplasmic reticulum; LD, lipid droplets; M, mitochondria; V, vacuole; Cp, capsular primordium; N, nucleoli; VB, vesicular body. Scale bar: A= 2 µm; B= 5 µm; C= 2 µm; D= 1 µm; E= 0.2 µm; F-G= 1 µm.

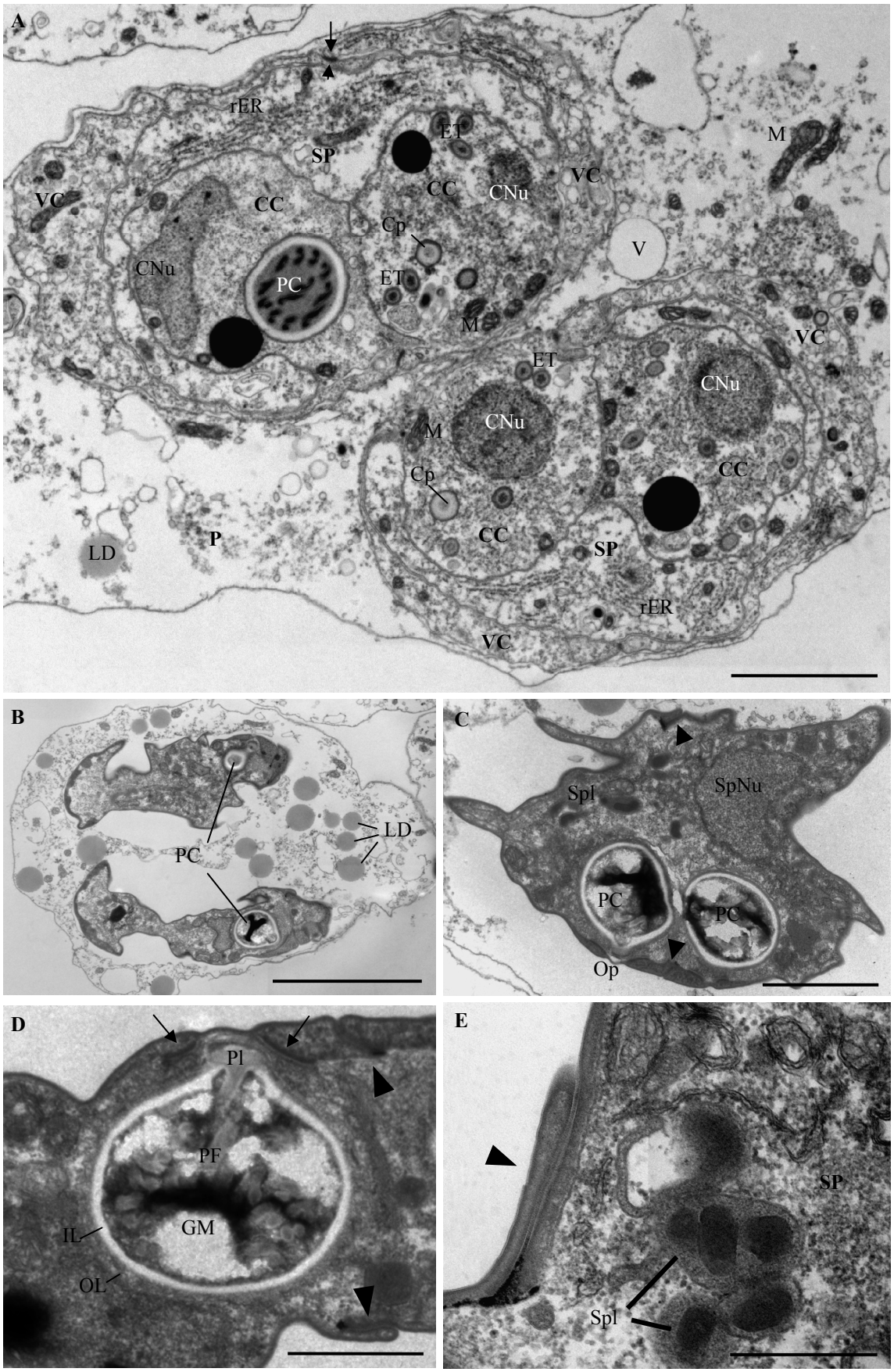

Figure 7.7 Legend on following page.

Figure 7.7 Sporogenesis of *Ceratomyxa puntazzi* from the bile of *Diplodus puntazzo* (TEM). A) Pseudoplasmodium harbouring two sporoblasts, with capsulogenic cells in different stages of maturation. One capsulogenic cell has a mature polar capsule, where sections of the coiled, twisted polar filament can be observed. The other three capsulogenic cells show an external tube and capsular primordium in their cytoplasm. Note abundant rough endoplasmic reticulum in the cytoplasm of the sporoplasmogenic cell. Formation of suture line between valvogenic cells can be observed (arrows). B) Two mature spores inside a P cell. Abundant lipid droplets are present in the degenerated P cell. C) Mature spore with two polar capsules, the opening for the extrusion of the polar filament, the suture (arrow head), one sporoplasm nucleus and sporoplasmosomes present in the sporoplasm cytoplasm. D) Detail of a mature polar capsule with twisted appearance of polar filament, capsular plug; polar capsule with an outer electron-dense layer and an inner electron-lucent layer. Apical junctions of the mature spore, surrounded by fibrous material between the capsulogenic cell and the valve cell (arrows). Suture between valves (arrow head). E) Detail of a mature spore: desmosome-like junction of the suture (arrow head) and sporoplasmosomes in sporoplasm cytoplasm. Abbreviations: CC, capsulogenic cell; CNu, capsulogenic nucleus; SP, sporoplasmogenic/sporoplasm cell; SpNu, sporoplasmogenic/sporoplasm nucleus; VC, valvogenic cell; PC, polar capsule; Cp, capsular primordium; ET, external tube; M, mitochondria; rER, rough endoplasmic reticulum; LD, lipid droplets; Spl, sporoplasmosomes; Op, opening for the extrusion of the polar filament; Pl, plug; IL, inner electron-lucent layer; OL, outer electron-dense layer; GM, granular matrix. Scale bar: A= 2 µm; B= 5 µm; C= 2 µm; D= 1 µm; E= 0.5 µm.

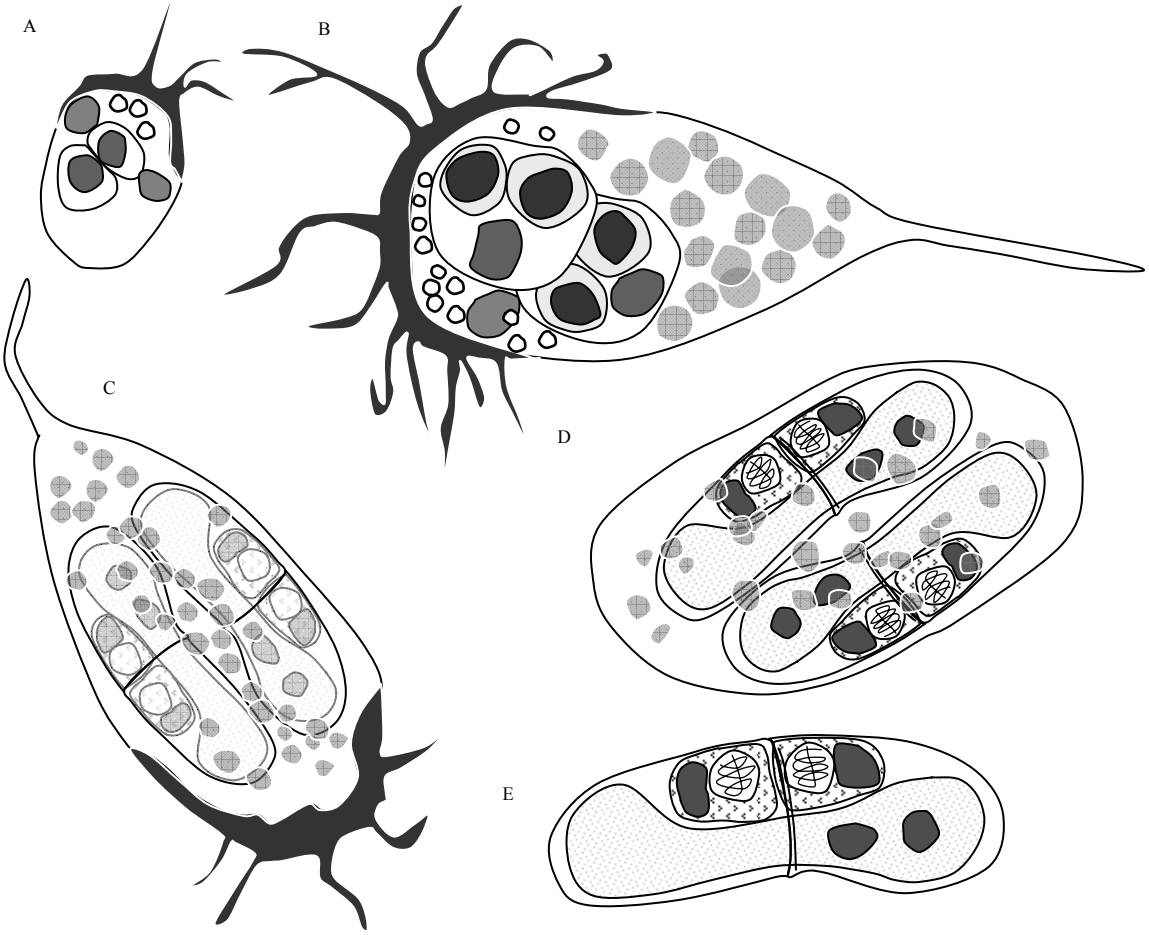

Figure 7.8 Schematic diagrams of some developmental stages of *Ceratomyxa puntazzi* observed in the bile of *Diplodus puntazzo*. A) Early, active ellipsoidal stage with a few small filopodia at anterior part, showing two primary nuclei and two secondary nuclei and refractive granules. B) Active, pyriform stage, with many filopodia, at anterior part, some of them ramified. This stage possesses a primary nucleus and two secondary cells with two tertiary cells each, abundant lipid droplets, and refractive granules at rounded side. C) Sporogonic stage with two forming spores, still showing motility and abundant lipid droplets. D) Sporogonic stage close to the end of spore development, with loss of motility and reduced size and number of lipid droplets. E) Mature spore with a binucleate sporoplasm, showing two capsulogenic cells with their nuclei and two polar capsules.

7.4. Discussion

The in-depth study of the different stages of development of *C. puntazzi* from the bile of *D. puntazzo*, using a combination of light microscopy, scanning and transmission electron microscopy and three-dimensional confocal laser microscopy, contributed novel information on the structure and morphology of ceratomyxid parasite stages in the bile, and provided unique insights into parasite composition and cell motility in myxozoans, which had not previously been studied in detail.

The combination of DAPI-stained parasites and TEM allowed for the detection of the sequence of stages of cellular development. It was demonstrated that the parasite shows two developmental pathways in the bile, 1. pre-sporogonic proliferation and 2. spore formation. This allows parasite multiplication directly prior to spore formation and thus increases the parasite's chance of infecting the invertebrate host considerably. The co-location of proliferative and sporogonic cycles in the same organ has also been reported for other *Ceratomyxa* spp. (e.g. Georgévitch 1917, 1929; Noble 1941; Sitjà-Bobadilla et al. 1995; Morrison et al. 1996; Cho et al. 2004).

CLSM presented itself as an extremely useful tool for exploring the three-dimensional morphology of the parasites as well as for determining the presence and location of certain cellular components. The three-dimensional view combined with nucleic acid staining by DAPI allowed for the rapid determination of the number of nuclei in each stage and in the buds produced during pre-sporogonic proliferation. Nile Red had not previously been used for CLSM in myxozoans, but allowed for the visualisation of the distribution of lipid droplets during parasite development. Lipid droplets were extremely common in medium-sized pyriform stages and less common in the smallest, ellipsoid stages or in late sporogonic stages. Lipid droplets were almost exclusively present in the P cell. This was also observed in *Enteromyxum* spp. (Redondo et al. 2003a; Cuadrado et al. 2008). However, lipid droplets have been observed in S and T cells, *e.g.* in sporoplasmogenic cells (Sitjà-Bobadilla & Alvarez-Pellitero 1993a; Adriano et al. 2005) or in capsulogenic cells (Sitjà-Bobadilla & Alvarez-Pellitero 1992; Sitjà-Bobadilla & Alvarez-Pellitero 1995). In the case of *C. puntazzi*, the high concentration of lipid droplets in the P cell and the presence of considerably more rough endoplasmic reticulum and ribosomes in the S cells than in the P cell, may be indicative of differential cell functions. In this respect, the non-dividing P cell may serve as a "container" and potential energy supplier for S and T cells, which divide frequently and

are actively synthesizing cellular components. Thus, the lipid droplets might represent energy reserves for parasite proliferation and sporogony. At the same time, the lipid droplets might have some hydrostatic function, keeping the parasites neutrally buoyant in the bile. Surface enlargement by the formation of pseudopodia and the presence of small blebs on the surface of the parasite's P cell might also help keeping the parasites in suspension. Apart from the structures passively increasing hydrostasis, active locomotion may contribute to buoyancy. In *C. puntazzi* and possibly in other myxozoans inhabiting liquid-filled body cavities, motility of the parasites is achieved by a highly active cytoplasm area, the ectoplasm, an area which is formed by cell membrane protrusions, lamellipodia which further produce filopodia. In contrast to the inactive, rather rigid cytoplasmic extensions observed at the posterior end of the parasites, the pseudopodia showed a very high degree of mobility. The use of phalloidin, for the first time in myxozoan proliferative stages, suggests that F-actin is an important effector of cell motility in myxozoans. Concentration of F-actin in the lamellipodium and the filopodia, which are located at the anterior pole of the parasite and which were found to extend forward in the direction of swimming and then be moved postero-laterally, is thought to facilitate directional movement.

Other *Ceratomyxa* spp. in the bile have been described to possess cytoplasmic extensions (e.g. Morrison et al. 1996; Cho et al. 2004; Maíllo-Bellón & Gracia-Royo 2007). However, these have been related predominantly to anchorage in the host epithelium and to a potential increase in the absorptive surface which is in contact with host cells (Sitjà-Bobadilla & Alvarez-Pellitero 1993d; Lom & Dyková 1996; Sitjà-Bobadilla & Alvarez-Pellitero 2001; Cuadrado et al. 2007). In myxozoans, pinocytosis has been observed as a means of energy transfer from host to parasite, with the P cell taking up material from the surrounding host cell, but also from P cells to S cells (Morris & Adams 2008). In the case of *C. puntazzi,* none of the cytoplasmic extensions detected were found to be in contact with the epithelium of the gall bladder, and all parasites were found to be in suspension in the bile. While it is suggested that the filopodia of *C. puntazzi* have a locomotive rather than an anchoring or energy providing function, it remains unclear, where the parasite's energy to fabricate new cellular components comes from.

Information on the occurrence and distribution of effectors of cell motility in myxozoans is scarce. F-actin has been previously described to be present in the stinging tube of polar capsules and in the cytoplasm of the amoeboid sporoplasm of

actinosporean spores of *Myxobolus pseudodispar* Gorbunova 1936 (Uspenskaya & Raikova 2004). However, this is the first report of the presence of an F-actin rich cytoskeleton in proliferating stages, confirming the active role of these stages. Almost mature pseudoplasmodia showed much more dispersed F-actin and less locomotive activity and flexibility. The loss of F-actin may reflect the end of the active swimming period and may cause sinking and thus allow expulsion from the gall bladder via the common bile duct, resulting in the release of spores via the intestine.

The present study further demonstrates for the first time, that F-actin also seems to be of great importance in the process of budding. Budding has previously been observed in many members of the genus *Ceratomyxa*, e.g. in *Ceratomyxa appendiculata* Thélohan 1892, *C. herouardi*, *Ceratomyxa blennius* Noble 1938 and *Ceratomyxa protopsettae* Fujita 1923 (Georgévitch 1917; Noble 1941; Cho et al. 2004; Maíllo-Bellón & Gracia-Royo 2007). However, a mechanism resulting in the separation of newly formed buds has so far not been suggested. It has been demonstrated during cytokinesis of yeast, that F-actin polymerization is important for the assembly, maintenance and closure of the contractile ring between two cells (Pelham & Chang 2002). In the present study, no F-actin rich contractile ring was observed during the budding process. Separating buds were always found to "head" away from the "mother" parasite, demonstrating polarization of the F-actin cytoskeleton at the opposite end of its attachment to the "mother" parasite, thus resulting in the active separation of buds. A polarized distribution of F-actin has been observed in the early development of monospores from a marine red alga indicating that F-actin asymmetry is evolutionally conserved in relation to the establishment of cell polarity in migration of eukaryotic cells (Li et al. 2008).

Plasmotomy was found to be the process leading to the division of the P cell during exogenous budding as observed in SEM of *C. puntazzi*. Plasmotomy has also been reported from other marine coelozoic myxosporeans (Georgévitch 1917; Noble 1941; Diamant et al. 2004). However, despite the large number of sections examined, the exact composition of "daughter" parasites remained unknown. The resultant "daughter" parasites contained 1-3 S cells, harbouring 0-2 T cells each but it is unclear whether they contained a P cell nucleus. However, in the present study, the P cells of *C. puntazzi* appeared to be rather inactive with no more than 2 nuclei present in any parasite stage at any time, when compared with S and T cells, which multiplied frequently and were present in larger numbers. This suggests that "daughter" parasites do not contain a P cell

nucleus but only part of the P cell cytoplasm, which probably disintegrates or is being reabsorbed resulting in the liberation of S cells enveloping T cells. Support for this idea is found in the observation that some small stages of one cell enveloping another one were found to have a very electron-dense cytoplasm (Figure 7.3H), similar to that of S and T cells found within the P cell (Figure 7.4E) and remnants of a cell membrane (presumably that of the P cell) attached to it. According to the general scheme for myxozoans presented by Morris & Adams (2008) separated buds containing T cells would then initiate sporogony. However, according to our observations on the rapid and massive multiplication of *C. puntazzi* in the gall bladder, the exclusion of the P cell from involvement in proliferative processes, and the frequency of budding, it seems unlikely that all buds transform into sporogonic stages without further proliferation. However, this question cannot be answered by the current observations. Nevertheless, these observations are supported by other reports in the literature: Pre-sporogonic proliferation of *C. shasta* was recently detected in the endothelium of the blood vessels in the gills, and it was suggested that they produce S cells containing T cells which may re-invade the endothelium of gills' blood vessels or migrate to the intestinal epithelium where another cycle of proliferation takes place before sporogony is initiated (Bjork & Bartholomew 2010). Furthermore, the involvement of T cells in proliferative development was also described for *M. cerebralis* where intra- and intercellular production and release of cell-doublets (S cells containing T cells) was observed to take place in the epidermis, subcutis and the central nervous system before proliferation and sporogony takes place in the cartilage (El-Matbouli et al. 1995).

Despite the large number of sections examined, the mechanism producing S or T cells in *C. puntazzi* could not be determined with certainty, however S cells engulfing other S cells were observed. Engulfment of one cell by another to form an S-T cell doublet was clearly demonstrated for *C. sparusaurati* (Sitjà-Bobadilla et al. 1995) and supports the idea that T cells are generally produced by engulfment (Morris 2010), however, this process has never been observed in P cells (resulting in the formation of S cells), and further ultrastructural study of sequential sections is necessary to clarify whether engulfment is the only process of endogenous cell formation in myxozoans.

Cell junctions between S cells have previously been observed in other myxozoans (Morrison et al. 1996; Cuadrado et al. 2008). S cell junctions in *C. puntazzi* might make it easier for one S cell to envelop another S cell, and this might explain why they occur frequently. It is likely that, after mitosis, S cells remain somehow attached, establishing

the observed cell junctions. Independent vacuolar membranes surrounding groups of S cells were observed in *C. sparusaurati* (Sitjà-Bobadilla et al. 1995) but were never detected in *C. puntazzi*.

Many ultrastructural details of *C. puntazzi* are similar to that of other Myxozoa, however, there are some structures that differ or are extraordinary and these are discussed briefly in the following section:

The P cells of *C. puntazzi* presented a very large number of vacuoles, sometimes filled with granular material. Their function is unclear. In the case of *Enteromyxum scophthalmi* Palenzuela, Redondo & Alvarez-Pellitero 2002*,* a nutritional role was ascribed to vacuoles in the P cell, with transport of nutrients to the S cells (Redondo et al. 2003a). However, as the composition of the vacuoles is unknown, an excretory function could also be assigned. Additionally, the bile is rich in salts and vacuoles of the P cell could have an osmotic function, offsetting the loss of water of the parasite.

Shrinkage of the stages during fixation and staining may explain the discrepancy in the size of the vacuoles of the P cell between fresh LM samples and fixed TEM samples. A similar phenomenon was reported for myxozoan spores (Kudo 1921; Parker & Warner 1970).

Mitochondria were considerably smaller in S cells than in early P cells, where extremely large mitochondria were observed. This could be related to the high energy production required for the motility of the highly active parasite stages, with locomotive actions likely to be conducted exclusively by the P cell.

A vesicular body was observed in the cytoplasm of the sporoplasmogenic cell, and it was found to be associated with the two capsulogenic cells, often demonstrating the only structure located between the membranes of the capsulogenic cells. A similar structure, described as aggregates of microtubules, was described in the capsulogenic cells of *Ceratomyxa tenuispora* Kabata 1960 (Casal et al. 2007), however, the diameter of the microtubules was slightly smaller (25 nm) than that of the vesicles (32-60 nm) of the vesicular body in *C. puntazzi.* Furthermore, both distribution and morphology were different. In *Polysporoplasma mugilis* Sitjà-Bobadilla & Alvarez-Pellitero 1995 from *Liza aurata* L., icosahedral virus-like particles measuring 18-20 nm were observed (Sitjà-Bobadilla & Alvarez-Pellitero 1996). These virus-like particles and the vesicular body of *C. puntazzi* share similarities: both structures represent a cluster of small vesicles surrounded by membranes, with an electron-dense core and are associated with the capsulogenic cell. However, the vesicular body in *C. puntazzi* differed considerably

with regard to vesicle size, lacked icosahedral shape and was not associated with pathological effects. The vesicular body observed in the present study was previously reported in *Unicapsula pflugfelderi* (Schubert, Sprague & Reinboth 1975) where vesicles measured 40-60 nm. In *U. pflugfelderi* the vesicular body was also found in close vicinity to developing polar capsules, and a secretory function was suggested (see Chapter 5, Sections 5.3.1.1 & 5.4). Due to its location and its vesicular structure it is suggested that the presence and function of the vesicular body is related to capsulogenesis, possibly secreting carbohydrates or other substances required for polar capsule formation.

Summarizing, the present study demonstrates that the combination of a three-dimensional microscopy method applying different specific stains together with the details of the cellular ultrastructure of the different parasite stages is the best approach to capture and understand the developmental cycles of myxozoan parasites, which are still poorly understood, due to their extremely reduced size and the lack of information on the basic principles of cell-in-cell formation. The material from the present study and comparison with existing reports showed that the development of *Ceratomyxa* spp. in the bile seems to follow a sequence which includes pre-sporogonic proliferation by budding and spore formation. Previously undescribed details on the concentration of F-actin in certain cytoplasmic areas and the formation of active cytoplasmic extensions provided a first insight into the fascinating locomotive behaviour of myxozoans and the mechanisms underlying the unique process of budding. The use of other specific stains in CSLM is strongly encouraged as they are likely to provide further information on these processes and on the distribution and function of other important cellular components.

CHAPTER 8. *Ceratomyxa puntazzi* seasonality and pathways in the host determined by natural and experimental transmissions studies

8.1. Background

Information about the transmission and the life cycles of marine myxozoans is scarce as finding specific invertebrate hosts in a large, extremely diverse and invertebrate-rich environment is difficult (Køie et al. 2004). Despite these obstacles, in the genus *Ceratomyxa*, two life cycles have been elucidated to date and both of them involve a polychaete alternate host: 1. The atypical ceratomyxid *C. shasta* (see Chapter 6, Section 6.1) which occurs in salmonid freshwater habitats in North America and alternates between the polychaete *Manayunkia speciosa* Leidy 1858 and Chinook salmon (Bartholomew et al. 1997), and 2. The bile-inhabiting, marine species *Ceratomyxa auerbachi* Kabata 1962, which cycles between *Chone infundibuliformis* Krøyer 1856 and the herring *Clupea harengus* L. (Køie et al. 2008).

The ceratomyxid actinosporean spores released from *M. speciosa* and from *C. infundibuliformis* measure less than 10 µm. Due to the miniature size of these infective stages and most other marine actinospores (Køie et al. 2004, 2007, 2008; Rangel et al. 2009), their elimination from the incoming water source in aquaculture tank systems is tricky. Fine mesh filters quickly clog up and UV treatment may not be feasible. In sea cages, it is impossible to control water-borne myxozoan infection, however, knowledge of the seasonality and transmission of a myxozoan species allows for designing management strategies aiming at reducing the exposure to infective stages. Currently, this seems to be the most effective means to control myxozoan diseases. In *T. bryosalmonae* e.g. reduced water temperature suppress the effects of the disease (Clifton-Hadley et al. 1986) and fish exposed late in the season, before ambient temperatures fall, survive the infection and appear less susceptible to the disease the following year.

By exposure of sentinel fish to a *C. puntazzi*-enzooic environment, the present part of the thesis aimed to investigate the seasonality of this myxozoan in order to be able to suggest management strategies for *C. puntazzi* in *D. puntazzo* cultures in the Mediterranean. Furthermore, the exposure of fish to an infective environment for a known duration of time should allow for the reconstruction of the parasite's route of infection and pathway in the host.

In many parasites, the order of development of different stages is genetically determined and cannot be reversed (Mueller et al. 2005). Thus, not all stages in the life cycle can develop further if transferred to different tissues or hosts in the life cycle of a certain

parasite. The use of myxosporean spores in experimental transmission studies have not succeeded to infect naïve receptor fish (McGeorge et al. 1996; Moran et al. 1999b), however, different pre-sporogonic stages have been shown to have infective capacity (Grossheider & Körting 1993; Hedrick et al. 1993; Diamant 1997; Moran et al. 1999b; Redondo et al. 2002; Diamant et al. 2006). For the pathogenic species of the genus *Enteromyxum*, direct fish-to-fish transmission of pre-sporogonic stages inside epithelial cells of the intestine has been demonstrated by means of dislodgement of infected host epithelial cells and waterborne contamination of naïve fish (Diamant 1997; Redondo et al. 2002). Thus, in order to determine which stages in the piscine life cycle of *C. puntazzi* are capable of resuming their development or cause the development of other parasite stages in receptor fish, artificial infection with different developmental stages of the parasite were conducted. Blood stages, pre-sporogonic stages and sporogonic stages from the bile were used to infect naïve fish. Artificial infection was attempted via four different routes: 1. Oral, 2. Intracoelomic, 3. Bath and 4. Cohabitation. The present chapter thus investigates in detail *C. puntazzi* pathways and development in the sharpsnout seabream and the seasonality of the infection in the Mediterranean environment.

8.2. Materials and methods

8.2.1. Experimental transmission of different parasite stages in the laboratory

Transmission of *C. puntazzi* infected bile

Donor fish

In 2007, wild specimens of *D. puntazzo* (n=67; 24.5-29.2 cm total length; 223.2-448.6 g) were obtained from San Pedro del Pinatar by local shore fishing (Spanish Mediterranean coast; see Table 3.1). Donor fish presented a prevalence of 26.87%. Bile of several fishes containing pre-sporogonic and sporogonic stages of *C. puntazzi* isolated as described in Chapter 6, Section 6.2.2 was used for infection. From the bile suspension used for infection, 4 µl were placed on a microscope slide, covered with a cover-slip and examined using light microscopy at 400x magnification. 3 µl of bile were used for counting the *C. puntazzi* stages in a haemocytometer. The number of stages in the total volume of bile was then calculated, and initially, 10 µl of bile equaling 3160 stages units were used for oral infection. Due to high mortalities experienced in the fish, probably due to the aggressive bile composition, the protocol was then changed. The

mixture of bile and parasite stages from different fish was centrifuged at 800 RCF, the supernatant was discarded and the pellet of *C. puntazzi* stages was resuspended in 0.1M PBS at a concentration of 212 stages per µl, including pre-sporogonic proliferative and sporogonic stages as described in Chapter 7, Section 7.3, as well as mature spores. Parasite stages were viable in PBS as determined by neutral red uptake. The mixture was homogenised and refrigerated until further use within the next hour.

Transmission of *C. puntazzi* infected blood

Donor fish

In May 2010, wild sharpsnout seabream *D. puntazzo* in their first year (n=8; 10-11.5 cm total length; 16.1-25.66 g) were obtained from San Pedro del Pinatar by local shore fishing (Spanish Mediterranean coast; see Table 3.1). Donor fish contained a microscopic prevalence of 87.5% in the bile. The bile presented abundant pre-sporogonic proliferative, sporogonic stages and only few mature spores. Due to the natural infection profile (see section 8.4.3), it was assumed that these fish would harbour blood stages. Immediately after arrival at the laboratory, blood samples were taken from the caudal fin of all fish, using a heparinised syringe with a fine needle (0.3mm diameter). The blood samples were checked for the presence of *C. puntazzi* stages by Diff Quick® staining of blood smears and by PCR of DNA extracted from 4 microliter of the mixture. The blood samples of all fish were pooled and maintained refrigerated until use for infection (max. 1 hour).

Receptor fish were from the same stock but of different age as experimental infections were conducted several times over a period of 2 years. Details are provided in the following section.

Experimental design and receptor fish maintenance

Infection using bile stages: Naïve *D. puntazzo* from a Greek hacthery (n=105; 9.1-12.8 cm total length; 9.5-28.8 g, see Table 3.1) were used as receptor fish. Experimental infections were carried out as follows:

1. *Oral transmission (OT)* (n=30): Fish were intubated with 50 µl of PBS-parasite mixture (10.600 parasite stages). The mixture was injected by using a micropipette. The opening of the tip was placed into the oesophagus past the gill region.

2. *Intracoelomic transmission (IT)* (n=30): A syringe with a 0.3mm diameter needle was used for intracoelomic injection of 50 µl of the prepared mixture (10.600 parasite stages) per fish.
3. *Bath transmission (BT)* (n=10): Receptor fish were exposed to 3.5 ml of the prepared mixture (742.000 parasite stages) in 12.2 L of seawater. Fish were moved to a 60-L tank after 4 days.
4. *Cohabitation transmission (CT)* (n=20): Receptor fish were maintained in a 750-L fibreglass tank with infected sharpsnout sea bream (donors).

Infection using blood stages: Naïve sharpsnout seabream (n=5; 22.5-24 cm total length; 212.4-277.3 g) were used for:

5. *Intracoelomic blood transmission (IBT)* (n=5): Each receptor fish received an intracoelomic injection of 0.2 ml of the pooled, heparinised blood sample obtained from infected fish. Thereafter, fish were kept in 750-L fibreglass tank.

For OT and IT, the receptor fish were sedated with 60 ppm of 1:10 clove oil:ethanol. All fish were maintained at a water temperature between 18 and 20ºC. After infection, all groups were kept in 60-L tanks, except for the CT and IBT group, which were kept in a 750-L tank. Control fish (n=10) were not exposed to the parasite and reared in a 20-L tank.

Parasitological analysis of artificially infected fish

Gall bladders were analysed for light microscopy as described in Chapter 6, Section 6.2.2. Blood (4µl), obtained from the caudal vein after dissection of the tail, bile (20-30 µl) and liver (approx 2 mm^3) were sampled for DNA extraction and PCR analysis. Control fish, OT, IT and BT were sampled at 13, 21, 28, 35, 50, 64, 78, 92 and 113 days post infection (p.i.). Each sampling day 1 control fish, 2 OT fish, 2 IT fish and 1 BT fish were sampled. On the last sampling, at 113 days the remaining fish were sampled (2 Control, 8 OT, 11 IT and 2 BT fish). CT fish were sampled at 27 (n=2), 49 (n=2), 77 (n=2) and 102 (n=4) days p.i. IBT fish were sampled at 60 (n=3) and 75 (n=2) days p.i. Mortalities during the experiment were recorded only for OT (n=6) and IT (n=3). These fish, condition permitting, were necropsied and examined as described above.

8.2.2. Natural infections in a *C. puntazzi*-enzooic habitat in the Mediterranean

Exposure

Between December 2008 and November 2009, naïve sharpsnout seabream *D. puntazzo* (n=194; 10.2-20 cm total length; 13.5- 113.5 g, see Table 3.1) were exposed to the sea close to the Cape of San Antonio, Jávea, Alicante (38º 47' 56.0'' N; 0º 11' 32.9'' E) (Figure 8.1). Fourteen to twenty naïve *D. puntazzo* were exposed to the infective environment for 7 days every month, throughout a complete year. Environmental parameters such as sea water temperature, visibility and water conditions prevailing during exposure and recovery of the sea cages were recorded (Table 8.2). Sentinel fish were placed in a handmade cage (73 x 28 x 29 cm) with a size mesh of 2 cm and a plexiglass support on all sides, which was intended to protect the fish from the water motion which would force them against the wire mesh and cause severe damage to the skin. Holes of 7 mm diameter were drilled into the plexiglass to allow for water exchange. The sentinel sea cage was attached to a deadweight at 9.2 m depth with chains. After 7 days, fish were recovered and carried live to the facilities at the University of Valencia. There, fish were maintained in seawater at 20-23ºC in tanks of 80-120-L. Fish were sampled at arrival from the sea each month, 1 day post exposure (p.e.) and at 60 days p.e. Number of fish sampled at day 1 and 60 days p.e. as well as mortalities and their causes and number of samples molecularly analysed are detailed in Table 8.1. Control fish (n=10) were not exposed in the sea and were reared in a 20-L tank in the aquaria facilities of the University.

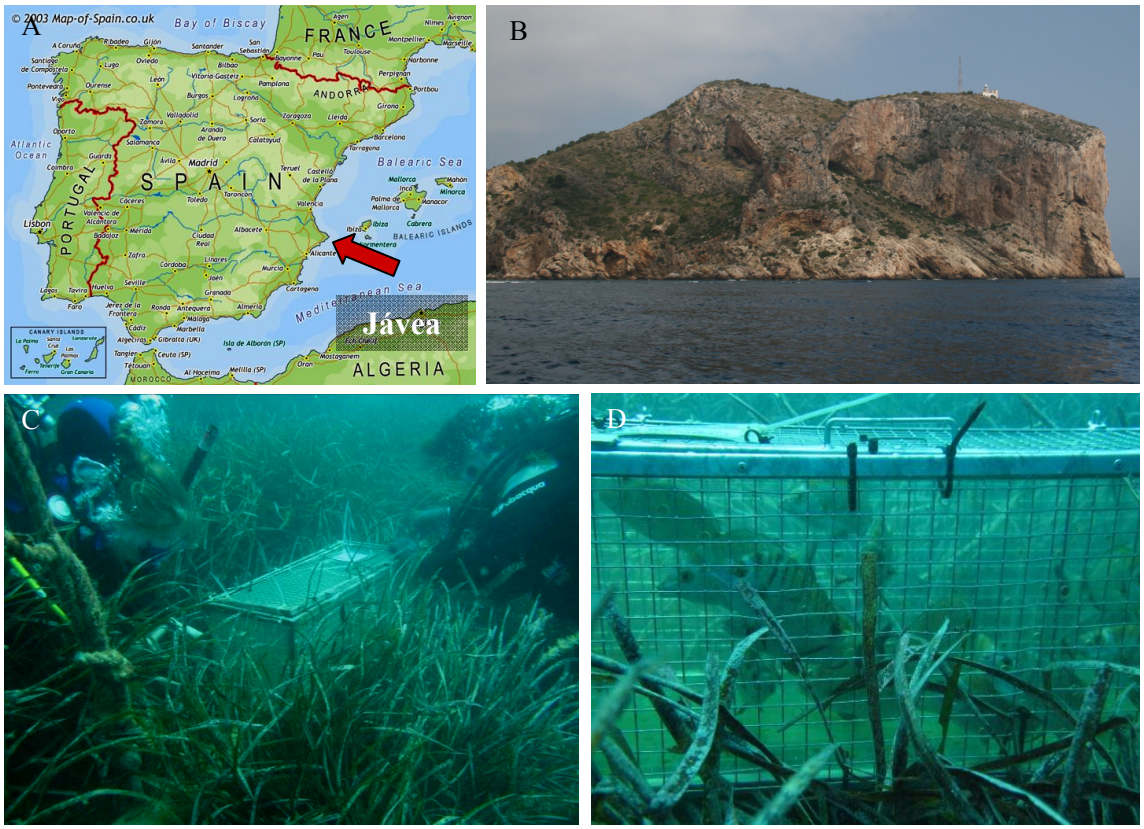

Figure 8.1 A) Location of exposure site of sentinel fish at the Cape of San Antonio, Jávea, Alicante, South East Mediterranean Coast (Spain). B) Cape of San Antonio, Jávea, Spain. C) Sentinel handmade sea cage anchoraged to a deadweight at 9.2 m depth. D) Naïve sharpsnout seabream inside exposed sea cage.

Parasitological analysis of naturally infected/sentinel fish

From fish sampled 1 day p.e. skin and fins were observed macroscopically for ectoparasites. From all fish sampled, blood (4µl), liver (approx 2 mm^3) and gall bladder (half of the bladder plus bile) were sampled and preserved in liquid nitrogen (LN_2) and quickly transferred to -20ºC until subsequent molecular analysis. In order to avoid cross contamination 10% H_20_2 was used routinely to clean scissors and tweezers for molecular sampling. Fish analysed 60 days p.e., were processed as before and in addition gall bladder, kidney and intestine were observed in fresh smears at 400X magnification and brain, eyes, gills, heart, spleen, digestive system and muscle were scrutinized for the presence of parasites at 80X magnification. Blood smears stained by Diff Quick® were analysed for the presence of *C. puntazzi* stages. Fish that died during the experiment, condition permitting, were necropsied and examined as described above.

8.2.3. Molecular analysis of fish samples

DNA extraction and PCR of selected fish samples (see Table 8.1) were conducted as described in Chapter 3, Section 3.3.1. Partial SSU rDNA fragments were amplified from the genomic ribosomal DNA (rDNA) gene tandems using specific primers (see below). Selected samples were sequenced as described in Chapter 3, Section 3.3.1 to confirm specificity.

Based on the sequences obtained from *C. puntazzi* (see Chapter 6, Section 6.3.1, Appendix 1) and their alignment with closely related taxa, specific primers were designed using Primo Pro 3.4 (Chang Bioscience, Inc) or the Primer Express Software (Applied Biosystems, Life Technologies Corporation, California, USA). Specific primers CDF and CDR (Table 3.2) were tested to exclude self-complementary binding or primer dimers, checked for cross-reaction by BLAST search, and they were then applied in a single-round polymerase chain reaction (PCR) assay and tested for their optimal annealing temperature in a gradient PCR reaction.

Table 8.1 Number of fish analysed each month, mortalitiy and the causes of death (1.- During transport or in the sea cage; 2.- Unknown etiology; 3.- Caligid infection; 4.- Cannibalism). Number of blood samples analysed by PCR at 1 and 60 days p.e. and total of gall bladder samples analysed by PCR.

Month	**n**	**n (1 p.e.)**	**n (60 p.e.) Microscopically analysed**	**Mortality**	**Blood PCR**		**Gall Bladder PCR**
					1 p.e.	60 p.e.	
January	20	5	15	$4^{(1)}$	5	6	11
February	20	18	2	$14^{(1,2)}$	6	2	8
March	20	5	15	$3^{(1,2)}$	5	5	10
April	15	3	12	$3^{(2)}$	3	12	15
May	15	5	10	$8^{(1,3,4)}$	4	8	11
June	14	4	10	$3^{(3)}$	4	10	11
July	14	4	10	$5^{(1,2)}$	1	9	11
August	14	1	13	-	1	9	9
September	14	-	14	-	-	9	10
October	14	7	7	$8^{(1,2)}$	4	5	11
November	14	5	9	$11^{(1,2)}$	5	7	12
December	20	5	15	$1^{(2)}$	5	10	13
Total of fish	194				135		132

8.3. Results

8.3.1. Experimental transmission of different parasite stages in the laboratory

None of the fish experimentally infected with *C. puntazzi* via OT, IT and CT, showed parasite stages at the end of the experiment, neither microscopically in the bile nor molecularly by PCR of blood, bile or liver. In the transmission trial using infected blood of donor fish, blood stages proved to be present by PCR but were not numerous enough to be visible in stained blood smears. However, *C.puntazzi* was not detected in IBT receptor fish, neither microscopically in the bile nor molecularly by PCR of blood, bile or liver. The control group was never found parasitized by *C. puntazzi* either.

8.3.2. Natural infections in the sea

Environmental parameters recorded during the monthly exposures of the fish are summarized in Table 8.2 Sentinel fish were found infected with *C. puntazzi*, both microscopically and by PCR screening, showing a marked seasonality in the piscine host. The control group was never found to harbour *C. puntazzi*.

8.3.2.1. *C. puntazzi* seasonality

Infection prevalence and intensity in the bile

Prevalences of *C. puntazzi* showed a marked seasonality throughout the year (Figure 8.2). Microscopical detection of spores and pre-sporogonic stages of *C. puntazzi* in the bile was only possible between April and November, when these stages were numerous enough to be seen. Microscopical detection of *C. puntazzi* was first possible in April when sea water temperature had increased by 4ºC in with respect to the winter months. In June and July a decrease in infection prevalence was observed. Thereafter, prevalence rates increased again, with a maximum prevalence in October. Thus, two peaks of infection levels were observed: in April-May and in October. During the winter months (December-March), neither spores no pre-sporogonic stages were detected microscopically in the bile.

While microscopical detection of *C. puntazzi* was possible only between April and November, PCR analysis detected the parasite throughout the whole year. In general, prevalence of the parasite by PCR was higher than by microscopical detection, as it allowed for detection of the parasite during winter months. In some cases, similar prevalence values were observed between microscopical and PCR detection (April, May

and October, Figure 8.2). Similar to the microscopical observations, prevalence rates estimated by PCR showed two peaks, in April/May and in October. Lowest *C. puntazzi* prevalences (PCR) were observed in June/July and during the winter months.

Prevalence of infection in the bile at 1 day p.e. by PCR varied between 20-100% (data not shown), except for April, August and October where no infection was detected at 1 day p.e. Similar values were observed in the PCR analysis of bile samples at 60 days p.e. (16.7-100%; data not shown). No clear pattern of increase or decrease of prevalence was observed between 1 day p.e. and 60 days p.e each month.

Infection prevalence and intensity in the blood

PCR proved the presence of *C. puntazzi* in the blood of sharpsnout seabream and thus indicates that this myxozoan forms blood stages for dissemination. PCR detection of *C. puntazzi* in the blood revealed that, in contrast to the bile, the parasite showed very high infection prevalence all year round, reaching 100% almost every month (Figure 8.3). The prevalence of infection in the blood at 60 days p.e. were lower than at 1 day a.e. in March, April, June, November and December.

Table 8.2 Fish data and sea parameters during natural transmission experiment: number of fish analysed per month, total length and weight, sea water temperature, visibility and sea condition (calm water, swell, storms, water sediment) at exposure and recovery of the sea cage.

MONTH	FISH			SEA CONDITIONS					
				Exposure			Recovery		
	n	Length (cm)	Weight (g)	Exposure Temperature (°C)	Expousure Visibility (m)	Other	Recovery Temperature (°C)	Recovery Visibility (m)	Other
January	20	11.5-13.5	22.1-38	11	3-5	Calm	11	< 1	Ground swell
February	20	11-14.9	29.2-51.2	11	5-6	Calm	12	5-6	Ground swell
March	20	13.4-15.7	29.6-53.3	12	3	Calm	13	3-4	-
April	15	13.3-16.5	39-61	16	9	Calm	16	3	Ground swell
May	15	13.6-16.5	34.6-62.7	16	3-5	Calm	19	3-5	-
June	14	16.2-17.6	57.1-80.7	20	9	Ground swell	24	9	-
July	14	15.8-17.5	57-74.2	24	3-5	-	24	2	-
August	14	15.2-18.3	44.4-89.9	24	5-6	-	24	3-5	Ground swell
September	14	17-19.2	63.5-92.9	21	6-7	-	21	< 1	Storm, river sediment
October	14	16-19.5	58-98.5	21	2	Ground swell	19	4	-
November	14	17-20	78.1-113.5	17	8	-	17	10	-
December	20	10.2-13.9	13.5-28.3	14	3-5	-	14	< 1	-

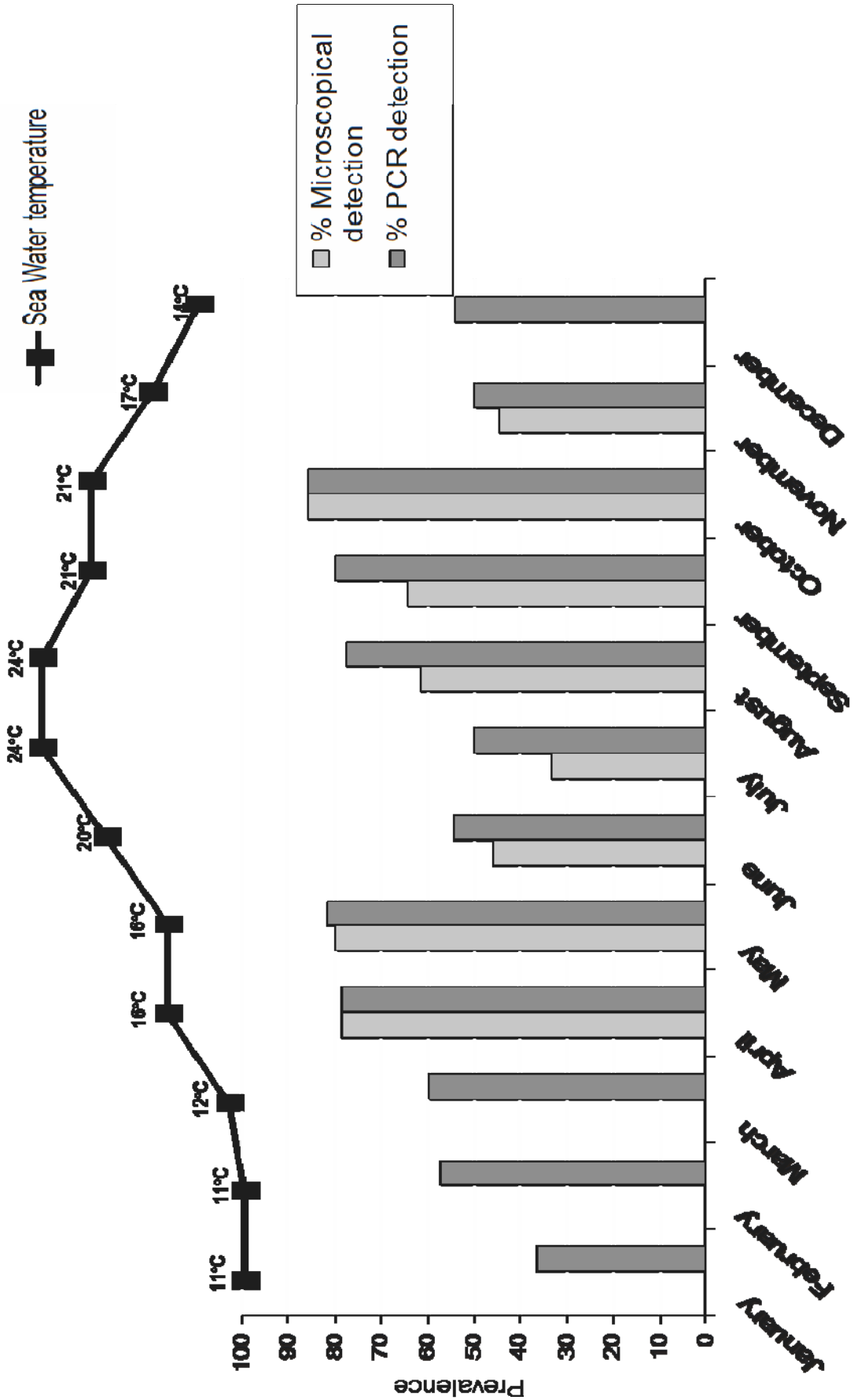

Figure 8.2 *Ceratomyxa puntazzi* prevalence (%) in the bile by microscopical (only 60 days p.e. analysed fish) and PCR detection (total analysed fish) plotted together with sea water temperature each month.

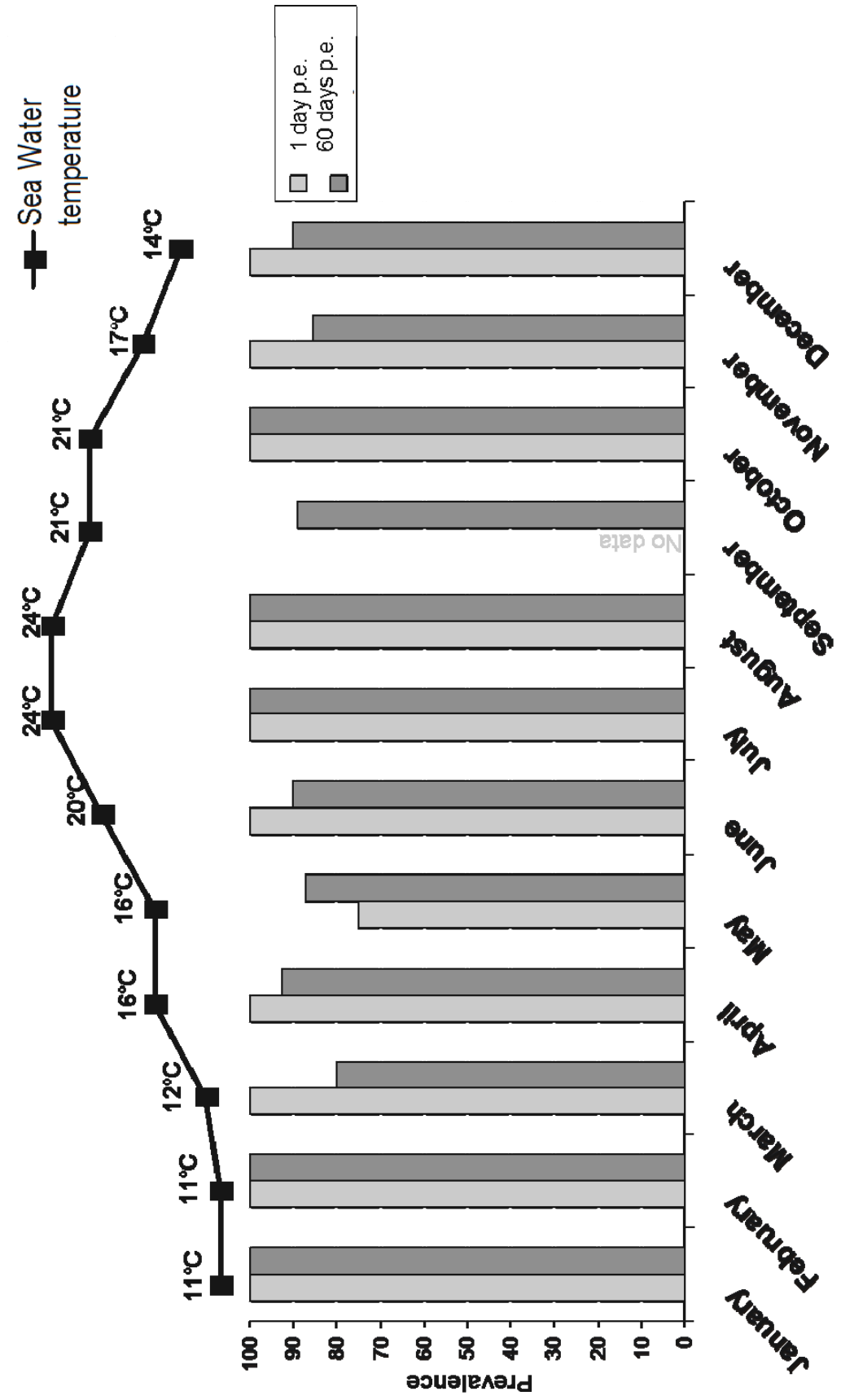

Figure 8.3 *Ceratomyxa puntazzi* prevalence (%) in the blood at 1 and at 60 days p.e. by PCR detection plotted together with sea water temperature each month.

C. puntazzi infection in the liver

PCR was conducted on DNA extracted from selected liver samples (n=28) throughout the year. Special care was taken to analyse samples that were from fish which proved to have infection in the blood but not in the bile, vice versa or in both locations. The results (summarized in Table 8.3) showed that when blood and bile were PCR positive for *C. puntazzi* (42.9% of cases), the parasite was always present in the liver. When the parasite was detected in the blood but not in the gall bladder (35.7% of cases), it was always detected in the liver. Finally, when blood stages were not detected but *C. puntazzi* was present in the bile, the liver proved to be PCR positive in 14.3% and PCR negative in 7.1% of fish.

Table 8.3 Pattern of PCR results from blood, liver and bile.

Blood	Liver	Bile	Prevalence of cases
+	+	+	42.9%
+	+	-	35.7%
-	+	+	14.3%
-	-	+	7.1%
Route of infection			100%

8.3.2.2. Other parasites detected in sentinel fish

The following parasites were found occasionally in sentinel *D. puntazzo*:

Myxozoa

- *Enteromyxum* sp. (Figure 8.4A): Spores not matching any previous descriptions of known *Enteromyxum* spp. were detected in the intestine of fish sampled in May (60 days p.e.), but in no other month out of the year. Prevalence of *Enteromyxum* sp. was 18.2% (2/11) in May.

- *Enteromyxum leei* (Figure 8.4B): Spores of *E. leei* were found in the gall bladder (prevalence= 66.7%; 10/15) and in the intestine (prevalence=86.7%; 13/15) exclusively in fish sampled in December (60 days p.e.).

Copepoda

- Caligidae sp.: A caligid species was found on the skin of *D. puntazzo* from May until August with a maximum prevalence of 75% (3/4) in the fish sampled 1 day p.e. In some cases, the number of the caligids increased considerably during the 60 days of maintenance in the aquaria and severe skin injuries and even mortalities were observed in the fish after this period.

Isopoda

-*Gnathia* sp. (Figure 8.4C): These parasites were observed occasionally on the gills and skin of fish exposed in January, May, June and August, at 1 day p.e. Prevalence in these months reached from 20 to 50% (1/5 to 2/4).

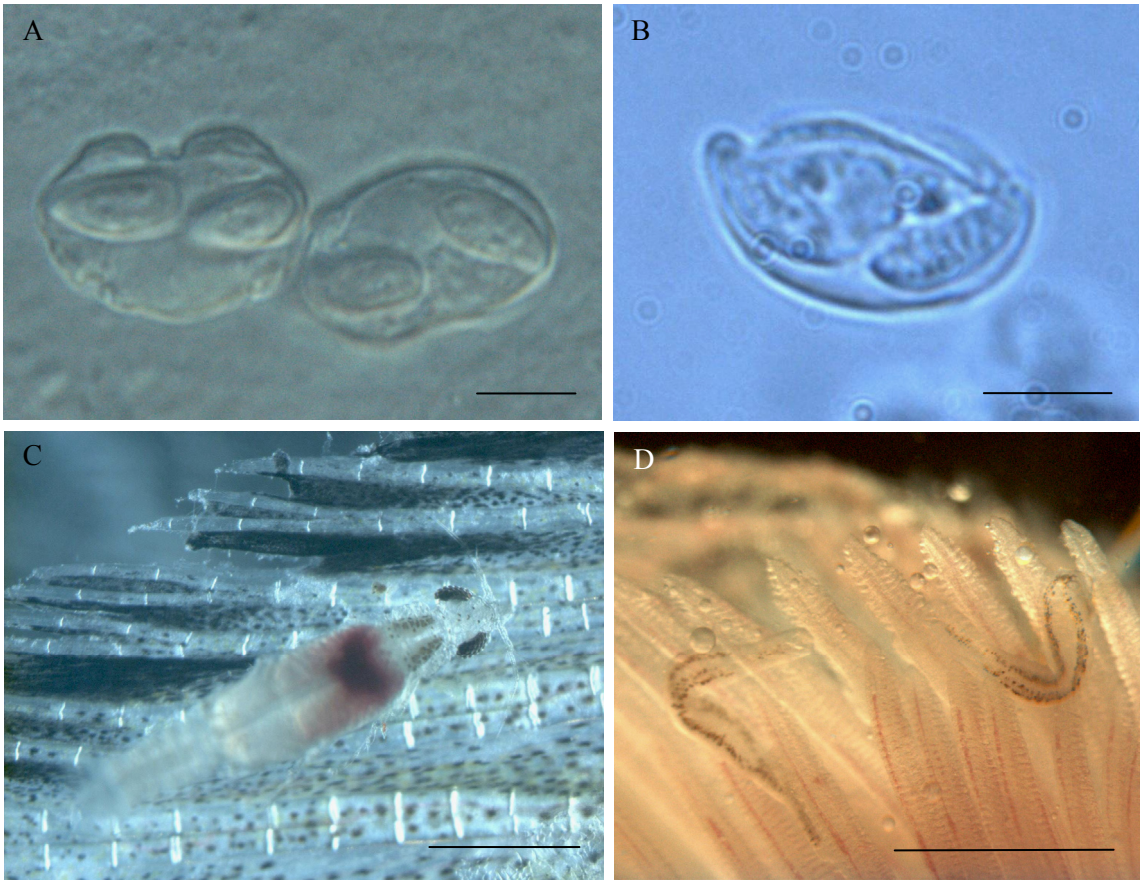

Figure 8.4 Occasional parasites found in sentinel *Diplodus puntazzo* during the natural transmission study. A) *Enteromyxum* sp. found in the intestine. B) *Enteromyxum leei* from the intestine. C) Live *Gnathia* sp. on dorsal fin. D) Live microcotílids attached to the gill filaments. Scale bar: A-B= 10 µm; C-D= 1 mm.

Monogenea

-Microcotylidae sp. (Figure 8.4D): Monogeneans were observed in the gills of *D. puntazzo* exposed in May and at 60 days p.e., showing a prevalence of 27.3% (3/11).

8.4. Discussion

8.4.1. Artificial transmission of *C. puntazzi*

Fish-to fish transmission of different developmental stages of a bile-inhabiting myxozoan has not been attempted previously. In the present case, transmission of *C. puntazzi* pre-sporogonic proliferative and sporogonic stages from the bile was neither achieved by oral, nor by bath treatment or cohabitation. These routes of transmission were chosen for trial because it was thought that it might be possible that, after ingestion, the parasite may be able to enter the gall bladder from the intestine by migration along the common bile duct, as pre-sporogonic stages of *C. puntazzi* from the bile were found to be extremely mobile (see Chapter 7, Section 7.3). However, the highly motile stages are possibly not resistant enough to cope with the strong pH and osmolarity changes and the cocktail of digestive enzymes in the intestine. In enteric myxozoans of the genus *Enteromyxum*, parasite developmental stages that can be transmitted to receptor fish are less exposed to such an environment, as they are located within and protected by host intestinal tissue and mucosa remnants (Redondo et al. 2003b; Diamant et al. 2006). In contrast, *C. puntazzi* proliferative stages are "naked" stages floating in the bile with the only defence against external challenges being their delicate cell membrane. Oral transmission has been reported as an irregular infection pathway. However, some oral transmission experiments resulted in high prevalence of infection (Redondo et al. 2002; Sitjà-Bobadilla et al. 2007) but in other cases, oral intubation was unsuccessful (Bower 1985; Estensoro et al. 2010). This variability has been explained by varying digestive conditions i.e. physical, chemical and enzymatic processes affecting the survival of the stages (Diamant et al. 2006). Changes in osmolarity could be an additional obstacle for parasite transmission in the host gut, as marine fish drink large volumes of seawater (Perrot et al. 1992). Short survival time of developmental stages of *E. scophthalmi* in seawater was observed (Redondo et al. 2003b). Due to the delicacy of pre-sporogonic *C. puntazzi* stages, a limited viability in seawater can also be expected, and possibly explain the failure of transmitting these stages via oral and bath application.

The mixture used for transmission studies in the present case consisted of pre-sporogonic stages but also a large number of mature spores. Mature spores are designed to endure environmental changes but did not cause infection in receptor fish either. As observed in numerous other studies (Grossheider & Körting 1993; McGeorge et al. 1996; Moran et al. 1999b), mature myxosporean spores are not capable of re-infecting their fish hosts, this suggests that spores exclusively infect only the alternate invertebrate host, which is probably the case also in *C. puntazzi*.

Intracoelomic injection of proliferative and sporogonic stages of *C. puntazzi* from the bile also failed to transmit the infection. This could indicate that these stages might not be able to reverse their development, i.e. migrate to the blood and establish as "blood stages". The concentration of parasite stages in the bile was extremely high, and it is unlikely that the failure to establish infection in the receptor fish is due to an insufficient dose of infective parasites.

A different scenario may have occurred in the trial aiming at the transmission of *C. puntazzi* blood stages. The number of stages was so low, that they could not be detected microscopically in blood smears, and only PCR was able to prove their presence. The number of blood stages present in the fish may vary according to the stage of infection as shown in *C. shasta*, where two peaks in the concentration of blood stages (qPCR) were observed, one relating to their initial entry after proliferation in the blood vessel endothelium of the gills and one at re-entry into the blood from the digestive tissues (Bjork & Bartholomew 2010; personal communication). The amount of stages needed successful transmission is unknown, but it is recommended that this trial be repeated experimentally with a higher number of blood stages from more heavily infected fish. Successful transmission of blood stages by intracoelomic injection has previously been reported in other myxozoan species (Kent & Hedrick 1985; Molnár & Kovács-Gayer 1986; Moran et al. 1999b). *Kudoa thrysites* (Gilchrist 1924) infection was successfully transmitted by intracoelomic injection of infected blood, however, in contrast to the blood stages, intubation of spores from infected muscle of Atlantic salmon (Moran et al. 1999b) did not cause infection in the receptor fish. This, once again, emphasizes the importance of the developmental stage of myxozoans for successful fish-to-fish transmission.

Water temperature is another relevant factor in experimental transmissions. In general, high water temperatures allow for earlier establishment of infections and, in many cases, for higher numbers of parasites (Redondo et al. 2002). Water temperatures below 12-

15ºC suppress the development of enteromyxosis, with absence of symptoms and mortalities (Redondo et al. 2002; Yanagida et al. 2006). First signs of infection in *E. leei* appear after 13 days at 24ºC (Diamant et al. 2006). In *D. puntazzo*, *E. leei* was observed as short as 10 days p.e in fish held a 18-20.5ºC (Alvarez-Pellitero et al. 2008). However, in the present study, a relatively high experimental rearing temperature (18-20 ºC) was used and sufficient time was provided for parasite proliferation in the receptor fish. It is thus believed that these factors were not the ones impeding parasite development in the host in the present transmission studies of *C. puntazzi*.

M. cerebralis infection in salmonids was observed to be age or size dependent (Markiw 1992; Thompson et al. 1999; Ryce et al. 2004). Older fish were more resistant to the disease and mortalities were substantially reduced (Ryce et al. 2004). In the intracoelomic blood transmission trial of *C. puntazzi*, receptor fish were much older than donor fish or than the fish used in the other experimental trials, however, they were all previously unexposed, from the same stock and did become infected under natural conditions throughout a whole year, indicating that the age difference may be a negligible factor for *C. puntazzi* infection.

Artificial transmission of *C. puntazzi* from fish to fish was not possible in the present study. In contrast, *Enteromyxum* spp. transmission by cohabitation or waterborne contamination are natural modes of transmission of the disease (Redondo et al. 2002) and "opportunistic direct transmission" has been suggested as an strategy of direct transmission for *E. leei* without the need of an alternate host (Diamant et al. 2006). However, a recent study revealed that it is likely that even *Enteromyxum* spp. have an alternate host (Rangel et al. 2011). Our observations on *C. puntazzi* indicate that this species requires an obligatory alternate host to complete its cycle and that fish-to-fish transmission is not likely to occur in culture conditions.

8.4.2. Natural infections

Natural infection of *D. puntazzo* by exposure to *C. puntazzi*-enzootic waters was possible throughout the whole year. This is the first study providing detailed data on the presence of *C. puntazzi* infective actinosporeans over a full year and the course of the infection in sentinel fish. Monthly exposures have not previously been conducted in a similar way for any marine myxozoan. Thus, this study contributed significantly to our knowledge of the course and the seasonality of infections in marine myxozoans in the Mediterranean environment.

C. puntazzi infection in sentinel fish revealed a marked, temperature-related profile of prevalence and intensity of infection. Spores and pre-sporogonic stages in the bile were detected microscopically from April until November. A similar seasonal trend was reported for *C. shasta* in the Fraser river, despite considerably different water temperatures (4-15ºC) (Ching & Munday 1984; Hendrickson et al. 1989). PCR detection of *C. puntazzi* in the bile was possible all year round despite the absence of sporogonic stages, demonstrating that the parasite must be present in low numbers throughout the winter months. Significant proliferation and spore formation of the parasite only takes place above temperatures of 16ºC degrees. A strong relationship between intensity of infection and water temperature has previously been described for other myxosporeans (Redondo et al. 2002; Yanagida et al. 2006; Estensoro et al. 2010). The first detectable peak of infection was registered in April-May when seawater temperature reached 16ºC. In June and July, when seawater temperatures reached 20-24ºC lower prevalence levels of *C. puntazzi* infection were observed. This may be explained by a reduction in the viability of actinospores at high water temperatures, as observed in *C. shasta* and *P. minibicornis,* where infection declined when temperatures increased above 18ºC (Foott et al. 2007). In contrast, when seawater temperatures started to decrease in October, infection levels of *C. puntazzi* increased again, producing a second peak of infection. This second peak might be explained by a higher production of actinospores during summer time as observed *e.g.* in *Thelohanellus hovorkai* Achmerov 1960*,* which showed an increase in production at 20-25ºC (Liyanage et al. 2003). This suggests that temperature regulates both aspects: the onset of the production of actinospores in the alternate host and the survival of actinospores in the seawater, which probably leads to a fine balance and self-regulation of the infection, thus avoiding massive parasite numbers and mortalities in the fish. Another explanation for the double-peaked prevalence in fish may be the coordination of actinospore release with the invertebrate life cycle (Rangel et al. 2009; 2011). Polychaetes show a varying number of cohorts a year (e.g. Sardá & Martin 1993; Zajac 1991a; Nithart 1998) and actinospore release may take place only during a certain period. *Nereis diversicolor* Müller 1776 e.g. is monotelic and dies immediately after spawning (Andries 2001). Only males are infected with *Zschokkella mugilis* Sitjà-Bobadilla & Alvarez-Pellitero 1993 and they release actinospores at the same time as gametes, once in their life by rupture of their body wall and subsequent death (Rangel et al. 2009).

Alternatively, polychaete densities may be strongly impacted by predation. The densities of *Streblospio benedicti* Webster 1879 decreased sharply in July and August because they were drastically reduced by predation from fish and crabs (Sardá & Martin 1993). Similar dynamics may affect the alternate host of *C. puntazzi* explaining peaks of actinosporean abundance in the seawater. Supporting the idea that the number of actinosporeans is related to the course of the infection in fish, is the fact that not all fish from which PCR-positive blood samples were obtained, developed a microscopically visible infection despite their maintenance at 20-23ºC in the aquarium for 60 days p.e. This was the case in the winter months and suggests that a lower infective dose of actinospores is present in the water during the winter time, possibly due to a lower number of alternate hosts during the harsh winter conditions which lead to increased development time, reduced activity and growth rates of polychaetes, producing shifts in the demography (Zajac 1991b). In future, it would thus be especially useful to analyse water samples throughout the year and determine the concentration of infective actinospores in the water column in each month.

8.4.3. Route of *C. puntazzi* in the fish host and location of latent infection

The combined PCR analysis of blood, liver and gall bladder in infected fish suggests the following route of infection for *C. puntazzi*: The sporoplasm of the unknown actinospore probably enters the blood through the gills, as described for another species of *Ceratomyxa* (Bjork & Bartholomew 2010) and other myxozoans (e.g. Yokoyama & Urawa 1997; Belem & Pote 2001; Holzer et al. 2003). *C. puntazzi* then exits the blood system and enters the liver tissue, penetrates the bile ducts, through which the parasite finally reaches the gall bladder, where it starts pre-sporogonic proliferation and, subsequently, sporogony. Spores are then released with the bile via the intestine into the environment (see Chapter 7, Section 7.3.2). An identical route of infection has been suggested for the bile-infecting freshwater myxozoan *Chloromyxum truttae* Léger 1906 (Holzer et al. 2006b). *C. shasta* invades the fish host through the gills, where it forms large proliferative stages below the blood vessel endothelium in the gills. These stages then release smaller stages into the blood vessels, which migrate into the intestine, where another cycle of proliferation takes place before sporogenesis begins (Bjork & Bartholomew 2010). In the case of *C. puntazzi* it is unclear whether a proliferative cycle takes place in the gills but it would be desirable to determine the exact location and morphology of all parasite stages in the future, by using *in situ* hybridisation, which has

been proven extremely effective in detecting small, cryptic parasite stages (Holzer et al. 2003; Holzer et al. 2010; Bjork & Bartholomew 2010). This may also help to reveal the blood stages which were not detected in regular, Diff Quick-stained blood smears.

The relevance of the blood system for the dispersion of myxozoan parasites and for reaching the target organ cannot be underestimated as blood stages have been reported from many myxozoans from different phylogenetic clades (McGeorge et al. 1994; Holzer et al. 2006b; Holzer et al. 2010; Bjork & Bartholomew 2010). *C. puntazzi* infection in the blood presented a very high prevalence after exposure and all year round. However, possibly dependent on their number and/or the immunological condition of the host, blood stages may be lost or cleared over time, so that not all fish initially infected establish an infection in the bile. Unspecific cellular and humoral effectors can be involved as early as several hours after parasite infection and antibody response in *E. scophthalmi* was observed to appear 50-100 days p.e., limiting the establishment of the parasite (Sitjà-Bobadilla et al. 2006). In *O. mykiss* exposed to *M. cerebralis* specific antibodies first occurred 12 weeks p.e. (Ryce 2003). Loss or clearance of *C. puntazzi* from the blood may be related to an immunological response of the host. However, although some level of innate and acquired immunity might be developed, complete elimination of the parasite is not achieved. This may be due to the bile being an immunoprotective site for continuing parasite development (Sitjà-Bobadilla 2008). According to our observations, reared wild infected *D. puntazzo*, without any possibility of re-infection due to their rearing in our aquaria facilities, maintained *C. puntazzi* infection for more than 2 years (microscopically and/or molecularly, personal observation). Re-activation of infection or last-long infections have been reported from other myxozoans (Higgins et al. 1993; Moran et al. 1999b). Higgins et al. (1993) indicate that some developmental stages of *Myxidium salvelini* Shulman & Konovalov 1966 persist in the kidney tubules, another immunoprotective site, of the anadromous *Oncorhynchus nerka* Walbaum 1792, when the fish return from the sea.

The liver functions as an “antigen trap” showing a high prevalence of macrophages and granulocytes and *C. puntazzi* stages might be eliminated quickly from this organ. This suggest that the stages responsible for last-long infections of *C. puntazzi* occur in the gall bladder. According to the present results they occur in the bile in small numbers (PCR positive), not microscopically detectable, allowing persistent infections during winter time. This might explain why wild stock of sharpsnout seabream,

microscopically negative for *C. puntazzi* in the bile, developed abundant pres-sporogonic proliferative and sporogonic stages in short periods of time (3-4 weeks) when transferred to higher temperatures (18ºC to 24ºC) (authors, unpublished data). This, once again, corroborates highly temperature dependence for the proliferation and sporogony of this parasite. Estensoro et al. (2010) indicates the importance of false negatives by parasite latency in epidemiological surveys during winter time. This emphasises the need of molecular tools to check for infections in parasitological studies. The present chapter provides novel and detailed information about the prevalence and the seasonality of infection of *C. puntazzi* in the sharpsnout seabream *D. puntazzo* and analyses these aspects for the first time in a marine myxozoan. The results allow for the design of new strategies of control of this parasite, e.g. by first exposure of sharpsnout seabream to *C. puntazzi* in sea cages in late autumn, which could provide some immunization previous to the exposure to large numbers of parasites in the following summer.

CHAPTER 9. Conclusions

The present thesis investigates aporocotylid and myxozoan parasites in novel aquaculture species and aquaculture candidate species belonging to the family Sparidae, in the Mediterranean region. The following section concludes and interprets the findings with regard to their relevance for both science and the aquaculture sector:

1) A detailed description of a new blood fluke taxon, *Skoulekia meningialis* n. gen., n. sp. from the common two-banded seabream *D. vulgaris* was provided and the erection of the new genus was strongly supported by morphological data as well as molecular phylogeny and differentiation from the closely related genera, *Psettarium* and *Pearsonellum*. The importance of characterising aporocotylids molecularly using markers of different evolutionary rates (in this study SSU, ITS2 and LSU rDNA) has to be stressed, as commonly used regions (ITS2 rDNA) are not conserved enough to allow for phylogenetic analyses of more distantly related taxa. This probably explains why a phylogenetical hypothesis for this family is still missing.

2) In contrast to the majority of aporocotilids, which usually inhabit the heart or the blood vessels of the gills, *S. meningialis* was found to inhabit a special location, the ectomeningeal veins surrounding the optic lobes of the brain of *D. vulgaris*. While blood fluke pathology is normally almost exclusively related to the eggs trapped within the gill vessels, it is the adults of *S. meningialis* which were found to cause mild, chronic, localised meningitis. *S. meningialis* does not seem to cause any important pathological effect on wild *D. vulgaris*, but special attention has to be paid when establishing *D. vulgaris* in aquaculture systems, due to its extraordinary location surrounding the brain, a vital organ.

3) Macroscopic, elongate plasmodia containing myxosporean spores belonging to the genus *Unicapsula* in the skeletal muscle of the striped seabream, *L. mormyrus* where found to be conspecific with *Unicapsula pflugfelderi* described from the picarel *Spicara smaris*. The comparison of the spore morphology between the different hosts demonstrated that only minor differences exist, and molecular sequences (SSU rDNA) were identical. Disruption of the muscle tissue (myoliquefaction) is common for species of *Unicapsula* and *Kudoa* and may render fillets unmarketable. Enzymatic degradation or myoliquefaction was not found to occur in *U. pflugfelderi*, however, the massive presence of macroscopic plasmodia in the fillets of *L. mormyrus* could produce

marketing problems due to rejection by the consumer. This has to be kept in mind when considering the potential of the striped seabream as an aquaculture candidate.

4) A new species of ceratomyxid *Ceratomyxa puntazzi* n. sp. was described from the gall bladder of the sharpsnout seabream *D. puntazzo*, using morphological and molecular (SSU rDNA) analyses and by comparison with existing reports of ceratomyxids. Analysis of ceratomyxid species of some sparids sharing the habitat with *D. puntazzo*, showed that a species of *Ceratomyxa* was present in *D. annularis*, which was morphologically undistinguishable from *C. puntazzi* but showed an SSU rDNA divergence of 27 bases (1.7%). This, as well as the case of *U. pflugfelderi* demonstrates again that only the combination of morphological and molecular data allows for the erection of new taxa or the identification of conspecific ones, in the Myxozoa. This is of special importance in this parasitic phylum as morphology often contradicts phylogenetic clustering.

5) *C. puntazzi* was found to cause necrosis and loss of epithelial cells in the gall bladder, and it was shown to provoke pericholangitis in the liver tissue which surrounds the bile ducts of *D. puntazzo*. No direct mortalities were related to *C. puntazzi*, however *C. puntazzi* may figure as an opportunistic parasite in immunocompromised hosts as demonstrated for *C. diplodae* in *D. puntazzo* in a previous study.

6) Preliminary data from ceratomyxids from sparids sharing the habitat with *D. puntazzo* indicate that the genus *Ceratomyxa* is very host-specific in sparids and that a high species diversity can be expected in sparids from the Mediterranean. Phylogenetical analyses revealed that all ceratomyxid species of sparids from the Mediterranean rise from a common ancestor. In order to determine whether this relationship is based on geographic or host features, it would be important to analyse additional SSU rDNA sequences from ceratomyxids in sparids from other geographic localities.

7) The combination of microscopic methods *i.e.* light microscopy, electron microscopy and, as a novelty in myxozoan research, confocal laser scanning microscopy using live parasites and specific fluorescent stains, provided unique insights into the development and cellular organisation of the myxozoan *C. puntazzi*. Confocal

laser scanning microscopy had not previously been applied on developmental stages of myxozoans but is strongly recommended for future use and combination with different specific stains. The successful outcome of this study emphasizes the need to apply new techniques in myxozoan research as they can help to elucidate important gaps in our knowledge of this phylum.

8) The combined microscopical study of *C. puntazzi* parasite stages from the bile showed that two developmental pathways can be found in the bile of *D. puntazzo*, i.e. pre-sporogonic proliferation and sporogony. Presporogonic stages demonstrated a high degree of motility, of cellular divisions and of budding by plasmotomy while sporogonic stages were characterised by the formation and maturation of spores.

9) For the first time in myxozoans, locomotive behaviour and the distribution of potential effectors of motility were analysed. The present study provided the following unique information on the processes of directional locomotion and budding in *C. puntazzi*: F-actin rich cytoskeletal elements were found to concentrate at one end of the parasite, which produces localised filopodia, thus facilitating parasite motility. Furthermore, the mechanism of budding was identified, for the first time, as an F-actin dependent process with F-actin concentrating at opposite ends of the separating stages, thus causing their active separation. The study of the behaviour of the stages as a response to external and internal stimuli and the determination of other cellular components involved in motility are future plans initiating from the present work.

10) Ultrastructural studies were found to be of special importance in the study of microparasites like myxozoans. In *C. puntazzi*, lipid droplets and external blebs were detected which might facilitate buoyancy of the parasites. Furthermore, in both *C. puntazzi* and *U. pflugfelderi* an intracellular vesicular body is reported for the first time, and its location and position in sporogonic stages suggests it may be related to the production of material for capsulogenesis.

11) Monthly exposures of sharpsnout seabream to *C. puntazzi*-enzooic environment throughout a full year demonstrate the first attempt of conducting a seasonality study in marine myxozoans. The results showed that *C. puntazzi* demonstrates a marked temperature-related seasonality, with microscopical detection of

proliferative stages and spores exclusively between April and November. However, using a specifically designed PCR assay for *C. puntazzi,* a covert infection was detected in the bile during the winter months. Blood stages were detected all year round and with a high prevalence, when using PCR. This indicates that actinospores are present in the sea water and the blood of exposed fish is invaded throughout the whole year. However, blood stages were found to be lost or cleared, probably in the case of low numbers and due to some immunological response of the fish host. Covert infection in the winter months, blood invasion all year round and the presence of long-lasting infections stresses the importance of diagnosing myxozoan infections in routine examinations by using molecular tools. Ongoing work analyses sea water samples from different depths throughout the year, in order to be able to mirror parasite dynamics in the fish and determine the patterns of actinospore production by the polychaete alternate host. The natural exposure study suggests that initial exposure of fish/transfer from the hatchery to sea cages is best done in late autumn/early winter, as the parasite would then establish in low number and potentially cause some kind of immunization, potentially resulting in higher resistance to re-infection with high numbers of parasites in the following summer. This has been demonstrated in other myxozoans and is an important implication for control measures of *D. puntazzo*.

12) The combinations of PCR results from different organs of the fish exposed to *C. puntazzi* suggests the following route of infection of *C. puntazzi* in the fish host: gills are the portals of entry, from where the parasites enter the blood stream, then exits into the liver tissue and into the bile ducts through which the gall bladder is reached. In the gall bladder, *C. puntazzi* undergoes pre-sporogonic proliferation and sporogony with the consequent release of spores with the bile via the intestine into the environment.

13) The artificial transmission of blood stages, as well as pre-sporogonic and sporogonic stages from the bile of *C. puntazzi* infected sharpsnout seabream to naïve donor fish showed that the parasite cannot be transmitted orally, by injection in coelomic cavity, by bath or by cohabitation with infected fish. This indicates that fish-to-fish transmission of *C. puntazzi* in *D. puntazzo* culture is unlikely to occur and that an alternate invertebrate host is required, unlike in the case of *Enteromyxum* spp.

Reflections

Species diversification is an important strategy in Mediterranean aquaculture in order to combat the saturation of the market and the decrease of prices. Thus, the continuity of the sector strongly depends on basic research in new aquaculture species and their pathogens, and on innovation in the area of strategic disease intervention. Parasite research of new and candidates culture fish should thus be carried on, as the range of parasite species and their pathological potential are still undiscovered. For prevention of parasitic diseases in aquaculture systems of new species, future research should focus on life cycle studies to determine whether the required invertebrate hosts are likely to constitute the biofouling fauna of sea cages. Furthermore, host specificity of parasite taxa should be determined to obtain data about the possibility of cross infection between existent and newly established cultures. Mixed parasitic infections and their dynamics should be studied as they are likely to occur and to have a much stronger impact on the host than single infections. In general, it is of great importance that applied and basic research are combined, in the same way as traditional and new techniques, whose use is currently limited to parasites of human or veterinary importance, in which research has progressed much further. These techniques can provide invaluable insights into yet unexplored areas of research on fish parasites, which is of considerable importance in a world which depends more and more on fish as a valuable protein source for human consumption.

"We must plant the sea and herd its animals using the sea as farmers instead of hunters. That is what civilization is all about - farming replacing hunting." Jacques Yves Cousteau (Interview 17 July 1971).

CHAPTER 10. Appendix

Sequences obtained in the present study, gene fragment, their length and GenBank Accession Number.

Sequence Name	Host	Gene	Lenght (bp)	GenBank® Accession Number
Trematoda				
Skoulekia meningialis	*Diplodus vulgaris*	SSU rDNA	1668	FN652294
		LSU rDNA	1506	FN652293
		ITS2 rDNA	580	FN652292
Myxozoa				
Unicapsula pflugfelderi	*Lithognathus mormyrus*	SSU rDNA	736	AM931470
		LSU rDNA	594	AM931468
Unicapsula pflugfelderi	*Spicara smaris*	SSU rDNA	732	AM931471
		LSU rDNA	594	AM931469
Ceratomyxa puntazzi	*Diplodus puntazzo*	SSU rDNA	1708	JF820290
Ceratomyxa sp.	*Diplodus annularis*	SSU rDNA	1766	JF820291
Ceratomyxa sp. 1	*Sparus aurata*	SSU rDNA	1769	JF820292
Ceratomyxa sp. 2	*Sparus aurata*	SSU rDNA	1743	JF820293

CHAPTER 11. Scientific publications from the present thesis

- **Alama-Bermejo, G**., Cuadrado, M., Raga, J. A. and Holzer, A. S. (2009), Morphological and molecular redescription of the myxozoan *Unicapsula pflugfelderi* from two teleost hosts in the Mediterranean. A review of the genus *Unicapsula* Davis 1924. **Journal of Fish Diseases**, 32: 335–350. doi: 10.1111/j.1365-2761.2008.01000.x

- **Alama-Bermejo, G**., Montero, F.E., Raga, J. A. and Holzer, A. S. (2011) *Skoulekia meningialis* n. gen., n. sp. (Digenea: Aporocotylidae Odhner, 1912) a parasite surrounding the brain of the Mediterranean common two-banded seabream *Diplodus vulgaris* (Geoffroy Saint-Hilaire, 1817) (Teleostei: Sparidae): Description, molecular phylogeny, habitat and pathology. **Parasitology International**, 60, 34–44. doi:10.1016/j.parint.2010.10.001

- **Alama-Bermejo, G**., Raga, J. A. and Holzer, A. S. Host-parasite relationship of *Ceratomyxa puntazzi* n. sp. (Myxozoa: Myxosporea) and sharpsnout seabream *Diplodus puntazzo* (Walbaum, 1792) from the Mediterranean with first data on ceratomyxid host specificity in sparids. **Veterinary Parasitology** In press, doi:10.1016/j.vetpar.2011.05.012

- **Alama-Bermejo, G**., Bron J.E., Raga, J. A. and Holzer, A. S. Motility, three-dimensional morphology, ultrastructure and composition of *Ceratomyxa puntazzi* proliferative and sporogonic stages (Submitted).

- **Alama-Bermejo, G,** Raga J. A. and Holzer A. S. Experimental transmission and seasonality of the myxozoan *Ceratomyxa puntazzi* in the Mediterranean (in preparation)

CHAPTER 12. References

Abdel-Ghaffar F., Ali M.A., Al Quraishy S., Al Rasheid K., Al Farraj S., Abdel-Baki A.S., Bashtar A.R. 2008. Four new species of *Ceratomyxa* Thélohan 1892 (Myxozoa: Myxosporea: Ceratomyxidae) infecting the gallbladder of some Red Sea fishes. Parasitology Research 103: 559–565.

Adriano E.A., Arana S., Cordeiro N.S. 2005. Histology, ultrastructure and prevalence of *Henneguya piaractus* (Myxosporea) infecting the gills of *Piaractus mesopotamicus* (Characidae) cultivated in Brazil. Diseases of Aquatic Organisms 64: 229-235.

Agius C., Tanti J. 1997. Production. In: Status of fish diseases in the Mediterranean. Diseases in Asian aquaculture III, Flegel T.W., MacRae I.H. (eds), Fish Health Section, Asian Fisheries Society, Manila, Philippines, pp. 49-58.

Ali M., Abdel-Baki A., Sakran T. 2006. *Myxidium elmatboulii* n. sp. and *Ceratomyxa ghaffari* n. sp. (Myxozoa: Myxosporea) parasitic in the gallbladder of the Red Sea houndfish *Tylosurus choram* (Rüppell, 1837) (Teleostei: Belonidae) from the Red Sea, Egypt. Acta Protozoologica 45: 97–103.

Alvarez-Pellitero P., Sitjà-Bobadilla A. 1993a. *Ceratomyxa* spp. (Protozoa: Myxosporea) infections in wild and cultured sea bass (*Dicentrarchus labrax*) from the Spanish Mediterranean area. Journal of Fish Biology 42: 889-901.

Alvarez-Pellitero P., Sitjà-Bobadilla A. 1993b. Pathology of Myxosporea in marine fish culture. Diseases of Aquatic Organisms 17: 229-238.

Alvarez-Pellitero P., Palenzuela O., Sitjà-Bobadilla A. 2008. Histopathology and cellular response in *Enteromyxum leei* (Myxozoa) infections of *Diplodus puntazzo* (Teleostei). Parasitology International 57: 110-120.

Anderson G.R, Barker S.C. 1998. Inference of phylogeny and taxonomy within the Didymozoidae (Digenea) from the second internal transcribed spacer (ITS2) of ribosomal DNA. Systematic Parasitology 41: 87–94.

Andries J.C. 2001. Endocrine and environmental control of reproduction in 317 Polychaeta. Canadian Journal of Zoology 79: 254-270.

Asahida T., Kobayashi T., Saitoh K., Nakayama I. 1996. Tissue preservation and total DNA extraction from fish stored at ambient temperature using buffers containing high concentration of urea. Fisheries Science 62: 727–730.

Aseeva N.L., Krasin V.K. 2001. On new records of the family Trilosporidae (Myxosporida: Multivalvulida) from fishes of Pacific ocean. Zoological Journal 35: 353-356 (in Russian).

Aseeva N.L. 2002. Myxosporidian fauna from the Gadidae in Far Eastern seas. Parazitologiya 36:167-174.

Athanassopoulou F., Prapas Th., Rodger H. 1999. Diseases of *Puntazzo puntazzo* C. in marine aquaculture systems in Greece. Journal of Fish Diseases 22: 215–218.

Atkinson S.D., Bartholomew J.L. 2009. Alternate spore stages of *Myxobilatus gasterostei*, a myxosporean parasite of three-spined sticklebacks (*Gasterosteus aculeatus*) and oligochaetes (*Nais communis*). Parasitology Research 104: 1173-1181.

Aurboonyawat T., Suthipongchai S., Pereira V., Ozanne A., Lasjaunias P. 2007. Patterns of cranial venous system from the comparative anatomy in vertebrates - Part I, Introduction and the dorsal venous system. Interventional Neuroradiology 13: 335-344.

Barazi-Yeroulanos L. 2010. Regional synthesis of the Mediterranean marine finfish aquaculture sector and development of a strategy for marketing and promotion of Mediterranean aquaculture (MedAquaMarket). In: GFCM Stud. Rev. 88, 195 pp.

Barta J.R., Martin D.S., Liberator P.A., Dshkevicz M., Anderson J.W., Feighner S.D., Elbrecht A., Perkins-Barrow A., Jenkins M.C., Danforth H.D., Ruff M.D., Profous-Juchelka H. 1997. Phylogenetic relationships among eight *Eimeria* species infecting domestic fowl inferred using complete small subunit ribosomal DNA sequences. Journal of Parasitology 83: 262-271.

Bartholomew J.L., Smith C.E., Rohovec J.S., Fryer J.L. 1989a. Characterization of the host response to the myxosporean parasite, *Ceratomyxa shasta* (Noble), by histology, scanning electron microscopy, and immunological techniques. Journal of Fish Diseases 12: 509–522.

Bartholomew J.L., Rohovec J.S., Fryer J.L. 1989b. *Ceratomyxa shasta*, a myxosporean parasite of salmonids. In: Fish Disease Leaflet, F.W.S. 80, pp 8.

Bartholomew J.L., Whipple M.J., Stevens D.G., Fryer J.L. 1997. The life cycle of *Ceratomyxa shasta*, a myxosporean parasite of salmonids, requires a freshwater polychaete as an alternate host. Journal of Parasitology 83: 859-868.

Bartholomew J.L., Ray E., Torell B., Whipple M.J., Heidel J.R. 2004. Monitoring *Ceratomyxa shasta* infection during a hatchery rearing cycle: Comparison of molecular, serological and histological methods. Diseases of Aquatic Organisms 62: 85-92.

Bartholomew J.L., Atkinson S.D., Hallett S.L., Lowenstine L.J., Garner M.M., Gardiner C.H., Rideout B.A., Keel M.K., Brown J.D. 2008. Myxozoan parasitism in waterfowl. International Journal for Parasitology 38: 1199-1207.

Bartošová P., Fiala I., Hypša V. 2009. Concatenated SSU and LSU rDNA data confirm the main evolutionary trends within myxosporeans (Myxozoa: Myxosporea) and provide an effective tool for their molecular phylogenetics. Molecular Phylogenetics and Evolution 53: 81-93.

Belem A.M.G., Pote L. 2001. Portals of entry and systemic localization of proliferative gill disease organisms in channel catfish *Ictalurus punctatus*. Diseases of Aquatic Organisms 48: 37–42.

Bjork S.J., Bartholomew J.L. 2010. Invasion of *Ceratomyxa shasta* (Myxozoa) and comparison of migration to the intestine between susceptible and resistant fish hosts. International Journal for Parasitology 40: 1087-1095.

Bower S.M. 1985. *Ceratomyxa shasta* (Myxozoa:Myxosporea) in juvenile Chinook salmon (*Onchorhynchus tshawystscha*): experimental transmission and natural infections in the Fraser River, British Columbia. Canadian Journal of Zoology 63: 1737-1740.

Branson E., Riaza A., Alvarez-Pellitero P. 1999. Myxosporean infection causing intestinal disease in farmed turbot, *Scophthalmus maximus* (L.), (Teleostei: Scophthalmidae). Journal of Fish Diseases 22: 395–399.

Bullard S.A., Overstreet R.M. 2006. *Psettarium anthicum* sp. n. (Digenea: Sanguinicolidae) from the heart of cobia *Rachycentron canadum* (Rachycentridae) in the Northern Gulf of Mexico. Folia Parasitologica 53: 117-124.

Bullard S.A., Overstreet R.M., Carlson J.K. 2006. *Selachohemecus benzi* n. sp. (Digenea: Sanguinicolidae) from the blacktip shark *Carcharhinus limbatus* (Carcharhinidae) in the northern Gulf of Mexico. Systematic Parasitology 63: 143-154.

Bullard S.A., Jensen K. 2008. Blood flukes (Digenea: Aporocotylidae) of stingrays (Myliobatiformes: Dasyatidae): *Orchispirium heterovitellatum* from *Himantura imbricata* in the bay of Bengal and a new genus and species of Aporocotylidae from *Dasyatis Sabina* in the northern Gulf of Mexico. Journal of Parasitology 94: 1311-1321.

Bullard S.A., Overstreet R.M. 2008. Digeneans as enemies of fishes, fish flukes whose adults, eggs, or miracidia harm the definitive host fish, Aporocotylidae. In: Fish Diseases, Vol. 2. Eiras J.C., Segner H., Wahli T., Kapoor G.B. (eds.) Plymouth, pp. 908–928.

Bullard S.A., Snyder S.D., Jensen K., Overstreet R.M. 2008. New genus and species of Aporocotylidae (Digenea) from a basal actinopterygian, the American paddlefish, *Polyodon spathula*, (Acipenseriformes:Polyodontidae) from the Mississippi Delta. Journal of Parasitology 94: 487-495.

Bullard S.A., Jensen K., Overstreet R.M. 2009. Historical account of the two family-group names in use for the single accepted family comprising the "fish blood flukes". Acta Parasitologica 54: 78-84.

Bullard S.A. 2010. *Littorellicola billhawkinsi* n. gen., n. sp. (Digenea: Aporocotylidae) from the myocardial lacunae of Florida pompano, *Trachinotus carolinus* (Carangidae) in the Gulf of Mexico; with a comment on the interrelationships and functional morphology of intertrabecular aporocotylids. Parasitology International 59: 587-598.

Bush A.O., Lafferty K.D., Lotz J.M., Shostak A.W. 1997. Parasitology meets ecology on its own terms: Margolis et al. revisited. Journal of Parasitology 83: 575-583.

Canning E.U., Curry A., Anderson C.L., Okamura B. 1999. Ultrastructure of *Myxidium trachinorum* sp. nov. from the gallbladder of the lesser weever fish *Echiichthys vipera*. Parasitology Research 85: 910-919.

Canning E.U., Okamura B. 2004. Biodiversity and evolution of the myxozoa. Advances in Parasitology 56:43-131.

Caruncho H.J., Pinto da Silva P., Anadon R. 1993. The morphology of teleost meningocytes as revealed by freezefracture. Journal of Submicroscopic Cytology and Pathology 25: 397-406.

Casal G., Costa G., Azevedo C. 2007. Ultrastructural description of *Ceratomyxa tenuispora* (Myxozoa), a parasite of the marine fish *Aphanopus carbo* (Trichiuridae), from the Atlantic coast of Madeira Island (Portugal). Folia Parasitologica 54: 165-171.

Castresana J. 2000. Selection of conserved blocks from multiple alignments for their use in phylogenetic analysis. Molecular Biology and Evolution 17: 540-552.

Charras G., Paluch E. 2008. Blebs lead the way: how to migrate without lamellipodia. Nature Reviews Molecular Cell Biology 9: 730-736.

Ching H.L., Munday D.R. 1984. Geographic and seasonal distribution of the infectious stage of *Ceratomyxa shasta* Noble, 1950, a myxozoan salmonid pathogen in the Fraser River system. Canadian Journal of Zoology 62: 1075-1080.

Cho J.B., Kwon S.R., Kim S.K., Nam Y.K., Kim K.H. 2004. Ultrastructure and development of *Ceratomyxa protosettae* Fujita, 1923 (Myxosporea) in the gallbladder of cultured Olive Flounder, *Paralichthys olivaceus*. Acta protozoologica 43: 241-250.

Clifton-Hadley R.S., Bucke D., Richards R.H. 1986. Economic importance of proliferative kidney disease in salmonid fish in England and Wales. Veterinary Record 119: 305–306.

Colquitt S.E., Munday B.L., Daintith W. 2001. Pathological findings in southern bluefin tuna, *Thunnus maccoyii* (Castelnau), infected with *Cardicola forsteri* (Cribb, Daintith & Munday, 2000) (Digenea: Sanguinicolidae), a blood fluke. Journal of Fish Diseases 24: 225-229.

Company R., Sitjà-Bobadilla A., Pujalte M.J., Garay E., Alvarez-Pellitero P., Pérez-Sánchez J. 1999. Bacterial and parasitic pathogens in cultured common dentex, *Dentex dentex* L. Journal of Fish Diseases 22: 299-309.

Crespo S., Grau A., Padrós F. 1992. Sanguinicoliasis in the cultured amberjack *Seriola dumerili* Risso, from the Spanish Mediterranean area. Bulletin European Association of Fish Pathologists 12: 157-159.

Crespo S., Grau A., Padrós F. 1994. The intensive culture of 0-group amberjack in the western Mediterranean is compromised by disease problems. Aquaculture International 2: 262-265.

Cribb T.H., Anderson G.R., Adlard R.D., Bray R.A. 1998. A DNA-based demonstration of a three-host life-cycle for the Bivesiculidae (Platyhelminthes: Digenea). International Journal for Parasitology 28: 1791–1795.

Cribb T.H., Bray R.A., Littlewood D.T.J., Pichelin S.P., Herniou E.A. 2001a. The Digenea. In: Interrelationships of the Platyhelminthes. Littlewood D.T.J., Bray R.A. (eds.) Taylor and Francis, London, pp. 168–185.

Cribb T.H., Bray R.A., Littlewood D.T.J. 2001b. The nature and evolution of the association among digeneans, molluscs and fishes. International Journal for Parasitology 31: 997-1011.

Cribb T.H. 2005. Digenea (endoparasitic flukes). In: Marine parasitology. Rohde K. (ed.) CSIRO Publishing. Collingwood, Vic, pp. 76-87.

Cuadrado M., Albinyana G., Padrós F., Redondo M.J., Sitjà-Bobadilla A., Álvarez-Pellitero P., Palenzuela O., Diamant A., Crespo S. 2007. An unidentified epi-epithelial myxosporean in the intestine of gilthead sea bream *Sparus aurata* L. Parasitology Research 101: 403-411.

Cuadrado M., Marques A., Diamant A., Sitjà-Bobadilla A., Palenzuela O., Alvarez-Pellitero P., Padrós F., Crespo S. 2008. Ultrastructure of *Enteromyxum leei* (Diamant, Lom, and Dyková, 1994) (Myxozoa), an enteric parasite infecting gilthead sea bream (*Sparus aurata*) and sharpsnout sea bream (*Diplodus puntazzo*). Journal of Eukaryotic Microbiology 55: 178-184.

Current W.L. 1979. *Henneguya adiposa* Minchew (Myxosporidia) in the channel catfish: ultrastructure of the plasmodium wall and sporogenesis. Journal of Protozoology 26: 209-217.

Davis H.S. 1924. A new myxosporidian parasite, the cause of "wormy" halibut. Report of United States Commission on Fisheries 1923: 1-5.

Day J.J. 2002. Phylogenetic relationships of the Sparidae (Teleostei: Percoidei) and implications for convergent trophic evolution. Biological Journal of the Linnean Society 76: 269-301.

Diamant A., Lom J., Dykova I. 1994. *Myxidium leei* n. sp. a pathogenic myxosporean of cultured sea bream *Sparus aurata*. Diseases of Aquatic Organisms 20: 137-141.

Diamant A. 1997. Fish-to-fish transmission of a marine myxosporean. Diseases of Aquatic Organisms 30: 99-105.

Diamant A. 1998. Red drum *Sciaenops ocellatus* (Sciaenidae), a recent introduction to Mediterranean mariculture, is susceptible to *Myxidium leei* (Myxosporea). Aquaculture 162: 33-39.

Diamant A., Whipps C.M., Kent M.L. 2004. A new species of *Spaheromyxa* (Myxosporea: Sphaeromyxina: Sphaeromyxidae) in devil firefish, *Pterois miles* (Scorpaenidae), from the northern red sea: morphology, ultrastructure, and phylogeny. Journal of Parasitology 90: 1434-1442.

Diamant A., Ucko M., Paperna I., Colorni A., Lipshitz A. 2005. *Kudoa iwatai* (Myxosporea: Multivalvulida) in wild and cultured fish in the Red sea: redescription and molecular phylogeny. Journal of Parasitology 91: 1175–1189.

Diamant A., Ram S., Paperna I. 2006. Experimental transmission of *Enteromyxum leei* to freshwater fish. Diseases of Aquatic Organisms 72: 171-178.

Diebakate C., Fall M., Faye N., Toguebaye B.S. 1999. *Unicapsula marquesi* n.sp. (Myxosporea, Multivalvulida) parasite des branchies de *Polydactylus quadrifilis* (Cuvier, 1829) (Poisson, Polynemidae) des côtes sénégalaises (Afrique de l'Ouest). Parasite 6: 231-235 (in French).

Egusa S. 1986. The order Multivalvulida Shulman, 1959 (Myxozoa: Myxosporea): a review. Fish Pathology 21: 261-274.

Eiras J.C. 2006. Synopsis of the species of *Ceratomyxa* Thélohan, 1892 (Myxozoa: Myxosporea: Ceratomyxidae). Systematic Parasitology 65: 49-71.

El-Matbouli M., Hoffmann R.W., Mandok C. 1995. Light and electron microscopic observations on the route of the triactinomyxon-sporoplasm of *Myxobolus cerebralis*

from epidermis into the rainbow trout (*Oncorhynchus mykiss*) cartilage. Journal of Fish Biology 46: 919–935.

Estensoro I., Redondo M.J., Alvarez-Pellitero P., Sitjà-Bobadilla A. 2010. Novel horizontal transmission route for *Enteromyxum leei* (Myxozoa) by anal intubation of gilthead sea bream *Sparus aurata*. Diseases of Aquatic Organisms 92: 51-58.

Eszterbauer E., Kallert D.M., Grabner D., El-Matbouli M. 2009. Differentially expressed parasite genes involved in host recognition and invasion of the triactinomyxon stage of *Myxobolus cerebralis* (Myxozoa). Parasitology 136: 367-377.

Evans N.M., Holder M.T., Barbeitos M.S., Okamura B., Cartwright P. 2010. The Phylogenetic position of Myxozoa: Exploring conflicting signals in phylogenomic and ribosomal data sets. Molecular Biology and Evolution 27: 2733-2746.

Feist S.W., Peeler E.J., Gardiner R., Smith E., Longshaw M. 2002. Proliferative kidney disease and renal myxosporidiosis in juvenile salmonids from rivers in England and Wales. Journal of Fish Diseases 25: 451–458.

Feist S.W., Longshaw M. 2006. Phylum Myxozoa. In: Fish Diseases and Disorders, Volume 1: Protozoan and Metazoan Infections, 2nd edition. Woo P.T.K. (ed.) CABI, Oxfordshire, U.K., pp. 230-296.

Fiala I. 2006. The phylogeny of Myxosporea (Myxozoa) based on small subunit ribosomal RNA gene analysis. International Journal for Parasitology 36: 1521-1534.

Fiala I., Bartošová P. 2010. History of myxozoan character evolution on the basis of rDNA and EF-2 data. BMC Evolutionary Biology 10: 228.

Firat K., Saka S., Kamaci H.O. 2005. Embryonic and larval development of striped seabream (*Lithognathus mormyrus* L. 1758). Israeli Journal of Aquaculture- Bamidgeh 57: 131-140.

Foott J.S., Stone R., Wiseman E., True K., Nichols K. 2007. Longevity of *Ceratomyxa shasta* and *Parvicapsula minibicornis* actinospore infectivity in the Klamath River. Journal of Aquatic Animal Health 19: 77-83.

George-Nascimento M., Lobos V., Torrijos C., Khan R. 2004. Species composition of assemblages of *Ceratomyxa* (Myxozoa), parasites of lings *Genypterus* (Ophidiidae) in the southeastern Pacific Ocean: an ecomorphometric approach. Journal of Parasitology 90: 1352-1355.

Georgévitch J. 1917. Recherches sur le développement de *Ceratomyxa herouardi* Georgévitch. Archives de zoologie expérimentale et générale 56: 375-399 (in French).

Georgévitch J. 1929. Recherches sur *Ceratomyxa maenae* nov. sp. Archive fur Protistenkunde 65: 106-123 (in French).

Georgiev B.B., Biserkov V., Genov T. 1986. *In toto* staining method for cestodes with iron acetocarmine. Helminthologia 23: 279-281.

Gibson D.I. 2002a. Class Trematoda Rudolphi, 1808. In: Keys to the Trematoda Vol. 1. Gibson D.I., Jones A., Bray R.A. (eds.), CAB International Cambridge, Wallingford, pp. 1-3.

Gibson D.I. 2002b. Subclass Digenea Carus 1863. In: Keys to the Trematoda Vol. 1. Gibson D.I., Jones A., Bray R.A. (eds.), CAB International Cambridge, Wallingford, pp. 15-16.

Goto S., Ozaki Y. 1930. Brief notes on new trematodes III. Japanese Journal of Zoology 3: 73-82.

Grabner D.S., El-Matbouli M. 2010a. Experimental transmission of malacosporean parasites from bryozoans to common carp *Cyprinus carpio* and minnow *Phoxinus phoxinus*. Parasitology 137: 629-639.

Grabner D.S., El-Matbouli M. 2010b. *Tetracapsuloides bryosalmonae* (Myxozoa: Malacosporea) portal of entry into the fish host. Diseases of Aquatic Organisms 90: 197-206.

Grenacher H. 1879. Untersuchen ber das Sehorgan der Arthropoden, insbesondere der Spinnen, Insekten und Crustaceen. Vandenhoeck & Ruprecht, Gottingen, Germany, 185 pp (in German).

Griffin M.J., Khoo L.H., Torrans L., Bosworth B.G., Quiniou S.M., Gaunt P.S., Pote L.M. 2009. New data on *Henneguya pellis* (Myxozoa: Myxobolidae), a parasite of blue catfish *Ictalurus furcatus*. Journal of Parasitology 95: 1455-1467.

Grossheider G., Körting W. 1993. Experimental transmission of *Sphaerospora renicola* to common carp *Cyprinus carpio*. Diseases of Aquatic Organisms 16: 91–95.

Gunter N.L., Adlard R.D. 2008. Bivalvulidan (Myxozoa: Myxosporea) parasites of damselfishes with description of twelve novel species from Australia's Great Barrier Reef. Parasitology 135: 1165–1178.

Gunter N.L., Adlard R.D. 2009. Seven new species of *Ceratomyxa* from the gall bladders of serranids from the Great Barrier Reef, Australia. Systematic Parasitology 73: 1–11.

Gunter N.L., Whipps C.M., Adlard R.D. 2009. *Ceratomyxa* (Myxozoa: Bivalvulida): Robust taxon or genus of convenience? International Journal for Parasitology 39: 1395-1405.

Gunter N., Adlard R. 2010. The demise of *Leptotheca* Thélohan, 1895 (Myxozoa: Myxosporea: Ceratomyxidae) and assignment of its species to *Ceratomyxa* Thélohan, 1892

(Myxosporea: Ceratomyxidae), *Ellipsomyxa* Køie, 2003 (Myxosporea: Ceratomyxidae), *Myxobolus* Bütschli, 1882 and *Sphaerospora* Thélohan, 1892 (Myxosporea: Sphaerosporidae). Systematic Parasitology 75: 81-104.

Gunter N.L., Burger M.A.A., Adlard R.D. 2010a. Morphometric and molecular characterisation of four new *Ceratomyxa* species (Myxosporea: Bivalvulida: Ceratomyxidae) from fishes off Lizard Island, Australia. Folia Parasitologica 57: 1-10.

Gunter N.L., Cribb T.H., Adlard R.D. 2010b. Extraordinary richness of *Ceratomyxa* (Myxozoa) infecting Australian coral reef fishes. In: 12th International Congress of Parasitology, understanding the global impact of parasites-from genomes to function and disease, Melbourne, Australia, August 2010.

Hall T.A. 1999. BioEdit: a user-friendly biological sequence alignment editor and analysis program for Windows 95/98/NT. Nucleic Acids Symp. Ser. 41: 95-98.

Hallett S.L., Atkinson S.D., Holt R.A., Banner C.R., Bartholomew J.L. 2006. A new myxozoan from feral goldfish (*Carassius auratus*). Journal of Parasitology 92: 357-363.

Hedrick R.P., MacConnell E., de Kinkelin P. 1993. Proliferative kidney disease of salmonid fish. In: Annual review of fish diseases, Faisal M., Hetrick F.M. (eds), Pergamon Press, New York, pp. 277–290.

Hedrick R.P., Baxa D.V., de Kinkelin P., Okamura B. 2004. Malacosporean-like spores in urine of rainbow trout react with antibody and DNA probes to *Tetracapsuloides bryosalmonae*. Parasitology Research 92: 81-88.

Heiniger H., Gunter N.L., Adlard R.D. 2008. Relationships between four novel ceratomyxid parasites from the gall bladders of labrid fishes from Heron Island, Australia. Parasitology International 57: 158–165.

Hemmingsen W. 2008. Emerging diseases in mariculture. In: Afonso-Dias I., Menezes G., Mackenzie K., Eiras J.C. Eds. Proceedings of the International Workshop on Marine Parasitology: Applied Aspects of Marine Parasitology. Arquipélago. Life and Marine Sciences, pp. 1-6.

Hendrickson G.L., Carleton A., Manzer D. 1989. Geographic and seasonal distribution of the infective stage of *Ceratomyxa shasta* (Myxozoa) in Northern California. Diseases of Aquatic Organisms 7: 165-169.

Herbert B.W., Shaharom-Harrison F.M., Overstreet R.M. 1994. Description of a new blood-fluke, *Cruoricola lates* n. g., n. sp. (Digenea: Sanguinicolidae), from sea-bass *Lates calcarifer* (Bloch, 1790) (Centropomidae). Systematic Parasitology 29: 51-60.

Herbert B.W., Shaharom F.M., Anderson I.G. 1995. Histopathology of cultured sea bass (*Lates calcarifer*) (Centropomidae) infected with *Cruoricola lates* (Trematoda: Sanguinicolidae) from Pulau Ketam, Malaysia. International Journal for Parasitology 25: 3-13.

Higgins M.J., Margolis L., Kent M.L. 1993. Arrested development in a freshwater myxosporeans *Myxidium salvelini*, following transfer of its host, the sockeye salmon (*Onchorhynchus nerka*), to sea water. Journal of Parasitology 79: 403-407.

Hillis D.M., Dixon M.T. 1991. Ribosomal DNA: molecular evolution and phylogenetic inference. Quarterly Review of Biology 66: 411-453.

Hofer B. 1903. Über die Drehkrankheit der Regenbogenforelle. Allgemeinen Fischerei-Ztg., Jahrg 28: 7-8 (in German).

Hogge C.I., Campbell M.R., Johnson K.A. 2008. A new species of myxozoan (Myxosporea) from the brain and spinal cord of rainbow trout (*Oncorhynchus mykiss*) from Idaho. Journal of Parasitology 94: 218-222.

Holland J.W., Okamura B., Hartikainen H., Secombes C.J. 2010. A novel minicollagen gene links cnidarians and myxozoans. Proceedings of the Royal Society B: Biological Sciences 278: 546-553.

Holmes J.C. 1971. Two new sanguinicolid blood flukes (Digenea) from scorpaenid rockfishes (Perciformes) of the Pacific Coast of North America. Journal of Parasitology 57: 209–216.

Holzer A.S., Sommerville C., Wootten R. 2003. Tracing the route of *Sphaerospora truttae* from the entry locus to the target organ of the host, *Salmo salar* L., using an optimized and specific in situ hybridization technique. Journal of Fish Diseases 26: 647-655.

Holzer A.S., Sommerville C., Wootten R., 2004. Molecular relationships and phylogeny in a community of myxosporeans and actinosporeans based on their 18S rDNA sequences. International Journal for Parasitology 34: 1099–1111.

Holzer A.S, Sommerville C., Wootten R. 2006a. Molecular identity, phylogeny and life cycle of *Chloromyxum schurovi* Shul'man and Ieshko 2003. Parasitology research 99: 90-96.

Holzer A.S., Sommerville C., Wootten R. 2006b. Molecular studies on the seasonal occurrence and development of five myxozoans in farmed *Salmo trutta* L. Parasitology 132: 193-205.

Holzer A.S., Wootten R., Sommerville C. 2007. The secondary structure of the unusually long 18S ribosomal RNA of the myxozoan *Sphaerospora truttae* and structural

evolutionary trends in the Myxozoa. International Journal for Parasitology 37: 1281-1295.

Holzer A.S., Montero F.E., Repullés A., Nolan M.J., Sitjà-Bobadilla A., Alvarez-Pellitero P., Zarza C., Raga J.A. 2008. *Cardicola aurata* sp. n. (Digenea: Sanguinicolidae) from Mediterranean *Sparus aurata* L. (Teleostei: Sparidae) and its unexpected phylogenetic relationship with *Paradeontacylix* McIntosh, 1934. Parasitology International 57: 472-482.

Holzer A.S., Stewart S., Tildesley A., Wootten R., Sommerville C. 2010. Infection dynamics of two renal myxozoans in hatchery reared fry and juvenile Atlantic cod *Gadus morhua* L. Parasitology 137: 1501-1513.

Ikeda J. 1912. Studies on some sporozoan parasites of sipunculoids. I. The life history of an Actinomyxidian, *Tetractinomyxon intermedium* g. et. sp. nov. Archiv für Protistenkunde 25: 240-242.

Iqbal N.A.M., Sommerville C. 1984. Developmental cycle and seasonal rhythms of *Sanguinicola inermis* (Digenea: Sanguinicolidae) in carp under constant conditions. In: Fourth European Multicolloquium of Parasitology, Tumbay E., Yasarol S., Ozcel M. A. (eds), Turkey, p.191.

Ishizaki H. 1960. A new myxosporidian parasite of the genus *Leptotheca*. Bulletin Fukuoka Gakugei University 10: 113-116.

Jiménez-Guri E., Philippe H., Okamura B., Holland P.W.H. 2007. *Buddenbrockia* is a cnidarian worm. Science 317: 116-118.

Jirkù M., Bolek M.G., Whipps C.M., Janovy Jr.J., Kent M.L., Modrý D. 2006. A new species of *Myxidium* (Myxosporea: Myxidiidae), from the western chorus frog, *Pseudacris triseriata triseriata*, and Blanchard's cricket frog, *Acris crepitans blanchardi* (Hylidae), from eastern Nebraska: Morphology, phylogeny, and critical comments on amphibian *Myxidium* taxonomy. Journal of Parasitology 92: 611-619.

Kalavati C., MacKenzie K. 1999. The genera *Ceratomyxa* Thélohan, 1892, *Leptotheca* Thélohan, 1895 and *Sphaeromyxa* Thélohan, 1892 (Myxosporea: Bivalvulida) in gadid fish of the Northeast Atlantic. Systematic Parasitology 43: 209-216.

Kallert D.M., Eszterbauer E., Grabner D., El-Matbouli M. 2009. In vivo exposure of susceptible and non-susceptible fish species to *Myxobolus cerebralis* actinospores reveals non-specific invasion behaviour. Diseases of Aquatic Organisms 84: 123-130.

Kallert D.M., Bauer W., Haas W., El-Matbouli M. 2010. No shot in the dark: Myxozoans chemically detect fresh fish. International Journal for Parasitology 41: 271-276.

Kallianiotis A., Torre M., Argyri A. 2005. Age, growth, mortality, reproduction and feeding habits of the striped seabream, *Lithognathus mormyrus* (Pisces: Sparidae), in the coastal waters of the Thracian Sea, Greece. Scientia Marina 69: 391-404.

Katharios P., Garaffo M., Sarter K., Athanassopoulou F., Mylonas C.C. 2007. A case of high mortality due to heavy infestation of *Ceratomyxa diplodae* in sharpsnout sea bream (*Diplodus puntazzo*) treated with reproductive steroids. Bulletin European Association of Fish Pathologists 27: 43-47.

Kent M.L., Hedrick R.P. 1985. PKX, the causative agent of proliferative kidney disease (PKD) in Pacific salmonid fishes and its affinities with the Myxozoa. Journal of Protozoology 32: 254-260.

Kent M.L., Poppe T.T. 1998. Diseases of Seawater Netpen-reared Salmonids. Pacific Biological Station Press, Nanaimo, British Columbia, Canada, 138 pp.

Kent M.L., Andree K.B., Bartholomew J.L., El-Matbouli M., Desser S.S., Devlin R.H., Feist S.W., Hedrick R.P., Hoffmann R.W., Khattra J., Hallett S.L., Lester R.J.G., Longshaw M., Palenzuela O., Siddall M.E., Xiao C.X. 2001. Recent advances in our knowledge of the Myxozoa. The Journal of Eukaryotic Microbiology 48: 395-413.

Kirk R.S., Lewis J.W. 1992. The laboratory maintenance of *Sanguinicola inermis* Plehn, 1905 (Digenea: Sanguinicolidae). Parasitology 104: 121-127.

Kirk R.S., Lewis J.W. 1993. The life cycle and morphology of *Sanguinicola inermis* Plehn, 1905 (Digenea: Sanguinicolidae). Systematic Parasitology 25: 125-133.

Kirk R.S., Lewis J.W. 1998. Histopathology of *Sanguinicola inermis* infection in carp, *Cyprinus carpio.* Journal of Helminthology 72: 33-38.

Køie M. 1982. The redia, cercaria and early stages of *Aporocotyle simplex* Odhner, 1900 (Sanguinicolidae) – a digenetic trematode which has a polychaete annelid as the only intermediate host. Ophelia 21: 115–145.

Køie M., Petersen M.E. 1988. A new annelid intermediate host (*Lanassa nordenskioeldi* Malmgren, 1866) (Polychaeta: Terebellidae) for *Aporocotyle* sp. and a new final host family (Pisces: Bothidae) for *Aporocotyle simplex* Odhner, 1900 (Digenea: Sanguinicolidae). Journal of Parasitology 74: 499–502.

Køie M., Whipps C.M., Kent M.L. 2004. *Ellipsomyxa gobii* (Myxozoa: Ceratomyxidae) in the common goby *Pomatoschistus microps* (Teleostei: Gobiidae) uses *Nereis* spp. (Annelida: Polychaeta) as invertebrate hosts. Folia Parasitologica 51: 14-18.

Køie M., Karlsbakk E., Nylund A. 2007. A new genus *Gadimyxa* with three new species (Myxozoa, Parvicapsulidae) parasitic in marine fish (Gadidae) and the two-host life cycle of *Gadimyxa atlantica* n. sp. Journal of Parasitology 93: 1459-1467.

Køie M., Karlsbakk E., Nylund A. 2008. The marine herring myxozoan C*eratomyxa auberbachi* (Myxozoa: Ceratomyxidae) uses *Chone infundibuliformis* (Annelida: Polychaeta: Sabellidae) as invertebrate host. Folia Parasitologica 55: 100-104.

Kudo R.R. 1919. Studies on Myxosporidia: a synopsis of genera and species of Myxosporidia. Illinois Biological Monographs 5: 1–265.

Kudo R.R. 1921. On the effect of some fixatives upon Myxosporidian spores. Transactions of the American Microscopical Society 40: 161-167.

Lester R.J.G. 1982. *Unicapsula seriolae* n. sp. (Myxosporea, Multivalvulida) from Australian Yellowtail Kingfish *Seriola lalandi*. Journal of Protozoology 29: 584-587.

Lin D., Hanson L.A., Pote L.M., 1999. Small subunit ribosomal RNA sequence of *Henneguya exilis* (Class Myxosporea) identifies the actinosporean stage from an oligochaete host. Journal of Eukaryotic Microbiology 46: 66-68.

Li L., Saga N., Mikami K. 2008. Phosphatidylinositol 3-kinase activity and asymmetrical accumulation of F-actin are necessary for establishment of cell polarity in the early development of monospores from the marine red alga *Porphyra yezoensis*. Journal of Experimental Botany 59: 3575-3586.

Littlewood D.T.J., Olson P.D. 2001. Small subunit rDNA and the phylum Platyhelminthes: signal, noise, conflict and compromise. In: Interrelationships of the Platyhelminthes, Littlewood D.T.J., Bray R.A. (eds), Taylor and Francis, London, pp. 262–278.

Liyanage Y.S., Yokoyama H., Wakabayashi H. 2003. Dynamics of experimental production of *Thelohanellus hovorkai* (Myxozoa: Myxosporea) in fish and oligochaete alternate hosts. Journal of Fish Diseases 26: 575-582.

Lockyer A.E., Olson P.D., Littlewood D.T.J. 2003. Utility of complete large and small subunit rRNA genes in resolving the phylogeny of the Neodermata (Platyhelminthes): implications and a review of the cercomer theory. Biological Journal of the Linnean Society 78: 155–171.

Lom J., Arthur R. 1989. A guideline for the preparation of species descriptions in Myxosporea. Journal of Fish Diseases 12: 151–156.

Lom J., Dyková I. 1992. Myxosporidia (Phylum Myxozoa). In: Protozoan Parasites of Fishes. Developments in Aquaculture and Fisheries Science. 26. Elsevier, Amsterdam, 167. pp. 159-235.

Lom J., Dyková I. 1996. Notes on the ultrastructure of two myxosporean (Myxozoa) species, *Zschokkella pleomorpha* and *Ortholinea fluviatilis*. Folia Parasitologica 43: 189-202.

Lom J., Dyková I. 2006. Myxozoan genera: definition and notes on taxonomy, life-cycle terminology and pathogenic species. Folia Parasitologica 53: 1-36.

Lubat V., Radujković B., Marques A., Bouix G. 1989. Parasites de poissons marins du Montenegro: Myxosporidies. Acta Adriatica 30: 31–50 (in French).

Maíllo-Bellón P.A., Gracia-Royo M.P. 2007. Vegetative stages, sporogenesis and spore morphology of *Ceratomyxa appendiculata*, Thélohan, 1892 (Myxozoa: Bibalvulida), from the gall bladder of *Lophius budegassa*, Spinola, 1807 (Teleostei: Lophiidae). Acta Protozoologica 46: 247-256.

Manter H.W. 1947. The digenetic trematodes of marine fishes of Tortugas, Florida. American Midland Naturalist Journal 38: 257-416.

Markiw M.E. 1992. Experimentally induced whirling disease. I. Dose response of fry and adults of rainbow trout exposed to the triactinomyxon stage of *Myxobolus cerebralis*. Journal of Aquatic Animal Health 4: 40–43.

McGeorge J., Sommerville C., Wootten R. 1994. Light and electron microscope observations on extrasporogonic and sporogonic stages of a myxosporean parasite of the genus *Sphaerospora* Thelohan, 1892 from Atlantic salmon, *Salmo salar* L., in Scotland. Journal of Fish Diseases 17: 227-238.

McGeorge J., Sommerville C., Wootten R. 1996. Transmission experiments to determine the relationship between *Sphaerospora* sp. from Atlantic salmon, *Salmo salar*, and *Sphaerospora truttae*: A revised species description for *S. truttae*. Folia Parasitologica 43: 107-116.

McGurk C., Morris D.J., Bron J.E., Adams A. 2005. The morphology of *Tetracapsuloides bryosalmonae* (Myxozoa: Malacosporea) spores released from *Fredericella sultana* (Bryozoa: Phylactolaemata). Journal of Fish Diseases 28: 307-312.

Meglitsch P. 1960. Some coelozoic myxosporidia from New Zealand fishes I.- General, and family Ceratomyxidae. Transactions of the Royal Society of New Zealand 88: 265–356.

Merella P., Cherchi S., Salati F., Garippa G. 2005. Parasitological survey of sharpsnout seabream *Diplodus puntazzo* (Cetti, 1777) reared in sea cages in Sardinia (western Mediterranean). Bulletin of the European Association of Fish Pathologists 25: 140-147.

Mitchison T.J. 1995. Evolution of a dynamic cytoskeleton. Philosophical Transactions of the Royal Society B: Biological Sciences 349: 299-304.

Mladineo I., Bočina I. 2006. *Ceratomyxa thunni* sp. n. (Myxozoa: Ceratomyxidae) in Atlantic northern bluefin tuna (*Thunnus thynnus*) caught in the Adriatic Sea, Island of Jabuka. Zootaxa 1224: 59–68.

Molnár K., Kovács-Gayer E. 1986. Biology and histopathology of *Thelohanellus hovorkai* Achmerov, 1960 (Myxosporea, Myxozoa), a protozoan parasite of the common carp (*Cyprinus carpio*). Acta Veterinaria Hungarica 34: 67-72.

Monteiro A.S., Okamura B., Holland P.W.H. 2002. Orphan worm finds a home: *Buddenbrockia* is a myxozoan. Molecular Biology and Evolution 19: 968-971.

Montero F.E., Aznar F.J., Fernández M., Raga J.A. 2003. Girdles as the main infection site for *Paradeontacylix kampachi* (Sanguinicolidae) in the greater amberjack *Seriola dumerili.* Disesases of Aquatic Organisms 53: 271–272.

Montero F.E., Kostadinova A., Raga J.A. 2009. Development and habitat selection of a new sanguinicolid parasite of cultured greater amberjack, *Seriola dumerili*, in the Mediterranean. Aquaculture 288: 132-139.

Moran J.D.W., Whitaker D.J., Kent M.L. 1999a. A review of the myxosporean genus *Kudoa* Meglitsch, 1947, and its impact on the international aquaculture industry and commercial fisheries. Aquaculture 172: 163-196.

Moran J.D.W., Whitaker D.J., Kent M.L. 1999b. Natural and laboratory transmission of the marine myxozoan parasite *Kudoa thyrsites* to Atlantic salmon. Journal of Aquatic Animal Health 11: 110-115.

Morris D.J., Adams A. 2006. Transmission of *Tetracapsuloides bryosalmonae* (Myxozoa: Malacosporea), the causative organism of salmonid proliferative kidney disease, to the freshwater bryozoan, *Fredericella sultana*. Parasitology 133: 701-709.

Morris D.J., Adams A. 2008. Sporogony of *Tetracapsuloides bryosalmonae* in the brown trout *Salmo trutta* and the role of the tertiary cell during the vertebrate phase of myxozoan life cycles. Parasitology 135: 1075-1092.

Morris D.J. 2010. Cell formation by myxozoan species is not explained by dogma. Proceedings of the Royal Society B: Biological Sciences 277: 2565-2570.

Morrison C.M., Martell D.J., Leggiadro C., O'Neil D. 1996. *Ceratomyxa drepanopsettae* in the gallbladder of Atlantic halibut, *Hippoglossus hippoglossus*, from the northwest Atlantic Ocean. Folia Parasitologica 43: 20-36.

Mueller A.K., Labaled M., Kappe S.H.I., Matuschewski K. 2005. Genetically modified *Plasmodium* parasites as a protective experimental malaria vaccine. Nature 433: 164-167.

Muñoz P., Cuesta A., Athanassopoulou F., Golomazou H., Crespo S., Padrós F., Sitjà-Bobadilla A., Albiñana G., Esteban M.A., Alvarez-Pellitero P., Meseguer J. 2007. Sharpsnout sea bream (*Diplodus puntazzo*) humoral immune response against the parasite *Enteromyxum leei* (Myxozoa). Fish Shellfish Immunology 23: 636-645.

Naidjenova N.N., Zaika V.E. 1970. Three new genera of myxosporidia-fish parasites from the Indian ocean. Zoological Journal 49: 451-454 (in Russian).

Nithart M. 1998. Population dynamics and secondary production of *Nereis diversicolor* in a North Norfolk Saltmarsh (UK). Journal of the Marine Biological Association of the United Kingdom 78: 131-143.

Noble E.R. 1941. Nuclear cycles in the life history of the protozoan genus *Ceratomyxa*. Journal of Morphology 69: 455-479.

Nolan M.J., Cribb T.H. 2004a. *Ankistromeces mariae* n. g., n. sp. (Digenea: Sanguinicolidae) from *Meuschenia freycineti* (Monacanthidae) from Tasmania. Systematic Parasitology 57: 151-157.

Nolan M.J., Cribb T.H. 2004b. Two new blood flukes (Digenea: Sangiunicolidae) from Epinephelinae (Percifomes: Serranidae) of the Pacific Ocean. Parasitology International 53: 327-335.

Nolan M.J., Cribb T.H. 2005. *Chaulioleptos haywardi* n. gen., n. sp. (Digenea: Sanguinicolidae) from *Filimanus heptadactyla* (Perciformes: Polynemidae) of Moreton Bay, Australia. Journal of Parasitology 91: 630-634.

Nolan M.J., Cribb T.H. 2006a. An exceptionally rich complex of Sanguinicolidae von Graff, 1907 (Platyhelminthes: Trematoda) from Siganidae, Labridae and Mullidae (Teleostei: Perciformes) from the Indo-West Pacific Region. Zootaxa 1218: 1-80.

Nolan M.J., Cribb T.H. 2006b. *Cardicola* Short, 1953 and *Braya* n. gen. (Digenea: Sanginicolidae) from five families of tropical Indo-Pacific fishes. Zootaxa 1265: 1-80.

Ogawa K., Andoh H., Yamaguchi M. 1993. Some biological aspects of *Paradeontacylix* (Trematoda: Sanguinicolidae) infection in cultured marine fish *Seriola dumerili*. Fish Pathology 28: 177–180.

Ogawa K., Hattori K., Hatai K., Saburoh S. 1989. Histopathology of cultured marine fish, *Seriola purpurascens* (Carangidae) infected with *Paradeontacylix* spp. (Trematoda: Sanguinicolidae) in its vascular system. Fish Pathology 24: 75-81.

Ogawa K., Nagano T., Akai N., Sugita A., Hall K.A. 2007. Blood fluke infection of cultured tiger puffer *Takifugu rubripes* imported from China to Japan. Fish Pathology 42: 91–99.

Ogawa K., Tanaka S., Sugihara Y., Takami I. 2010. A new blood fluke of the genus *Cardicola* (Trematoda: Sanguinicolidae) from Pacific bluefin tuna *Thunnus orientalis* (Temminck & Schlegel, 1844) cultured in Japan. Parasitology International 59: 44-48.

Okamura B., Curry A., Wood T.S., Canning E.U. 2002. Ultrastructure of *Buddenbrockia* identifies it as a myxozoan and verifies the bilaterian origin of the Myxozoa. Parasitology 124: 215-223.

Oldham-Ott C.K., Gilloteaux J. 1997. Comparative morphology of the gallbladder and biliary tract in vertebrates: Variation in structure, homology in function and gallstones. Microscopy Research and Technique 38: 571-597.

Orrell T.M., Carpenter K.E., Musick J.A., Graves J.E., McEachran J.D. 2002. Phylogenetic and Biogeographic Analysis of the Sparidae (Perciformes: Percoidei) from Cytochrome b Sequences. Copeia 3: 618-631.

Overstreet R.M., Køie M. 1989. *Pearsonellum corventum*, gen. et sp. nov. (Digenea: Sanguinicolidae), in Serranid fishes from the Capricornia section of the Great Barrier Reef. Australian Journal of Zoology 37: 71-79.

Overstreet R.M., Thulin J. 1989. Response by *Plectropomus leopardus* and other serranid fishes to *Pearsonellum corventum* (Digenea: Sanguinicolidae) including melanomacrophage centres in the heart. Australian Journal of Zoology 37: 129-142.

Padrós F., Zarza C., Crespo S. 2001. Histopathology of cultured seabream *Sparus aurata* infected with sanguinicolid trematodes. Diseases of Aquatic Organisms 44: 47–52.

Palenzuela O., Sitjà-Bobadilla A., Alvarez-Pellitero P. 1997. *Ceratomyxa sparusaurati* (Protozoa: Myxosporea) infections in cultured gilthead sea bream *Sparus aurata* (Pisces: Teleostei) from Spain: aspects of the host–parasite relationship. Parasitological Research 83: 539–548.

Palenzuela O., Álvarez-Pellitero P., Sitjà-Bobadilla A. 1999. Glomerular disease associated with *Polysporoplasma sparis* (Myxozoa) infections in cultured gilthead sea bream, *Sparus aurata* L. (Pisces: Teleostei). Parasitology 118: 245-256.

Palenzuela O., Redondo M.J., Alvarez-Pellitero P. 2002. Description of *Enteromyxum scophthalmi* gen. nov., sp. nov. (Myxozoa), an intestinal parasite of turbot (*Scophthalmus maximus* L.) using morphological and ribosomal RNA sequence data. Parasitology 124: 369-379.

Palenzuela O. 2006. Mixozoan infections in Mediterranean mariculture. Parassitologia 48: 27-29.

Paperna I., Dzikowski R. 2006. Digenea (Phylum Plathyhelminthes). In: Fish Diseases and Disorders, Volumen 1, Protozoan and Metazoan infections, second ed.,Woo P.T.K. (ed), C.A.B. International, Cambridge, p. 363.

Parker J.D., Warner M.C. 1970. Effects of fixation, dehydration and staining on dimensions of myxosporidan. Journal of wildlife diseases 6: 448-456.

Pelham R.J., Chang F. 2002. Actin dynamics in the contractile ring during cytokinesis in fission yeast. Nature 419: 82–86.

Perrott M.N., Grierson C.E., Hazon N., Balment R.J. 1992. Drinking behaviour in sea water and fresh water teleosts, the role of the renin-angiotensin system. Fish Physiology and Biochemistry 10: 161-168.

Posada D. 2008. jModelTest: Phylogenetic Model Averaging. Molecular Biology and Evolution 25: 1253-1256.

Prunescu C.C., Prunescu P., Puzek Z., Lom J. 2007. The first finding of myxosporean development from plasmodia to spores in terrestrial mammals: *Soricimyxum fegati* gen. et sp n. (Myxozoa) from *Sorex araneus* (Soricomorpha). Folia Parasitologica 54: 159-164.

Rambaut A. 2009. Tree Figure Drawing Tool. Versión 1.2.3. Institute of Evolutionary Biology, University of Edinburgh.

Rangel L.F., Santos M.J., Cech G., Székely C. 2009. Morphology, molecular data, and development of *Zschokkella mugilis* (Myxosporea, Bivalvulida) in a polychaete alternate host, *Nereis diversicolor*. Journal of Parasitology 95: 561-569.

Rangel L.F., Cech G., Székely C., Santos M.J. 2011. A new actinospore type Unicapsulactinomyxon (Myxozoa), infecting the marine polychaete, *Diopatra neapolitana* (Polychaeta: Onuphidae) in the Aveiro Estuary (Portugal). Parasitology 138: 698-712.

Redondo M.J., Palenzuela O., Riaza A., Macias A., Alvarez-Pellitero P. 2002. Experimental transmission of *Enteromyxum scophthalmi* (Myxozoa), an enteric parasite of turbot *Scophthalmus maximus*. Journal of Parasitology 88: 482-488.

Redondo M.J., Quiroga M.I., Palenzuela O., Nieto J.M., Alvarez-Pellitero P. 2003a. Ultrastructural studies on the development of *Enteromyxum scophthalmi* (Myxozoa),

an enteric parasite of turbot (*Scophthalmus maximus* L.). Parasitology Research 90: 192-202.

Redondo M.J., Palenzuela O., Alvarez-Pellitero P. 2003b. In vitro studies on viability and proliferation of *Enteromyxum scophthalmi* (Myxozoa), an enteric parasite of cultured turbot *Scophthalmus maximus*. Diseases of Aquatic Organisms 55: 133-144.

Redondo M.J., Palenzuela O., Alvarez-Pellitero P. 2004. Studies on transmission and life cycle of *Enteromyxum scophthalmi* (Myxozoa), an enteric parasite of turbot *Scophthalmus maximus*. Folia Parasitologica 51: 188–198.

Reed C.C., Basson L., Van As L.L., Dyková I. 2007. Four new myxozoans (Myxosporea: Bivalvulida) from intertidal fishes along the south coast of Africa. Folia Parasitologica 54: 283–292.

Repullés-Albelda A., Montero F.E., Holzer A.S., Ogawa K., Hutson K.S., Raga J.A. 2008. Speciation of the *Paradeontacylix* spp. (Sanguinicolidae) of *Seriola dumerili*. Two new species of the genus *Paradeontacylix* from the Mediterranean. Parasitology International 57: 405-414.

Riedl R. 1986. Fauna y flora del mar Mediterráneo, Omega, Barcelona. pp. 709, 711 (in Spanish).

Rigos G., Katharios P. 2010. Pathological obstacles of newly-introduced fish species in Mediterranean mariculture: A review. Reviews in Fish Biology and Fisheries 20: 47-70.

Ronquist F., Huelsenbeck J.P. 2003. MrBayes 3: Bayesian phylogenetic inference under mixed models. Bioinformatics 19: 1572-1574.

Ryce E.K.N. 2003. Factor Affecting the Resistance of Juvenile Rainbow Trout to Whirling Disease. PhD thesis, Montana State University, Bozeman, MT.

Ryce E.K.N., Zale A.V., MacConnell E. 2004. Effects of fish age and parasite dose on the development of whirling disease in rainbow trout. Diseases of Aquatic Organisms 59: 225-233.

Sardá R., Martin D. 1993. Populations of *Streblospio webster* (Polychaeta: Spionidae) on temperate zones: demography and production. Journal of the Marine Biological Association of the United Kingdom 73: 769-784.

Schell S.C. 1974. The life history of *Sanguinicola idahoensis* sp. n. (Trematoda: Sanguinicolidae), a blood parasite of steelhead trout, *Salmo gairdneri* Richardson. Journal of Parasitology 60: 561-566.

Schubert G., Sprague V., Reinboth R. 1975. Observations on a new species of *Unicapsula* (Myxosporida) in the fish *Maena smaris* (L.) by conventional and electronmicroscopy. Zeitschrift für Parasitenkunde 46: 245-252.

Schultz J., Maisel S., Gerlach D., Müller T., Wolf M. 2005. Common core of secondary structure of the internal transcribed spacer 2 (ITS2) throughout the Eukaryota. RNA 11: 361-364.

Seligman A.M., Wasserkrug H.L., Hanker J.S. 1966. A new staining method (OTO) for enhancing contrast of lipid droplets in osmium-tetraoxide-fixed tissue osmiophilic thiocarbohydrazide (TCH). Journal of Cell Biology 30: 424-432.

Sidall M.E., Martin D.S., Bridge D., Desser S.S., Cone D.K. 1995. The demise of a phylum of protists: Phylogeny of myxozoa and other parasitic cnidaria. Journal of Parasitology 81: 961-967.

Simón-Martín F., Rojo-Vázquez F., Simón-Vicente F. 1988. *Sanguinicola rutili* n. sp. (Digenea: Sanguinicolidae) parásito del sistema circulatorio de *Rutilus arcasi* (Cyprinidae) en la provincia de Salamanca. Revista Ibérica de Parasitología 47: 253-261.

Sitjà-Bobadilla A., Alvarez-Pellitero P. 1992. Light and electron microscopic description of *Sphaerospora dicentrachi* n. sp. (Myxosporea: Sphaerosporidae) from wild and cultured sea bass, *Dicentrarchus labrax* L. Journal of Protozoology 39: 273-281.

Sitjà-Bobadilla A., Alvarez-Pellitero P. 1993a. Ultrastructural and cytochemical observations on the sporogenesis of *Sphaerospora testicularis* (Protozoa: Myxosporea) from Mediterranean sea bass, *Dicentrarchus labrax* (L.). European Journal of Protistology 29: 219-229.

Sitjà-Bobadilla A., Alvarez-Pellitero P. 1993b. Pathologic effects of *Sphaerospora dicentrachi* Sitjà-Bobadilla and Alvarez-Pellitero, 1992 and *S. testicularis* Sitjà-Bobadilla and Alvarez-Pellitero, 1990 (Myxosporea:Bivalvulida) parasitic in the Mediterranean sea bass *Dicentrachus labrax* L. (Teleostei: Serranidae) and the cell-mediated immune reaction: a light and electron microscopy study. Parasitology Research 79: 119-129.

Sitjà-Bobadilla A., Alvarez-Pellitero P. 1993c. Light and electron microscopical description of *Ceratomyxa labracis* n. sp. and a redescription of *C. diplodae* (Myxosporea: Bivalvulida) from wild and cultured Mediterranean sea bass *Dicentrarchus labrax* (L.) (Teleostei: Serranidae). Systematic Parasitology 26: 215-223.

Sitjà-Bobadilla A., Alvarez-Pellitero P. 1993d. *Zschokkella mugilis* n. sp. (Myxosporea: Bivalvulida) from mullets (Teleostei: Mugilidae) of Mediterranean waters: Light and electron microscopic description. Journal of Eukaryotic Microbiology 40: 755-764.

Sitjà-Bobadilla A., Alvarez-Pellitero P. 1995. Light and electron microscopic description of *Polysporoplasma* n. g. (Myxosporea: Bivalvulida), *Polysporoplasma sparis* n. sp. from *Sparus aurata* (L.) and *Polysporoplasma mugilis* n. sp. from *Liza aurata* L. European Jornual of Protistology 31: 77-89.

Sitjà-Bobadilla A., Palenzuela O., Alvarez-Pellitero P. 1995. *Ceratomyxa sparusaurati* n. sp. (Myxosporea: Bivalvulida), a new parasite from cultured gilthead seabream (*Sparus aurata* L.) (Teleostei: Sparidae): light and electron microscopic description. Journal of Eukaryotic Microbiology 42: 529–539.

Sitjà-Bobadilla A., Alvarez-Pellitero P. 1996. Virus-like particles in *Polysporoplasma mugilis* (Protozoa: Myxosporea), parasitic in a marine fish (*Liza aurata* L.). International Journal for Parasitology 26: 457-459.

Sitjà-Bobadilla A., Alvarez-Pellitero P. 2001. *Leptotheca sparidarum* n. sp. (Myxosporea: Bivalvulida), a parasite from cultured common dentex (*Dentex dentex* L.) and gilthead sea bream (*Sparus aurata* L.) (Teleostei: Sparidae). Journal of Eukaryotic Microbiology 48: 627-639.

Sitjà-Bobadilla A., Redondo M.J., Bermúdez R., Palenzuela O., Ferreiro I., Riaza A., Quiroga I., Nieto J.M., Alvarez-Pellitero P. 2006. Innate and adaptive immune responses of turbot, *Enteromyxum scophthalmi* (L.) following experimental infection with *Enteromyxum scophthalmi* (Myxozoa: Myxosporea). Fish Shellfish Immunology 21: 485–500.

Sitjà-Bobadilla A., Diamant A., Palenzuela O., Alvarez-Pellitero P. 2007. Effect of host factors and experimental conditions on the horizontal transmission of *Enteromyxum leei* (Myxozoa) to gilthead sea bream, *Sparus aurata* L., and European sea bass, *Dicentrarchus labrax* (L.). Journal of Fish Diseases 30: 243-250.

Sitjà-Bobadilla A. 2008. Living off a fish: A trade-off between parasites and the immune system. Fish & Shellfish Immunology 25: 358-372.

Sitjà-Bobadilla A. 2009. Can Myxosporean parasites compromise fish and amphibian reproduction? Proceedings of the Royal Society B: Biological Sciences 276: 2861-2870.

Small J.V., Rottner K.R. 2010. Elementary cellular processes driven by actin assembly: lamellipodia and filopodia. In: Actin-based motility, Carlier M.F. (ed), Springer Science, pp 3-33.

Smith J.W. 1997. The blood flukes (Digenea: Sanguinicolidae and Spirorchidae) of cold-blooded vertebrates: Part 1. A review of the literature published since 1971, and bibliography. Helminthological Abstracts 66: 255-292.

Smith J.W. 2002. Familiy Sanguinicolidae von Graff, 1907. In: Keys to the Trematoda Vol. 1. Gibson D.I., Jones A., Bray R.A. (eds.), CAB International Cambridge, Wallingford, pp. 433-452.

Smothers J.F, Vondohlen C.D., Smith L.H., Spall R.D. 1994. Molecular evidence that the myxozoan protists are metazoans. Science 265: 1719-1721.

Štolc A. 1899. Actinomyxidia, eine neue Gruppe der Mesozoa, der Myxosporidien verwandt. Abhandlungen der Böhmischen Gesellschaft der Wissenschaften 8: 1-12.

Swofford D.L. 2002. PAUP*: Phylogenetic Analysis Using Parsimony, Ver.4.0b10. Sinauer Associates, Sunderland, MA.

Tamura K., Nei M. 1993. Estimation of the number of nucleotide substitutions in the control region of mitochondrial DNA in humans and chimpanzees. Molecular Biology and Evolution 10: 512-526.

Thiéry J.P 1967. Misé en evidence des polysaccarides sur coupes fines en microscopie électronique. Journal de Microscopie 6: 987-1018 (in French).

Thompson J.D., Gibson T.J., Plewniak F., Jeanmougin F., Higgins D.G. 1997. The ClustalX windows interface: flexible strategies for multiple sequence alignment aided by quality analysis tools. Nucleic Acids Research 25: 4876-4882.

Thompson K.G., Nehring R.B., Bowden D.C., Wygant T. 1999. Field exposures of 7 species or subspecies of salmonids to *Myxobolus cerebralis* in the Colorado River, Middle Park, Colorado. Journal of Aquatic Animal Health 11: 312–329.

Thoney D.A., Hargis W.J. 1991. Monogenea (Platyhelminthes) as hazards for fish in confinement. Annual Review of Fish Diseases 2: 133–153.

Thulin J. 1980. A redescription of the fish blood-fluke *Aporocotyle simplex* Odhner, 1900 (Digenea: Sanguinicolidae) with comments on its biology. Sarsia 65: 35-48.

Uspenskaya A.V., Raikova O.I. 2004. F-actin and beta-tubulin localization in the myxospore stinging apparatus of *Myxobolus pseudodispar* Gorbunova, 1936 (Myxozoa, Myxosporea). Tsitologiia 46: 748-754.

Viehberger G. 1982. Apical surface of the epithelial cells in the gallbladder of the rainbow trout and the tench. Cell Tissue Research 224: 449-454.

Weill R. 1938. L'interpretation des Cnidosporidies et la Valeur Taxonomique de Leur Cnidome. Leur Cycle Compare a la Phase Larvaire des Narcomeduses Cuninides. Travaux de la Station. Zoologique de Wimereux 13: 727-744 (in French).

Whipps C.M., Adlard R.D., Bryant M.S., Kent M.L. 2003. Two unusual myxozoans, *Kudoa quadricornis* n. sp. (Multivalvulida) from the muscle of goldspotted trevally (*Carangoides fulvoguttatus*) and *Kudoa permulticapsula* n. sp. (Multivalvulida) from the muscle of Spanish mackerel (*Scomberomorus commersoni*) from the Great Barrier Reef, Australia. Journal of Parasitology 89: 168-173.

Whipps C.M., Grossel G., Adlard R.D., Yokoyama H., Bryant M.S., Munday B.L., Kent M.L. 2004. Phylogeny of the multivalvulidae (Myxozoa:Myxosporea) based on comparative ribosomal DNA sequence analysis. Journal of Parasitology 90: 618-622.

Whipps C.M., Kent M.L. 2006. Phylogeography of the cosmopolitan marine parasite *Kudoa thyrsites* (Myxozoa: Myxosporea). Journal of Eukaryotic Microbiology 53: 364-373.

Whitehead P.J.P., Bauchot M.L., Hureau J.C., Nielsen J., Tortonese E. 1986. Percomonphi. In: Fishes of the North-Eastern Atlantic and the Mediterranean, Whitehead P.J.P., Bauchot M.L., Hureau J.C., Nielsen J., Tortonese E. (eds), United Nations Educational, Scientic and Cultural Organization (UNESCO), Paris, pp. 896–897, 911.

Wolf K., Markiw M.E. 1984. Biology contravenes taxonomy in the Myxozoa- New discoveries show alternation of invertebrate and vertebrate hosts. Science 225: 1449-1452.

Woo P.T.K., Bruno D.W., Lim L.H.S. 2002. Diseases and disorders of finfish in cage culture. CABI, 354 pp.

Yanagida T., Sameshima M., Nasu H., Yokoyama H., Ogawa K. 2006. Temperature effects on the development of *Enteromyxum* spp. (Myxozoa) in experimentally infected tiger puffer *Takifugu rubripes* (Temminck & Schlegel). Journal of Fish Diseases 29: 561-567.

Yokoyama H., Urawa S. 1997. Fluorescent labeling of actinospores for determining the portals of entry into fish. Diseases of Aquatic Organisms 30: 165–169.

Zajac R.N. 1991a. Population ecology of *Polydora ligni* (Polychaeta: Spionidae). I. Seasonal variation in population characteristics and reproductive activity. Marine Ecology Progress Series 77: 197-206.

Zajac R.N. 1991b. Population ecology of *Polydora ligni* (Polychaeta: Spionidae): II. Seasonal demographic variation and its potential impact on life history evolution. Marine Ecology Progress Series 77: 207-220.

Zhao Y.J., Song W.B. 2003. Myxosporea in marine fishes in the Yellow Sea and Bohai Sea. In: Pathogenic protozoa in mariculture, Song W., Zhao Y., Xu K., Hu X., Gong J. (eds), Science Press, Beijing, pp. 217–224 (in Chinese).

Zrzavý J., Hypša V. 2003. Myxozoa, *Polypodium*, and the origin of the Bilateria: The phylogenetic position of "Endocnidozoa" in light of the rediscovery of *Buddenbrockia*. Cladistics 19: 164-169.